Rewiring of signaling pathways by HCMV-encoded GPCRs

Erik Slinger

The work described in this thesis was performed at the Leiden/Amsterdam Center for Drug Research (LACDR), Faculty of Exact Sciences, Division of Medicinal Chemistry, VU University Amsterdam, De Boelelaan 1083, 1081 HV Amsterdam, The Netherlands.

Rewiring of signaling pathways by HCMV-encoded GPCRs.

Erik Slinger

Cover: Activation of β-catenin in an intestinal adenoma
Cover design by Erik Slinger

This research was supported by the Netherlands Organisation for Scientific Research (NWO), ECHO grant 700.55.010.

Printed by Wöhrmann Print Service B.V., Zutphen, The Netherlands.

ISBN-978-94-6203-204-0

VRIJE UNIVERSITEIT

Rewiring of signaling pathways by HCMV-encoded GPCRs

ACADEMISCH PROEFSCHRIFT

ter verkrijging van de graad Doctor aan
de Vrije Universiteit Amsterdam,
op gezag van de rector magnificus
prof.dr. L.M. Bouter,
in het openbaar te verdedigen
ten overstaan van de promotiecommissie
van de Faculteit der Exacte Wetenschappen
op dinsdag 11 december 2012 om 11.45 uur
in de aula van de universiteit,
De Boelelaan 1105

door

Erik Slinger

geboren te Heemskerk

promotor: prof.dr. M.J. Smit
copromoter: dr. M.H. Siderius

Table of contents

Aim of the thesis

Viruses with oncogenic or oncomodulatory properties are known agents of oncogenesis. Human Cytomegalovirus (HCMV) infection has been associated with several cancers, such as colon cancer and glioblastomas. At least one of the HCMV-encoded viral G-protein coupled receptors (vGPCRs), US28, has been shown, strongly dependent on the cellular context, to induce proliferative and anti-apoptotic signaling. The other vGPCRs; UL33, UL78, and US27 are not as well described, although UL33 has been demonstrated to display constitutive signaling. Multiple signaling pathways are engaged by US28, and the proliferative behavior is the result of the integration of these pathways. This thesis aims to gain more understanding of the molecular mechanisms by which HCMV-encoded GPCRs induce this proliferative phenotype.

First, the signal transduction pathways activated by US28, involving the Janus kinase/Signal transducer and activator of transcription (JAK/STAT)-axis and interleukin-6 (IL-6) induced activation of STAT3 have been investigated in detail (**Chapter 3**). Next, the nature of the IL-6/STAT3 positive feedback loop was investigated using a systems biology approach (**Chapter 4**). In **Chapter 5**, US28-induced non-canonical signaling through the b-catenin pathway is explored. An characterization of the signalosome in **Chapter 6** has resulted in a proposed model that may explain the mechanism by which US28 induces Tcf/Lef activation. One of the other vGPCRs, UL33, also displays constitutive signaling and its potential for proliferative signaling is explored in **Chapter 7**.

Understanding the molecular mechanism by which HCMV exerts its oncomodulatory effects, is key to further understand the fundamental mechanisms in tumor biology. This holds true, especially for the first steps in transformation and the role that aberrant signaling may play in it. Furthermore, the complex nature of US28-induced signaling clearly highlights the importance of a systems biology approach to understand the interplay between the different induced pathways.

1

Introduction to virally encoded GPCRs

Adapted from:
Herpesvirus-encoded GPCRs rewire cellular signaling
Erik Slinger, Ellen Langemeijer, Marco Siderius, Henry F. Vischer, Martine J. Smit.
Molecular and Cellular Endocrinology, 2010

Leiden/Amsterdam Center for Drug Research, Division of Medicinal Chemistry, Faculty of Sciences, VU University Amsterdam, De Boelelaan 1083, 1081 HV Amsterdam, the Netherlands.

1.1 G-protein coupled receptors Human and viral chemokine receptors

G-protein coupled receptors (GPCRs) constitute a diverse family of membrane receptors which can be activated by ligands varying from light (as in rhodopsin) to proteins (e.g. the chemokine receptors). Despite being activated by such a variety of ligands, these receptors show a high degree of structure similarity. The GPCR superfamily can be divided into 3 major groups (*1*). The family A receptors, the largest family, contains the Rhodopsin-like GPCRs which are named after their prototypical receptor. The chemokine receptors belong to this family. The Secretin-like GPCRs constitute the family B receptors, which are often regulated by peptide ligands. The glucagon receptor is a member from this family. Finally, there are the family C GPCRs which includes the metabotropic glutamate receptors, $GABA_B$ receptors, and the taste receptors amongst others. The GPCRs constitute the most abundant family of signaling proteins encoded by the human genome (*2*). Because of their importance in cellular signaling and relative ease of access, the GPCRs have been an important drug target for the last decades with over 30% the currently marketed drugs targeting a GPCR (*3*).

Almost all GPCRs are composed of 7 transmembrane (TM) domains, and generally couple to hetero-trimeric G-proteins resulting in a plethora of cellular responses to receptor activation (*4*). GPCRs contain a number of conserved sites that are necessary for GPCR functionality. For example, the DRY motif located in TM3 controls coupling of the receptor to G-proteins. Mutations in these residues can result in constitutive activity (eg. VRY for the chemokine receptor CXCR2 (*5*)).

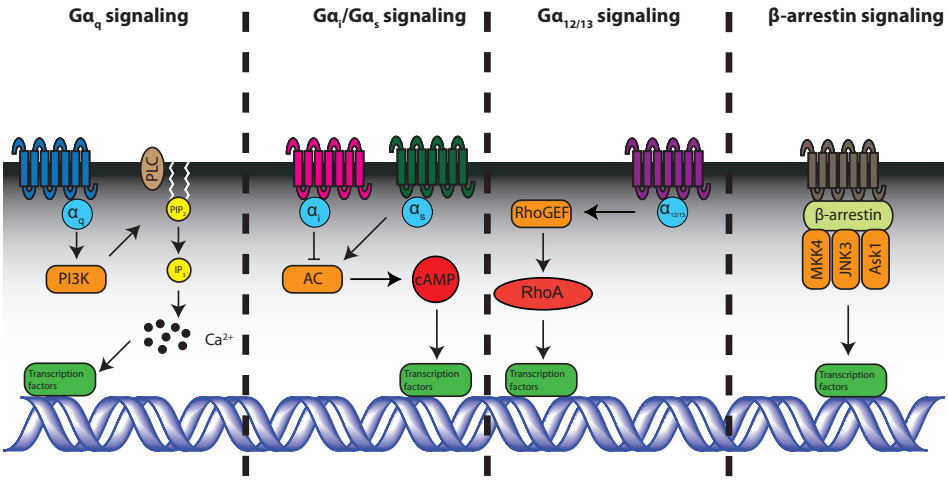

Figure 1. Models showing examples of the different modes of signaling by GPCRs. Signaling through $G\alpha_q$ results in activation of phosphotadyl-inositol-3-kinase (PI3K). Subsequently, PLC is activated which results in activation of Ca^{2+} stores which activates the transcription factors (eg. NFAT). Activation of $G\alpha_i$ inhibits adenylate cyclase (AC) which lowers cyclic-adenosine-mono-phosphate (cAMP) levels. In contrast, $G\alpha_s$ induces AC activation, increasing cAMP levels. Signaling through $G\alpha_{12/13}$ results into activation of RhoA via RhoGEF. Finally, G-protein independent signaling via β-arrestin involves scaffolding of the kinases MKK4, JNK3, and Ask1 on β-arrestin.

Conversely, other mutations can render a constitutive active receptor inactive (eg. DAY for US28 (*6*)). The G-proteins are composed of three constituents; the α, β, and γ subunits, of which the α subunit is the most variable and determines for a great part downstream signaling. However, the β and γ subunits were found to modulate downstream signaling. Figure 1 shows several different signaling pathways being activated by different Gα subunits: $G\alpha_q$, $G\alpha_s$, $G\alpha_{12/13}$ and $G\alpha_i$. For example, $G\alpha_q$ signaling typically activates phospholipase C β (PLCβ) signaling which in turn will activate Ca^{2+} signaling which then culminates in the activation of Nuclear Factor of Activated T-cells (NFAT). On the other hand, signaling via $G\alpha_i$ typically inhibits adenylyl cyclase which subsequently results in reduced cyclic-adenosine-monophosphate (cAMP) levels. In contrast, $G\alpha_s$ signaling is translated in increased activation of adenylyl cyclase. Finally, signaling via $G\alpha_{12/13}$ results in activation of RhoGEF, subsequently leading to RhoA activation and further downstream signaling. Once the receptor has been activated by a ligand, G-protein coupled receptor kinases (GRK) phosphorylate serine residues in the C-terminal tail. Upon C-tail phosphorylation, signaling through the G-proteins ceases. Subsequently, β-arrestins may bind to the phosphorylated GPCR and interact with clathrin and AP2, driving GPCR internalization into endosomes where the receptor is either recycled to the plasma membrane or degraded in lysosomes (*7*).

While most receptors are thought to activate only one pathway at a time this is not necessarily the case. It is possible for a GPCR to simultaneously activate multiple pathways resulting in GPCR-mediated promiscuous signaling. Furthermore, while GPCRs typically only signal upon binding of an agonist, some GPCRs show constitutive activity. Virally encoded GPCRs are especially known to display such behavior. In recent years another aspect of GPCR signaling has become apparent, G-protein independent signaling. In this type of GPCR-mediated signaling β-arrestin acts as a scaffold for Mitogen-activated protein kinases (MAPK) which then results in activation of c-Jun N-terminal kinase 3 (JNK3) (*8*). Another novel concept in GPCR signaling is ligand-directed signaling, where different ligands yield different responses upon binding to the receptor. Other names have been suggested for this behavior, including functional selectivity, biased agonism, agonist-directed trafficking, or protean agonism (*9*).

1.2 The chemokines and chemokine receptors

The mammalian chemokine (the name is derived from chemotactic cytokines) signaling system is composed of small protein ligands (the chemokines with a size around 8-10 kD) that bind and activate chemokine receptors. Together, chemokines and chemokine receptors are important mediators of the immune system. Chemokine nomenclature is based on conserved cysteine motifs and the chemokine family can be subdivided into 4 families, the CCL, CXCL, XCL and CX3CL. In this system, the chemokines themselves are noted with a 'L' at the end and the receptors with a 'R' at the end. As some chemokines activate multiple chemokine receptors the chemokine / chemokine receptor system is believed to be promiscuous (Figure 2).

The superfamily of chemokines is currently composed of at least 46 members, the majority of which belongs to either the CCL or the CXCL family. The XCL and CX3CL families only have two and one member, respectively (*10*).
The main function of chemokines, as the name suggests, is to attract cells to sites of inflammation. The different chemokines bind different kinds of cells, as each type of cell expresses distinct subsets of chemokine receptors. The CCL chemokines attract a variety of cells from the immune system, whereas the CXC chemokines mainly attract neutrophils and lymphocytes. Furthermore, the CXC chemokines possess angiomodulatory activity. The combination of these angiomodulatory properties and their homing response renders the CXC chemokines to be of special interest in tumor growth as well as in metastasis. Notably, in breast cancer, the combined effects of e.g. CXCR4 and CXCL12 are of importance for tumor development (*11*). Chemokine receptors are not only expressed in leukocytes, but are also present on cells that are of a non-hematopoietic origin such as endothelial cells and neurons (*12*). Furthermore, several of the CXC receptors have been reported to be associated with several tumors (9). This is not unexpected considering the observed angiomodulatory properties of some of the CXC chemokines described above.
Mammalian viruses have evolved multiple strategies to evade or subvert the host's immune system. Members of the Herpesviridae family are particularly successful in this respect, with some of them capable of achieving life-long infections in up to 90% of the general population. To be able to do this, several host genes have been 'hijacked' in the course of evolution by these viruses. This 'hijacked' genetic material includes genes encoding chemokines and chemokine receptors. The receptors and chemokines thus obtained have been severely modified and optimized for the virus's own benefit. Furthermore, these receptors often exhibit unique characteristics, such as receptors that show promiscuous binding of ligands and constitutive activity. The last years some of these vGPCRs have shown to be involved in virus-associated pathologies, by 'rewiring' the cellular signaling network, not only in the

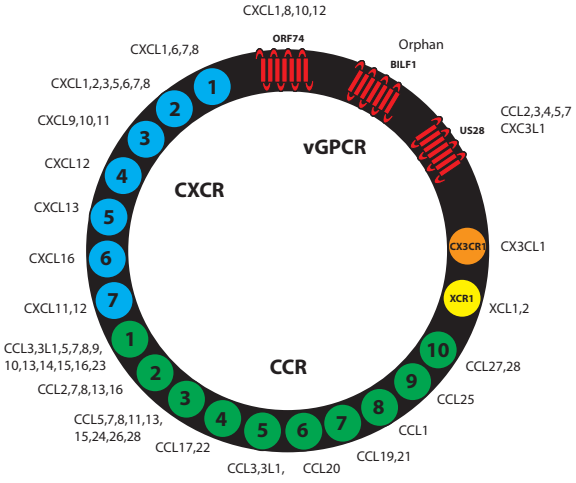

Figure 2. Schematic depiction of the chemokine/chemokine receptor system. Shown in blue are the different CXC-receptors with their respective ligands. Depicted in green are the CC-receptors and corresponding ligands. Finally, the viral receptors that are discussed in this review are shown in red with their ligands (if known). The XC-receptor and CX3C-receptor are also shown in yellow and orange, respectively.

cells expressing vGPCRs but also affecting neighboring cells by inducing secretion of different signaling factors. Examples of such signaling pathway subversions by vGPCRs are described in this thesis, and are also shown in Figure 3.

1.3 Kaposi Sarcoma associated herpes virus (KSHV)

KSHV or HHV8 is a γ-herpesvirus that was first identified in AIDS patients in the 1980's, when frequent occurrences of the usually rare Kaposi sarcoma (KS) were reported (*13*). The virus is endemic in Africa, with infection rates of over 50% in Central Africa, whilst infection rates in the rest of the world are much lower (between 0.2% and 10%). Currently three different variants of KS are recognized. Classic KS occurs mainly in Mediterranean men over the age of 50, and the lesions do not typically spread beyond the extremities. Endemic KS is common in particular parts of Africa. In Uganda, for example, KS accounts for up to 9% of the cancers. Finally, there is AIDS-associated KS, which was found initially predominantly in AIDS-affected patients, a particularly aggressive and often fatal variant of KS. In all the variants KS is characterized by highly vascularized lesions (*14*). Moreover, KHSV is found in nearly 100% of tumor isolates from patients. KSHV is also associated with primary effusion lymphoma and multicentric Castleman disease (*15, 16*).
The double stranded DNA genome of KSHV encodes 84 open-reading frames (*17*) and 12 microRNAs (miRNAs) (*18*). Open-reading frame 74 encodes a vGPCR, also referred to as ORF74. ORF74 is a close homologue of CXCR2 and binds multiple chemokines, particularly those of the CXC family, which is indicative for a role in the avoidance of the host immune system by KSHV. In addition, ORF74 displays

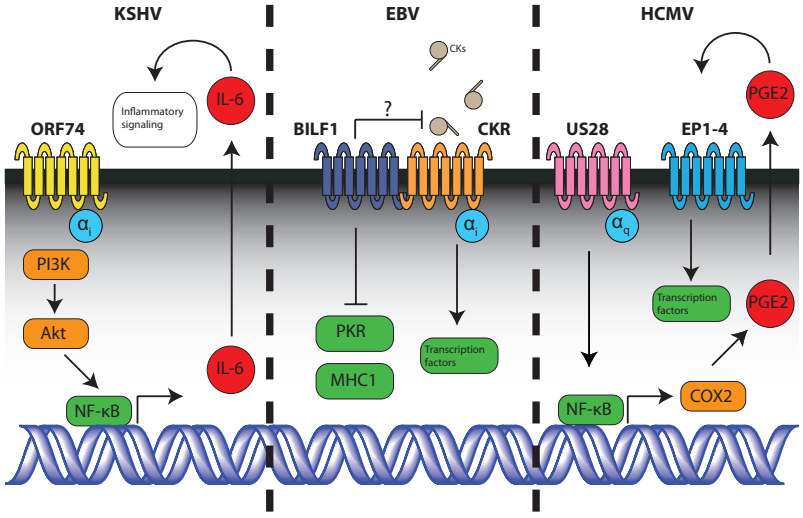

Figure 3. Methods by which the different viruses take over cellular signaling. Showing from the left to the right; ORF74 activating IL-6 transcription in a PI3K and Akt dependent manner. BILF1 displays constitutive Gαi signaling and downregulates PKR and MHC1. When forming dimers with endogenous chemokine receptors it may show negative binding cooperativity

constitutive activity, which has been correlated with oncogenesis *in vitro* and *in vivo* (*19, 20*). Furthermore, transgenic mice expressing ORF74 develop KS-like lesions (*21, 22*). Host cell signal transduction pathways activated by ORF74 include MAPKs, PLC, phosphoinositide-3-kinase (PI3K), and Akt (*23*). ORF74 has also been shown to activate NF-κB via PI3K and Akt. Moreover, the activation of NF-κB by ORF74 is accompanied by the release of inflammatory cytokines (*24*). The CXCL8 and CXCL1 chemokines act as (partial) agonists for ORF74 (*25*). In contrast, CXCL10 and CXCL12 act as inverse agonists (*26, 27*). Furthermore, ORF74 induces IL-6 release in infected cells, in the aforementioned manner via NF-κB. Subsequently, IL-6 triggers VEGF production both in a paracrine as well as autocrine manner (*24*). Moreover, KSHV encodes a viral IL-6 homologue (vIL-6) that may further strengthen inflammatory responses in the infected cells (*28*). Increased IL-6 levels induced by ORF74 produce an inflammatory environment that has been shown to promote transformation of cells and formation of tumors (*29*). IL-6 secretion and subsequent para- or autocrine activation of the JAK/STAT axis are thought to play an important role in these processes (*30, 31*). Interestingly, stimulation of cells neighboring the IL-6 producing cells may also induce an epigenetic switch, turning a transient event into a permanent change in phenotype of the affected cells, which has recently been described by Iliopoulos et al. (*32*) in a breast cancer model.
Only a small amount of the tumor cells in KS is actually KSHV positive in early KS. In later stages of the disease, more than 90% of the tumor cells are KSHV positive (*16*). In the latter case, only a small subset actually displays a gene expression profile typical for the lytic phase, including ORF74 expression (*33*). Although ORF74 is not the only oncogenic determinant in KSHV, this observation is striking. A small number of ORF74 expressing cells can alter the behavior of the surrounding tumor cells via paracrine signaling by inducing the production of factors like IL-6. Such a feed-forward mechanism creates an inflammatory environment that may be an important factor in KSHV related cancers. Indeed, for many cancers an inflammatory milieu promotes tumor development, and such tumor-associated inflammation may also invoke feed-forward mechanisms (*34*). However, the molecular mechanism how ORF74 accomplishes this, remains to be elucidated.

1.4 Epstein-Barr Virus (EBV)

EBV or HHV4 is another lymphotropic virus involved in proliferative diseases. This γ-herpesvirus was first identified in the 1960's. It infects over 90% of humans and persists during lifetime. Infection with EBV usually occurs by contact with oral secretions, causing infectious mononucleosis, also known as kissing disease. The virus replicates in cells in the oropharynx. B cells in the oropharynx are the primary site of infection and resting memory B cells are thought to be the site of persistence of EBV within the body. Shedding of EBV from the oropharynx is abolished in patients treated with acyclovir, whereas the number of EBV infected B cells in the circulation remains the same as before treatment (*35*).

EBV-related diseases are B cell- and epithelial cell-specific diseases, namely Burkitt's lymphoma, Hodgkin's lymphoma and nasopharyngeal carcinoma (*36*). All these diseases are particularly common in immune-suppressed patients like HIV-infected patients and recipients of organ or bone marrow transplants. Immune-compromised patients have impaired T-cell immunity and are unable to control the proliferation of EBV-infected B cells. EBV may play a pathogenic role in several other lymphoproliferative diseases and tumors in which EBV DNA or proteins have been detected as well.

The EBV genome consists of a linear DNA molecule that encodes approximately 94 ORFs or viral proteins. During viral replication, these proteins are important for regulation of the expression of viral genes, replicating viral DNA, forming structural components of the virion, and modulating the host immune response. Of the almost 100 viral genes that are expressed during replication, a small subset is expressed in latently infected B cells in vitro. Two types of non-translated RNA, six nuclear proteins, and two membrane proteins are expressed in these latently infected B cells (*37*).

Like KSHV, the EBV genome also contains a single viral GPCR, BILF1, a gene specifically expressed in the lytic phase of the viral replication cycle. BILF1 presents (low) homology to chemokine receptor CXCR4, a chemokine receptor known to be involved in many cancers (*11*). In contrast with ORF74 from KSHV, BILF1 does not seem to display oncogenic properties in vitro (unpublished observations Smit *et al*). Attempts that were undertaken so far to deorphanize BILF1 have not been successful. However, downstream signaling by BILF1 can be studied as this receptor, like other vGPCRs, signals in a constitutive manner through Gai (*38, 39*). It has been suggested that EBV may use BILF1 to control Gai-activated pathways during viral lytic replication, thereby affecting disease progression (*38*).

The function of BILF1 has also been examined in the context of immune evasion. Expression of BILF1 constitutively inhibits the phosphorylation of RNA-dependent protein kinase (PKR) (*39*). Upon viral infection, PKR is phosphorylated and activated, causing the overall cellular translational machinery to stop, thereby prohibiting viral replication (*40*). This mechanism serves to prevent viral spreading by elimination of the infected cells. Thus, the inhibition of PKR by BILF1 may help EBV by preventing a cellular antiviral response. Moreover, Zuo *et al.* showed recently that BILF1 reduces the levels of MHC class I at the cell surface of epithelial and melanoma cells (*41*). Targeting these molecules for lysosomal degradation, results in impaired recognition by immune T cells. Together with two other EBV lytic cycle genes BGLF5 and BNLF2A, BILF1 is the third gene in a group that cooperates to interfere with MHC class I antigen processing. This underscores the importance of the need for EBV to be able to evade CD8+ T cell responses during the lytic replication cycle. The effect on MHC class I degradation is independent of constitutive BILF1 signaling functions and the molecular mechanisms are distinct. It involves physical association of BILF1 with MHC class I molecules, an increased turnover from the cell surface, and enhanced degradation via lysosomal proteases (*41*).

In addition to the above mentioned immune-escape mechanisms, viral GPCRs may also affect the properties of human receptors by means of receptor oligomerization and/or cross-talk between downstream signaling pathways. GPCR proteins can physically interact, thereby modifying intracellular signaling and cellular functions (*42*). B lymphocyte migration and function is controlled by chemokines, acting on their cognate receptors. Using bioluminescence resonance energy transfer (BRET), time-resolved fluorescence resonance energy transfer (trFRET) and co-immunoprecipitation techniques, we recently have shown that BILF1 heterodimerizes with various chemokine receptors endogenously expressed in B lymphocytes. The oligomerization of BILF1 with chemokine receptors involved in B lymphocyte migration may change the receptors responsiveness to chemokines, resulting in altered homing and homeostasis of infected B lymphocytes. This might be an essential step for EBV dissemination or in EBV-induced pathogenesis in general (*43*). Negative binding cooperativity of both cognate chemokines and small drug-like compounds has been shown for CCR2/CCR5 and CCR2/CXCR4 chemokine receptor heterodimers (*44*). Since BILF1 is still an orphan GPCR, such binding cooperativity cannot be investigated at this moment. On the other hand, the active conformation of the constitutive active BILF1 may affect the function of partnering receptors in a hetero-oligomer, as previously shown for other GPCR dimers (*45*). As BILF1 seems to play a role in preventing the immune system from clearing the virus from the body, this may present an extra venue that can be targeted in treatment of EBV infection. Furthermore, a study by Kledal *et al.* has shown that BILF1 may display oncogenic signaling (*46*), which suggests a possible role for BILF1 in the development of EBV-related cancers.

1.5 Human Cytomegalovirus (HCMV)

Another member of the Herpesviridae family and β-herpesvirus subfamily is HCMV (HHV-5). HCMV is widely present among the general population, with up to 90% of the individuals harboring a latent infection (*47*). While HCMV infection is asymptomatic in immune-competent individuals, it can cause severe pathologies in immune-compromised patients (*48*). HCMV infection during pregnancy can result in aberrant development of the unborn child resulting in, for example, hearing loss (*49, 50*). Furthermore, HCMV infection has been correlated to several pathologies, such as arthrosclerosis (*51*).

HCMV proteins, DNA, and mRNA have been detected in multiple tumors that, together with epidemiological data, suggest a role for HCMV in cancer (*52, 53*). Furthermore, HCMV preferably infects cancer cells (*54*). However, unlike KSHV and EBV, HCMV is not considered an oncogenic virus and it is unlikely that HCMV by itself can act as an oncogenic factor. Alternatively, HCMV may have an oncomodulatory role, to catalyze an oncogenic process that has already been initiated.

The HCMV genome is the largest of any human virus known thus far, being 236 kb in size. The genome can be divided into two parts, a long and short part named UL and US, respectively. Also, a number of miRNAs have been found to be present

on the HCMV genome (*55*). In contrast with KSHV, the HCMV genome encodes four vGPCRs: US27, US28, UL33, and UL78. All of these genes encode chemokine receptor homologues, indicating that they were most likely pirated from the human -or another mammalian- genome at some point during evolution (*56, 57*). Homologues of UL33 and UL78 are conserved throughout the β-herpesvirus family, whereas homologues of US28 and US27 have been identified only in primate CMVs closely related to HCMV. Furthermore, two chemokines have been pirated from the human genome, vCXC1 and vCXC2 (*58*).

Only US28 has been shown to bind to chemokines, and has been most intensively studied. US28 binds promiscuously to several different members of the CC family, including CCL5 and CCL2, and also binds CX3CL1. Upon binding of chemokines, US28 is rapidly internalized, reflecting a possible function as a chemokine sink in the viral life cycle (*59*). Like ORF74 and BILF1, US28 displays constitutive signaling, activating PLCβ and NF-κB (*60*) as well as NFAT and CREB (*61*) via Gαq and Gαi. The constitutive signaling through CREB has been found to play a role in the regulation of the viral genome, specifically by stimulating the immediate-early gene promoter (*62*). Signaling via Gα12 results in SMC migration (*63*). Interestingly, US28 has been shown to possess tumorigenic properties when expressed in a NIH-3T3 murine fibroblast cell line, upregulating VEGF production and Cyclin D1. In a mouse xenograft model, tumors were formed when US28 expressing NIH-3T3 cells were injected (*64*). Further investigation revealed that release of PGE2 via US28-induced NF-κB activation of COX2 results in the activation of VEGF and Cyclin D1. This signaling cascade can be perturbed using pharmacological inhibitors of COX2 (eg. Celecoxib) (*65*). These data suggest a role of US28 in HCMV-related cancers that may be reminiscent of ORF74's role in KSHV, with the important distinction that HCMV, and thus US28, are probably not direct causative agents. However, as stated above, US28 most likely has an oncomodulatory role. This is strongly suggested by the observations that in many cell lines prolonged US28 expression results in apoptosis (*66*), indicating an interference of US28 in critical signaling pathways which, depending on cellular context results in either proliferation or apoptosis. It remains to be seen whether US28 also induces a local environmental change reminiscent of ORF74, but the US28-induced release of PGE2 and IL-6 suggests such a possibility. The fact that NF-κB is activated by US28 supports this notion, since NF-κB is known to induce the secretion of inflammatory factors.

Another vGPCR encoded by HCMV is UL33, which has been shown to signal in a constitutive manner via $G\alpha_q$, $G\alpha_i$, and $G\alpha_s$ (*67*). UL33's mouse homologue M33 has a function in viral dissemination within the host. Interestingly, a ΔM33 MCMV (viral strain lacking expression of M33) strain can be complemented with UL33, which suggests that UL33 may serve a role in the HCMV life-cycle (*68*). Supporting such a role for UL33 in HCMV is the presence of UL33 on the virion itself (*69*). Although US28 has never been detected in the viral envelope, there are indications that this is also the case. For instance, the rhesus macaque CMV homologue RhUS28.5 has been found in the viral envelope (*70*). Furthermore, the envelope proteins gB

and gH have been found to co-localize with US28 (*71*). In Chapter 7 we show that infected cells bind CCL5 directly after infection, well before any US28 has been synthesized from the viral genome. Presence of vGPCRs on the viral particle likely enhances binding to target cells, considering that US28 recognizes the membrane-bound chemokine CX3CL1 (*72*). However, in experiments *in vitro* with viral strains lacking either US28 or UL33 (ΔUS28 and ΔUL33, respectively) no reduced infectivity was observed (*73*). Of note, *in vitro* there is no real necessity for viral dissemination and UL33 would not be necessary. The biochemical properties of the remaining two vGPCRs, US27 and UL78, remain thus far largely uncharacterized. US27 has been shown to localize on the plasma membrane as well as in endosomes (*71*). The mouse and rat homologues of UL78, M78 and R78 respectively, have been shown to contribute to efficient viral cell-cell spread (*74, 75*). Interestingly, UL33 and UL78 have been shown to be able to form heterodimers with US28, which inhibits US28-induced activation of NF-κB, while induction of inositol phosphate accumulation was not affected (*76*).

It is clear that US28 and its constitutive activity may rewire cellular signaling and by this means play a potential role in HCMV-related pathologies. However, the exact signaling pathways involved still remain to be resolved. This will be critical for further understanding of HCMV-mediated oncomodulatory effects. Since US28 and UL33 are expressed at different times during the viral cycle (*77*), their expression will most likely modulate distinct signaling pathways at different times post infection.

1.6 Conclusions

The chemokine system, responsible for immune responses and as such an important mediator of the mammalian defense system against invasion of pathogens, has been corrupted by several β-herpesviruses. These viruses have hijacked and subverted many of the components of the chemokine system, both the ligands as well as the receptors. Although the three herpesviruses described above all have hijacked chemokine receptors, the role these vGPCRs play in the viral life cycle and the impact they have on host cell's signaling differs widely. Figure 3 depicts the different ways virus-encoded chemokine receptors take over signaling in their respective target cells. KSHV's ORF74 induces NF-κB signaling via PI3K and its downstream kinase Akt, resulting in IL-6 release and the establishment of an inflammatory environment, beneficial for tumorigenesis. EBV's BILF1 appears to be mainly involved in immune avoidance, which is demonstrated by both the hijacking and subversion of both the PKR and the MHC1 signaling pathways. In addition, BILF1 may act as a chemokine receptor scavenger, possibly modulating chemokine receptor affinity for their ligands by means of negative binding cooperativity. This is in contrast with ORF74 and US28, that both negatively influence the immune system by binding the chemokines themselves. The HCMV encoded vGPCR US28 has been shown -at least in a specific cellular context- to be able to induce a proliferative phenotype. US28 may exert this effect by creating a pro-inflammatory microenvironment by activation of COX2 expression leading to PGE2 production.

Furthermore, by modulating signaling through ROCK via Gα12, US28 is also able to promote smooth muscle cell migration. In cells without Gα12, US28 cannot induce migration further underlining the importance of cellular context.
In the cases described above, cellular signaling networks have been rewired to the benefit of the virus. In some cases radical alterations of cellular signaling can have unforeseen consequences and may result in or aggravate a transformed phenotype. To further understand the molecular basis behind the mechanisms described above we investigated signaling pathways induced by the HCMV-encoded GPCR US28. In this thesis two more US28-induced signaling pathways are described: STAT3 and β-catenin. Therefore a general background of these two pathways is given in the next chapter.

References

1. S. M. Foord *et al.*, International Union of Pharmacology. XLVI. G protein-coupled receptor list. *Pharmacol Rev* **57**, 279 (Jun, 2005).
2. T. Schoneberg, M. Hofreiter, A. Schulz, H. Rompler, Learning from the past: evolution of GPCR functions. *Trends Pharmacol Sci* **28**, 117 (Mar, 2007).
3. J. P. Overington, B. Al-Lazikani, A. L. Hopkins, How many drug targets are there? *Nat Rev Drug Discov* **5**, 993 (Dec, 2006).
4. D. M. Rosenbaum, S. G. Rasmussen, B. K. Kobilka, The structure and function of G-protein-coupled receptors. *Nature* **459**, 356 (May 21, 2009).
5. M. Burger *et al.*, Point Mutation Causing Constitutive Signaling of CXCR2 Leads to Transforming Activity Similar to Kaposi's Sarcoma Herpesvirus-G Protein-Coupled Receptor. *J Immunol* **163**, 2017 (August 15, 1999, 1999).
6. M. Waldhoer *et al.*, The carboxyl terminus of human cytomegalovirus-encoded 7 transmembrane receptor US28 camouflages agonism by mediating constitutive endocytosis. *J Biol Chem* **278**, 19473 (May 23, 2003).
7. S. L. Ritter, R. A. Hall, Fine-tuning of GPCR activity by receptor-interacting proteins. *Nat Rev Mol Cell Biol* **10**, 819 (2009).
8. P. H. McDonald *et al.*, Beta-arrestin 2: a receptor-regulated MAPK scaffold for the activation of JNK3. *Science* **290**, 1574 (Nov 24, 2000).
9. M. C. Michel, A. E. Alewijnse, Ligand-directed signaling: 50 ways to find a lover. *Mol Pharmacol* **72**, 1097 (Nov, 2007).
10. A. Zlotnik, O. Yoshie, H. Nomiyama, The chemokine and chemokine receptor superfamilies and their molecular evolution. *Genome Biology* **7**, 243 (2006).
11. J. A. Burger, T. J. Kipps, CXCR4: a key receptor in the crosstalk between tumor cells and their microenvironment. *Blood* **107**, 1761 (Mar 1, 2006).
12. T. Fischer, F. Nagel, S. Jacobs, R. Stumm, S. Schulz, Reassessment of CXCR4 chemokine receptor expression in human normal and neoplastic tissues using the novel rabbit monoclonal antibody UMB-2. *PLoS One* **3**, e4069 (2008).
13. Y. Chang *et al.*, Identification of herpesvirus-like DNA sequences in AIDS-associated Kaposi's sarcoma. *Science* **266**, 1865 (Dec 16, 1994).
14. K. Antman, Y. Chang, Kaposi's sarcoma. *N Engl J Med* **342**, 1027 (Apr 6, 2000).
15. E. Cesarman, Y. Chang, P. S. Moore, J. W. Said, D. M. Knowles, Kaposi's sarcoma-associated herpesvirus-like DNA sequences in AIDS-related body-cavity-based lymphomas. *N Engl J Med* **332**, 1186 (May 4, 1995).
16. N. Dupin *et al.*, Distribution of human herpesvirus-8 latently infected cells in Kaposi's sarcoma, multicentric Castleman's disease, and primary effusion lymphoma. *Proc Natl Acad Sci U S A* **96**, 4546 (Apr 13, 1999).
17. D. Martin, J. S. Gutkind, Kaposi's sarcoma virally encoded, G-protein-coupled receptor: a paradigm for paracrine transformation. *Methods Enzymol* **460**, 125 (2009).
18. X. Cai *et al.*, Kaposi's sarcoma-associated herpesvirus expresses an array of viral microRNAs in latently infected cells. *Proc Natl Acad Sci U S A* **102**, 5570 (Apr 12, 2005).
19. L. Arvanitakis, E. Geras-Raaka, A. Varma, M. C. Gershengorn, E. Cesarman, Human herpesvirus KSHV encodes a constitutively active G-protein-coupled receptor linked to cell proliferation. *Nature* **385**, 347 (Jan 23, 1997).
20. C. Bais *et al.*, G-protein-coupled receptor of Kaposi's sarcoma-associated herpesvirus is a viral oncogene and angiogenesis activator. *Nature* **391**, 86 (Jan 1, 1998).
21. T. Y. Yang *et al.*, Transgenic expression of the chemokine receptor encoded by human herpesvirus 8 induces an angioproliferative disease resembling Kaposi's sarcoma. *J Exp Med* **191**, 445 (Feb 7, 2000).
22. H. G. Guo *et al.*, Kaposi's sarcoma-like tumors in a human herpesvirus 8 ORF74 transgenic mouse. *J Virol* **77**, 2631 (Feb, 2003).
23. M. J. Smit *et al.*, Kaposi's sarcoma-associated herpesvirus-encoded G protein-coupled receptor ORF74 constitutively activates p44/p42 MAPK and Akt via G(i) and phospholipase C-dependent signaling pathways. *J Virol* **76**, 1744 (Feb, 2002).
24. S. Pati *et al.*, Activation of NF-kappaB by the human herpesvirus 8 chemokine receptor ORF74: evidence for a paracrine model of Kaposi's sarcoma pathogenesis. *J Virol* **75**, 8660 (Sep, 2001).
25. M. C. Gershengorn, E. Geras-Raaka, A. Varma, I. Clark-Lewis, Chemokines activate Kaposi's sarcoma-associated herpesvirus G protein-coupled receptor in mammalian cells in culture. *J Clin Invest* **102**, 1469 (Oct 15, 1998).

26. E. Geras-Raaka, A. Varma, H. Ho, I. Clark-Lewis, M. C. Gershengorn, Human interferon-gamma-inducible protein 10 (IP-10) inhibits constitutive signaling of Kaposi's sarcoma-associated herpesvirus G protein-coupled receptor. *J Exp Med* **188**, 405 (Jul 20, 1998).
27. E. Geras-Raaka, A. Varma, I. Clark-Lewis, M. C. Gershengorn, Kaposi's sarcoma-associated herpesvirus (KSHV) chemokine vMIP-II and human SDF-1alpha inhibit signaling by KSHV G protein-coupled receptor. *Biochem Biophys Res Commun* **253**, 725 (Dec 30, 1998).
28. F. Neipel *et al.*, Human herpesvirus 8 encodes a homolog of interleukin-6. *J Virol* **71**, 839 (Jan, 1997).
29. C. Y. Yu *et al.*, STAT3 activation is required for interleukin-6 induced transformation in tumor-promotion sensitive mouse skin epithelial cells. *Oncogene* **21**, 3949 (Jun 6, 2002).
30. H. Yu, D. Pardoll, R. Jove, STATs in cancer inflammation and immunity: a leading role for STAT3. *Nat Rev Cancer* **9**, 798 (Nov, 2009).
31. S. Rebouissou *et al.*, Frequent in-frame somatic deletions activate gp130 in inflammatory hepatocellular tumours. *Nature* **457**, 200 (Jan 8, 2009).
32. D. Iliopoulos, H. A. Hirsch, K. Struhl, An epigenetic switch involving NF-kappaB, Lin28, Let-7 MicroRNA, and IL6 links inflammation to cell transformation. *Cell* **139**, 693 (Nov 13, 2009).
33. C. J. Chiou *et al.*, Patterns of gene expression and a transactivation function exhibited by the vGCR (ORF74) chemokine receptor protein of Kaposi's sarcoma-associated herpesvirus. *J Virol* **76**, 3421 (Apr, 2002).
34. S. I. Grivennikov, F. R. Greten, M. Karin, Immunity, inflammation, and cancer. *Cell* **140**, 883 (Mar 19, 2010).
35. J. I. Cohen, Epstein-Barr virus infection. *The New England journal of medicine* **343**, 481 (Aug 17, 2000).
36. J. L. Hsu, S. L. Glaser, Epstein-barr virus-associated malignancies: epidemiologic patterns and etiologic implications. *Crit Rev Oncol Hematol* **34**, 27 (Apr, 2000).
37. J. M. Middeldorp, A. A. Brink, A. J. van den Brule, C. J. Meijer, Pathogenic roles for Epstein-Barr virus (EBV) gene products in EBV-associated proliferative disorders. *Crit Rev Oncol Hematol* **45**, 1 (Jan, 2003).
38. S. J. Paulsen, M. M. Rosenkilde, J. Eugen-Olsen, T. N. Kledal, Epstein-Barr virus-encoded BILF1 is a constitutively active G protein-coupled receptor. *Journal of virology* **79**, 536 (Jan, 2005).
39. P. S. Beisser *et al.*, The Epstein-Barr virus BILF1 gene encodes a G protein-coupled receptor that inhibits phosphorylation of RNA-dependent protein kinase. *Journal of virology* **79**, 441 (Jan, 2005).
40. M. A. Garcia *et al.*, Impact of protein kinase PKR in cell biology: from antiviral to antiproliferative action. *Microbiol Mol Biol Rev* **70**, 1032 (Dec, 2006).
41. J. Zuo *et al.*, The Epstein-Barr virus G-protein-coupled receptor contributes to immune evasion by targeting MHC class I molecules for degradation. *PLoS pathogens* **5**, e1000255 (Jan, 2009).
42. G. Milligan, G-protein-coupled receptor heterodimers: pharmacology, function and relevance to drug discovery. *Drug Discov Today* **11**, 541 (Jun, 2006).
43. H. F. Vischer, S. Nijmeijer, M. J. Smit, R. Leurs, Viral hijacking of human receptors through heterodimerization. *Biochemical and biophysical research communications* **377**, 93 (Dec 5, 2008).
44. J. Y. Springael, E. Urizar, S. Costagliola, G. Vassart, M. Parmentier, Allosteric properties of G protein-coupled receptor oligomers. *Pharmacology & therapeutics* **115**, 410 (Sep, 2007).
45. Y. Han, I. S. Moreira, E. Urizar, H. Weinstein, J. A. Javitch, Allosteric communication between protomers of dopamine class A GPCR dimers modulates activation. *Nat Chem Biol* **5**, 688 (Sep, 2009).
46. R. Lyngaa *et al.*, Cell transformation mediated by the Epstein-Barr virus G protein-coupled receptor BILF1 is dependent on constitutive signaling. *Oncogene* **29**, 4388 (2010).
47. M. K. Gandhi, R. Khanna, Human cytomegalovirus: clinical aspects, immune regulation, and emerging treatments. *Lancet Infect Dis* **4**, 725 (Dec, 2004).
48. C. Soderberg-Naucler, Does cytomegalovirus play a causative role in the development of various inflammatory diseases and cancer? *J Intern Med* **259**, 219 (Mar, 2006).
49. C. A. Alford, S. Stagno, R. F. Pass, W. J. Britt, Congenital and perinatal cytomegalovirus infections. *Rev Infect Dis* **12 Suppl 7**, S745 (Sep-Oct, 1990).
50. J. Verbeeck *et al.*, Detection of perinatal cytomegalovirus infection and sensorineural hearing loss in belgian infants by measurement of automated auditory brainstem response. *J Clin Microbiol* **46**, 3564 (Nov, 2008).
51. J. L. Melnick, C. Hu, J. Burek, E. Adam, M. E. DeBakey, Cytomegalovirus DNA in arterial walls of patients with atherosclerosis. *J Med Virol* **42**, 170 (Feb, 1994).
52. C. S. Cobbs *et al.*, Human cytomegalovirus infection and expression in human malignant glioma. *Cancer Res* **62**, 3347 (Jun, 2002).
53. L. Harkins *et al.*, Specific localisation of human cytomegalovirus nucleic acids and proteins in human colorectal cancer. *Lancet* **360**, 1557 (Nov 16, 2002).
54. J. Cinatl, Jr., J. U. Vogel, R. Kotchetkov, H. Wilhelm Doerr, Oncomodulatory signals by regulatory proteins

encoded by human cytomegalovirus: a novel role for viral infection in tumor progression. *FEMS Microbiol Rev* **28**, 59 (Feb, 2004).

55. F. Grey, J. Nelson, Identification and function of human cytomegalovirus microRNAs. *J Clin Virol* **41**, 186 (Mar, 2008).
56. M. S. Chee, S. C. Satchwell, E. Preddie, K. M. Weston, B. G. Barrell, Human cytomegalovirus encodes three G protein-coupled receptor homologues. *Nature* **344**, 774 (Apr 19, 1990).
57. U. A. Gompels, H. A. Macaulay, Characterization of human telomeric repeat sequences from human herpesvirus 6 and relationship to replication. *J Gen Virol* **76 (Pt 2)**, 451 (Feb, 1995).
58. M. E. Penfold *et al.*, Cytomegalovirus encodes a potent alpha chemokine. *Proc Natl Acad Sci U S A* **96**, 9839 (Aug 17, 1999).
59. J. R. Randolph-Habecker *et al.*, The expression of the cytomegalovirus chemokine receptor homolog US28 sequesters biologically active CC chemokines and alters IL-8 production. *Cytokine* **19**, 37 (Jul 7, 2002).
60. P. Casarosa *et al.*, Constitutive signaling of the human cytomegalovirus-encoded chemokine receptor US28. *J Biol Chem* **276**, 1133 (Jan 12, 2001).
61. K. A. McLean, P. J. Holst, L. Martini, T. W. Schwartz, M. M. Rosenkilde, Similar activation of signal transduction pathways by the herpesvirus-encoded chemokine receptors US28 and ORF74. *Virology* **325**, 241 (Aug 1, 2004).
62. D. Q. Wen *et al.*, Human cytomegalovirus-encoded chemokine receptor homolog US28 stimulates the major immediate early gene promoter/enhancer via the induction of CREB. *J Recept Signal Transduct Res* **29**, 266 (2009).
63. R. M. Melnychuk *et al.*, Human cytomegalovirus-encoded G protein-coupled receptor US28 mediates smooth muscle cell migration through Galpha12. *J Virol* **78**, 8382 (Aug, 2004).
64. D. Maussang *et al.*, Human cytomegalovirus-encoded chemokine receptor US28 promotes tumorigenesis. *Proc Natl Acad Sci U S A* **103**, 13068 (Aug 29, 2006).
65. D. Maussang *et al.*, The human cytomegalovirus-encoded chemokine receptor US28 promotes angiogenesis and tumor formation via cyclooxygenase-2. *Cancer Res* **69**, 2861 (Apr 1, 2009).
66. O. Pleskoff *et al.*, The human cytomegalovirus-encoded chemokine receptor US28 induces caspase-dependent apoptosis. *Febs J* **272**, 4163 (Aug, 2005).
67. P. Casarosa *et al.*, Constitutive signaling of the human cytomegalovirus-encoded receptor UL33 differs from that of its rat cytomegalovirus homolog R33 by promiscuous activation of G proteins of the Gq, Gi, and Gs classes. *J Biol Chem* **278**, 50010 (Dec 12, 2003).
68. R. Case *et al.*, Functional analysis of the murine cytomegalovirus chemokine receptor homologue M33: ablation of constitutive signaling is associated with an attenuated phenotype in vivo. *J Virol* **82**, 1884 (Feb, 2008).
69. B. J. Margulies, H. Browne, W. Gibson, Identification of the human cytomegalovirus G protein-coupled receptor homologue encoded by UL33 in infected cells and enveloped virus particles. *Virology* **225**, 111 (Nov 1, 1996).
70. M. E. Penfold, T. L. Schmidt, D. J. Dairaghi, P. A. Barry, T. J. Schall, Characterization of the rhesus cytomegalovirus US28 locus. *J Virol* **77**, 10404 (Oct, 2003).
71. A. Fraile-Ramos *et al.*, Localization of HCMV UL33 and US27 in endocytic compartments and viral membranes. *Traffic* **3**, 218 (Mar, 2002).
72. T. N. Kledal, M. M. Rosenkilde, T. W. Schwartz, Selective recognition of the membrane-bound CX3C chemokine, fractalkine, by the human cytomegalovirus-encoded broad-spectrum receptor US28. *FEBS Lett* **441**, 209 (1998).
73. J. Vieira, T. J. Schall, L. Corey, A. P. Geballe, Functional analysis of the human cytomegalovirus US28 gene by insertion mutagenesis with the green fluorescent protein gene. *J Virol* **72**, 8158 (Oct, 1998).
74. S. A. Oliveira, T. E. Shenk, Murine cytomegalovirus M78 protein, a G protein-coupled receptor homologue, is a constituent of the virion and facilitates accumulation of immediate-early viral mRNA. *Proc Natl Acad Sci U S A* **98**, 3237 (Mar 13, 2001).
75. P. S. Beisser, G. Grauls, C. A. Bruggeman, C. Vink, Deletion of the R78 G protein-coupled receptor gene from rat cytomegalovirus results in an attenuated, syncytium-inducing mutant strain. *J Virol* **73**, 7218 (Sep, 1999).
76. P. Tschische, K. Tadagaki, M. Kamal, R. Jockers, M. Waldhoer, Heteromerization of human cytomegalovirus encoded chemokine receptors. *Biochem Pharmacol* **82**, 610 (Sep 15, 2011).
77. B. Bodaghi *et al.*, Chemokine sequestration by viral chemoreceptors as a novel viral escape strategy: withdrawal of chemokines from the environment of cytomegalovirus-infected cells. *J Exp Med* **188**, 855 (Sep 7, 1998).

2

Oncogenic signaling pathways

2.1 Oncogenic signaling pathways

The development of cancer is dependent on the aberrant regulation of cell cycle regulation and apoptosis (1). Understanding the signaling pathways that govern growth, anti-growth and apoptosis is therefore paramount for understanding cancer development. In the case of this thesis we restricted ourselves to two different signaling pathways, JAK/STAT and β-catenin signaling. These two pathways came to our attention as a result of an angiogenesis array and a micro-array analysis, respectively. Therefore, an introduction and more details about both pathways is given below. Additionally, VEGF signaling and regulation will be discussed.

2.2 The JAK/STAT axis

2.2.1 The JAK and STAT family proteins

The signal transducers and activators of transcription (STAT) are important mediators of growth factor and cytokine-directed signaling. There are 7 members of STAT family known to date, STAT1, STAT2, STAT3, STAT5A, STAT5B, and STAT6 (2). The different STATs, their ligands and some of their target genes are shown in Table 1. The receptors generally responsible for STAT activation are composed of multiple subunits. They consist of receptor subunits that actually bind to the ligand (eg. IL-6) and the gp130 subunit that interacts with Janus kinases (JAK). Ligand binding results in receptor dimerization which results in activation of JAK which, in turn results in phosphorylation and dimerization of STAT (Figure 1). The resulting STAT-dimer subsequently translocates to the nucleus where it engages its respective target genes. The receptor complex consist of, as mentioned above, multiple subunits which can form different functional receptors. For example, the IL-6 receptor complex is composed of the IL-6-Receptor (IL-6R) and two gp130 subunits. The other receptors belonging to this family form a similar complex. They always contain the gp130 in combination with different ligand-recognizing subunits (3). However, activation of JAK/STAT is not limited to the cytokine receptors, as GPCRs can also directly acti-

Table 1. STAT protein family members with examples of their respective ligands and target genes.

STAT family member	Ligands	Target genes	References
STAT1	IFNα,β, and γ	Inflammatory and pro-apoptotic factors (eg. IL-12, caspases)	(*1*)
STAT2	IFNα and β	Inflammatory and pro-apoptotic factors (eg. CD80)	(*1*)
STAT3	IL-5, IL-6, IL-10, IFNγ and LIF	Anti-apoptotic, proliferation inducing, angiogenic, and inflammatory. (eg. VEGF, Cyclin D1, IL-6)	(*2-6*)
STAT4	IL-12 and IL-23	IFNγ	(*1*)
STAT5A/STAT5B	IL-2, IL-7, IL-15, GM-CSF, IL-3, IL-5, and growth hormones	Anti-apoptotic, proliferation inducing. (eg. Cyclin D2, BCL-XL)	(*7*)
STAT6	IL-4 and IL-13	Anti-apoptotic (eg. BCL-2)	(*1*)

vate the JAK/STAT axis. The chemokine receptor CXCR4 was shown to do just this. Upon stimulation with CXCL12, CXCR4 associates with JAKs within minutes, which then results in phosphorylation of STAT1, 2, and 3 (4). The JAK family encompasses four members; JAK1, JAK2, JAK3, and Tyk2. These proteins have a molecular mass between 120 and 140 kD.

JAK1

JAK1 first was identified in a PCR-based screening for novel kinases (5), and was shown to associate with IL-2 and IL-6 receptors. Other cytokine-mediated responses for which JAK1 is critical are those triggered by interferon, IL-4, and IL-10. When a receptor is activated, the JAKs are recruited to the receptor and phosphorylate each other, a process that is also known as transphosphorylation. Of note, this can occur between two different JAKs (eg. JAK1 and JAK3). This was shown by Witthuhn et al. using the IL-2 receptor. They observed that using kinase-dead JAK1 and a wild-type JAK3 resulted in phosphorylation of JAK1 but not JAK3. However wild-type JAK1 was not capable of phosphorylating kinase-dead JAK3 (6). This suggests that the transphosphorylation between different JAK-pairs may be time-dependent, requiring one of the JAKs to be phosphorylated first (2).

JAK2

The second member of the JAK family is JAK2, which mediates response to IL-3, erythropoietin (Epo), and GMCSF among others. Being involved with erythropoietin and GMCSF suggest an important role in hematopoiesis. This was confirmed

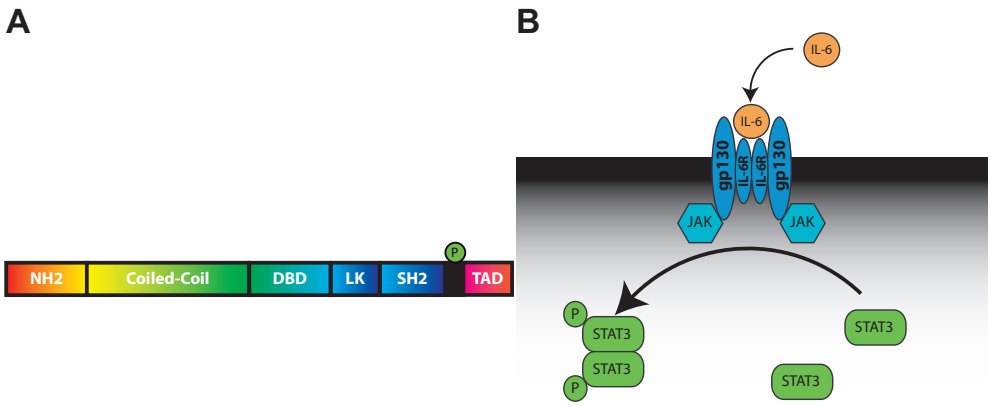

Figure 1. General structure of cytokine receptors and STAT-family proteins. (**A**) Shown are 7 conserved domains present in all proteins of the STAT-family: the amino-terminal (NH2), coiled-coil, DNA-binding domain (DBD), linker (LK), SH2, tyrosine phosphorylation site (in black with the phospho-group depicted in green), and the transcriptional activation domain (TAD). (**B**) Model showing the basic layout of a cytokine receptor, using the IL-6 receptor as an example. The IL-6R subunit is the actual IL-6 sensing unit, while the gp130 subunits bind to JAK. Upon ligand binding the receptor complex recruits STAT3 which then becomes phosphorylated and dimerizes. Subsequently the STAT3-dimers translocate to the nucleus where they activate their target genes.

with the generation of JAK2 knockout mice that die of anemia during embryogenesis. In the case of erythropoietin, the erythropoietin receptor (EpoR) recruits two JAK2 proteins upon activation which subsequently transphosphorylate each other. This was demonstrated using EpoR-dihydrofolate reductase (DHFR) chimeras that resulted in a receptor that only had DHFR functionality when the two parts of the enzyme were in close proximity. Using fluorescently labeled methotraxate, which binds to DHFR, the conformational change of the EpoR upon binding Epo resulted in fluorescence (7).

JAK3

The third member, JAK3, is an important mediator of IL-2 signaling. The IL-2-receptor is composed of 3 chains, a, b, and g. JAK3 interacts exclusively with the g-chain. The g-chain is also a key component of other receptors, such as IL-4, IL-7, IL-9, IL-15, and IL-21 (2). In contrast to JAK1 and JAK2, where knockout mice die during embryogenesis, JAK3 knockout mice are viable. However, these mice display immune deficiencies. Interestingly, human mutations in JAK3 have been described, and these cases show severe combined immune deficiency (SCID). Individuals with mutated JAK3 completely lack T-cells and NK-cells leaving them effectively without a functioning immune system (8).

Tyk2

The fourth and last member of the JAK kinases is Tyk2. This kinase interacts with receptors responding to interferon (IFN) type I cytokines, as well as cytokines from the IL-6, IL-10, IL-12, and IL-23 families (2). Unlike the other JAKs, Tyk2 knockout mice do not show a pronounced phenotype, other than a slight defect in interferon-α and β response (9). Humans exhibiting mutations in Tyk2 show a somewhat more severe phenotype with increased susceptibility to viral, bacterial, and fungal infections (10).

The STAT proteins have a size of about 80 kD, and contain seven conserved domains shown in Figure 5A. An example of cytokine receptor composition (in this case the IL-6 receptor with STAT3) is shown in Figure 5B. The SH2 domain of these proteins is of special interest, as this domain is critical for the formation of dimers. Upon phosphorylation the SH2 domain binds to the phosphorylated tyrosine of another STAT molecule, resulting in the formation of an anti-parallel dimer (2, 11). Activated STAT dimers typically bind to GAS sites (TTTCCNGGAAA), STAT1-STAT2 heterodimers are an exception and bind to ISRE (AGTTTN3TTTCC) sites instead.

STAT1

The first STAT protein to be identified, and was first discovered as an ISRE binding factor. STAT1 is mainly involved in IFN signaling, being activated by IFNα, β, γ, λ, and ω. Two splice variants of STAT1 exist, a full length STAT1α of 91 kD, and a truncated isoform STAT1β having a molecular mass of 84 kD (12). Tyrosine phosphorylation of

Y701 is essential for dimerization.
STAT1 is an important factor in the immune system, having a key role in the defense against bacterial and viral infection. STAT1 is generally thought of as an anti-proliferative and pro-apoptotic factor, as evidenced by the inhibition of cell growth (13) and induction of caspase expression (14). Moreover, induction of apoptosis by IL-21 is dependent on STAT1, involving STAT1 target genes such as BIK, NIP3, and HARAKIRI (15). Also, STAT1 potentiates p53 activity, either by inhibiting Mdm2 expression (16) or by promoting p53 activation (17). This, and data from experiments showing increased tumor incidence in STAT1 knock-out mice, as well as the observation that STAT1 expression is diminished in several cancers (18, 19), cause STAT1 to be regarded as a tumor suppressor.
Interestingly, STAT1 was shown to be activated by the EBV protein LMP1 in Burkitt's lymphoma. This STAT1-activation is indirect, driven by constitutive NF-κB activation by LMP1 resulting in the induction of IFNs that subsequently activate STAT1 (20, 21). However, it is not entirely clear how STAT1 is exactly involved in EBV-associated cancers.

STAT2

The largest STAT protein, with a size of 113 kD, it is also the most mysterious one. While STAT2 has been shown to be essential for IFNα and β signaling, the existence of STAT2 homo-dimers remains to be demonstrated (2). Thus far, STAT2 has only been shown to possess transcriptional activity when forming a hetero-dimer with STAT1 (2). Consequently, it shares quite a lot of the signaling characteristics (e.g. target genes, receptors) with STAT1. However, in contrast with STAT1 and the other STAT proteins, except for STAT6, STAT2 does not possess a serine phosphorylation site (22).
Despite the large overlap with STAT1-associated signaling, STAT2 appears to have a specific signaling role, as was shown by analysis of STAT2 genetic polymorphisms in humans which indicate that STAT2 may play a role in the development of asthma (23). Furthermore, the HCMV protein immediate early gene 1 (pUL123) inhibits STAT2-mediated IFN signaling (24), further indicating a key role for STAT2 in IFN signaling.

STAT3

Originally, STAT3 was identified as the down-stream effector of IL-6 (25). However, since its first identification STAT3 has been recognized to mediate signaling for a wide variety of ligands. Among the activating ligands are the IL-6 and IL-10 cytokine families, as well as IFNγ (26, 27). Dimerization is controlled by phosphorylation of Y705. It also features a serine phosphorylation at S727 (22). Like STAT1, STAT3 is differentially phosphorylated depending on the upstream receptor, thyroid stimulating hormone (TSH), for example, induces both Y705 and S727 phosphorylation, while IFNγ results in Y705 phosphorylation but not in S727 phosphorylation (28). In the case of TSH, the S727 phosphorylation is associated with STAT3 inactivation. Serine

phosphorylation of STAT3 is not as well defined as it is for STAT1. Nevertheless, studies have shown that stimulating the TrkA receptor with nerve growth factor (NGF) induces STAT3 phosphorylation at S727 but not at Y705. Interestingly, despite being only phosphorylated at S727, STAT3 still displays DNA binding (29). Moreover, constitutively active mutant TrkA, which acts as an oncogene, still induces STAT3 phosphorylation at S727. In both cases, serine phosphorylation of STAT3 is mediated by p44/p42 as was demonstrated by treating cells with the MEK1/2 inhibitor U0126, which inhibited STAT3 phosphorylation at S727 (29, 30). Serine phosphorylation of STAT3 does not appear to be only function as a transcriptional activator, it also serves to target STAT3 to a role in the cell's metabolism. Reconstitution experiments in murine STAT3-/- pro-B cells showed that STAT3 is required for full mitochondrial activity. Moreover, the S727 phosphorylation was shown to be critical for this function, while the Y705 phosphorylation was not required. Co-immunoprecipitation experiments indicated that STAT3 is present inside the mitochondria existing in both mitochondrial protein complex I and II (31).
Mutants of STAT3 that display constitutive activity have been found in solid tumors and lymphomas (32, 33). As mentioned above, target genes of STAT3 include genes that promote proliferation, such as the Cyclin D1 gene. Another important feature that highlights STAT3's importance in cancer development is its control over VEGF expression. In multiple cases, STAT3 directly drives VEGF expression (34). For example, STAT3 activation promotes brain metastasis of melanoma, which is accompanied by STAT3 driven VEGF expression (35).
Interestingly, expression of IL-6 is induced by STAT3 activation (36), which allows for a positive feedback loop, which is an interesting possibility considering the possibility of induction of IL-6 production by viruses like HMCV (37) or KSHV (38) with the latter even producing a viral variant of IL-6 (39). STAT3's propensity towards proliferation and survival can be explained by the role that inflammation is thought to have in cancer development. Moreover, mitochondrial STAT3 has an important function in regulating cellular respiration (31), and has been shown to support Ras dependent transformation (40). As mentioned earlier, an inflammatory environment may provide an environment that promotes transformation and survival of transformed cells. For example, liver cancer often arises from chronic hepatitis (41), and stomach cancer is strongly associated with chronic gastritis (42).

STAT4

Originally STAT4 was discovered via its homology with STAT1. STAT4 is a 86 kD protein, which plays a critical role in IL-12 and IL-23 signaling. IL-12 signaling through STAT4 is key for differentiation of lymphocytes into Th1 cells (2). Furthermore, STAT4 also mediates activation of NK cells by IL-12. An important STAT4 target gene is IFNγ. Like STAT1 and STAT3, STAT4 is also phosphorylated both on tyrosine (Y694) and serine (S722) residues. Phosphorylation of S722 is required for STAT4-induced IFNγ production, and is mediated by p38 (43). Because of the role of IL-12 and IL-23 in immune-modulation STAT4 is mainly associated with auto-immune diseases and al-

lergies (44, 45), although there may also be a role for STAT4 in tumor development as IL-23 is over-expressed in various human cancers (46).

STAT5a and STAT5b

These two STATs are actually tandem genes that both show high homology to Drosphila STAT (dSTAT). Together with STAT3, STAT5a and 5b are the closest homologues to this primordial STAT. The different mammalian STATs are thought to have evolved from a single STAT by gene duplication, of which STAT5a and 5b are the most recent examples (47). Consequently, both STAT5 isoforms mediate signaling for a variety of ligands and as such display a diverse functionality ranging from lymphoid development (48) and hematopoeisis (49) to lactogenesis (50) and growth (51).

Like most of the other STAT proteins, both STAT5a and STAT5b undergo serine phosphorylation (S726 and S731, respectively) separately from tyrosine phosphorylation (Y694 and Y699, respectively). While STAT5a and STAT5b show high sequence similarity and are largely functionally redundant, they possess different signaling capabilities. For example, STAT5a mediates prolactin signaling, while STAT5b is responsible for transducing signaling upon stimulation with growth hormone (2, 50). Consistent with these signaling differences, STAT5 serine phosphorylation also differs for the two isoforms. STAT5a phosphorylation at S726, is controlling STAT5a activity upon stimulation with prolactin (52). On the other hand, S731 phosphorylation of STAT5b is associated with EGF signaling (53).

Both 5a and the 5b isoforms are associated with several cancers, which is consistent with their role in development and proliferation. Breast cancer cells require STAT5a for anchorage-independent growth and survival, while suppressing cell motility as was shown by overexpression of constitutive active STAT5a and knockdown experiment using siRNA. In contrast, nor overexpression of constitutive active STAT5b or downregulating expression with siRNA, showed any significant change in survival and proliferation or motility (54). While STAT5b may not play an important role in breast cancer, there are indications that it has a role in supporting renewal of leukemia stem cells (55). Also, both isoforms have been shown to be required for survival and growth of prostate cancer cells, although STAT5b appeared to be more important in this case of survival as was demonstrated with siRNA experiments (56).

STAT6

The final member of the STAT-proteins, STAT6, is a 94 kD protein transducing signals for IL-4 and IL-13. It is involved in T-cell differentiation as well as regulating B-cell proliferation and maturation. IL-4 and IL-13 are related proteins, and this is reflected by sharing of receptor components (57). According to the role that IL-13 plays in the defense against parasites, mice that are deficient for STAT6 are rendered more susceptible to infection of the parasite Mesocestoides corti. Furthermore, IL-13 is also reported to have an inhibitory effect on cancer surveillance. The latter was shown using a recurrent-tumor model in transgenic mice that were deficient in either STAT6, IL-4, IL-13 or IL-4Rα. In this model the mice that did not express STAT6,

IL-13 or the IL-4Rα were more resistant against tumor recurrence, while the IL-4 knockout mice did not gain any resistance against tumor formation (58).
Interestingly, both EBV and KSHV influence STAT6 signaling. In the case of EBV STAT6 signaling is hijacked to drive LMP-1 expression. Either IL-4 or IL-13 are capable of inducing LMP-1 expression, even in the absence of EBNA-2 which is normally required for LMP-1 expression (59). The KSHV encoded protein LANA inhibits STAT6 transcriptional activity by preventing IL-4-induced STAT6 phosphorylation at Y641, effectively blocking B-cell activation (60).

2.2.1 Regulation of STAT mediated signaling

Normally, signaling by STAT-proteins, characterized by both a rapid onset and decay, is a transient event. As described earlier, STATs translocate to the nucleus upon activation, which already starts within minutes after stimulating the cell with a ligand. However, within a few hours after stimulation the STAT proteins will have been expelled from the nucleus. Negative regulation of signaling through the JAK/STAT axis can be subdivided into three main categories.

Phosphatases

Phosphorylation of STATs is essential for dimerization and signaling, and consequently phosphatases are an important mechanism of downregulation. STAT dephosphorylation is governed by multiple phosphatases, among which are SHP-2 and TC-PTP (61).

Regulation by nuclear import/export

STAT dimers are quite large, consisting of 2 ~80 kD subunits, while nuclear accumulation is rapid. Considering that only ions and proteins smaller than 40 kD can enter nucleus freely (62), it follows that this is an active process and is therefore subject to regulation. The transcriptional activity of the STAT proteins is controlled by subcellular localization and until the cell is stimulated with a ligand, the balance is towards nuclear export. However, when the cells are stimulated by a ligand, the balance rapidly shifts towards nuclear import and then as the signal decays, again towards nuclear export. To this end the STATs contain multiple nuclear export sequences (NES), as well as nuclear localization sequences (NLS). This also means that the total amount of STATs does not really change in the cell upon activation, but rather their subcellular localization.

The SOCS protein family

The family of Suppressor Of Cytokine Signaling (SOCS) proteins are essential components of immune regulation, as excessive or untimely activation of inflammatory pathways can result in auto-immunity, chronic inflammation or even septic shock. An example of the latter is the strong induction of cytokines by lipopolysaccharide (LPS), from Gram-negative bacteria (63). The SOCS proteins are defined by the presence of a conserved SOCS box domain in the C-terminus. The SOCS box functions as

a binding site for E3 ligase which targets for ubiquitin-induced degradation. Another conserved domain, is the SH2 binding domain. The SH2 binding domain recognizes tyrosine phosphorylation within specific motifs (64). For example, SOCS1 recognizes activated JAKs and down-regulates signaling by the JAK/STAT axis (65). Other SOCS-proteins that can down-regulate JAK/STAT signaling are SOCS3 (66), SOCS4, and SOCS5 (67).

The mechanisms described above are responsible for the correct signaling, and considering the potential for an out of control positive feedback loop (eg. IL-6 and STAT3) the need for tight regulation is clear.
While STAT3 activation normally is tightly controlled via the mechanisms described above, in a transformed cellular background parts of this control can be lost. For example, epigenetic silencing of SOCS3 has been correlated to prostate cancer aggressiveness (68). Furthermore, overexpression of SOCS3 in human non-small cell lung cancer cells resulted in growth inhibition and increased sensitivity to radiation (68). Cells with an impairment of SOCS3 functionality may more likely evoke a detrimental IL-6 positive feedback-loop that was mentioned before.

In the context of oncomodulatory viruses conditional activation of positive feedback loops may have interesting implications. A virally infected cell itself does not need to be transformed, as viral proteins can elicit secretion of factors that can affect cells in a paracrine fashion. In such a case only a small fraction of a tumor needs to express the protein in question as is seen in KSHV (69) and for US28 (70).
It is clear that the STAT proteins have a pivotal role in controlling cell survival, proliferation, and apoptosis. Therefore, it is not surprising that many of the STAT proteins are involved in cancer development be it as an oncogen or in the role of a tumor suppressor. In this light, subversion of STAT signaling by some of the viruses discussed earlier has the potential of instigating an oncomodulatory effect, especially considering the possibility of paracrine signaling and the initiation of positive feedback loops.

2.4 Wnt/β-catenin signaling

Another pathway that is activated by US28 is the Wnt/β-catenin pathway.
The Wnt signaling pathway is an evolutionary conserved pathway that is present in virtually all multicellular creatures. Even the most simple multicellular organisms, the placozoans, possess a functional Wnt signaling pathway (71). As such, Wnt signaling is a key component in the development of many organisms, and was also first discovered as an important factor in Drosphila melanogaster development. Consistent with the complex nature of Wnt signaling, there are many Wnt ligands. Moreover, signal transduction triggered by Wnt is accomplished via complex signaling routes. Wnt ligands typically initiate signaling by binding to Frizzled receptors, which are GPCRs, as shown in Figure 2, although other receptors also have been de-

scribed. The canonical Wnt/Frizzled pathway utilizes the transcription factor β-catenin, which is normally degraded by the destruction complex (72). Subsequently, free β-catenin activates genes regulated by Tcf/Lef, such as Cyclin D1 (73) and VEGF (74). Following their key role in development, which requires precise control of cell proliferation, survival, and apoptosis, aberrant Wnt signaling has been associated with cancer development in humans, in particular colon cancer (75-77).

The Wnt ligands

To date, 19 different Wnt proteins have been identified. Considering that they are secreted, these glycoproteins have a relative large size, with a molecular mass of around 40 kD. The different human Wnt ligands are listed in Table 2, with their char-

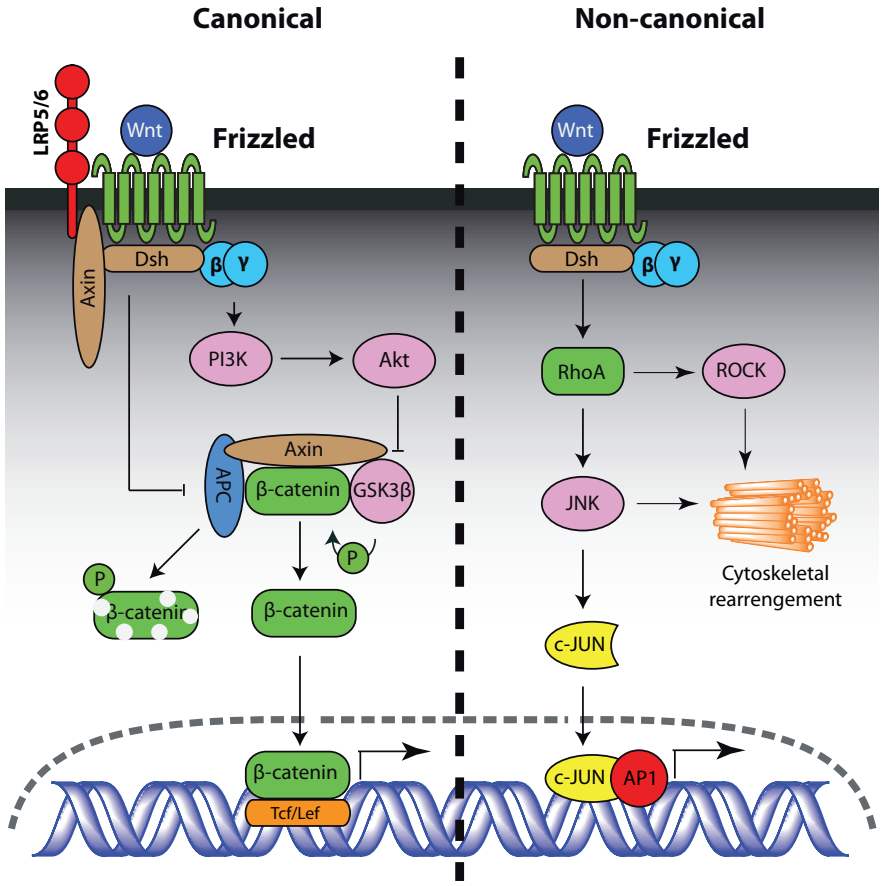

Figure 2. Model showing canonical Wnt signaling. Upon activation by a Wnt ligand Frizzled and LRP5/6 destabilize the destruction complex that is composed of Axin, APC and GSK3β that normally targets the transcription factor β-catenin for proteosomal destruction. The destruction complex is inhibited by recruitment of Axin by the activated receptor complex, as well as inhibition of GSK3β activity via G-protein mediated activation of Akt. The free non-phosphorylated β-catenin can then translocate to the nucleus and together with Tcf/Lef activate its target genes. An example of non-canonical signaling is signaling via RhoA which then activates the kinases ROCK and JNK. Both ROCK and JNK can subsequently induce cytoskeletal rearrangements, and JNK also activates the transcription factor c-JUN which, together with AP1, can activate target genes.

acteristics and, if known, associated diseases. The first mammalian Wnt ligand to be purified, because of its relatively efficient expression, was the murine homolog of Wnt3a (101). Analysis revealed that Wnt3a is post-translationally N-glycosylated. In addition these proteins also undergo lipidations, like palmitoylations and acylations, which are thought to attribute to the general poor solubility displayed by Wnt proteins (93). Mutations to these residues result in impaired secretion and retention in the endoplasmic reticulum (S209 acylation) or reduced signaling capability (C77) (102). These observations, coupled with studies performed on the D. melanogaster Wnt homolog wingless (Wg) instigated the hypothesis that Wnt proteins may be secreted linked to lipoprotein particles. Studies on Wg and its homolog in the nematode Caenorhabditis elegans, EGL-20, have resulted in a detailed understanding of Wnt biogenesis and secretion, displayed in Figure 3. The membrane protein Porcupine, which may possess acyltransferase activity, has been proposed to perform some of the acylations on Wnt (102, 103).
Experiments performed on C. elegans identified a protein complex called the retromer complex as an important mediator for Wnt signaling in Wnt producing cells. Using RNAi screening, a homolog of the yeast retromer subunit Vps35p was shown

Table 2. The different Wnt ligands with their putative glycosylation sites and their respective associated diseases

Wnt ligand	Size (aa)	Glycosylation sites	Associated disease	References
Wnt1	370	N29, N316, N346, N359	Breast cancer	(*79-81*)
Wnt2	360	N295	Malignant glioma	(*82-85*)
Wnt2b	391	N117, N283	Leukemia	(*86*)
Wnt3	355	N90, N301	Tetra-amelia	(*87*)
Wnt3a	352	N87, N298	Melanoma	(*88*)
Wnt4	351	N88, N297	SERKAL syndrome and Müllerian-duct regression	(*89, 90*)
Wnt5a	380	N114, N120, N312, N326	Pancreatic cancer	(*91, 92*)
Wnt5b	359	N93, N99, N291, N305	Type 2 diabetes	(*93*)
Wnt6	365	N86, N311	N/A	
Wnt7a	349	N83, N127, N295	Fuhrmann syndrome	(*94*)
Wnt7b	349	N83, N127, N295	N/A	
Wnt8a	351	N103, N262, N281	N/A	
Wnt8b	351	N103, N259	Gastric cancer	(*95*)
Wnt9a	365	N103	N/A	
Wnt9b	357	N99	N/A	
Wnt10a	417	N106, N363	Odonto-onycho-dermal dysplasia	(*96, 97*)
Wnt10b	389	N93, N335	Obesity, Split-hand/foot malformation	(*98, 99*)
Wnt11	354	N40, N90, N160, N300, N304	Hepatocellular carcinoma	(*100*)
Wnt16	365	N143, N189, N311	Leukemia	(*101*)

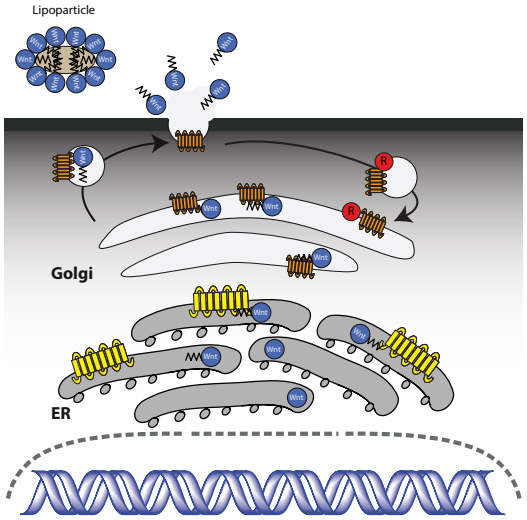

Figure 3. Schematic representation detailing the currently proposed model for Wnt ligand biogenesis and secretion. Newly synthesized Wnt post-translationally modified in the endoplasmatic reticulum (ER), which among others, entails acylation by Porcupine. Subsequently, the acylated Wnt is recognized by Wntless. Wntless targets vesicles containing Wnt to the plasma membrane, where Wnt is secreted into the extra-cellular milieu. The Wnt ligand then presumably clusters together into lipoparticles. The retromer complex is responsible for recruiting Wntless from endosomes.

to be essential for EGL-20 mediated patterning in C. elegans development. Furthermore, C. elegans EGL-20 null mutants display a similar phenotype as Vps35 deficient mutants, indicating a similar role in signaling. Further experiments showed that both in C. elegans as well as in mammalian cells Vps35 homologs are critical for Wnt ligand secretion (104). The retromer complex is composed of five subunits and is a mediator of protein trafficking between the endosomal compartment and the Golgi apparatus. Another protein that was determined to be indispensable for Wnt secretion is Wntless (Wls), Wls is a transmembrane protein that is localized to the Golgi and the plasma membrane and it can bind to the acylated residues of Wnt ligands, targeting it to the plasma membrane for secretion. Furthermore, the retromer complex has a key role in recruiting Wls from endosomes to the Golgi (105). However, while this proposed model is elegant, it must be noted that all this data has been gathered for Wnt3a and its homologs. Caution is necessary for extrapolating these characteristics onto the other Wnt ligands, considering that they differ in the extent in amount of lipidation. Moreover, there is at least one Wnt ligand that does neither require Porcupine nor Wls for secretion (106).

As is shown in Table 2, the Wnt ligands mostly have a critical role in development and mutations in the ligands are usually associated with severe birth defects, like Tetra-amelia or Fuhrmann syndrome (86, 93). Up- or down-regulation of several of these ligands is associated with multiple cancers.

Although there is clearly a specific role for each Wnt ligand, exactly which pathway is engaged by a Wnt ligand is not completely clear. Based on biological assays a subdivision between canonical (ligands that primarily engage the canonical signal pathway) and non-canonical (ligands that primarily signal via non-canonical pathways) ligands was made. In this subdivision Wnt1, Wnt3a, and both Wnt8s are considered canonical ligands, while Wnt5a and Wnt11 are thought of mainly activating non-canonical pathways. However, this classification of Wnt ligands is somewhat artificial as Wnt signaling is dependent on the cellular context. For example, Wnt5a activates

Table 3. The Frizzled receptor family, with their respective ligands and mutant phenotype

Receptor name	Size (aa)	Wnt ligand	Mutant phenotype	References
Frizzled-1	647	Wnt1, 2, 3a, 5a, 7b	N/A	(*110, 111*)
Frizzled-2	565	Wnt5a	N/A	(*112*)
Frizzled-3	666	Wnt3a	N/A	(*113*)
Frizzled-4	537	Wnt1, 2, 3a	Criswick-Schepens syndrome	(*114-116*)
Frizzled-5	585	Wnt5a	N/A	(*108*)
Frizzled-6	706	Wnt4	N/A	(*117*)
Frizzled-7	574	Wnt3	Loss of embryonic stem cell self-renewal	(*118, 119*)
Frizzled-8	694	Wnt3a, 5a, 5b, 9b	N/A	(*120*)
Frizzled-9	591	Wnt2	N/A	(*121*)
Frizzled-10	581	Wnt1, 8	N/A	(*122*)
Smoothened	787	No known Wnt ligand. Binds Hedgehog instead	N/A	(*123*)

canonical β-catenin signaling when the receptor Frizzled-5 is present (107). Moreover, Wnt5a and Wnt11 have been shown to form dimers that can induce β-catenin activation (108). These findings show that the Wnt ligands cannot be easily qualified as canonical or non-canonical.

The Frizzled receptors

The cognate receptors for the Wnt ligands are 7 trans-membrane receptors, that share a similar structure with the GPCRs, which together form the family of Frizzled receptors. The Frizzled receptor family contains 11 members which are listed in Table 3. Because the Wnt ligands are poorly soluble, and dependence on cellular context, the pharmacology of most of the receptors and their ligands are ill defined. In some cases the cell-type on which the receptor is present determines whether a Wnt ligand acts as an agonist or antagonist. Although this fits with the complex role these receptors play in development and embryogenesis, it also indicates that these receptors and their ligands have a complex interplay with each other. GPCR signaling in general can be complicated by their ability to form dimers. Frizzled receptors are no exception and to this and has been at least one report of a Frizzled receptor forming dimers (123).

Although the Frizzled receptors share the 7 trans-membrane architecture with the rest of the GPCRs, they constitute an unconventional class of GPCRs. The Frizzled receptors exhibit signaling characteristics that are unconventional among the GPCRs. For example, signaling through Disheveled/b-catenin is unique for this class of receptors (124). The smoothened receptor shares the structure of the other Frizzled receptors, but unlike the other receptors of this family, it does not appear to recognize a Wnt ligand. Instead it binds to protein ligands from the Hedgehog family that serve a similar role in body development as the Wnt ligands do. Smoothened

can signal via both Gαi and Gα12/13 (125, 126).
Another set of receptors that play a pivotal in Wnt signaling are LRP5 and 6. These receptors form a complex together with Frizzled en Wnt. Subsequently LRP5/6 are phosphorylated by the kinases CK1 and GSK3β (127). The phosphorylation of LRP5/6 creates a docking site for Axin, which is a critical component of the destruction complex (Figure 6). Other receptors that bind Wnt are structurally unrelated to the Frizzled receptors; the single transmembrane receptors from the Ryk and Ror families. Both these receptors seem to engage non-canonical signaling. The Ryk proteins have been reported to transduce signaling through the kinase Src in D. melanogaster (128). Experiments performed with mice deficient for the Ror family member Ror2, have shown that Ror2 signaling involves Rho-GTPases, and, further downstream, JNK (129).
The Frizzled receptors do not exclusively bind Wnt ligands, a multitude of other factors have been described. For example, a small family of ligands known as the R-spondins have been shown to activate canonical signaling via the Frizzled receptors (130).

Key component of Wnt-signaling: β-catenin
The transcriptional regulator β-catenin has a pivotal role in Wnt signaling. It is a 88 kD protein, it is characterized by the presence of so-called armadillo repeats, which are named after the D. melanogaster β-catenin homolog Armadillo. As mentioned before, β-catenin is normally rendered inactive by the destruction complex. The destruction complex is composed of four proteins, besides β-catenin itself: Adenomatous Polyposis Coli (APC), Axin CK1, and GSK3β. These four proteins all perform a different role in β-catenin regulation, as is shown in Figure 6. While APC and Axin act as a scaffold, CK1 kinases and GSK3β phosphorylate β-catenin (CK1 phosphorylates at S45, and GSK3β at S33, S37, and T41), targeting it for ubiquitination, and subsequent proteasomal degredation. Highlighting β-catenin's role as a powerful regulator of cell proliferation and survival, mutations in APC and Axin are associated with the development of cancer. Mutations in APC are known to be associated with cancer, especially colon cancer, with familial adenomateous polyposis as an important risk factor for developing colon cancer. Mutations in Axin, on the other hand, are associated with several other cancers, such as liver cancer and medullablastoma. Stabilizing mutations in β-catenin have also been described to promote oncogenesis, which is understandable, considering the importance of phosphorylation for regulating β-catenin abundance.
Activation of β-catenin is mediated by destabilizing the destruction complex, increasing levels of cytoplasmic non-phosphorylated β-catenin. The free β-catenin subsequently translocates to the nucleus where it can transcriptionally activate expression of its target genes (eg. Cyclin D1). Disruption of the destruction complex is of key importance for activation of β-catenin. However, the exact molecular mechanisms triggering this event are not fully understood. There are currently three proposed models, starting with a model which involves Axin binding Disheveled

resulting in a conformational change in Axin disrupting the complex thus freeing β-catenin. In the second model, LRP5/6 are the main mediators of destruction complex inhibition, by binding to Axin which subsequently results in disruption of the destruction complex. Finally, the last model entails inhibition of GSK3β, preventing β-catenin phosphorylation (131). These three possible models are not mutually exclusive, and quite possibly happen in concert.

It is important to note that there are alternative pathways besides the canonical signaling of Frizzled receptors through β-catenin. For example, Frizzled can also signal via other pathways such as JNK and ROCK (Figure 6). Conversely, other GPCRs may activate β-catenin via alternative signaling routes. For example, stimulation of the EP2 and EP4 receptors with PGE2 results in the stablization and activation of β-catenin. In the case of the EP2 receptor this is effected by signaling via Gas and, further downstream, PKA which results in inhibition of GSK3b (132). The EP4 receptor achieves b-catenin activation by PI3K dependent inhibition of GSK3b, a process which is dependent on Gaq activation (133). Additionally, Gas has been reported to be able to bind with the RGS domain of Axin, which also facilitates binding of APC to Axin (134, 135). This results in a loss of binding of GSK3b to Axin. In contrast to Gas, Gai is not capable of binding to Axin (134).

The existence of these different pathways means that care must be taken when analyzing b-catenin signaling, since autocrine and paracrine signaling through either the canonical or one of the non-canonical pathways may also signal at the same time through the same pathway.

2.5 VEGF signaling

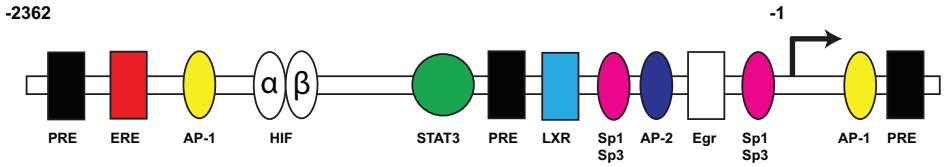

Figure 4. Architecture of the human VEGF promoter region. The response elements are indicated in differently colored shapes. The promoter region is approximately 2.5 kb in size. The different elements, and examples of stimuli are listed below:

Element	Activated by	Location
PRE	Polycomb	-1865/-1860, -716/-711, +679/+684
ERE	Estrogen	-1525/-1514
AP-1	Activating protein 1	-1168/-1015, +418/+425
HIF-1	Hypoxia-inducible factor	-975/-968
STAT3	IL-6/Oncostatin	-848/-850
LXR	Liver-X receptor response element	-317-302
Sp1/Sp3	Retinoic acid, TNFa	-238/-233, -94/-89, -84/-79, -73/-68, -57/-52
AP-2	Activating protein 2	-79/-72
Egr	Early growth response	-77/-70

Vascular endothelial growth factor (VEGF) is an important angiogenic factor, that specifically acts on endothelial cells. Currently, there are five VEGF isoforms known that are expressed from a single gene through alternative splicing. The VEGF gene constitutes 8 exons and the coding sequence is approximately 14 kb in size. The VEGF promoter region contains multiple consensus sites which tend to be well conserved between different species (Figure 4). The promoter region contains response elements for Sp1/Sp3, AP-2, Egr-1, STAT3, and HIF1 (136). The presence of multiple response elements allows for signal integration from multiple pathways. For example, induction of VEGF expression in chronic myeloid leukemia (CML) is achieved through activation of Erk, JAK/STAT and PI3-kinase signaling (137). Factors that induce signaling through these pathways include TNF-a, PDGF, IL-1b, IL-6, Interferon a, estrogen, and retinoic acid.

A STAT3 response element is located between -848 and -840 of the human VEGF promoter. This predicted site was experimentally confirmed to be a STAT3 response site by chromatin immunoprecipitation experiments (34). Furthermore, experiments where a dominant negative form of STAT3 was expressed resulted in a down-regulation of VEGF promoter activity. Conversely, a constitutive active form of STAT3 up-regulates VEGF promoter activity (138). In the context of cancer, STAT3 activation by Oncostatin and IL-6 has been shown to be an essential factor in the pathogenesis of glioblastoma (139) and cervical cancer (140). In both cases VEGF expression is induced by either ligand through the JAK/STAT axis.

Regulation of VEGF expression is controlled by multiple signaling pathways, and because of that complex. Many tumors exist in an inflammatory micro-environment. The presence of response elements that are associated with inflammatory signaling (e.g. Sp1/Sp3, STAT3, Liver-X-receptor, AP-1, AP-2) indicates that the presence of inflammation can induce VEGF production.

There are three VEGF receptors, VEGFR-1, VEGFR-2, and VEGFR-3. These receptors are all tyrosine kinase receptors and members of the PDGF receptor family. Reflecting their critical role in vasculogenesis, knock-out mice for any one of these receptors are not viable and die at different stages of embryonic development (141-143). Upon binding to their respective VEGF ligand, VEGF receptors homo- or heterodimerize which results in receptor kinase activity, (auto)phosphorylation and, ultimately, downstream signaling. Signaling through VEGFR-2 has been extensively studied and plays a pivotal role in endothelial cell migration, differentiation, and survival. Activation of VEGFR-2 results in signaling through PLCg. Subsequently, MAPK becomes activated, promoting endothelial cell proliferation (144). PLCg also triggers calcium release, which in turn activates PKC pathways (145). These two pathways ultimately induce NFAT and EGR-1. Both these transcription factors are involved in effecting the angiogenic response in endothelial cells (146).

2.6 Conclusions

In this chapter several oncogenic signaling were discussed: STAT3, b-catenin, and VEGF. Although there are of course more oncogenic pathways, investigation of US28-induced proliferation described in this thesis found that the HCMV-encoded viral GCPRs US28 and UL33 constitutively activate STAT3 and b-catenin. The next chapters will describe the molecular mechanisms underlying activation of STAT3 and b-catenin by US28 in particular.

Of course, oncogenic signaling in general encompasses more pathways than the two pathways mentioned above. Additionally, the possibility of interplay between the different pathways adds greatly to the complexity of oncogenic signaling. By reducing complexity using model systems (**Chapter 3 and 5**) and constructing mathematical models, as described in **Chapter 4**, that give good approximations of the 'real world' we can learn a great deal about the nature of oncogenic signaling pathways in different settings.

References

1. D. Hanahan, R. A. Weinberg, The hallmarks of cancer. Cell 100, 57 (Jan 7, 2000).
2. C. Schindler, D. E. Levy, T. Decker, JAK-STAT signaling: from interferons to cytokines. J Biol Chem 282, 20059 (Jul 13, 2007).
3. S. A. Jones, J. Scheller, S. Rose-John, Therapeutic strategies for the clinical blockade of IL-6/gp130 signaling. J Clin Invest 121, 3375 (Sep, 2011).
4. A. J. Vila-Coro et al., The chemokine SDF-1alpha triggers CXCR4 receptor dimerization and activates the JAK/STAT pathway. FASEB J 13, 1699 (Oct, 1999).
5. A. F. Wilks, Two putative protein-tyrosine kinases identified by application of the polymerase chain reaction. Proc Natl Acad Sci U S A 86, 1603 (Mar, 1989).
6. B. A. Witthuhn, M. D. Williams, H. Kerawalla, F. M. Uckun, Differential substrate recognition capabilities of Janus family protein tyrosine kinases within the interleukin 2 receptor (IL2R) system: Jak3 as a potential molecular target for treatment of leukemias with a hyperactive Jak-Stat signaling machinery. Leuk Lymphoma 32, 289 (Jan, 1999).
7. I. Remy, I. A. Wilson, S. W. Michnick, Erythropoietin receptor activation by a ligand-induced conformation change. Science 283, 990 (Feb 12, 1999).
8. L. D. Notarangelo et al., Mutations in severe combined immune deficiency (SCID) due to JAK3 deficiency. Hum Mutat 18, 255 (Oct, 2001).
9. M. Karaghiosoff et al., Partial impairment of cytokine responses in Tyk2-deficient mice. Immunity 13, 549 (Oct, 2000).
10. Y. Minegishi et al., Human tyrosine kinase 2 deficiency reveals its requisite roles in multiple cytokine signals involved in innate and acquired immunity. Immunity 25, 745 (Nov, 2006).
11. U. Vinkemeier, Getting the message across, STAT! Design principles of a molecular signaling circuit. The Journal of Cell Biology 167, 197 (October 25, 2004, 2004).
12. C. Schindler, X. Y. Fu, T. Improta, R. Aebersold, J. E. Darnell, Jr., Proteins of transcription factor ISGF-3: one gene encodes the 91-and 84-kDa ISGF-3 proteins that are activated by interferon alpha. Proc Natl Acad Sci U S A 89, 7836 (Aug 15, 1992).
13. J. F. Bromberg, C. M. Horvath, Z. Wen, R. D. Schreiber, J. E. Darnell, Jr., Transcriptionally active Stat1 is required for the antiproliferative effects of both interferon alpha and interferon gamma. Proc Natl Acad Sci U S A 93, 7673 (Jul 23, 1996).
14. C. K. Lee, E. Smith, R. Gimeno, R. Gertner, D. E. Levy, STAT1 affects lymphocyte survival and proliferation partially independent of its role downstream of IFN-gamma. J Immunol 164, 1286 (Feb 1, 2000).
15. P. Gelebart et al., Interleukin-21 effectively induces apoptosis in mantle cell lymphoma through a STAT1-dependent mechanism. Leukemia 23, 1836 (Oct, 2009).
16. P. A. Townsend et al., STAT-1 interacts with p53 to enhance DNA damage-induced apoptosis. J Biol Chem 279, 5811 (Feb 13, 2004).
17. P. A. Townsend et al., STAT-1 facilitates the ATM activated checkpoint pathway following DNA damage. J Cell Sci 118, 1629 (Apr 15, 2005).
18. S. E. Dovhey, N. S. Ghosh, K. L. Wright, Loss of interferon-gamma inducibility of TAP1 and LMP2 in a renal cell carcinoma cell line. Cancer Res 60, 5789 (Oct 15, 2000).
19. L. H. Wong et al., Interferon-resistant human melanoma cells are deficient in ISGF3 components, STAT1, STAT2, and p48-ISGF3gamma. J Biol Chem 272, 28779 (Nov 7, 1997).
20. I. Najjar et al., Latent membrane protein 1 regulates STAT1 through NF-kappaB-dependent interferon secretion in Epstein-Barr virus-immortalized B cells. J Virol 79, 4936 (Apr, 2005).
21. M. Vaysberg, S. L. Lambert, S. M. Krams, O. M. Martinez, Activation of the JAK/STAT pathway in Epstein Barr virus+-associated posttransplant lymphoproliferative disease: role of interferon-gamma. Am J Transplant 9, 2292 (Oct, 2009).
22. M. M. Brierley, E. N. Fish, Stats: multifaceted regulators of transcription. J Interferon Cytokine Res 25, 733 (Dec, 2005).
23. Y. Y. Hsieh, L. Wan, C. C. Chang, C. H. Tsai, F. J. Tsai, STAT2*C related genotypes and allele but not TLR4 and CD40 gene polymorphisms are associated with higher susceptibility for asthma. Int J Biol Sci 5, 74 (2009).
24. E. E. Marshall, A. P. Geballe, Multifaceted evasion of the interferon response by cytomegalovirus. J Interferon Cytokine Res 29, 609 (Sep, 2009).
25. C. Lutticken et al., Association of transcription factor APRF and protein kinase Jak1 with the interleukin-6 signal transducer gp130. Science 263, 89 (Jan 7, 1994).
26. H. Yu, D. Pardoll, R. Jove, STATs in cancer inflammation and immunity: a leading role for STAT3. Nat Rev

Cancer 9, 798 (Nov, 2009).
27. H. A. Bluyssen et al., IFN gamma-dependent SOCS3 expression inhibits IL-6-induced STAT3 phosphorylation and differentially affects IL-6 mediated transcriptional responses in endothelial cells. Am J Physiol Cell Physiol 299, C354 (Aug, 2010).
28. E. S. Park et al., Thyrotropin induces SOCS-1 (suppressor of cytokine signaling-1) and SOCS-3 in FRTL-5 thyroid cells. Mol Endocrinol 14, 440 (Mar, 2000).
29. Y. P. Ng, Z. H. Cheung, N. Y. Ip, STAT3 as a downstream mediator of Trk signaling and functions. J Biol Chem 281, 15636 (Jun 9, 2006).
30. C. Miranda et al., Role of STAT3 in in vitro transformation triggered by TRK oncogenes. PLoS One 5, e9446 (2010).
31. J. Wegrzyn et al., Function of mitochondrial Stat3 in cellular respiration. Science 323, 793 (Feb 6, 2009).
32. J. F. Bromberg et al., Stat3 as an oncogene. Cell 98, 295 (Aug 6, 1999).
33. T. J. Mitchell, S. John, Signal transducer and activator of transcription (STAT) signalling and T-cell lymphomas. Immunology 114, 301 (Mar, 2005).
34. G. Niu et al., Constitutive Stat3 activity up-regulates VEGF expression and tumor angiogenesis. Oncogene 21, 2000 (Mar 27, 2002).
35. T. X. Xie et al., Activation of stat3 in human melanoma promotes brain metastasis. Cancer Res 66, 3188 (Mar 15, 2006).
36. H. Sumimoto, F. Imabayashi, T. Iwata, Y. Kawakami, The BRAF-MAPK signaling pathway is essential for cancer-immune evasion in human melanoma cells. J Exp Med 203, 1651 (Jul 10, 2006).
37. J. Dumortier et al., Human cytomegalovirus secretome contains factors that induce angiogenesis and wound healing. J Virol 82, 6524 (Jul, 2008).
38. S. Pati et al., Activation of NF-kappaB by the human herpesvirus 8 chemokine receptor ORF74: evidence for a paracrine model of Kaposi's sarcoma pathogenesis. J Virol 75, 8660 (Sep, 2001).
39. F. Neipel et al., Human herpesvirus 8 encodes a homolog of interleukin-6. J Virol 71, 839 (Jan, 1997).
40. D. J. Gough et al., Mitochondrial STAT3 supports Ras-dependent oncogenic transformation. Science 324, 1713 (Jun 26, 2009).
41. R. P. Beasley, Hepatitis B virus. The major etiology of hepatocellular carcinoma. Cancer 61, 1942 (May 15, 1988).
42. R. M. Peek, Jr., M. J. Blaser, Helicobacter pylori and gastrointestinal tract adenocarcinomas. Nat Rev Cancer 2, 28 (Jan, 2002).
43. A. Morinobu et al., STAT4 serine phosphorylation is critical for IL-12-induced IFN-gamma production but not for cell proliferation. Proc Natl Acad Sci U S A 99, 12281 (Sep 17, 2002).
44. K. Kikly, L. Liu, S. Na, J. D. Sedgwick, The IL-23/Th(17) axis: therapeutic targets for autoimmune inflammation. Curr Opin Immunol 18, 670 (Dec, 2006).
45. J. N. Temblay, E. Bertelli, J. L. Arques, M. Regoli, C. Nicoletti, Production of IL-12 by Peyer patch-dendritic cells is critical for the resistance to food allergy. J Allergy Clin Immunol 120, 659 (Sep, 2007).
46. J. L. Langowski et al., IL-23 promotes tumour incidence and growth. Nature 442, 461 (Jul 27, 2006).
47. K. Miyoshi et al., Structure of the mouse Stat 3/5 locus: evolution from Drosophila to zebrafish to mouse. Genomics 71, 150 (Jan 15, 2001).
48. Z. Yao et al., Stat5a/b are essential for normal lymphoid development and differentiation. Proc Natl Acad Sci U S A 103, 1000 (January 24, 2006, 2006).
49. J. J. Schuringa, K. Wu, G. Morrone, M. A. Moore, Enforced activation of STAT5A facilitates the generation of embryonic stem-derived hematopoietic stem cells that contribute to hematopoiesis in vivo. Stem Cells 22, 1191 (2004).
50. X. Liu et al., Stat5a is mandatory for adult mammary gland development and lactogenesis. Genes Dev 11, 179 (Jan 15, 1997).
51. G. B. Udy et al., Requirement of STAT5b for sexual dimorphism of body growth rates and liver gene expression. Proc Natl Acad Sci U S A 94, 7239 (Jul 8, 1997).
52. H. Yamashita et al., Role of serine phosphorylation of Stat5a in prolactin-stimulated [beta]-casein gene expression. Mol Cell Endocrinol 183, 151 (2001).
53. A. M. Weaver, C. M. Silva, S731 in the transactivation domain modulates STAT5b activity. Biochem Biophys Res Commun 362, 1026 (2007).
54. J.-Z. Tang et al., Signal Transducer and Activator of Transcription (STAT)-5A and STAT5B Differentially Regulate Human Mammary Carcinoma Cell Behavior. Endocrinology 151, 43 (January 1, 2010, 2010).
55. M. Heuser et al., Modeling the functional heterogeneity of leukemia stem cells: role of STAT5 in leukemia stem cell self-renewal. Blood 114, 3983 (November 5, 2009, 2009).
56. L. Gu et al., Transcription Factor Stat3 Stimulates Metastatic Behavior of Human Prostate Cancer Cells in Vivo, whereas Stat5b Has a Preferential Role in the Promotion of Prostate Cancer Cell Viability and

Tumor Growth. Am J Pathol 176, 1959 (April 1, 2010, 2010).
57. T. A. Wynn, IL-13 effector functions. Annu Rev Immunol 21, 425 (2003).
58. M. Terabe et al., NKT cell-mediated repression of tumor immunosurveillance by IL-13 and the IL-4R-STAT6 pathway. Nat Immunol 1, 515 (Dec, 2000).
59. L. L. Kis et al., The STAT6 signaling pathway activated by the cytokines IL-4 and IL-13 induces expression of the Epstein-Barr virus-encoded protein LMP-1 in absence of EBNA-2: implications for the type II EBV latent gene expression in Hodgkin lymphoma. Blood, (Sep 27, 2010).
60. Q. Cai, S. C. Verma, J. Y. Choi, M. Ma, E. S. Robertson, Kaposi's sarcoma-associated herpesvirus inhibits interleukin-4-mediated STAT6 phosphorylation to regulate apoptosis and maintain latency. J Virol 84, 11134 (Nov, 2010).
61. T. Mustelin, T. Vang, N. Bottini, Protein tyrosine phosphatases and the immune response. Nat Rev Immunol 5, 43 (Jan, 2005).
62. M. Suntharalingam, S. R. Wente, Peering through the pore: nuclear pore complex structure, assembly, and function. Dev Cell 4, 775 (Jun, 2003).
63. B. Beutler, E. T. Rietschel, Innate immune sensing and its roots: the story of endotoxin. Nat Rev Immunol 3, 169 (Feb, 2003).
64. D. J. Hilton, Negative regulators of cytokine signal transduction. Cell Mol Life Sci 55, 1568 (Sep, 1999).
65. T. A. Endo et al., A new protein containing an SH2 domain that inhibits JAK kinases. Nature 387, 921 (1997).
66. M. Kubo, T. Hanada, A. Yoshimura, Suppressors of cytokine signaling and immunity. Nat Immunol 4, 1169 (2003).
67. A. N. Bullock, M. C. Rodriguez, J. E. Debreczeni, Z. Songyang, S. Knapp, Structure of the SOCS4-Elongin-B/C complex reveals a distinct SOCS box interface and the molecular basis for SOCS-dependent EGFR degradation. Structure 15, 1493 (Nov, 2007).
68. F. Pierconti et al., Epigenetic silencing of SOCS3 identifies a subset of prostate cancer with an aggressive behavior. The Prostate, n/a (2010).
69. C. J. Chiou et al., Patterns of gene expression and a transactivation function exhibited by the vGCR (ORF74) chemokine receptor protein of Kaposi's sarcoma-associated herpesvirus. J Virol 76, 3421 (Apr, 2002).
70. E. Slinger, E. Langemeijer, M. Siderius, H. F. Vischer, M. J. Smit, Herpes virus-encoded GPCRs rewire cellular signaling. Mol Cell Endocrinol, (Apr 14, 2010).
71. M. Srivastava et al., The Trichoplax genome and the nature of placozoans. Nature 454, 955 (Aug 21, 2008).
72. K. Orford, C. Crockett, J. P. Jensen, A. M. Weissman, S. W. Byers, Serine phosphorylation-regulated ubiquitination and degradation of beta-catenin. J Biol Chem 272, 24735 (Oct 3, 1997).
73. O. Tetsu, F. McCormick, [beta]-Catenin regulates expression of cyclin D1 in colon carcinoma cells. Nature 398, 422 (1999).
74. V. Easwaran et al., beta-Catenin regulates vascular endothelial growth factor expression in colon cancer. Cancer Res 63, 3145 (Jun 15, 2003).
75. E. Lara et al., Epigenetic repression of ROR2 has a Wnt-mediated, pro-tumourigenic role in colon cancer. Mol Cancer 9, 170 (2010).
76. C. Muller-Tidow et al., Translocation products in acute myeloid leukemia activate the Wnt signaling pathway in hematopoietic cells. Mol Cell Biol 24, 2890 (Apr, 2004).
77. P. Nava et al., Desmoglein-2: a novel regulator of apoptosis in the intestinal epithelium. Mol Biol Cell 18, 4565 (Nov, 2007).
78. A. Glejzer et al., Wnt1 and BMP2: two factors recruiting multipotent neural crest progenitors isolated from adult bone marrow. Cell Mol Life Sci, (Oct 26, 2010).
79. E. Cohn, L. Ossowski, S. Bertran, C. Marzan, E. F. Farias, RARalpha1 control of mammary gland ductal morphogenesis and wnt1-tumorigenesis. Breast Cancer Res 12, R79 (Oct 5, 2010).
80. R. W. Cho et al., Isolation and molecular characterization of cancer stem cells in MMTV-Wnt-1 murine breast tumors. Stem Cells 26, 364 (Feb, 2008).
81. P. Pu et al., Downregulation of Wnt2 and beta-catenin by siRNA suppresses malignant glioma cell growth. Cancer Gene Ther 16, 351 (Apr, 2009).
82. D. Klein et al., Wnt2 acts as an angiogenic growth factor for non-sinusoidal endothelial cells and inhibits expression of stanniocalcin-1. Angiogenesis 12, 251 (2009).
83. G. Hauptmann, T. Gerster, Regulatory gene expression patterns reveal transverse and longitudinal subdivisions of the embryonic zebrafish forebrain. Mech Dev 91, 105 (Mar 1, 2000).
84. A. M. Goss et al., Wnt2/2b and beta-catenin signaling are necessary and sufficient to specify lung progenitors in the foregut. Dev Cell 17, 290 (Aug, 2009).

85. N. I. Khan, K. F. Bradstock, L. J. Bendall, Activation of Wnt/beta-catenin pathway mediates growth and survival in B-cell progenitor acute lymphoblastic leukaemia. Br J Haematol 138, 338 (Aug, 2007).
86. S. Niemann et al., Homozygous WNT3 mutation causes tetra-amelia in a large consanguineous family. Am J Hum Genet 74, 558 (Mar, 2004).
87. A. J. Chien et al., Activated Wnt/beta-catenin signaling in melanoma is associated with decreased proliferation in patient tumors and a murine melanoma model. Proc Natl Acad Sci U S A 106, 1193 (Jan 27, 2009).
88. H. Mandel et al., SERKAL syndrome: an autosomal-recessive disorder caused by a loss-of-function mutation in WNT4. Am J Hum Genet 82, 39 (Jan, 2008).
89. A. Biason-Lauber, D. Konrad, F. Navratil, E. J. Schoenle, A WNT4 mutation associated with Mullerian-duct regression and virilization in a 46,XX woman. N Engl J Med 351, 792 (Aug 19, 2004).
90. S. Ripka et al., WNT5A--target of CUTL1 and potent modulator of tumor cell migration and invasion in pancreatic cancer. Carcinogenesis 28, 1178 (Jun, 2007).
91. T. Saitoh, M. Katoh, Expression and regulation of WNT5A and WNT5B in human cancer: up-regulation of WNT5A by TNFalpha in MKN45 cells and up-regulation of WNT5B by beta-estradiol in MCF-7 cells. Int J Mol Med 10, 345 (Sep, 2002).
92. A. Kanazawa et al., Association of the gene encoding wingless-type mammary tumor virus integration-site family member 5B (WNT5B) with type 2 diabetes. Am J Hum Genet 75, 832 (Nov, 2004).
93. C. G. Woods et al., Mutations in WNT7A cause a range of limb malformations, including Fuhrmann syndrome and Al-Awadi/Raas-Rothschild/Schinzel phocomelia syndrome. Am J Hum Genet 79, 402 (Aug, 2006).
94. T. Saitoh, T. Mine, M. Katoh, Up-regulation of WNT8B mRNA in human gastric cancer. Int J Oncol 20, 343 (Feb, 2002).
95. L. Adaimy et al., Mutation in WNT10A is associated with an autosomal recessive ectodermal dysplasia: the odonto-onycho-dermal dysplasia. Am J Hum Genet 81, 821 (Oct, 2007).
96. A. Bohring et al., WNT10A mutations are a frequent cause of a broad spectrum of ectodermal dysplasias with sex-biased manifestation pattern in heterozygotes. Am J Hum Genet 85, 97 (Jul, 2009).
97. C. Christodoulides et al., WNT10B mutations in human obesity. Diabetologia 49, 678 (Apr, 2006).
98. S. A. Ugur, A. Tolun, Homozygous WNT10b mutation and complex inheritance in Split-Hand/Foot Malformation. Hum Mol Genet 17, 2644 (Sep 1, 2008).
99. T. Toyama, H. C. Lee, H. Koga, J. R. Wands, M. Kim, Noncanonical Wnt11 inhibits hepatocellular carcinoma cell proliferation and migration. Mol Cancer Res 8, 254 (Feb, 2010).
100. J. Mazieres et al., Inhibition of Wnt16 in human acute lymphoblastoid leukemia cells containing the t(1;19) translocation induces apoptosis. Oncogene 24, 5396 (Aug 11, 2005).
101. K. Willert et al., Wnt proteins are lipid-modified and can act as stem cell growth factors. Nature 423, 448 (May 22, 2003).
102. R. Takada et al., Monounsaturated fatty acid modification of Wnt protein: its role in Wnt secretion. Dev Cell 11, 791 (Dec, 2006).
103. L. M. Galli, T. L. Barnes, S. S. Secrest, T. Kadowaki, L. W. Burrus, Porcupine-mediated lipid-modification regulates the activity and distribution of Wnt proteins in the chick neural tube. Development 134, 3339 (Sep, 2007).
104. D. Y. Coudreuse, G. Roel, M. C. Betist, O. Destree, H. C. Korswagen, Wnt gradient formation requires retromer function in Wnt-producing cells. Science 312, 921 (May 12, 2006).
105. T. Y. Belenkaya et al., The retromer complex influences Wnt secretion by recycling wntless from endosomes to the trans-Golgi network. Dev Cell 14, 120 (Jan, 2008).
106. W. Ching, H. C. Hang, R. Nusse, Lipid-independent secretion of a Drosophila Wnt protein. J Biol Chem 283, 17092 (Jun 20, 2008).
107. X. He et al., A member of the Frizzled protein family mediating axis induction by Wnt-5A. Science 275, 1652 (Mar 14, 1997).
108. S. W. Cha et al., Wnt11/5a complex formation caused by tyrosine sulfation increases canonical signaling activity. Curr Biol 19, 1573 (Sep 29, 2009).
109. A. Gazit et al., Human frizzled 1 interacts with transforming Wnts to transduce a TCF dependent transcriptional response. Oncogene 18, 5959 (Oct 28, 1999).
110. Z. Wang, W. Shu, M. M. Lu, E. E. Morrisey, Wnt7b activates canonical signaling in epithelial and vascular smooth muscle cells through interactions with Fzd1, Fzd10, and LRP5. Mol Cell Biol 25, 5022 (Jun, 2005).
111. L. Ma, H. Y. Wang, Suppression of cyclic GMP-dependent protein kinase is essential to the Wnt/cGMP/Ca2+ pathway. J Biol Chem 281, 30990 (Oct 13, 2006).
112. Y. Endo et al., Wnt-3a and Dickkopf-1 stimulate neurite outgrowth in Ewing tumor cells via a Frizzled3- and c-Jun N-terminal kinase-dependent mechanism. Mol Cell Biol 28, 2368 (Apr, 2008).

113. J. Robitaille et al., Mutant frizzled-4 disrupts retinal angiogenesis in familial exudative vitreoretinopathy. Nat Genet 32, 326 (Oct, 2002).
114. Q. Xu et al., Vascular development in the retina and inner ear: control by Norrin and Frizzled-4, a high-affinity ligand-receptor pair. Cell 116, 883 (Mar 19, 2004).
115. K. Planutis et al., Regulation of norrin receptor frizzled-4 by Wnt2 in colon-derived cells. BMC Cell Biol 8, 12 (2007).
116. J. P. Lyons et al., Wnt-4 activates the canonical beta-catenin-mediated Wnt pathway and binds Frizzled-6 CRD: functional implications of Wnt/beta-catenin activity in kidney epithelial cells. Exp Cell Res 298, 369 (Aug 15, 2004).
117. M. Kim et al., Functional interaction between Wnt3 and Frizzled-7 leads to activation of the Wnt/beta-catenin signaling pathway in hepatocellular carcinoma cells. J Hepatol 48, 780 (May, 2008).
118. K. Melchior et al., The WNT receptor FZD7 contributes to self-renewal signaling of human embryonic stem cells. Biol Chem 389, 897 (Jul, 2008).
119. E. Bourhis et al., Reconstitution of a frizzled8.Wnt3a.LRP6 signaling complex reveals multiple Wnt and Dkk1 binding sites on LRP6. J Biol Chem 285, 9172 (Mar 19, 2010).
120. T. Karasawa, H. Yokokura, J. Kitajewski, P. J. Lombroso, Frizzled-9 Is Activated by Wnt-2 and Functions in Wnt/β-Catenin Signaling. J Biol Chem 277, 37479 (October 4, 2002, 2002).
121. C. Garcia-Morales, C.-H. Liu, M. Abu-Elmagd, M. K. Hajihosseini, G. N. Wheeler, Frizzled-10 promotes sensory neuron development in Xenopus embryos. Dev Biol 335, 143 (2009).
122. C.-h. Wu, R. Nusse, Ligand Receptor Interactions in the Wnt Signaling Pathway inDrosophila. J Biol Chem 277, 41762 (November 1, 2002, 2002).
123. C. Carron et al., Frizzled receptor dimerization is sufficient to activate the Wnt/beta-catenin pathway. J Cell Sci 116, 2541 (Jun 15, 2003).
124. G. Schulte, V. Bryja, The Frizzled family of unconventional G-protein-coupled receptors. Trends Pharmacol Sci 28, 518 (Oct, 2007).
125. K. Kasai et al., The G12 family of heterotrimeric G proteins and Rho GTPase mediate Sonic hedgehog signalling. Genes Cells 9, 49 (Jan, 2004).
126. N. A. Riobo, B. Saucy, C. Dilizio, D. R. Manning, Activation of heterotrimeric G proteins by Smoothened. Proc Natl Acad Sci U S A 103, 12607 (Aug 15, 2006).
127. T. P. Rao, M. Kuhl, An Updated Overview on Wnt Signaling Pathways: A Prelude for More. Circ Res 106, 1798 (June 25, 2010, 2010).
128. R. R. Wouda, M. R. Bansraj, A. W. de Jong, J. N. Noordermeer, L. G. Fradkin, Src family kinases are required for WNT5 signaling through the Derailed/RYK receptor in the Drosophila embryonic central nervous system. Development 135, 2277 (Jul, 2008).
129. I. Oishi et al., The receptor tyrosine kinase Ror2 is involved in non-canonical Wnt5a/JNK signalling pathway. Genes Cells 8, 645 (Jul, 2003).
130. K. A. Kim et al., R-Spondin proteins: a novel link to beta-catenin activation. Cell Cycle 5, 23 (Jan, 2006).
131. D. Kimelman, W. Xu, beta-catenin destruction complex: insights and questions from a structural perspective. Oncogene 25, 7482 (Dec 4, 2006).
132. S. Hino, C. Tanji, K. I. Nakayama, A. Kikuchi, Phosphorylation of beta-catenin by cyclic AMP-dependent protein kinase stabilizes beta-catenin through inhibition of its ubiquitination. Mol Cell Biol 25, 9063 (Oct, 2005).
133. H. Fujino, K. A. West, J. W. Regan, Phosphorylation of glycogen synthase kinase-3 and stimulation of T-cell factor signaling following activation of EP2 and EP4 prostanoid receptors by prostaglandin E2. J Biol Chem 277, 2614 (Jan 25, 2002).
134. M. D. Castellone, H. Teramoto, B. O. Williams, K. M. Druey, J. S. Gutkind, Prostaglandin E2 promotes colon cancer cell growth through a Gs-axin-beta-catenin signaling axis. Science 310, 1504 (Dec 2, 2005).
135. K. E. Spink, P. Polakis, W. I. Weis, Structural basis of the Axin-adenomatous polyposis coli interaction. EMBO J 19, 2270 (May 15, 2000).
136. G. Pages, J. Pouyssegur, Transcriptional regulation of the Vascular Endothelial Growth Factor gene--a concert of activating factors. Cardiovasc Res 65, 564 (Feb 15, 2005).
137. L. S. Steelman et al., JAK/STAT, Raf/MEK/ERK, PI3K/Akt and BCR-ABL in cell cycle progression and leukemogenesis. Leukemia 18, 189 (Feb, 2004).
138. D. Wei et al., Stat3 activation regulates the expression of vascular endothelial growth factor and human pancreatic cancer angiogenesis and metastasis. Oncogene 22, 319 (Jan 23, 2003).
139. P. Repovic, C. Y. Fears, C. L. Gladson, E. N. Benveniste, Oncostatin-M induction of vascular endothelial growth factor expression in astroglioma cells. Oncogene 22, 8117 (Nov 6, 2003).
140. L. H. Wei et al., Interleukin-6 promotes cervical tumor growth by VEGF-dependent angiogenesis via a STAT3 pathway. Oncogene 22, 1517 (Mar 13, 2003).

141. F. Shalaby et al., Failure of blood-island formation and vasculogenesis in Flk-1-deficient mice. Nature 376, 62 (Jul 6, 1995).
142. G. H. Fong, J. Rossant, M. Gertsenstein, M. L. Breitman, Role of the Flt-1 receptor tyrosine kinase in regulating the assembly of vascular endothelium. Nature 376, 66 (Jul 6, 1995).
143. D. J. Dumont et al., Cardiovascular failure in mouse embryos deficient in VEGF receptor-3. Science 282, 946 (Oct 30, 1998).
144. D. J. Lyttle, K. M. Fraser, S. B. Fleming, A. A. Mercer, A. J. Robinson, Homologs of vascular endothelial growth factor are encoded by the poxvirus orf virus. J Virol 68, 84 (Jan, 1994).
145. T. Takahashi, S. Yamaguchi, K. Chida, M. Shibuya, A single autophosphorylation site on KDR/Flk-1 is essential for VEGF-A-dependent activation of PLC-gamma and DNA synthesis in vascular endothelial cells. EMBO J 20, 2768 (Jun 1, 2001).
146. E. Hofer, B. Schweighofer, Signal transduction induced in endothelial cells by growth factor receptors involved in angiogenesis. Thromb Haemost 97, 355 (Mar, 2007).

3

HCMV-encoded chemokine receptor US28 mediates proliferative signaling through the IL-6/STAT3 axis.

Adapted from:
Erik Slinger[1], David Maussang[1], Andreas Schreiber[1], Marco Siderius[1], Afsar Rahbar[2], Alberto Fraile-Ramos[3,4], Sergio A. Lira[5], Cecilia Söderberg-Nauclér[2], and Martine J. Smit[1]
Science Signaling **3** (133), ra58, 2010.

[1]Leiden/Amsterdam Center for Drug Research, Division of Medicinal Chemistry, Faculty of Sciences, VU University Amsterdam, De Boelelaan 1083, 1081 HV Amsterdam, the Netherlands. [2]Department of Medicine, Center for Molecular Medicine, Karolinska University Hospital Solna and Karolinska Institutet, 171 76 Stockholm, Sweden. [3]Department of Molecular and Cell Biology, Centro Nacional de Biotecnologia, Consejo Superior de Investigaciones Cientificas, Campus Universidad Autonoma de Madrid, 28006 Madrid, Spain. [4]MRC Laboratory for Molecular Cell Biology, University College London, London WC1E 6BT, UK. [5]Immunology Institute, Mount Sinai School of Medicine, New York, NY 10029, USA.

3.1 Abstract

US28 is a viral G protein-coupled receptor encoded by the human cytomegalovirus (HCMV). In addition to binding and internalizing chemokines, US28 constitutively activates signaling pathways linked to cell proliferation. Here, we show increased concentrations of vascular endothelial growth factor (VEGF) and interleukin (IL)-6 in supernatants of US28-expressing NIH-3T3 cells. Increased IL-6 was associated with increased activation of the signal transducer and activator of transcription 3 (STAT3), through upstream activation of the Janus activated kinase JAK1. We used conditioned growth medium, IL-6-neutralizing antibodies, an inhibitor of the IL-6 receptor, and shRNA targeting IL-6 to show that US28 activates the IL-6-JAK1-STAT3 signaling axis to elicit a positive feedback loop. This loop is initiated in an US28-dependent manner through activation of the NF-κB transcription factor and the consequent production of IL-6. Treatment of cells with a specific inhibitor of STAT3 inhibited US28-dependent [^{3}H]-thymidine incorporation and foci formation, further suggesting a key role for STAT3 in the US28-mediated proliferative phenotype. US28 also elicits STAT3 activation and IL-6 secretion in HCMV-infected cells. Analysis of tumor specimens from glioblastoma patients demonstrates co-localization of US28 and phosphorylated STAT3 in the vascular niche of these tumors. Moreover, increased phospho-STAT3 expression correlated with poor patient outcome. Taken together, US28 induces proliferation via a novel signaling pathway, by establishing a positive feedback loop via activation of the IL-6/STAT3 axis, which defines a novel pathway activated in HCMV-infected tumors.

3.2 Introduction

Human cytomegalovirus (HCMV), a member of the family of β-herpesviruses, is widespread, persisting as a latent infection in up to 90% of the population (*1*). Although HCMV is asymptomatic in immunocompetent individuals, it may cause such pathologies as pneumonitis, hepatitis, and retinitis in immunocompromised hosts (*1*). Furthermore, HCMV has been proposed to promote the development of colon cancer (*2*) and malignant glioma (*3*). HCMV has also been detected as an active infection in several forms of cancer, including prostate cancer, colon cancer, and malignant glioblastoma. However, the exact role of HCMV as a promoting factor in these tumors remains elusive. HCMV-encoded proteins are thought to drive these processes either directly, through activation or inhibition of cellular signaling pathways, or indirectly, through induction of autocrine and paracrine signaling. One of the HCMV-encoded proteins, known to induce a proliferative and angiogenic phenotype in vitro and in vivo, is the viral chemokine receptor US28 (*4*).

The presence of four G protein-coupled receptors (GPCR) that are structurally similar to human chemokine receptors in the HCMV genome--US28, US27, UL33, and UL78-- (*5, 6*) is intriguing. Chemokine receptors are involved in regulation of the immune system (*7*), and have also been implicated in various aspects of oncogenesis (*8*). The HCMV-encoded GPCR US28, which is structurally similar to the human chemokine receptor CCR1 (*9*), has been studied most extensively (*10*). US28 binds various chemokines, including: CCL2, CCL5, and CX3CL1 (*11*), and may thereby suppress the host immune response (*12*). In addition, US28 also signals constitutively and shows G-protein promiscuity, traits that enable it to hijack the host cell's signaling machinery (*13*).

Like chemokine receptors, viral GPCRs appear to play a role in oncogenesis and tumor growth (*14, 15*). Transgenic mice expressing ORF74, the chemokine receptor encoded by Kaposi sarcoma-associated herpesvirus (KSHV), develop lesions resembling Kaposi sarcoma (*16*). Similarly, US28 induces various oncogenic responses, including increased cyclin D1 and cyclooxygenase-2 (COX2) production, as well as that of vascular endothelial growth factor (VEGF), when expressed in NIH-3T3 fibroblasts (*4, 17*). Moreover, US28 enhances HCMV-induced VEGF promoter activity and COX2 expression in HCMV-infected cells (*4, 17*), and promotes tumor formation in a mouse xenograft model (*4, 17*).

To investigate the molecular mechanism by which US28 contributes to oncogenesis, we analyzed US28-induced release of angiogenic factors. We used an antibody array that recognized different chemokines, growth factors, and cytokines to identify factors secreted by US28-expressing NIH-3T3 cells. US28 increased the production of interleukin (IL)-6, which is induced by HCMV infection (*18, 19*) and has been implicated in oncogenesis (*20, 21*). In addition, we identified a key role for the IL-6-STAT3 (signal transducer and activator of transcription 3) axis in US28-mediated proliferative signaling. Our data thus reveal a positive feedback loop initiated by US28 that is crucial for the proliferative phenotype shown by US28-expressing cells.

3.3 Results

3.3.1 US28 increases the secretion of IL-6 and VEGF

NIH-3T3 cells stably expressing US28 display oncogenic properties (*4, 17*). For instance, injection of US28-transformed NIH-3T3 cells into nude mice results in tumor formation (*4*). Because angiogenic factors are required for formation of large tumors (*22*), we assessed their secretion by US28-expressing NIH-3T3 cells. We analyzed conditioned medium from US28-expressing NIH-3T3 cells and compared it to that from mock-transfected NIH-3T3 cells using a mouse antibody array for angiogenic factors. The array analysis showed a marked increase in both IL-6 (296% ± 3%) and VEGF (271% ± 45%) in medium from the US28-expressing cells (Fig. 1); the latter finding was consistent with earlier observations (*4*). Medium concentration of CCL2, a chemokine that binds US28, was decreased (13% ± 2%) (*11*), whereas the medium concentration of CCL11 and CXCL4, which do not bind US28, was unaffected. Because IL-6 has been implicated in oncogenesis (*22, 23*), we investigated the role of IL-6 in US28-induced proliferative signaling.

3.3.2 US28 induces STAT3 phosphorylation and STAT3-driven transcriptional activation

IL-6 binds to its cognate receptor, the IL-6 receptor, to activate STAT3 signaling (*24*); therefore, we assessed the phosphorylation status of STAT3. Consistent with the observed increase in IL-6 concentration in the supernatant of stably US28-transfected cells, STAT3 phosphorylation was markedly increased in US28-expressing cells,

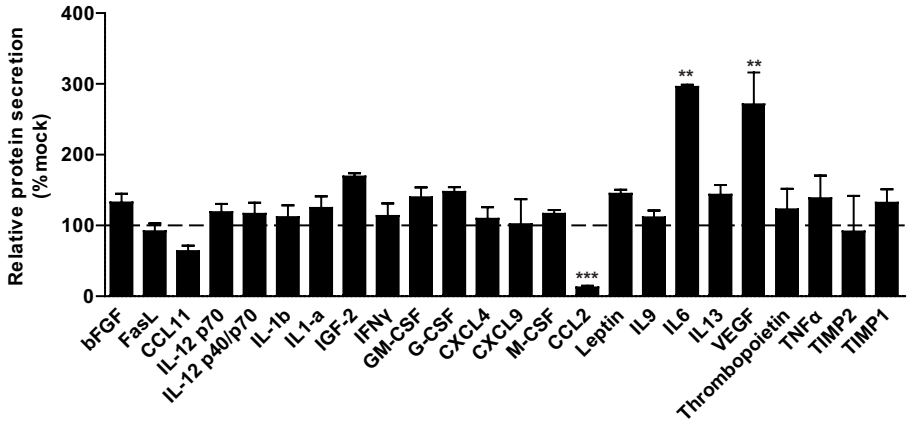

Figure 1. Increased IL-6 and VEGF secretion in US28 transfected cells. Medium from NIH-3T3 cells stably transfected with US28 was compared with medium obtained from mock transfected cells. Excreted cytokines and growth factors were analyzed using an antibody array. The mean result of three separate experiments is shown as a percentage of protein levels in US28 expressing cells compared to mock transfected cells. CCL2 secretion is significantly downregulated in US28 expressing cells (***$p < 0.001$) whereas IL-6 and VEGF secretion are both significantly upregulated (**$p < 0.01$).

compared to mock-transfected cells (Fig. 2A). In contrast, no STAT3 phosphorylation was observed in cells stably transfected with the US28-$R^{129}A$ mutant, which fails to couple to G proteins (*25*). Furthermore, a luciferase-based reporter assay showed that STAT3-driven transcriptional activation was increased in HEK293T transiently transfected with a plasmid encoding US28, but not in mock- or US28-$R^{129}A$-transfected cells (Fig. 2B). The presence of US28 in transfected HEK293T (Fig. 2C), and NIH-3T3 (Fig. 2D) cells was verified using [^{125}I]-CCL5 binding.

3.3.3 JAK1 and NF-κB mediate US28-induced STAT3 signaling

Next, we used specific inhibitors to identify components of the signaling pathway leading from US28 to STAT3 activation (*26, 27*). We performed these analyses both in transiently-transfected HEK293T cells, in which we assessed STAT3 activity using STAT3 reporter gene assays, and in NIH-3T3 cells stably transfected with US28, in which we determined STAT3 phosphorylation using Western blot analysis. Overnight treatment with 10 µM Pyridone-6 (P6, a pan-JAK inhibitor) inhibited STAT3-dependent reporter gene activity by 51.6% ±1.5% in HEK293T cells transfected with US28 (Fig. 3A). In contrast, overnight exposure to several other kinase inhibitors [10 µM AG-490 (JAK2 inhibitor), PP-2 (Src inhibitor), or Tyrene CR-4 (Abl inhibitor)] failed to affect STAT3 signaling. Signaling through the $G\alpha_o$ family of G proteins has been described to activate STAT3 (*28*). Therefore, we assessed the effects on US28-induced STAT3 signaling of treating cells with 100 ng/ml of the $G\alpha_{i/o}$

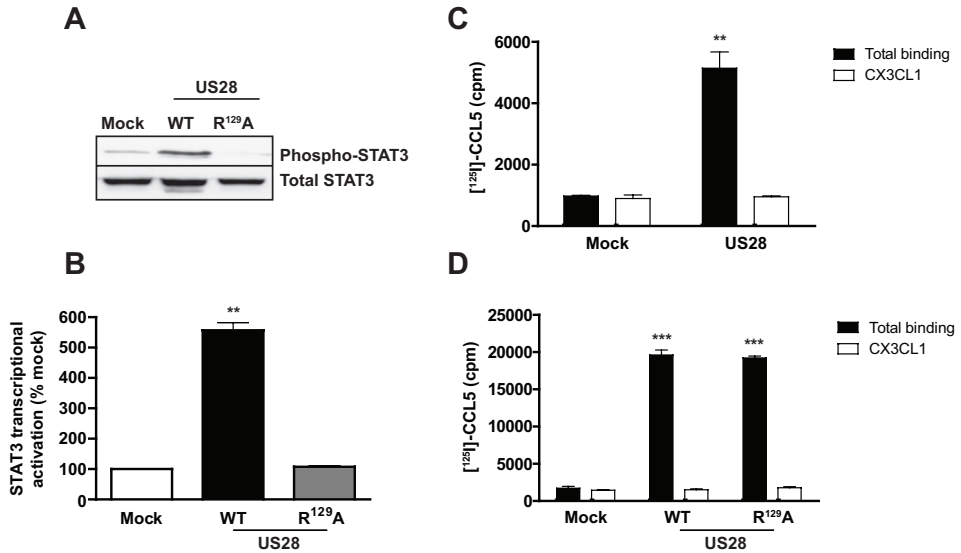

Figure 2. Increased STAT3 activity in NIH-3T3 and HEK293T transfected with US28. (**A**) STAT3 phosphorylation levels are increased in NIH-3T3 stably transfected with US28, whereas in the G-protein uncoupled mutant US28-R129A shows no increased STAT3 phosphorylation. (**B**) In HEK293T cells, STAT3-driven transcriptional activation is only observed when the US28 wild-type receptor is expressed (**p < 0.01 compared to mock). (**C**) [125I]-CCL5 binding to US28, displacement with 10-7 M CX3CL1 in HEK293T (**p < 0.01 compared to mock). (**D**) [125I]-CCL5 binding to US28 and US28 R129A, displacement with 10-7 M CX3CL1 in stably transfected NIH-3T3 (**p < 0.01 for both wild-type and US28 R129A compared to mock).

inhibitor pertussis toxin (PTX) and observed no significant effect on STAT3 reporter gene activity (Fig. 3A). Because IL-6 production is enhanced by the transcription factor nuclear factor κB (NF-κB) (*29, 30*), which is constitutively activated through both $G\alpha_q$ and Gβγ in cells expressing US28 (*12*), we treated cells with the NF-κB inhibitor BAY11-7082 (*31, 32*). BAY11-7082 reduced the transcriptional activation of reporter genes by STAT3 78.7% (±4.2%) (Fig. 3A).
We also assessed the effects of the kinase inhibitors P6, AG-490, and Tyrene on STAT3 phosphorylation in US28-expressing NIH-3T3 cells treated for 30 minutes with 10 μM of each inhibitor. We observed a strong reduction of STAT3 phosphorylation only after treatment with P6 (Fig. 3B), implicating JAK1 in mediating US28-dependent STAT3 phosphorylation.

3.3.4 US28 activates the IL-6-STAT3 axis in a paracrine and autocrine fashion

To assess whether US28 directly or in a paracrine or autocrine fashion, via activation of NF-κB, induces increased IL-6 production, we investigated the importance of US28-mediated IL-6 release in STAT3 activation. We observed a marked increase in STAT3 phosphorylation as assessed by Western blot analysis in mock- and US28-expressing NIH-3T3 cells treated with 10 ng/ml IL-6 (Fig. 4A). Moreover, conditioned medium from US28-expressing NIH-3T3 cells induced STAT3 phosphorylation in both mock- and US28-R^{129}A-transfected cells (Fig. 4B), whereas incubation of US28-expressing NIH-3T3 cells with a neutralizing antibody to IL-6 attenuated STAT3 phosphorylation (Fig. 4C). Treatment of US28-expressing NIH-3T3 cells with 10 μM

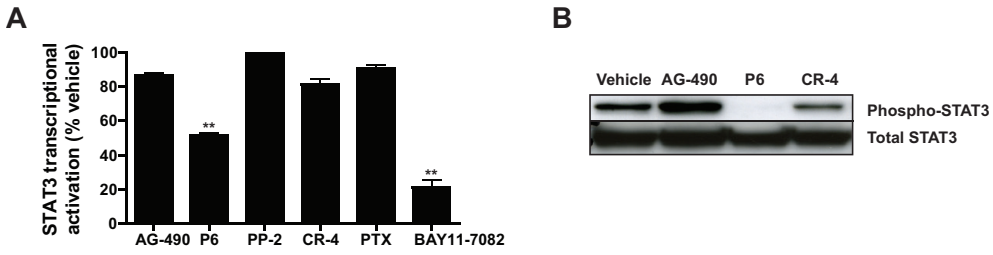

Figure 3. US28 induced STAT3 phosphorylation and transcriptional activaty is mediated by JAK1. (A) STAT3-driven transcriptional activation was inhibited by treatment with 10 μM of Pyridone 6 (P6, pan-JAK kinase inhibitor) (**p < 0.01 compared to vehicle treated), whereas similar concentrations AG-490 (JAK-2 inhibitor), PP-2 (Src inhibitor), and Tyrene CR-4 (Abl inhibitor) had little or no effect. 100 ng/ml pertussis toxin (PTX) had no effect on STAT3 activation. The NF-κB inhibitor BAY11-7082 reduced STAT3-dependent reporter gene activation approximately 80% (**p < 0.01 compared to vehicle). (**B**) NIH-3T3 cells stably transfected with US28 were treated for 30 minutes with the different kinase inhibitors. Only 10 μM P6 inhibited STAT3 phosphorylation (~6% compared to vehicle treated cells).

Madindoline-A, which inhibits the formation of gp130 homodimers and thereby signaling of the IL-6Rα-gp130 complex (*33*), completely inhibited US28-induced STAT3 phosphorylation (Fig. 4D).

To investigate the involvement of IL-6 in the US28-induced activation of STAT3 in HEK293T cells, we expressed shIL-6, the shRNA targeting and downregulating IL-6 (*23*), in conjunction with the STAT3 reporter gene. Co-transfection of shIL-6 completely abolished US28-induced STAT3 transcriptional activity, whereas expression of scrambled shRNA (shEmpty) did notaffect STAT3 transcriptional activity (Fig. 4E). In contrast, co-transfecting shIL-6 with a NFAT (nuclear factor of activated T cells) reporter gene did not significantly alter US28-induced NFAT signaling (Fig. 4F). These results indicate that, in both HEK293T and NIH-3T3 cells, US28 induces IL-6 release, resulting in STAT3 activation by way of the IL-6Rα-gp130 complex.

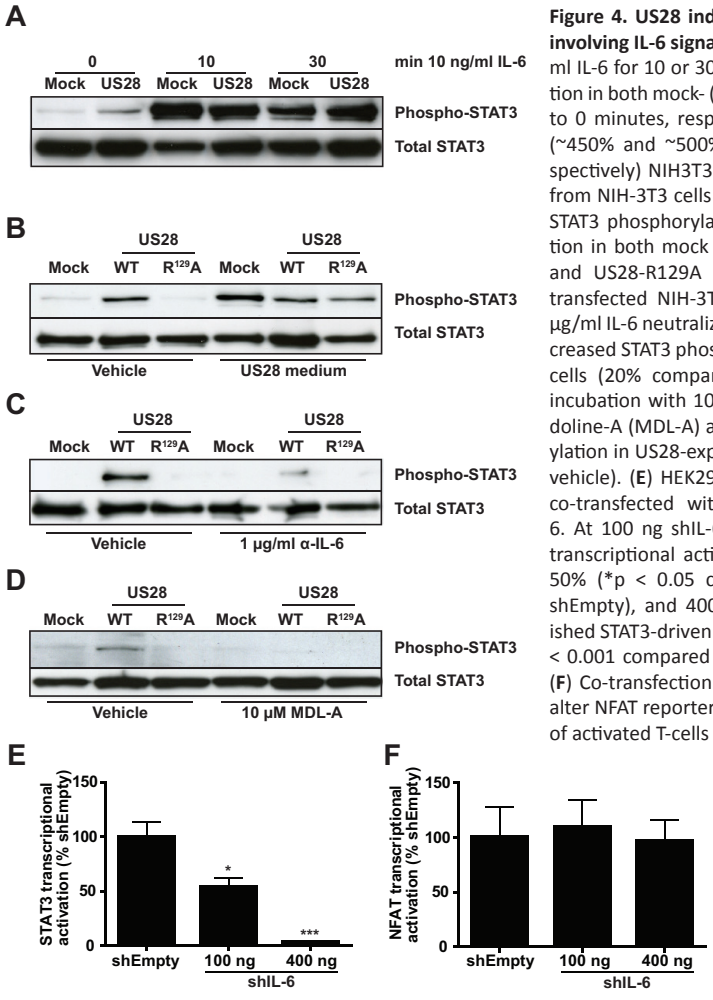

Figure 4. US28 induces a positive feedback loop involving IL-6 signaling. (**A**) Incubation with 10 ng/ml IL-6 for 10 or 30 min elicits STAT3 phosphorylation in both mock- (~2500% and ~1800% compared to 0 minutes, respectively) and US28-transfected (~450% and ~500% compared to 0 minutes, respectively) NIH3T3 cells. (**B**) Conditioned medium from NIH-3T3 cells transfected with US28 induced STAT3 phosphorylation after a 90 minute incubation in both mock (~1300% compared to vehicle) and US28-R129A (~760% compared to vehicle) transfected NIH-3T3 cells. (**C**) Incubation with 1 µg/ml IL-6 neutralizing antibody for 90 minutes decreased STAT3 phosphorylation in US28-expressing cells (20% compared to vehicle). (**D**) Overnight incubation with 10 µM of gp130 inhibitor Madindoline-A (MDL-A) also decreased STAT3 phosphorylation in US28-expressing cells (~4% compared to vehicle). (**E**) HEK293T cells expressing US28 were co-transfected with different amounts of shIL-6. At 100 ng shIL-6 / 106 cells STAT3-dependent transcriptional activation was reduced by almost 50% (*$p < 0.05$ compared to transfection with shEmpty), and 400 ng shIL-6 per 106 cells abolished STAT3-driven transcriptional activation (***$p < 0.001$ compared to transfection with shEmpty). (**F**) Co-transfection of shIL-6 failed to significantly alter NFAT reporter gene activation. Nuclear factor of activated T-cells (NFAT).

3.3.5 STAT3 is involved in the US28-induced proliferative phenotype

Next, we used inhibitors of STAT3 and JAK1 to determine whether IL-6-driven STAT3 signaling was involved in the US28-mediated proliferative phenotype. The specific STAT3 inhibitor JSI-124 (*34*) inhibited US28-mediated STAT3 signaling in HEK293T cells (Fig. 5A) with an IC_{50} of approximately 500 nM. Next, we used a [^{3}H]-thymidine incorporation assay to determine the effect of various inhibitors of the IL-6-STAT3 pathway on the proliferation of mock- and US28-expressing NIH-3T3 cells. We found that treatment with either the STAT3 inhibitor JSI-124 or the JAK inhibitor P6 strongly reduced proliferation of US28-transfected cells (Fig. 5B). Because US28 increases expression of the gene encoding VEGF (*4*), which in part is regulated by STAT3 (*35*), we examined whether IL-6 was involved in US28-mediated transcriptional activation of the VEGF promoter. Co-expression of shIL-6 with US28 resulted in reduced US28-induced activation of the VEGF promoter (Fig. 5C). Furthermore, inhibition of STAT3 with JSI-124 partially inhibited US28-induced VEGF promoter activity (Fig. 5D). COX-2 has previously been shown also to mediate US28-induced VEGF-production (*17*); therefore we investigated whether combined inhibition of STAT3 and COX-2 with JSI-124 and Celecoxib had a synergistic effect. Indeed, treatment with both inhibitors resulted in a 67.8% ± 4.2% reduction of VEGF promoter activation, compared to 35.1 ± 7.7 % and 48.1 ± 5.6 % reduction when treated with either JSI-124 or Celecoxib, respectively (Fig. 5D). In addition, the transforming potential of US28 was inhibited by treatment with JSI-124, resulting in a 48% ± 4% and 77% ± 8% reduction in number of foci when treated with 250 and 500 nM JSI-124, respectively, in a focus formation assay with NIH-3T3 cells (Fig. 5E).

3.3.6 HCMV infection results in STAT3 activation

To investigate the contribution of US28 to STAT3 activation during HCMV infection, we infected U373 MG (malignant glioblastomas) cells with HCMV Titan wild-type or a HCMV Titan ΔUS28 mutant at an multiplicity of infection (MOI) of 2. The presence of US28 or lack thereof was confirmed with [^{125}I]-CCL5 binding (Fig. 6A). The presence of US28 was further confirmed 24 hours post-infection by immunofluorescence using an antibody targeting US28. Infected cells (green) were visualized by means of GFP incorporated in HCMV Titan and US28 is shown in red (Fig. 6C, panel I and II). As previously shown, US28 is predominantly found in the perinuclear region of infected cells (*36*). In contrast, we did not detect any US28 in cells infected with HCMV Titan ΔUS28 (Fig. 6C, panel III and IV). We confirmed US28 functionality by measuring the intracellular accumulation of inositol phosphate, as described before (*4, 13*). We observed increased inositol phosphate accumulation in HCMV Titan-infected cells, whereas cells infected with the ΔUS28 strain did not show inositol phosphate accumulation (Fig. 6B).

Experiments using the STAT3 reporter gene showed increased STAT3 activity 48 hours post-infection in cells infected with the HCMV Titan strain, but significantly less activity in cells infected with the HCMV TitanΔUS28 mutant strain ($p<0.001$) (Fig. 6D). Consistent with the reporter gene data, Western blot analysis of cells in-

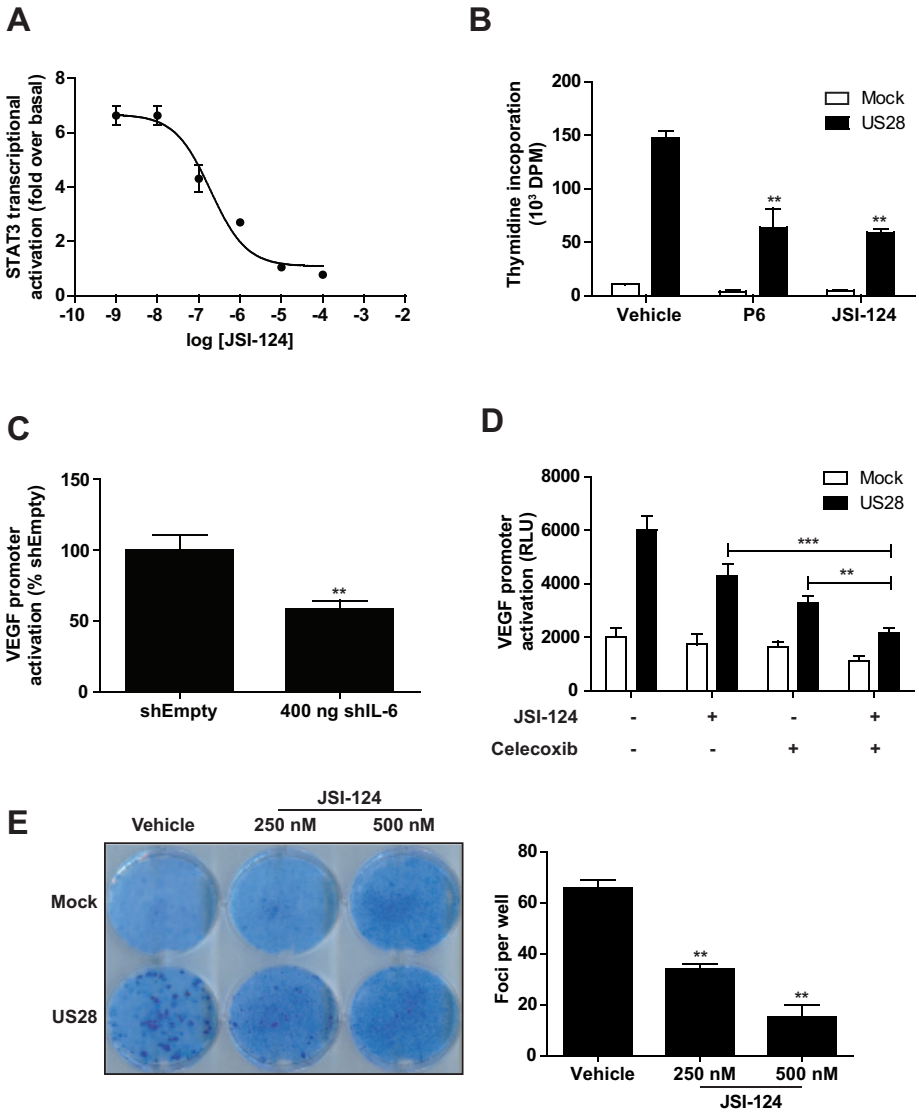

Figure 5. STAT3 plays a critical role in US28-induced proliferation. (**A**) The STAT3 inhibitor JSI-124 inhibited STAT3 response element activation in HEK293T after a 24 hour incubation. (**B**) Over-night treatment with either JSI-124 or P6 inhibited DNA synthesis in NIH-3T3 cells expressing US28 (**p < 0.01 compared with vehicle). (**C**) Knock-down of IL-6 with 400 ng shIL-6 / 106 cells in HEK293T cells expressing US28 inhibits transcriptional activation of the VEGF promoter (**p < 0.01). (**D**) Treatment of HEK293T cells co-transfected with US28 and a reporter gene containing the VEGF promoter with either 500 nM JSI-124 or 25 μM Celecoxib partially inhibits transcriptional activation of the VEGF promoter , and treatment with both compounds simultaneously has a synergistic effect (***p < 0.001 and **p < 0.01 compared to single treatment with JSI-124 or Celecoxib, respectively) . (**E**) Inhibition of foci formation by US28-expressing NIH-3T3 cells by either 250 nM or 500 nM JSI-124 (**p < 0.01 compared to vehicle).

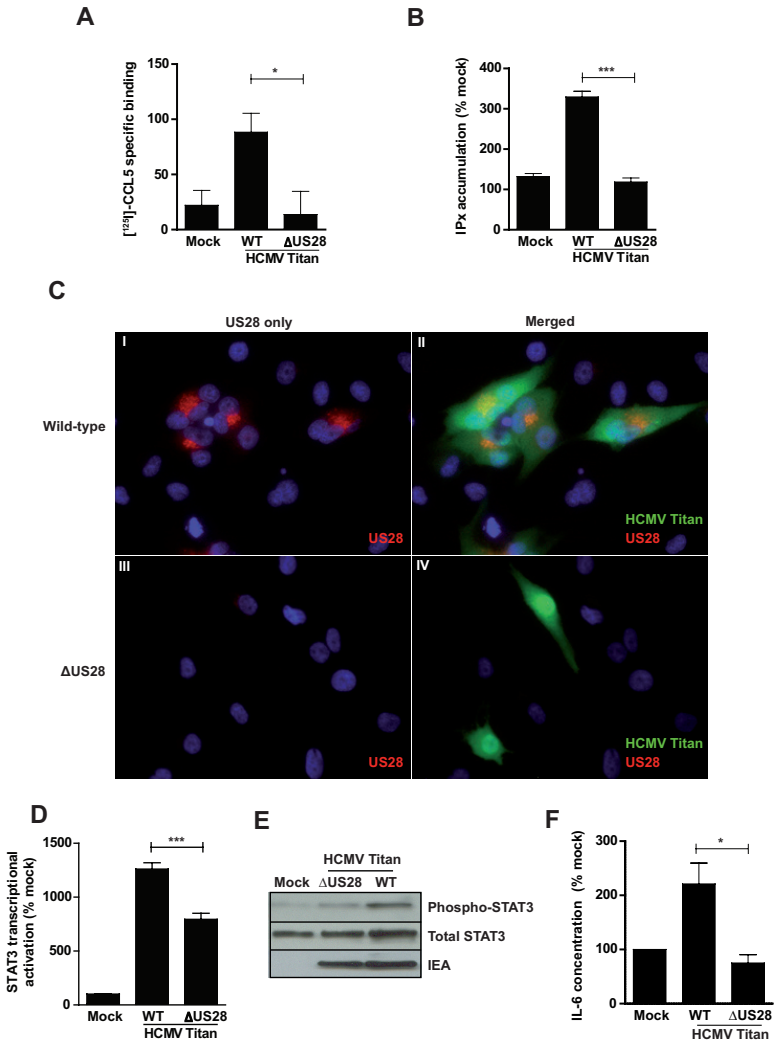

Figure 6. STAT3 activation during HCMV infection is partly mediated by US28. (**A**) [^{125}I]-CCL5 binding to US28 on U373 MG cells 48 hours post-infection with HCMV Titan; cells infected with the wild-type virus showed CCL5 binding, whereas those infected with ΔUS28 virus did not (*$p < 0.05$ compared to binding on HCMV Titan ΔUS28). (**B**) Accumulation of inositol phosphate in U373 MG cells 48 hours post-infection with HCMV Titan; cells infected with the wild-type virus showed increased inositol phosphate accumulation compared to both mock- and ΔUS28 mutant virus-infected cells (***$p < 0.001$ compared to HCMV Titan ΔUS28). (**C**) Anti-US28 stains U373 MG cells infected with HCMV Titan show specific staining of US28 (Red) in panel I and II, where in panel II infected cells are shown in green using a GFP-tag incorporated in the viral genome. In panel III and IV the same staining is performed on cells infected with HCMV Titan ΔUS28 as a negative control; in panel IV infected cells are also shown in green using the same GFP-tag. (**D**) STAT3-dependent transcriptional activation by HCMV Titan in U373 cells 48 hours post-infections with HCMV Titan, which is less prominent in the ΔUS28 mutant virus (***$p < 0.001$ compared to the wild-type virus). (**E**) STAT3 phosphorylation in U373 MG cells 24 hours post-infection with HCMV Titan, STAT3 phosphorylation is induced more strongly upon infection with wild-type virus (~250% compared to mock) compared to HCMV Titan ΔUS28 (~130% compared to mock), staining with anti-IEA confirms viral infection in both samples. (**F**) HCMV infection induces IL-6 secretion in U373 MG in a US28-dependent fashion, IL-6 concentration was measured 24 hours post-infection in serum starved cells (*$p < 0.05$). Human cytomegalovirus (HCMV), immediate early antigen (IEA), green fluorescent protein (GFP).

fected with the HCMV Titan strain showed increased STAT3 phosphorylation, which was significantly greater than that in cells infected with the HCMV TitanΔUS28 mutant strain (Fig. 6E). IL-6 concentration in the supernatant of HCMV-infected cells 24 hours post-infection was increased by 182% ± 13.8% compared to mock, whereas no increase in IL-6 concentration was apparent in cells infected with the HCMV Titan ΔUS28 strain (Fig. 6F).

3.3.7 Primary glioblastoma tumors show presence of US28 and activated STAT3

Finally, we examined whether US28, STAT3 phosphorylation, and IL-6 could be detected in primary tumor specimens from patients with malignant glioblastoma. We examined 21 different malignant glioblastoma specimens obtained from patients at debulking surgery, of which 20 were HCMV-positive and one HCMV-negative. The presence of HCMV was confirmed by staining with antibodies directed against US28 and HCMV immediate-early antigen (IEA) (Fig 7A and 7C). Cells containing US28 and showing STAT3 phosphorylation were mostly confined to the vascular wall, with a few cells scattered over the tumor. Double-staining with antibodies directed against phospho-STAT3 and US28 revealed a similar pattern (Fig. 7B and 7E; cells with phospho-STAT3 in brown and cells with US28 cells in red). HCMV IEA was present in tumor cells, smooth muscle cells (identified using SMC α-actin (Fig. 7D), and endothelial cells (Fig. 7G). IL-6 was abundant in tumor cells close to the vessels in all tissue samples (Fig. 7F; US28 in brown and IL-6 in red). As shown in figure 7G, CD31, an angiogenic marker, was consistently detected in HCMV-positive glioblastoma specimens. We did not observe either HCMV IEA- or US28-stained cells in the HCMV-negative tumor (Fig. 7I). In this HCMV-negative tumor phospho-STAT3 abundance was very low and only detected in <10% of the cells (Fig. 7J), in contrast with its abundance in HCMV-infected tumor samples.

The abundance of US28 and the extent of STAT3 phosphorylation differed among different individuals, allowing us to grade tumor samples accordingly and relate these values to patient outcome. Median overall survival (OS) and in patients (n=9) with <30% US28-positive cells in the tissue was 19.5 vs. 14.5 months in those (n=12) with > 30% US28-positive cells, (*p=0.7*), and median time to tumor progression (TTP) was 12 vs. 6.5 months, *p=0.28* (Table 1). Overall survival time and TTP were higher in patients (n=1) with <30% HCMV-IEA-positive cells (median OS: 34 vs. 14.5 months, median TTP: 17 vs7 months) than in those (n=17) with >30%

Table 1. Median overall survival and time to tumor progression in tumors with low (0-2) and high grade (3-5) US28, Phospho-STAT3, and HCMV-Immediate Early Antigen (IEA). (n = 21 patients per group). P-value was determined using the Log-rank (Mantel-Cox) test.

	Overall survival (months)			Time to tumor progression (months)		
	Grade 0 to 2	Grade 3 to 5	P	Grade 0 to 2	Grade 3 to 5	P
US28	19.5 (n=9)	14.5 (n=12)	>0.05	12 (n=9)	6.5 (n=12)	>0.05
Phospho-STAT3	21 (n=14)	11.5 (n=7)	<0.05	12 (n=14)	4.5 (n=7)	<0.01
HCMV-IEA	34(n=1)	14.5 (n=20)	-	17 (n=1)	7 (n=20)	-

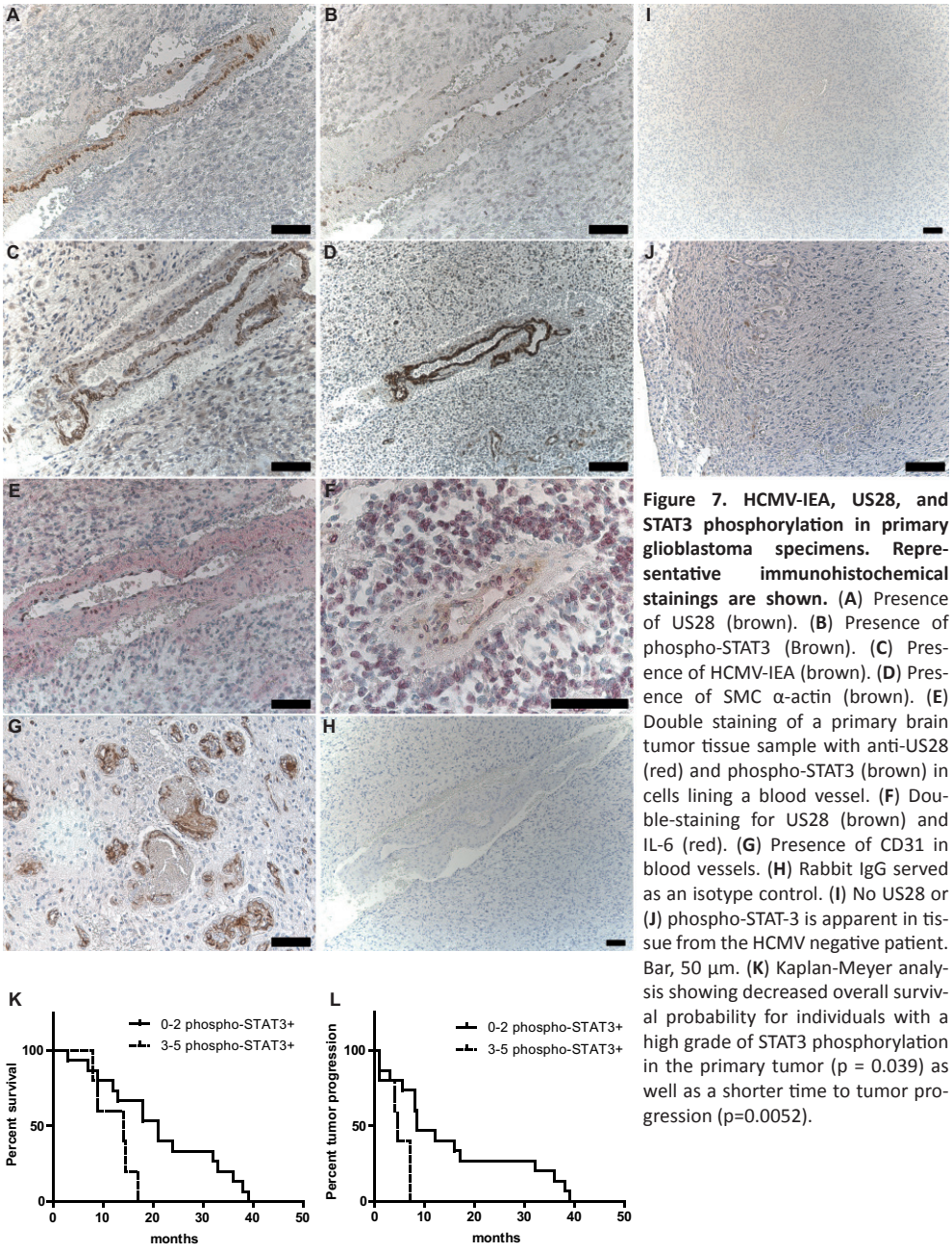

Figure 7. HCMV-IEA, US28, and STAT3 phosphorylation in primary glioblastoma specimens. Representative immunohistochemical stainings are shown. (**A**) Presence of US28 (brown). (**B**) Presence of phospho-STAT3 (Brown). (**C**) Presence of HCMV-IEA (brown). (**D**) Presence of SMC α-actin (brown). (**E**) Double staining of a primary brain tumor tissue sample with anti-US28 (red) and phospho-STAT3 (brown) in cells lining a blood vessel. (**F**) Double-staining for US28 (brown) and IL-6 (red). (**G**) Presence of CD31 in blood vessels. (**H**) Rabbit IgG served as an isotype control. (**I**) No US28 or (**J**) phospho-STAT-3 is apparent in tissue from the HCMV negative patient. Bar, 50 µm. (**K**) Kaplan-Meyer analysis showing decreased overall survival probability for individuals with a high grade of STAT3 phosphorylation in the primary tumor (p = 0.039) as well as a shorter time to tumor progression (p=0.0052).

infected cells (Table 1). Patients (n=14) with <30% phospho-STAT3-positive cells survived significantly longer (median OS: 21 vs. 11.5 months, *p=0.039* and median TTP: 12 vs. 4.5, *p=0.0052*) than those (n=7) with >30% phospho-STAT3-positive cells in their tumor tissue (Table 1, Fig. 7K, L). The presence of US28 was related to STAT3 phosphorylation (*p=0.006)* and STAT3 phosphorylation was related to the presence of IL-6 as determined by a Wald test (*p=0.041)*. Thus, although we analyzed only a limited number of samples, our data suggest that HCMV infection is related to STAT3 phosphorylation, IL-6 production and outcome for individuals with malignant glioblastomas.

3.4 Discussion

Convincing evidence has linked viral infection to several forms of cancer. For example, Kaposi sarcoma-associated herpes virus (KSHV) and Human Papilloma virus (HPV) are considered the etiological agents of Kaposi sarcoma and cervical cancer, respectively (*37, 38*). HCMV proteins and DNA have been detected in several tumors (*39-42*), but a causal relationship has yet to be demonstrated. Although HCMV is not considered an oncogenic virus like KSHV and HPV (*43*), accumulating evidence suggests that it may act as an oncomodulator (*44*). Furthermore, HCMV interferes with several key cellular signaling pathways, leading to enhanced tumor survival and angiogenesis, as well as alterations in cell motility and adhesion (*45*).

Here, we identified a signaling pathway involving NF-κB and IL-6/STAT3 through which US28 induces cell proliferation. Analysis of a set of secreted growth factors, chemokines, and cytokines enabled us to confirm increased VEGF secretion by US28-expressing cells (*4*). Medium concentration of CCL2 was decreased, reflecting its sequestration by US28 (*11*). Notably, the concentration of IL-6 was increased in the medium of US28-expressing cells. IL-6 is a pro-inflammatory cytokine that induces STAT3 phosphorylation by binding to its cognate receptor IL-6Rα and thereby activating the tyrosine kinase subunit of the IL-6 receptor, gp130 (*24*). Following IL-6 binding to IL-6Rα, the two gp130 subunits activate Janus kinases (JAKs), leading to activation of STAT3 and its target genes. IL-6 is a regulatory factor in melanoma, inhibiting proliferation, and may play a pivotal role in the switch from cellular senescence to oncogenesis (*23*). Moreover, STAT3 is a transcriptional regulator known to show increased activity in solid tumors (*46*), as well as in lymphomas (*47*). Recent studies have shown that constitutively active gp130 mutants are responsible for increased STAT3 phosphorylation in hepatocellular tumors (*48*). As such, IL-6 and STAT3 are considered promising anti-cancer drug targets (*49, 50*), stimulating the clinical use of IL-6 neutralizing antibodies (*51*) and the discovery of several STAT3 inhibitors (*34, 52*). The importance of IL-6 and STAT3 signaling in oncogenesis (*20, 21*) led us to investigate the role of the IL-6-STAT3 axis in US28-mediated proliferative signaling. The rise in IL-6 production and secretion in US28-expressing cells was associated with increased activation of STAT3, through the upstream activation of JAK1. This increase was only apparent in cells transfected with US28 and not in either mock-transfected cells or cells carrying the US28 mutant, US28-

$R^{129}A$. Using conditioned growth medium, IL-6 neutralizing antibodies, an inhibitor of the IL-6 receptor, and shRNA targeting IL-6, we showed that US28 activates the IL-6-JAK1-STAT3 signaling axis. Because IL-6 itself is transcriptionally activated by STAT3 (*53*), this creates a positive feedback loop. Both IL-6/STAT3 autocrine loops, as well as paracrine loops have been described in cancer cells (*54, 55*). A common factor in both US28 and IL-6 signaling is NF-κB, which is activated in response to US28 signaling (*13*) and drives the transcription of IL-6 (*29, 30, 56*). We found that NF-κB signaling was crucial to US28-mediated STAT3 activation. Using the G protein-uncoupled US28-R129A mutant, we demonstrate that similarly to NF-kB constitutive signaling (*13*), US28-induced STAT3 activation is G protein-dependent. Thus, a positive loop activating IL-6-JAK1-STAT3 is initiated in an US28-dependent manner through activation of NF-κB. Treatment of cells with the STAT3 inhibitor JSI-124 inhibited US28-induced [^{3}H]-thymidine incorporation, VEGF promoter activity, and foci formation, further demonstrating the relevance of the STAT3 pathway to the US28-induced proliferative phenotype. We previously identified a role for COX-2 in US28-induced VEGF production (*17*); our experiments here indicate that US28-induced VEGF promoter activation is regulated by both STAT3 and COX-2, suggesting that US28 acts as an oncomodulator through multiple mechanisms. We also observed increased STAT3 activity and IL-6 abundance in HCMV-infected U373 MG glioblastoma cells, both of which were attenuated in cells infected with a strain lacking US28. However, STAT3 activity was not fully abolished in cells infected with the ΔUS28 virus, suggesting that STAT3 activation is also promoted by other viral factors. Furthermore, HCMV-infected cells secrete large amounts of IL-5 (*57*), which activates STAT3 (*58*). The increased IL-6 production in HCMV-infected U373 MG cells appears to depend on US28. Increased IL-6 abundance and subsequent activation of the STAT3 axis have been reported in HCMV-infected HUVEC and U373 MG cells (*57, 59*). Moreover, gliomas, and some cancer stem cells, require IL-6 and STAT3 for tumor growth and survival (*60*). The presence of US28 and of STAT3 phosphorylation in cells lining the blood vessels in primary glioblastoma tumors suggest that US28 may be involved in the formation and maintenance of these tumors in within the vascular niche. The IL-6 receptor has shown to be present in glioblastomas and IL-6 triggers proliferation and migration in cerebral endothelial cells (*61, 62*). The specific localization of these cells suggest that they may play a role in vascularization of the tumor, particularly in light of our data showing IL-6-dependent VEGF secretion. Furthermore, IL-6 is known to induce expression of VEGF and other angiogenic factors in pulmonary hypertension (*63*). Moreover, increased IL-6 concentrations are associated with smooth muscle cell proliferation and VEGF release in human cerebrovascular smooth muscle cells (*62*). Cells expressing US28 may also influence neighboring cells in a paracrine manner, effectively reprogramming these cells to display a more malignant phenotype. This notion is further supported by our data on disease progression and patient survival. Increased number of cells showing HCMV-IEA and STAT3 phosphorylation in the glioblastoma specimens was associated with a poor prognosis, with median overall survival and time to tumor

progression significantly reduced. A similar trend was observed for the presence of US28. The fact that US28 abundance correlated with the degree of STAT3 phosphorylation in the tumor specimen indicates a potentially important role for US28 in glioblastoma: US28 and other viral factors that induce NF-κB signaling in infected cells may initiate a positive feedback loop activating the IL-6-STAT3 axis, thereby contributing to the severity of disease.

We suggest the following model for US28-induced STAT3 activation and subsequent proliferative signaling (Fig. 8). Cells carrying US28 produce IL-6 by way of a G-protein-dependent pathway involving NF-κB. IL-6 binds to the IL-6Rα subunit, subsequently activating the gp130 subunits of the IL-6 receptor , eliciting tyrosine phosphorylation of STAT3 by JAK1. Phospho-STAT3 dimerizes and translocates to the nucleus, to regulate target genes, including proliferative and angiogenic factors such as Cyclin D1 (*64*) and VEGF (*35*), respectively. IL-6 itself is a STAT3 target gene (*53*), leading to creation of a positive feedback loop. Our observations imply that, in cells infected with HCMV, US28 initiates a pathway leading to secretion of IL-6 and resulting in enhanced proliferative signaling in an autocrine feedback loop. In addition, IL-6 stimulates STAT3 activation in neighboring uninfected cells through paracrine signaling. By locally altering cytokine concentrations, US28 may facilitate tumor progression and vascularization, thereby contributing to the oncomodulatory properties of HCMV. Together, our data indicate that the HCMV-encoded chemokine receptor US28 mediates proliferative signaling by establishing a positive feedback loop involving activation of the IL-6-STAT3 axis. Targeting the IL-6-STAT3 axis with inhibitors effectively inhibited US28-induced proliferative signaling and VEGF secretion; the IL-6-STAT3 axis may thus represent a target for anti-angiogenic therapy, and specifically for HCMV-related tumor formation.

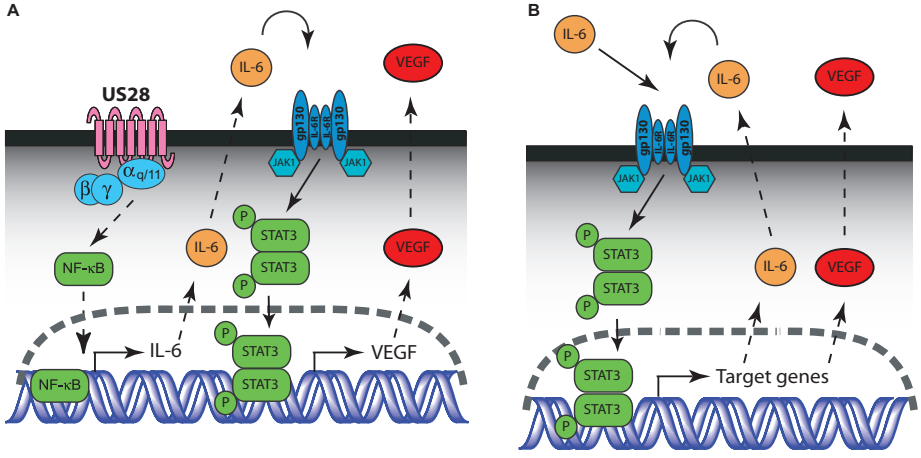

Figure 8. Model outlining the US28 positive feedback loop. (A) US28 activates STAT3 via autocrine stimulation initiated byinducing IL-6 production via the NF-κB pathway. IL-6 subsequently activates the IL-6 receptor which results in STAT3 phosphorylation and activation of its target genes (amongst others, VEGF). (**B**) IL-6 secreted by US28-expressing cells can also activate STAT3 in a paracrine fashion. In both cases IL-6 is a target gene of STAT3 and activation of the IL-6/STAT3 axis may result in a positive feedback loop. Arrows indicate direct interactions, dashed arrows indicate activation with intervening steps.

3.5 Materials and methods

Materials and reagents
Antibodies directed against phospho-STAT3 (Tyr^{705}) and STAT3 were purchased from Cell Signaling Technology (Boston, MA, USA). Neutralizing antibody against murine IL-6 was from BD Biosciences (Franklin Lakes, NJ, USA). Secondary antibodies used in the immunofluorescence experiments were obtained from Invitrogen (Paisley, UK). Pyridone 6 (pan-JAK inhibitor), Tyrene CR-4 (Abl inhibitor), AG-490 (JAK2 inhibitor), JSI-124 (STAT3 inhibitor), BAY11-7082 (NF-κB inhibitor) and PP-2 (Src inhibitor) were all purchased from Calbiochem (San Diego, CA, USA). Stocks were made in DMSO, except for JSI-124, which was dissolved in ethanol. The inhibitors were subsequently diluted in the culture medium. Madindoline-A was purchased from Alexis Biochemicals (Lausen, Switzerland). Tris base, pertussis toxin, and linear polyethylenimine (25 kD) were obtained from Sigma-Aldrich (St. Louis, MO); other chemicals were obtained from Applichem (Darmstadt, Germany). Recombinant human CCL5, human CX3CL1, and murine IL-6 were obtained from Peprotech (Rocky Hill, NJ, USA). Dulbecco's Modified Eagle Medium (DMEM) was purchased from PAA Laboratories (Pasching, Austria). Fetal bovine serum was purchased from Integro (Zaanstad, The Netherlands), and bovine serum was purchased from Invitrogen.

Cell culture
Human HEK293T, human U373 MG, and murine NIH-3T3 cells were cultured in Dulbecco's Modified Eagle Medium (DMEM) supplemented with 50 IU/ml penicillin, 50 µg/ml streptomycin, and 10% fetal bovine, heat inactivated fetal bovine and bovine sera, respectively. Transient transfections of HEK293T cells were performed using the polyethylenimine method (*65*). Transient transfections of U373 cells were performed using the lipofectamine method (*66*). The HCMV Titan strain described in (*4*) was used to infect U373 cells at an MOI of 2. Stable clones of NIH-3T3 expressing US28 or US28 R129A mutant (*4*) were kept under a selective pressure of 400 µg/ml neomycin in the culture medium to ensure homogenous receptor expression in the cells. Expression of US28 in HEK293T, U373 MG, and NIH-3T3 cells was confirmed using [^{125}I]-CCL5 binding (specific binding was determined using CX3CL1 10^{-7} M), as previously described (*13*).

Angiogenesis array
A mouse angiogenesis array (Raybiotech, Norcross, GA, USA) was used according to manufacturer's instructions to determine relative amounts of cytokines and chemokines involved in angiogenesis.

Measurement of IL-6 concentration in culture medium
Il-6 concentrations in culture medium supernatant from serum-starved U373 MG cells were measured 24 hours post-infection with either HCMV Titan wild-type or HCMV Titan ΔUS28. For the measurement the Human IL-6 Quantikine ELISA Kit from R&D Systems (Minneapolis, MN, USA) was employed according to manufacturer's instructions.

Western-blot analysis
A Biorad (Hercules, CA) minigel system was used to perform SDS/PAGE, and a Biorad electroblot system was used to transfer protein samples to a 0.45 µm nitrocellulose membrane. Cells were lysed in RIPA-buffer supplemented with α-complete protease inhibitor cocktail

from Hoffmann-La Roche (Basel, Switzerland), 1 mM PMSF, 1 mM $NaVO_4$, and 1 mM NaF added. Samples were normalized using the BCA total protein determination kit obtained from Thermo Fisher Scientific (Rockford, IL, USA). Blots were quantified using ImageJ (Rasband, W.S., U. S. National Institutes of Health, Bethesda, Maryland, USA). Data shown is representative of three independent experiments.

Reporter gene analysis

The Ly6E STAT3-response element luciferase construct (*28*) was used for STAT3 activity measurements. To determine STAT3 activity, 10^6 HEK293T cells were transfected with 625 ng Ly6E STAT3-response luciferase construct, with or without pcDEF3 containing a gene encoding HA-US28. U373 cells were transfected 24 hours before infection with 1300 ng STAT3 reporter gene. When inhibitors were used, they were added immediately following transfection. Total DNA amounts were kept constant by adding empty vector. Luciferase activity was measured 24 hours after transfection or 48 hours post-infection using a Victor^2 multilabel platereader from Perkin-Elmer (Waltham, MA, USA). The NFAT reporter gene, pNFAT-luc was purchased from Stratagene (La Jolla, CA, USA). To measure VEGF promoter activation, the pGL2-VEGF-Luciferase construct, kindly provided by Dr. G. Pages (Institute of Signalling Development Biology and Cancer, Nice, France).

IL-6 knock-down

IL-6 knock-down experiments were performed with the pRS-puro-shIL-6 (GAACTTATGTTGTTCTCTA) construct kindly provided by Dr. D. Peeper (Netherlands Cancer Institute, Amsterdam, the Netherlands) (*23*). For the knock-down, HEK293T cells were transiently transfected with shIL-6 and a STAT3, VEGF, or NFAT reporter gene. Luminescence measurements were made 48 hours post-transfection. As a negative control pRS-puro expressing a nonsense sequence (CCAATGCTTTGATGCCAAA) was used.

[^{3}H]-Thymidine incorporation

Cell proliferation in NIH-3T3 cells was measured using [^{3}H]-thymidine incorporation. [6-^{3}H]-Thymidine was obtained from GE Healthcare Life Sciences (Buckinghamshire, UK). Cells were serum-starved overnight before labeling in DMEM supplemented with 0.5% bovine serum containing 1 µCi/ml [6-^{3}H]-Thymidine together with inhibitors.

Focus formation assay

Focus formation potential of NIH-3T3 cells transfected with either US28 or empty vector was determined by seeding cells into a monolayer of native NIH-3T3 cells as previously described (*4*). Treatment with JSI-124 was initiated 48 hours after seeding. Medium containing JSI-124 or vehicle was replaced every 48 hours. After 2 weeks the cells were washed 3 times with phosphate buffered saline (PBS) and subsequently fixed in cold methanol for 10 minutes. Following this the cells were stained with 0.4% Methylene Blue in H_2O and the foci counted.

Inositol phosphate accumulation

U373 MG cells were labeled 48 hours post-infection in inositol-free DMEM supplemented with 2 µCi/ml *myo*-[2-^{3}H]-inositol and incubated overnight. The cells were subsequently incubated for 2 hours in DMEM with 10 mM LiCl added. The incubation was stopped with 10 mM cold formic acid, and inositol phosphates were isolated by anion exchange chromatography (Dowex AG1-X8 columns, Bio-Rad).

Generation of a rabbit antiserum against US28

To generate polyclonal antisera, rabbits were immunized with a synthetic peptide corresponding to the C-terminal 17 amino acids of the US28 protein (H_2N-SSDTLSDEVCRVSQIIP-CO_2H) coupled to keyhole limpet hemocyanin through the N-terminal amino group. The specificity of the antisera was assessed by immunoprecipitation followed by Western blot analysis and immunofluorescence (Fig. S1). Immunofluorescence was performed using Alexafluor568 conjugated anti-rabbit to detect anti-US28, and subsequent imaging was done on an Olympus FSX-100.

Patient Samples and Immunohistochemistry

Paraffin-embedded primary brain tumor specimens were obtained from one HCMV negative glioblastoma tumor and randomly from 20 GBM patients in our sample collection in the Biobank at the Karolinska University Hospital Sweden. Twelve of 21 patients received Temozolomide and radiation; 2 patients received gammaknife treatment; 5 patients received CCNU and radiation; and 2 patients received only CCNU after debulking surgery. Tissue sections (6 µm thickness) were stained for HCMV-IEA, US28, phospho-STAT3, CD31, and IL-6 using immunohistochemistry staining protocols as previously been described (*67*). Briefly, the sections were deparaffinized in xylene, rehydrated through an alcohol series, postfixed with 4% neutral buffered formalin, treated with pepsin (Biogenex, San Ramon, CA), and then incubated in citrate buffer (Biogenex). The sections were treated with 3% H_2O_2 (Sigma-Aldrich) to inactivate endogenous peroxidase, avidin/biotin blocking kit (DakoCytomation, Glostrup, Denmark), was used in order to block endogenous biotin/avidin, and FC receptor blocker (Innovex Biosciences) to block FC-R. Finally, the tissue sections were treated with Background Buster (Innovex Biosciences). Incubation with primary antibodies against US28 (created by Alberto Fraile-Ramos), phospho-STAT3 (Cell Signaling), CD31 (Dako Cytomation, Denmark), IL-6 (AbCam), Human cytomegalovirus-IEA (Chemicon, US), and Human cytomegalovirus-Late (Chemicon, US) was done overnight at 4°C. Antibodies against rabbit IgG (R&D Systems, Minneapolis, MN) and smooth muscle cells alpha actin (IgG2a, Dako) were used as isotype control. After incubation with primary antibodies, the sections were incubated with biotinylated anti-rabbit (Dako) or anti-mouse (Biogenex) antibodies. Finally, the antibodies were visualized using streptavidin-conjugated horseradish peroxidase and diaminobenzidine (Innovex Biosciences). For double-staining, the first staining was performed as described, and the second was performed using streptavidin-conjugated alkaline phosphatase (DakoCytomation) and FastRed (Dakocytomation). Hematoxylin (Sigma-Aldrich) was used for counterstaining and slides were mounted in permanent mounting medium (DakoCytomation).

The percentage number of cells expressing different factors in the tissue specimens were graded 1, 0-1+ to <10%; grade 2, ≥10% to 30%, grade 3, ≥30% to 50%, grade 4, ≥50 % to 70%, grade 5, >70%. This study was approved by the ethics committees at Karolinska Institutet.

Statistical analysis

All experiments were performed at least three times in triplicate. When comparisons between treated and vehicle-treated cells, or mock and infected cells were made, Student T-test was performed using the GraphPad Prism software (San Diego, CA, USA). Bars and error bars represent the mean and SEM, respectively. Median time to tumour progression (TTP) and survival were analyzed using Kaplan-Meier curves by using Long-rank (Mantel-Cox) test. Relationship between different stainings was determined using Wald statistics.

Acknowledgements

We thank Prof. Dr. M. Detlef (Abteilung Virologie, Universitätsklinikum Ulm, Germany) for providing both the HCMV Titan wild-type and ΔUS28 strain. We also thank Prof. Dr. D. Peeper (Netherlands Cancer Institute, Amsterdam, the Netherlands) for kindly providing us with the IL-6 shRNA, as well as Prof. Dr. C.M. Horvath (Northwestern University, Chicago, IL, USA) for providing us with the Ly6E STAT3-response luciferase construct. Finally, we would like to thank Prof. Dr. M. Marsh (MRC Laboratory for Molecular Cell Biology, London, UK) for his assistance in the generation of the US28 antibody. The Netherlands Organisation for Scientific Research, the Swedish Medical Research Council, the Swedish Children's cancer foundation, and the Cancer foundation are thanked for their financial support.

References

1. M. K. Gandhi, R. Khanna, Human cytomegalovirus: clinical aspects, immune regulation, and emerging treatments. *Lancet Infect Dis* **4**, 725 (Dec, 2004).
2. F. R. Stassen, X. Vega-Cordova, I. Vliegen, C. A. Bruggeman, Immune activation following cytomegalovirus infection: more important than direct viral effects in cardiovascular disease? *J Clin Virol* **35**, 349 (Mar, 2006).
3. L. Harkins *et al.*, Specific localisation of human cytomegalovirus nucleic acids and proteins in human colorectal cancer. *Lancet* **360**, 1557 (Nov 16, 2002).
4. D. Maussang *et al.*, Human cytomegalovirus-encoded chemokine receptor US28 promotes tumorigenesis. *Proc Natl Acad Sci U S A* **103**, 13068 (Aug 29, 2006).
5. M. S. Chee, S. C. Satchwell, E. Preddie, K. M. Weston, B. G. Barrell, Human cytomegalovirus encodes three G protein-coupled receptor homologues. *Nature* **344**, 774 (Apr 19, 1990).
6. U. A. Gompels, H. A. Macaulay, Characterization of human telomeric repeat sequences from human herpesvirus 6 and relationship to replication. *J Gen Virol* **76 (Pt 2)**, 451 (Feb, 1995).
7. M. Thelen, J. V. Stein, How chemokines invite leukocytes to dance. *Nat Immunol* **9**, 953 (Sep, 2008).
8. F. Balkwill, Cancer and the chemokine network. *Nat Rev Cancer* **4**, 540 (Jul, 2004).
9. J. L. Gao, P. M. Murphy, Human cytomegalovirus open reading frame US28 encodes a functional beta chemokine receptor. *J Biol Chem* **269**, 28539 (Nov 18, 1994).
10. H. F. Vischer, R. Leurs, M. J. Smit, HCMV-encoded G-protein-coupled receptors as constitutively active modulators of cellular signaling networks. *Trends Pharmacol Sci* **27**, 56 (Jan, 2006).
11. B. Bodaghi *et al.*, Chemokine sequestration by viral chemoreceptors as a novel viral escape strategy: withdrawal of chemokines from the environment of cytomegalovirus-infected cells. *J Exp Med* **188**, 855 (Sep 7, 1998).
12. J. R. Randolph-Habecker *et al.*, The expression of the cytomegalovirus chemokine receptor homolog US28 sequesters biologically active CC chemokines and alters IL-8 production. *Cytokine* **19**, 37 (Jul 7, 2002).
13. P. Casarosa *et al.*, Constitutive signaling of the human cytomegalovirus-encoded chemokine receptor US28. *J Biol Chem* **276**, 1133 (Jan 12, 2001).
14. A. Muller *et al.*, Involvement of chemokine receptors in breast cancer metastasis. *Nature* **410**, 50 (Mar 1, 2001).
15. S. Iwakiri *et al.*, Higher expression of chemokine receptor CXCR7 is linked to early and metastatic recurrence in pathological stage I nonsmall cell lung cancer. *Cancer* **115**, 2580 (Jun 1, 2009).
16. T. Y. Yang *et al.*, Transgenic expression of the chemokine receptor encoded by human herpesvirus 8 induces an angioproliferative disease resembling Kaposi's sarcoma. *J Exp Med* **191**, 445 (Feb 7, 2000).
17. D. Maussang *et al.*, The human cytomegalovirus-encoded chemokine receptor US28 promotes angiogenesis and tumor formation via cyclooxygenase-2. *Cancer Res* **69**, 2861 (Apr 1, 2009).
18. G. Halwachs-Baumann, G. Weihrauch, H. J. Gruber, G. Desoye, C. Sinzger, hCMV induced IL-6 release in trophoblast and trophoblast like cells. *J Clin Virol* **37**, 91 (Oct, 2006).
19. A. Rahbar *et al.*, Evidence of active cytomegalovirus infection and increased production of IL-6 in tissue specimens obtained from patients with inflammatory bowel diseases. *Inflamm Bowel Dis* **9**, 154 (May, 2003).
20. C. Y. Yu *et al.*, STAT3 activation is required for interleukin-6 induced transformation in tumor-promotion sensitive mouse skin epithelial cells. *Oncogene* **21**, 3949 (Jun 6, 2002).
21. L. H. Wei *et al.*, The anti-apoptotic role of interleukin-6 in human cervical cancer is mediated by up-regulation of Mcl-1 through a PI 3-K/Akt pathway. *Oncogene* **20**, 5799 (Sep 13, 2001).
22. D. Hanahan, R. A. Weinberg, The hallmarks of cancer. *Cell* **100**, 57 (Jan 7, 2000).
23. T. Kuilman *et al.*, Oncogene-induced senescence relayed by an interleukin-dependent inflammatory network. *Cell* **133**, 1019 (Jun 13, 2008).
24. P. C. Heinrich, I. Behrmann, G. Muller-Newen, F. Schaper, L. Graeve, Interleukin-6-type cytokine signalling through the gp130/Jak/STAT pathway. *Biochem J* **334 (Pt 2)**, 297 (Sep 1, 1998).
25. M. Waldhoer *et al.*, The carboxyl terminus of human cytomegalovirus-encoded 7 transmembrane receptor US28 camouflages agonism by mediating constitutive endocytosis. *J Biol Chem* **278**, 19473 (May 23, 2003).
26. P. J. Murray, The JAK-STAT signaling pathway: input and output integration. *J Immunol* **178**, 2623 (Mar 1, 2007).
27. H. Yu, M. Kortylewski, D. Pardoll, Crosstalk between cancer and immune cells: role of STAT3 in the tumour microenvironment. *Nat Rev Immunol* **7**, 41 (Jan, 2007).
28. P. T. Ram, C. M. Horvath, R. Iyengar, Stat3-mediated transformation of NIH-3T3 cells by the constitutively

active Q205L Galphao protein. *Science* **287**, 142 (Jan 7, 2000).
29. Y. H. Son *et al.*, Roles of MAPK and NF-kappaB in interleukin-6 induction by lipopolysaccharide in vascular smooth muscle cells. *J Cardiovasc Pharmacol* **51**, 71 (Jan, 2008).
30. T. A. Libermann, D. Baltimore, Activation of interleukin-6 gene expression through the NF-kappa B transcription factor. *Mol Cell Biol* **10**, 2327 (May, 1990).
31. J. W. Pierce *et al.*, Novel inhibitors of cytokine-induced IkappaBalpha phosphorylation and endothelial cell adhesion molecule expression show anti-inflammatory effects in vivo. *J Biol Chem* **272**, 21096 (Aug 22, 1997).
32. M. Lappas, K. Yee, M. Permezel, G. E. Rice, Sulfasalazine and BAY 11-7082 interfere with the nuclear factor-kappa B and I kappa B kinase pathway to regulate the release of proinflammatory cytokines from human adipose tissue and skeletal muscle in vitro. *Endocrinology* **146**, 1491 (Mar, 2005).
33. M. Hayashi *et al.*, Suppression of bone resorption by madindoline A, a novel nonpeptide antagonist to gp130. *Proc Natl Acad Sci U S A* **99**, 14728 (Nov 12, 2002).
34. M. A. Blaskovich *et al.*, Discovery of JSI-124 (cucurbitacin I), a selective Janus kinase/signal transducer and activator of transcription 3 signaling pathway inhibitor with potent antitumor activity against human and murine cancer cells in mice. *Cancer Res* **63**, 1270 (Mar 15, 2003).
35. G. Niu *et al.*, Constitutive Stat3 activity up-regulates VEGF expression and tumor angiogenesis. *Oncogene* **21**, 2000 (Mar 27, 2002).
36. A. Fraile-Ramos *et al.*, The human cytomegalovirus US28 protein is located in endocytic vesicles and undergoes constitutive endocytosis and recycling. *Mol Biol Cell* **12**, 1737 (Jun, 2001).
37. D. Ganem, KSHV and Kaposi's sarcoma: the end of the beginning? *Cell* **91**, 157 (Oct 17, 1997).
38. N. Munoz *et al.*, Epidemiologic classification of human papillomavirus types associated with cervical cancer. *N Engl J Med* **348**, 518 (Feb 6, 2003).
39. D. A. Mitchell *et al.*, Sensitive detection of human cytomegalovirus in tumors and peripheral blood of patients diagnosed with glioblastoma. *Neuro Oncol* **10**, 10 (Feb, 2008).
40. C. S. Cobbs *et al.*, Human cytomegalovirus infection and expression in human malignant glioma. *Cancer Res* **62**, 3347 (Jun, 2002).
41. L. Giuliani *et al.*, Detection of oncogenic viruses SV40, BKV, JCV, HCMV, HPV and p53 codon 72 polymorphism in lung carcinoma. *Lung Cancer* **57**, 273 (Sep, 2007).
42. M. Samanta, L. Harkins, K. Klemm, W. J. Britt, C. S. Cobbs, High prevalence of human cytomegalovirus in prostatic intraepithelial neoplasia and prostatic carcinoma. *J Urol* **170**, 998 (Sep, 2003).
43. B. Damania, Oncogenic gamma-herpesviruses: comparison of viral proteins involved in tumorigenesis. *Nat Rev Microbiol* **2**, 656 (Aug, 2004).
44. M. Michaelis, H. W. Doerr, J. Cinatl, The story of human cytomegalovirus and cancer: increasing evidence and open questions. *Neoplasia* **11**, 1 (Jan, 2009).
45. C. Soderberg-Naucler, Does cytomegalovirus play a causative role in the development of various inflammatory diseases and cancer? *J Intern Med* **259**, 219 (Mar, 2006).
46. J. F. Bromberg *et al.*, Stat3 as an oncogene. *Cell* **98**, 295 (Aug 6, 1999).
47. T. J. Mitchell, S. John, Signal transducer and activator of transcription (STAT) signalling and T-cell lymphomas. *Immunology* **114**, 301 (Mar, 2005).
48. S. Rebouissou *et al.*, Frequent in-frame somatic deletions activate gp130 in inflammatory hepatocellular tumours. *Nature* **457**, 200 (Jan 8, 2009).
49. R. Buettner, L. B. Mora, R. Jove, Activated STAT signaling in human tumors provides novel molecular targets for therapeutic intervention. *Clin Cancer Res* **8**, 945 (Apr, 2002).
50. M. Fulciniti *et al.*, A high-affinity fully human anti-IL-6 mAb, 1339, for the treatment of multiple myeloma. *Clin Cancer Res* **15**, 7144 (Dec 1, 2009).
51. T. Puchalski, U. Prabhakar, Q. Jiao, B. Berns, H. M. Davis, Pharmacokinetic and pharmacodynamic modeling of an anti-interleukin-6 chimeric monoclonal antibody (siltuximab) in patients with metastatic renal cell carcinoma. *Clin Cancer Res* **16**, 1652 (Mar 1, 2010).
52. D. Bhasin *et al.*, Design, synthesis, and studies of small molecule STAT3 inhibitors. *Bioorg Med Chem Lett* **18**, 391 (Jan 1, 2008).
53. H. Sumimoto, F. Imabayashi, T. Iwata, Y. Kawakami, The BRAF-MAPK signaling pathway is essential for cancer-immune evasion in human melanoma cells. *J Exp Med* **203**, 1651 (Jul 10, 2006).
54. D. S. Aaronson *et al.*, An androgen-IL-6-Stat3 autocrine loop re-routes EGF signal in prostate cancer cells. *Mol Cell Endocrinol* **270**, 50 (May 30, 2007).
55. J. C. Lieblein *et al.*, STAT3 can be activated through paracrine signaling in breast epithelial cells. *BMC Cancer* **8**, 302 (2008).
56. H. Shimizu, K. Mitomo, T. Watanabe, S. Okamoto, K. Yamamoto, Involvement of a NF-kappa B-like transcription factor in the activation of the interleukin-6 gene by inflammatory lymphokines. *Mol Cell Biol*

10, 561 (Feb, 1990).
57. J. Dumortier *et al.*, Human cytomegalovirus secretome contains factors that induce angiogenesis and wound healing. *J Virol* **82**, 6524 (Jul, 2008).
58. B. A. Stout, M. E. Bates, L. Y. Liu, N. N. Farrington, P. J. Bertics, IL-5 and granulocyte-macrophage colony-stimulating factor activate STAT3 and STAT5 and promote Pim-1 and cyclin D3 protein expression in human eosinophils. *J Immunol* **173**, 6409 (Nov 15, 2004).
59. C. Gealy *et al.*, Posttranscriptional suppression of interleukin-6 production by human cytomegalovirus. *J Virol* **79**, 472 (Jan, 2005).
60. H. Wang *et al.*, Targeting interleukin 6 signaling suppresses glioma stem cell survival and tumor growth. *Stem Cells* **27**, 2393 (Oct, 2009).
61. S. Goswami, A. Gupta, S. K. Sharma, Interleukin-6-mediated autocrine growth promotion in human glioblastoma multiforme cell line U87MG. *J Neurochem* **71**, 1837 (Nov, 1998).
62. J. S. Yao *et al.*, Interleukin-6 upregulates expression of KDR and stimulates proliferation of human cerebrovascular smooth muscle cells. *Journal of Cerebral Blood Flow and Metabolism* **27**, 510 (Mar, 2007).
63. M. K. Steiner *et al.*, Interleukin-6 overexpression induces pulmonary hypertension. *Circ Res* **104**, 236 (Jan 30, 2009).
64. D. Sinibaldi *et al.*, Induction of p21WAF1/CIP1 and cyclin D1 expression by the Src oncoprotein in mouse fibroblasts: role of activated STAT3 signaling. *Oncogene* **19**, 5419 (Nov 16, 2000).
65. E. J. Schlaeger, K. Christensen, Transient gene expression in mammalian cells grown in serum-free suspension culture. *Cytotechnology* **30**, 71 (Jul, 1999).
66. B. Dalby *et al.*, Advanced transfection with Lipofectamine 2000 reagent: primary neurons, siRNA, and high-throughput applications. *Methods* **33**, 95 (Jun, 2004).
67. M. Bellon, C. Nicot, Regulation of telomerase and telomeres: human tumor viruses take control. *Journal of the National Cancer Institute* **100**, 98 (Jan 16, 2008).

4

Development of a mathematical model describing STAT3 signaling

Authors:
Erik Slinger[1], Mannus Kempe[2], Frank Bruggeman[2], Marco Siderius[1], Martine J. Smit[1].

[1]Leiden/Amsterdam Center for Drug Research, Division of Medicinal Chemistry, Faculty of Sciences, VU University Amsterdam, De Boelelaan 1083, 1081 HV Amsterdam, the Netherlands.[2]Molecular Cell Physiology, VU University Amsterdam, De Boelelaan 1083, 1081 HV Amsterdam, The Netherlands.

4.1 Abstract

STAT3 signaling is an important mediator of cytokine signaling, and IL-6 in particular. In recent years it has become clear that STAT3 and IL-6 both play an important role in tumor biology. Recently, the virally encoded G-protein coupled receptor US28 has been shown to induce IL-6 production, which subsequently results in STAT3 activation. Furthermore, because STAT3 itself can also induce IL-6 expression there is the potential for establishing a positive feedback loop. In this study a systems biology approach was utilized to investigate the nature of US28-induced IL-6/STAT3 signaling. A mathematical model was developed of the basic IL6-signaling circuitry and cell-to-cell signaling mechanisms. Experiments could qualitatively reproduce model predictions of the consequence of US28-induced IL-6 production and STAT3 activation. Moreover, the model reveals that US28 can provoke an IL-6/STAT3 positive feedback loop, which can cause a population of cells to concertedly switch in states. The data presented here, show that a systems biology approach may be of great help in understanding signaling pathways and to identify new therapeutic targets.

4.2 Introduction

Human cytomegalovirus (HCMV) is a beta-herpesvirus establishing a latent infection of 30–70% (1) among residents in developed countries and up to 90% among residents of developing countries (2). HCMV infection has been proposed to promote the development of malignant glioma (3) and colon cancer (4). It has also been detected as an active infection in several cancer forms.

The genome of HCMV encodes four G-protein-coupled receptors (GPCR), which are homologous to human chemokine receptors (5, 6). Chemokine receptors are involved in immune system regulation (7) and participate in oncogenesis (8). One of the HCMV encoded GPCRs is US28. The presence of US28 causes suppression of the host' immune response against HCMV infection (9) and constitutively activates signaling pathways linked to proliferation (10, 11); mediated by IL6. HCVM-encoded viral GPCRs may play a role in oncogenesis and tumor growth. US28 is known to induce various oncogenic responses in vitro when expressed in NIH-3T3 fibroblasts. US28 is also capable of promoting tumor formation in mice (12).

To investigate the molecular mechanism by which US28 contributes to the progression of oncogenesis, we previously analyzed the US28-induced release of cytokines (11). Conditioned medium from US28-expressing NIH-3T3 cells was analyzed and compared to medium from mock-transfected NIH-3T3 cells. Analysis using an antibody array showed that Interleukin-6 (IL-6) levels were significantly higher in the medium taken from US28 expressing cells. Further investigation showed that US28 activates STAT3 signaling pathway in an indirect fashion. Furthermore, analysis of glioblastoma patients revealed localized expression of US28 around the blood vessels. In the aforementioned study US28-induced IL-6 secretion involved NF-κB. However, because STAT3 can also induce IL-6 expression (13), there is a potential for a positive feedback loop. This would imply that once cells have been exposed to certain IL-6 levels, they will be able to produce enough IL-6 in response to this stimulus to maintain signaling without an exogenous source of IL-6.

To obtain a better understanding of this mechanism we first describe a single cell model for US28 induced IL-6 production and autocrine IL-6 signaling that includes simplified NF-kB and STAT3 signaling. In the second part we organize these single cell models on a lattice. By studying the conditions for IL-6 spreading and IL-6 induced IL-6 synthesis on the lattice, we examined whether irreversible bistability of the single cell module is of key importance for the observed experimental behavior described in **Chapter 3**.

4.3 Results

4.3.1 Development of a single cell mathematical model with IL-6-induced IL-6 synthesis

The essential features of the biological model described in the introduction are illustrated in Figure 1. The US28-induced IL-6 synthesis is mediated by NF-kB signaling (*11, 28*). NF-kB induced transcription of IL-6 leads to the excretion of IL-6 protein in the extracellular fluid. In response to extracellular IL-6, STAT3 is phosphorylated. As mentioned before, STAT3 is a transcription factor regulating the il6 gene. IL-6 is degraded both internally and externally. The relation between the concentration of US28 and active NF-κB as well as the relation between the concentration of extracellular IL-6 (IL-6_E) and phosphorylated STAT3 (STAT3P) is unknown. We model their relation with a Hill equation. This provides the steady state concentrations of STAT3P and active NF-κB based on the concentrations of US28 and IL-6_E. The Hill equation used is noted below:

$$\mathrm{E}_{\mathrm{active}} = \frac{\mathrm{E}_{\mathrm{T}} S^n}{K_A{}^n + S^n}$$

where n is the Hill coefficient, describing the steepness of the curve. S is the concentration of activator and K_A equals the activator concentration at which E_{active} equals

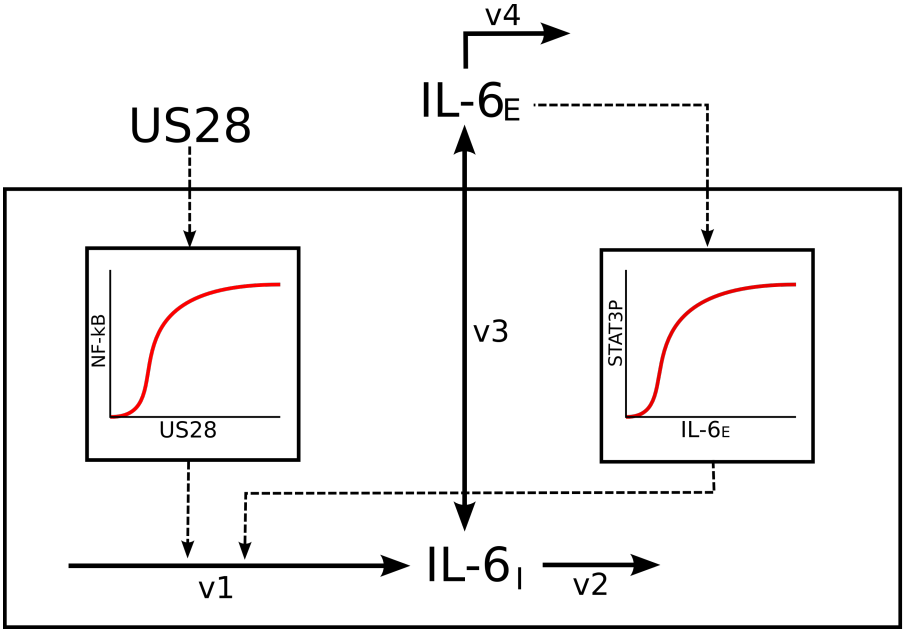

Figure 1. Schematic representation outlining the IL6 positive feedback loop. Two components, NF-κB and STAT3, influence the production rate of IL-6 (v1). v3 indicates the secretion rate and uptake rate of IL-6. v2 and v4 are the respective internal and external degradation rates of IL-6. The left graph gives a possible relation between US28 and NF-kB and the right one the relation between IL6 and active STAT3. Internal IL-6 is denoted as IL-6I and IL-6E denotes the extracellular IL-6.

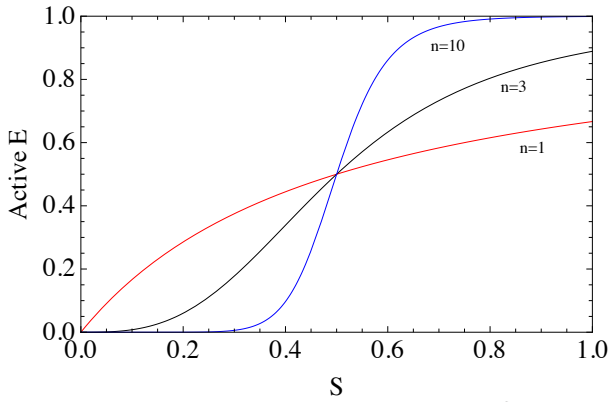

Figure 2. Behavior of the Hill equation for different n. On the y-axis the active portion of E and on the x-axis the input strength (S). When n=1 the Hill equation behaves as a normal saturation curve, n>1 gives a sigmoidal shaped relation.
Parameters: E_T=1, K_A=0.5.

0.5 E_T, where E_{active} denotes the amount of activation of a factor (e.g. STAT3) and E_T is a number that describes the level of activation by a stimulant (e.g. IL-6). When n=1, the Hill equation behaves as a normal saturation curve, n>1 gives sigmoidal behavior (Figure 2).

4.3.2 Analysis of the single cell model

The change of intracellular IL-6 ($IL\text{-}6_I$) over time is the balance between production, degradation and transport of IL-6. For $IL6_E$, the change over time is the result of transport and degradation. The differential equations for the model are:

$$\frac{dIL6_I}{dt} = k_1 NF\varkappa B_{\text{active}} + k_2 STAT3^P - k_3 IL6 + k_5 IL6_E$$

$$\frac{dIL6_E}{dt} = -k_6 IL6_E - k_5 IL6_E + k_4 IL6_E$$

$$NF\varkappa B_{\text{active}} = \frac{E_1 US28^{n1}}{K_1^{n1} + US28^{n1}}$$

$$STAT3^P = \frac{E_2 IL6_E^{n2}}{K_2^{n2} + IL6_E^{n2}}$$

Where k_x denotes the rate constant for the step under consideration, k_1-k_4 are used to describe the rate constant for v1-v4 while k_5 and k_6 describe uptake and degradation of extracellular IL-6, respectively.
Next the behavior of this model was investigated. In Figure 3A the rate of production and degradation is plotted for three different values of US28 activity. In the model the degradation rate only depends on $IL\text{-}6_E$ and is therefore insensitive to changes in US28 activity. The sigmoidal nature of the production rate originates from the sigmoidal relation between $IL\text{-}6_E$ and STAT3P (E_1=5, K_1=3, n_1=5). Due to the sigmoidality, the number of intersections between the rate of production and degradation varies with US28 activity. Each intersection between the two rates in-

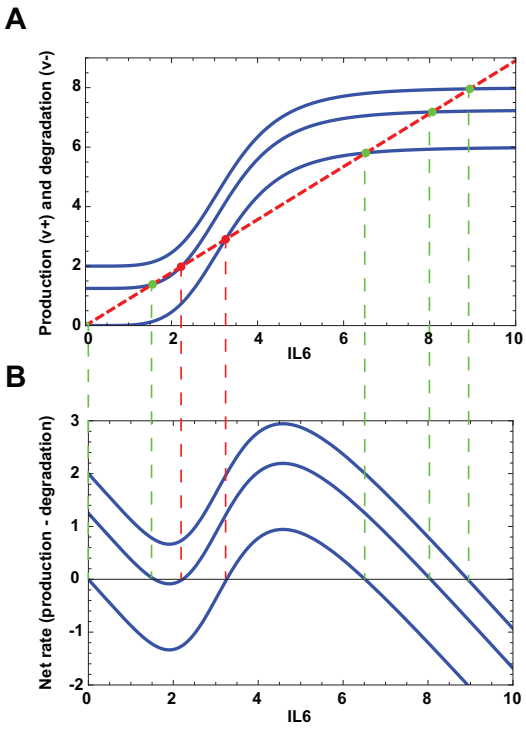

Figure 3. (**A**) Production rates (blue solid lines) and degradation rate (red dashed line) as a function of IL6. The production rate depends on the activity of US28 and is visualized for three different activities (US28activity=0, US28activity=1 US28activity=2). Stable steady state points are indicated in green and unstable steady state points in red. (**B**) Net rate of IL6 production as a function of IL6. The net rate of IL6 production is the difference between IL6 production and IL6 degradation. When the net rate of IL6 production is zero (production equals degradation) the system is at steady state. Parameters: k_1=1, k_2=1.2, k_3=0.9, k_4=10, k_5=1, k_6=0.9, E_1=5, K_1=3, n_1=1, E_2=5, K_2=3, n_2=5.

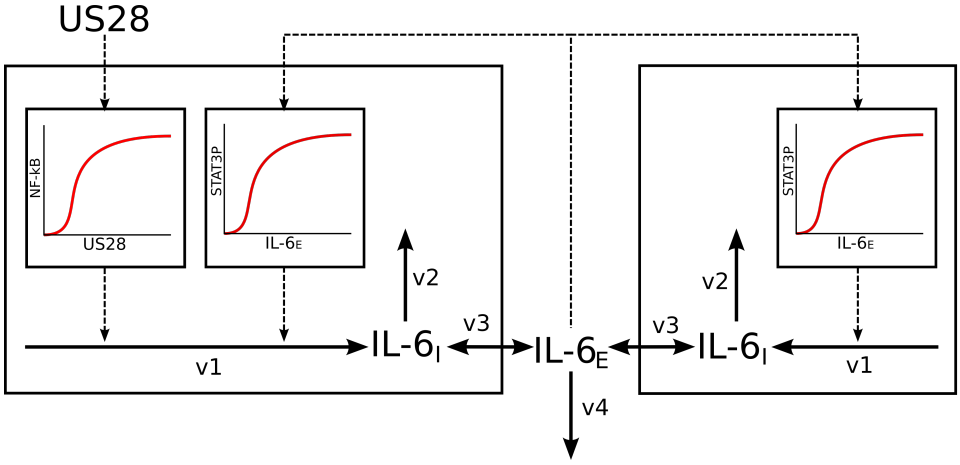

Figure 6. Schematic representation of the IL6 positive feedback loop in a multicellular context. The left hand of the figure corresponds to the single cell model, similar to Figure 6. On the right hand side a second cell is incorporated in the model. In this cell IL-6 production is not induced by US28, but rather by IL-6 originating from the neighboring cell.

dicates a steady state of the model. Different concentrations of the US28 receptor (higher US28 activity) can result in another number of steady state solutions.
The net rate of the system is plotted in Figure 3B. The steady state solutions are the crossings with the x-axis. There are regions for which the net-rate increases with IL-6 (d/dIL-6•dIL6/dt>0). A steady state situated in such a region is unstable; a small increase of IL-6 will lead to a higher production than degradation of IL-6 (positive dIL-6/dt). The system will not be able to return to its former (lower IL-6) state. There are regions for which the net-rate decreases with IL-6 (d/dIL-6•dIL-6/dt<0). A steady state situated in such a region is stable; a small increase of IL-6 will lead to a negative dIL6/dt. The system will return to its former (lower IL-6) state.
A steady state of a system is reached when the production rate equals the degradation rate. In this case they are obtained by solving:

$$0 = k_1 NF\varkappa B_{\text{active}} + k_2 STAT3^{\text{P}} - k_3 IL6_{\text{I}} - k_6 IL6_{\text{E}}$$

The solutions of the system is plotted against the activity of US28 in Figure 4, with the assumption $IL6_I$ and $IL6_E$ are in steady state. The solid lines indicate stable steady state solutions and the dashed line represents unstable ones. When US28 activity increases the steady state is low until a critical value ($US28_{critical}$) is reached. After this point the steady state of the system jumps to a higher value. A decrease in US28 activity will not yield the low steady state value again. Therefore this system is called an irreversible bistable switch. This behavior is called hysteresis; a system is in a certain state depending on its history. Depending on the chosen parameters, this model can also act as a reversible switch and a monostable model (Figure 7).
Apart from the dependence of the system on US28 activity, Figure 4 shows that when US28 activity is lower than $US28_{critical}$ (subcritical), the level of $IL6_E$ at t=0 controls whether the system will settle at the high or low steady state. Values of $IL6_E(0)$ higher than the unstable solution direct the system to the high steady state. The critical $IL6_E$ level ($IL6_{E,critical}$) depends on the US28 activity, for a cell with high US28 activity (but still subcritical) the $IL6_{E,critical}$ decreases.
Figure 5 shows this characteristic in an intuitive manner. Figure 5A shows analyses

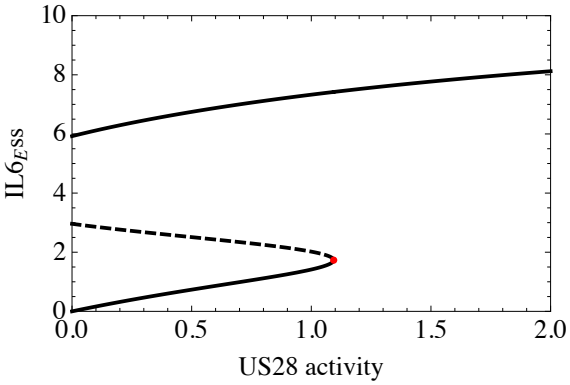

Figure 4. The bifurcation diagram of the single cell model shows the IL6 steady state concentration for different US28 activities. The solid lines represent stable steady states whereas the dotted line represents the unstable ones. For certain values of US28 activity the cell has two possible stable steady states, which one it occupies depends on the history of the cell, a process called hysteresis. The red dot indicates the critcal value of US28. If a cell has experienced an active US28 higher than US28critical in the past, the system will occupy the high steady state. Parameters: k_1=1, k_2=1.2, k_3=0.9, k_4=10, k_5=1, k_6=0.9, E_1=5, K_1=3, n_1=1, E_2=5, K_2=3, n_2=5.

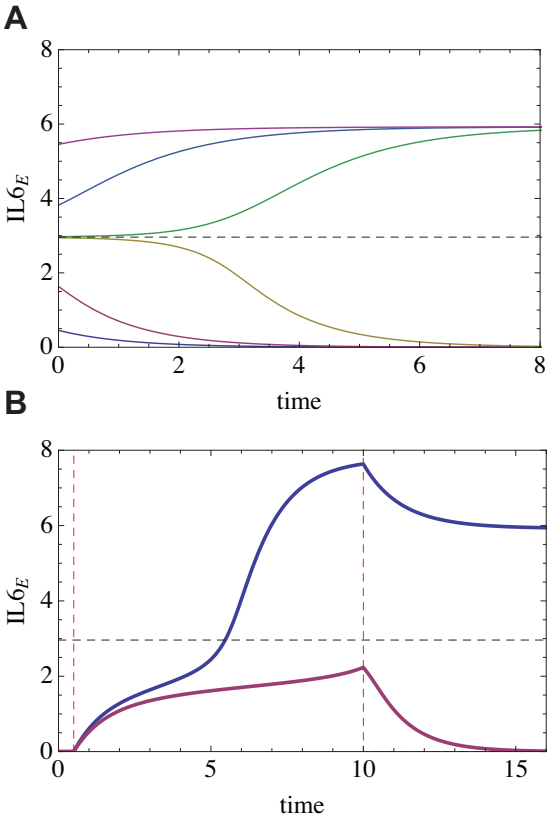

Figure 5. (**A**) Change in IL6 over time with no US28 activity present. The steady state reached by the cell depends on the IL6 present at t=0. The dashed line indicates the critical value of IL6, which determines which steady state is reached. (**B**) When US28 activity is temporal (between the red lines, 0.5 < t < 10), the strength of the signal determines the IL6 produced by the cell. When the activity is high enough to produce more IL6 than the critical IL6 level, the IL6 induced IL6 production is activated to a sufficient level to maintain the IL6 producing phenotype of the cell. Parameters: Parameters: k_1=1, k_2=1.2, k_3=0.9, k_4=10, k_5=1, k_6=0.9, E_1=5, K_1=3, n_1=1, E_2=5, K_2=3, n_2=5.

of $IL6_E$ in the time domain with a subcritical US28 activity (in this case $US28_{activity}$=0). The steady state reached by the system depends on the initial value of $IL6_E$. In the case of a temporal signal the same behavior is observed. When the US28 activity directs the $IL6_E$ above $IL6_{E,critical}$ the system will continue to occupy the high steady state even when the US28 activity is decreased (Figure 5B).

4.3.3 Development of a multicellular model.

As discussed before, STAT3 phosphorylation in NIH-3T3 cells can be induced by treating cells with conditioned medium from US28-expressing cells. This prompted us to study the single cell model in a multicellular context. In this case, a cell expressing US28 can affect the cells around it by secreting IL-6. Subsequently, the surrounding cells will also display STAT3 phosphorylation, resulting in further production of IL-6. This scenario is further explored below.

The single cell model (a US28-expressing cell, Figure 1) is first expanded with another cell that does not express US28, and therefore unable to initiate its own IL6 synthesis by US28. A schematic representation of such a system is given in Figure 6. The additional cell has all the same properties as the US28-expressing cell, except for of course the US28-induced IL-6 production. Therefore, production and degradation of such a cell is already visualized in the lowest sigmoidal line of Figure 3A,

where $US28_{activity}$=0. This figure indicates that there are multiple steady states for this cell, two stable ones and one unstable solution. The switch between the stable steady states is triggered by the IL-6 outside the cell as can be seen in the bifurcation diagram (Figure 4, by $US28_{activity}$=0). The critical external IL-6 level for non-virus-infected cells is visualized in Figure 3 where the steady state concentration of $IL\text{-}6_E$ is plotted against the $IL\text{-}6_E$ concentration at t=0.

This model still treats $IL\text{-}6_E$ in a similar manner as in the single cell model, using it directly as input for the cells. However, a multicellular environment is more complex than this. The secreted IL-6 is hindered to reach another cell in the medium due to diffusion and is subject to extracellular degradation. To study the behavior of cells in a multicellular context we developed a model for spreading of $IL\text{-}6_E$ (or any other substance) over distance and time with a discrete approximation of two dimensional diffusion. This model is expanded with single cell models covering a whole area of interest. Where available we used parameter values from literature for the single cell module and for the diffusion model. We implemented these in our model and we assigned values to the unknown parameters. Parameters for the Hill-equation of the relation between $IL\text{-}6_E$ and STAT3P were selected to obtain three different kinds of behavior of the single cell model. The first set was chosen to make the system act as an irreversible bistable switch. The second set of parameters makes the switch reversible and the third set results in a monostable cell (Table 1 and Figure 7).

In human blood mononuclear cells most IL-6 was found in the extracellular fluid, whereas between 5% and 15% remained in the intracellular compartment (14). Although we are aware that this pattern of secretion of IL-6 might be different in other cell types, we use these findings to choose a secretion rate of 10 s^{-1} and an uptake rate of 1 s^{-1}.

Diffusion of IL-6 in the medium depends on the diffusion coefficient of IL-6. By our knowledge, the exact diffusion coefficient of IL-6 is not documented. There are

Table 1. Overview of parameter settings.

Name	Function	Irr. bistable	Re. bistable	monostable	unit
k_1	Production of $IL6_I$ by signal	1	1	1	s-1
k_2	Production of $IL6_I$ by $IL6_E$	2	2	2	s-1
k_3	Degradation of $IL6_I$	0.01	0.01	0.01	s-1
k_4	Secretion of $IL6_I$	10	10	10	s-1
k_5	Uptake of $IL6_E$	1	1	1	s-1
k_6	Degradation of $IL6_E$	0.01	0.01	0.01	s-1
E_1	Total NfkB	3	3	3	*
K_1	Concentration where $NFkB_{active}$ = 0.5 $NFkB_{total}$	6	6	6	*
n_1	Steepness, Hill coefficient	1	1	1	-
E_2	Total STAT3	1	1	1	*
K_2	Concentration where $STAT3_{active}$ = 0.5 $STAT3_{total}$	**10**	**115**	**200**	*
n_2	Steepness, Hill coefficient	**5**	**5**	**1**	-

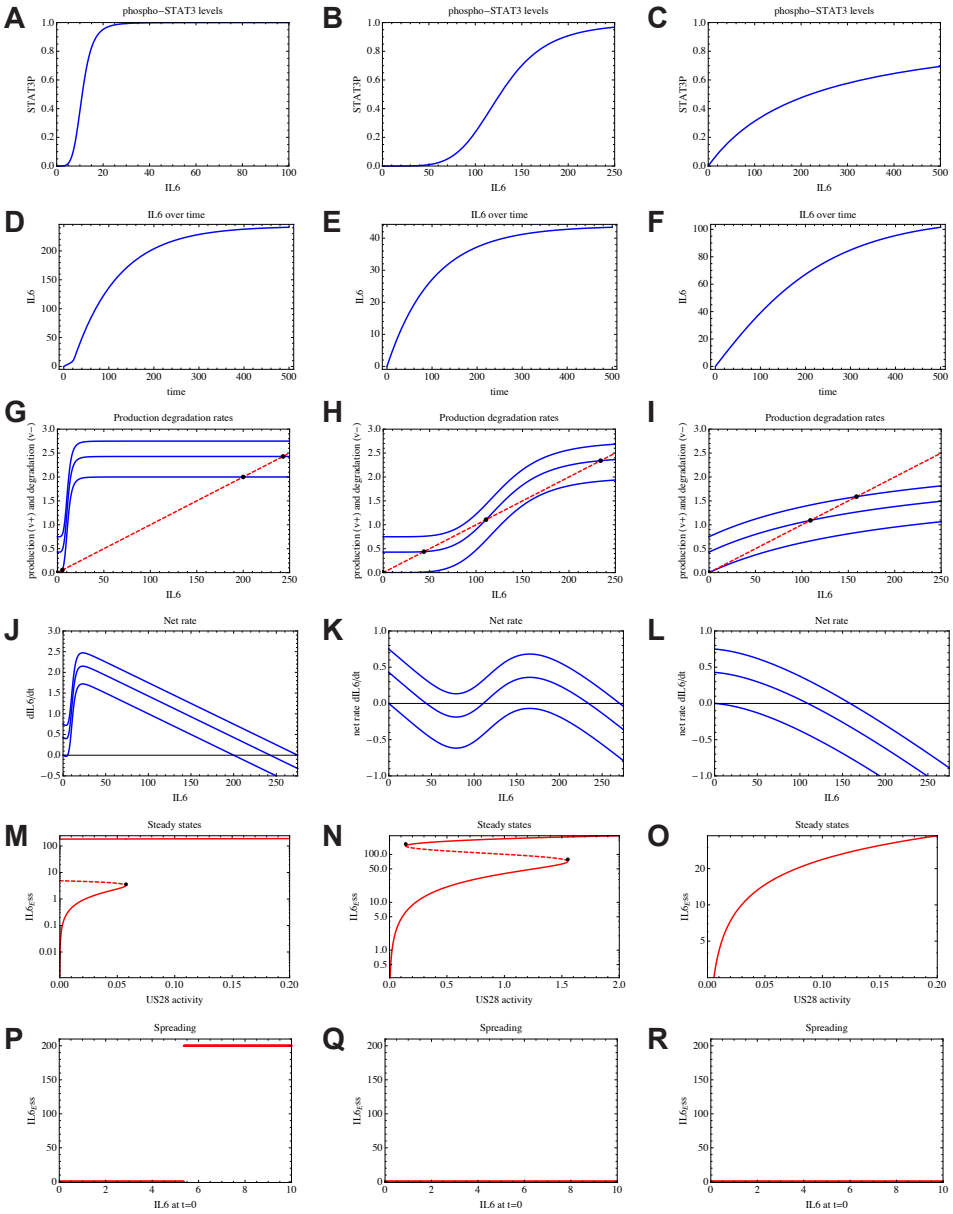

Figure 7. Overview of the behavior of the model for three different parameter settings for the relation between phosphorylated STAT3 and IL6. The parameter values of the three different situations are described in Table 1. The first column of pictures displays the behavior as result of a sigmoidal relation between STAT3P and IL6. This leads to an irreversible bistable system that is also described in the analyses of the single cell model. The second column shows the behavior of the system as a result of a sigmoidal relation between STAT3P and IL6, only here the result is a reversible bistable system. The last column shows the results of the model when STAT3P increases hyperbola as a function of IL6 present in the system. (**A-C**) The IL6 induced STAT3 phosphorylation patterns for the three different parameter settings. **A** and **B** show sigmoidal dependence whereas **C** shows a hyperbola relation. (**D-F**) The change in IL6 over time for the single cell model. The US28 activity is set to 1, which initiates IL6 production in the model. Depending on the parameters for the positive feedback mechanism of IL6 via STAT3 signaling there will be additional IL6 production. These figures show an increase in IL6 that implies an increase in STAT3P. Legend continues on the next page

Figure 7. Continued from previous page. (**G-I**) Production rates (blue solid lines) and degradation rate (red dashed line) as a function of IL6. The production rate depends on the activity of US28 and is visualized for three different activities ($US28_{activity}$=0, $US28_{activity}$=1 $US28_{activity}$=2). Stable steady state points are indicated in green and unstable steady state points in red. Note that with changing the US28 activity the number of steady state solutions varies in **G** and **H**. When there is no US28 activity only the irreversible bistable system has two stable steady state solutions. (**J-L**) The net rate of IL6 production as a function of IL6. When the net rate of IL6 production is zero (production equals degradation) the system is at steady state. As described in the text, a stable steady state is situated in a region where the net rate increases. (**M-O**) The steady state IL6 as a function of the US28 activity. The solid lines represent stable steady states whereas the dotted line represents the unstable ones. For certain values of US28 activity the cell has two possible stable steady states (bistability), which one it occupies depends on the history of the cell. The black dots indicate the critical values of US28 activity. At such point a small change in the US28 activity gives a large transition in the steady state value of IL6. M shows irreversible bistable behaviour, once occupying the high steady state solution branch, no critical US28 activity point is present to return to the low stable solution branch. N shows reversible bistability because such point of return is present. **L** shows that this system is monostable for all US28 activities. (**P-R**) The behavior of the models as a function of the initial IL6 concentration. Only the model with irreversible bistable behavior is sensitive to the initial present IL6. The critical IL6(0) value is the unstable steady state solution of the system.

methods, which estimate the diffusion coefficient of cytokines based on their molecular weight and the radius of gyration (15). This reference gives the diffusion coefficient in an aqueous solution of IL-5 ($9.39\ 10^{-7}\ cm^2s^{-1}$), a cytokine with a molecular weight of 26 kDa. The weight of IL-6 is, depending on the glycosylation and phosphorylation, between 21,5 and 28 kDa. We assume the diffusion coefficient of IL=6 to be in the same order, $D_{IL\text{-}6} = 1*10^{-6}\ cm^2s^{-1}$. An overview of the different parameter settings is described in Table 1. In Figure 7 the analyses using these parameters are shown.

As shown by the single cell analyses the STAT3P increases with ascending IL-6 in our model (Figure 7A-C). As a result of this induced STAT3P, the production rate of IL-6 will increase. We subjected the multicellular lattice model to a high amount of IL-6 (IL-6(0)=220) and followed its behavior over time. On the single cell level we used the three different parameter settings as given in Table 1 and no US28 activity. Given the high IL-6 levels the single cell models on the lattice start producing IL-6. Only the lattice with the irreversible bistable behavior of the single cell model keeps a stable IL-6 concentration on the lattice over time, implying a constant production of IL-6 since there is IL-6 turnover.

Autocrine signaling of IL6 enhances STAT3P and proliferative signaling. Furthermore, paracrine signaling can lead to induced STAT3 phosphorylation in other cells. In this manner, US28 may facilitate tumor progression. The next analysis shows that a single US28-expressing cells can enhance IL-6 production (as a function of enhanced STAT3P) in cells that are not expressing US28. This may enhance proliferative signaling in those cells too.

This experiment has also been done for an irreversible bistable, reversible bistable and mono stable model at the single cell level. The centre cell on the lattice is given a transient US28 activity. In response this cell starts IL6 production and secretion. The external IL6 will diffuse in space and stimulate IL6 production in its surrounding cells. When the single cell behavior is reversible bistable or monostable and no US28 activity is present, the IL6 feedback is too weak to maintain the high IL6 levels in the extracellular space. In fact this is already visualized in the bifurcation

diagrams (Figure 7N-O). When no US28 activity exists the only steady state for the single cell model is reached when IL6 is zero.

4.3.4 Experimental validation of the model

To confirm the models described previously experimentally, several conditions must be met. First of all, the model assumes a sigmoidal relationship between IL-6 levels and the amount STAT3 phosphorylation. Secondly, cells with US28 activity should be able to continue to display STAT3 phosphorylation after US28 activity has been ceased. Finally, medium of US28-expressing cells should be able to induce STAT3 phosphorylation in cells that are not expressing US28. The last condition has already shown to be true in **Chapter 3**, but the first two conditions have not been satisfied yet.

While ideally one would like to switch off US28 at will, this has proven to be difficult. Using inverse agonists on US28 would be preferable. However, while such inverse agonists have been generated (16-18), their potency is not high enough to inhibit proliferation (data not shown). An alternative would be to use an inducible system for controlling US28-expression, however that would entail the generation of several new cell line which would take a significant amount of time. Instead we have opted to reduce the role US28 in the specific case of STAT3 signaling to IL-6 production. In this scenario, US28 activity can be replaced with recombinant IL-6. Using recombinant IL-6, pulse-chase experiments were performed where the cells were pulsed with IL-6 and then followed in time. In Figure 8A, the cells were treated with 10 ng/ml IL-6 for 10 minutes (t=0). Then at t=3, t=8, t=24, and t=32, samples were taken and the phospho-STAT3 content was analyzed by Western-blot analysis. Following quantification and correction for loading using β-actin as loading control, the amount of STAT3 phosphorylation was plotted in a graph against time. This shows that cells treated with IL-6 indeed show sustained STAT3 phosphorylation, while the vehicle treated cells do not show STAT3 phosphorylation. In Figure 8B a similar experiment is shown, but in this case two additional conditions were taken along. In one case, following IL-6 treatment and washing the cells were treated with 1 μg/ml anti-IL-6 neutralizing antibodies. In the other case, the cells were treated with 30 μg/ml cycloheximide which is an inhibitor of protein synthesis. The treatment with anti-IL-6 failed to inhibit STAT3 phosphorylation, indicating that other factors that can activate STAT3 may also be present or that anti-IL-6 may not be able to bind all the IL-6 being secreted. Treatment with cycloheximide completely inhibits STAT3 phosphorylation; this indicates that the cells need to be able to produce new factors in order to display sustained STAT3 phosphorylation.

Utilizing a STAT3 reporter gene, we assessed the amount STAT3 transcriptional activation after treatment with different concentrations of recombinant IL-6 (Figure 8C). The reporter gene data indicates the dose-response of IL-6 treated HEK293T cells.

Thus far indirect methods have been used to assess IL-6 production following an IL-6 pulse. As an extra confirmation, a more direct approach in the form of quan-

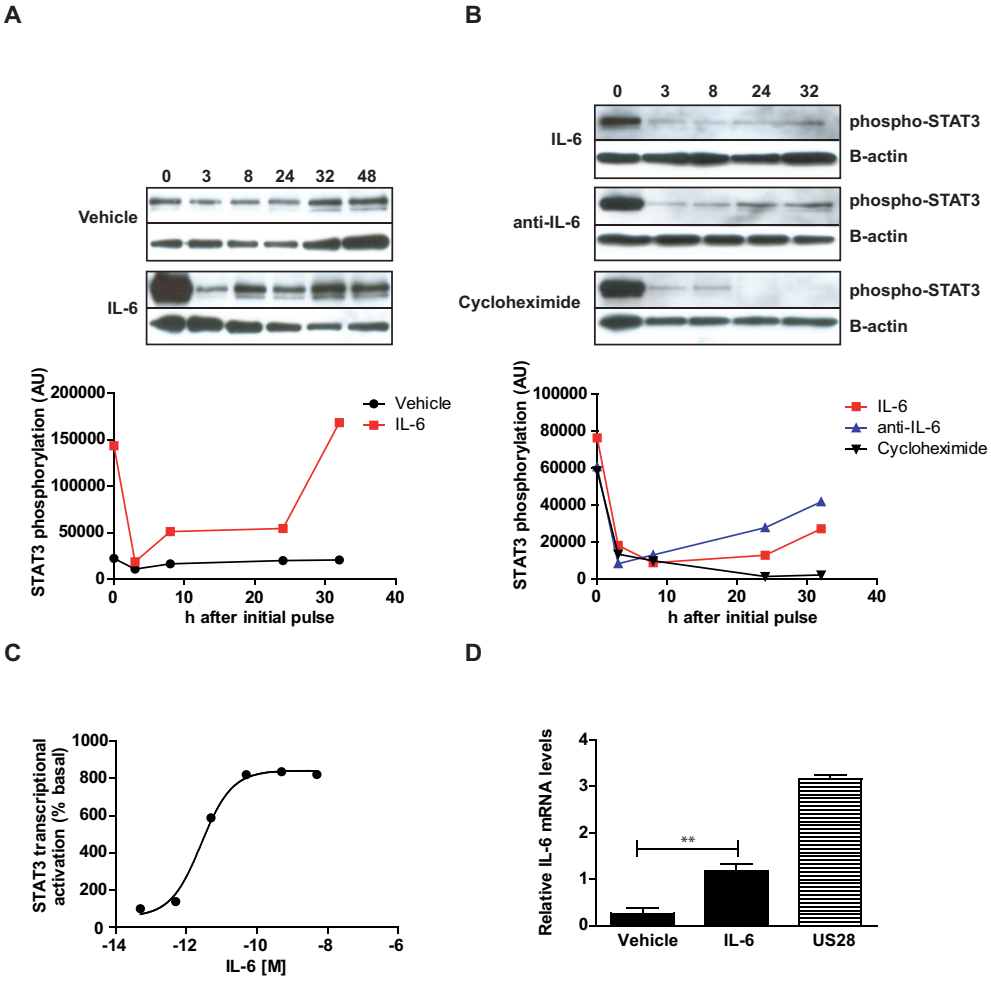

Figure 8. (**A**) A 10 minute pulse with 10 ng/ml recombinant IL-6 results in increased STAT3 phosphorylation in NIH-3T3 up until 32 hours post-pulse. Vehicle treated cells do not show this behaviour (**B**) IL-6-induced STAT3 phosphorylation after the initial treatment can be prevented using 30 ug/ml cycloheximide (protein synthesis inhibitor). However, anti-IL-6 neutralizing antibodies cannot prevent IL-6-induced STAT3 phosphorylation indicating either incomplete neutralization or other factors (eg. IL-5 or IL-10). (**C**) Treatment of NIH-3T3 with different concentrations of recombinant IL-6 shows a sigmoidal relationship between IL-6 concentration and STAT3 phosphorylation. (**D**) Assessment of IL-6 mRNA production shows a 1.2 fold increase of IL-6 mRNA 24 hours post-pulse, while vehicle treated cells show a 0.35 fold decrease of IL-6 mRNA production in the same time-span (**p<0.01). As a positive control US28-expressing cells were used, which show a 3.2 fold increase of IL-6 mRNA versus mock transfected cells.

titative RT-PCR was used to assess IL-6 mRNA production (Figure 8D). This analysis confirmed the result from Figure 8A, showing significantly higher IL-6 mRNA levels in IL-6 treated cells 24 hours after administering the IL-6 pulse ($p<0.01$). As a control US28 expressing cells were used, since these cells are known to produce IL-6 constitutively (11). These data together with those from **Chapter 3** indicate that the model may be a good approximation of what happens in the NIH-3T3 cells.

4.4 Discussion

In this study we investigate US28 activated STAT3 phosphorylation mediated by an IL-6 positive feedback loop. When a human cell is infected with HCMV, the viral gene that encodes the GPCR homologue US28 is transcribed. In proliferating cells, US28 constitutively activates IL-6 transcription mediated by NF-κB signaling. Subsequently, an IL-6 positive feedback loop is activated that includes phosphorylation of the transcription factor STAT3. STAT3P is known to regulate VEGF, an important factor in tumorigenesis (19). Furthermore, STAT3 activation has also been documented in brain tumors (20) and is known to hinder immune surveillance (21). Analyses of human glioblastoma tissue showed US28 expression and activated STAT3 in cells lining blood vessels (11), suggesting that US28 and its activation of STAT3 may play a role in tumor vascularization.

In order to investigate the IL-6 positive feedback mechanism we use a mathematical model based on the experimental data from **Chapter 3**. We model a single cell that includes simplified NF-κB and STAT3 signaling. We apply this to a multicellular set up where spreading of the STAT3-positive phenotype (due to STAT3P) occurs via IL-6 present in the extracellular matrix.

Figure 7J-L shows IL-6 production as a response to US28 activity in our model, for all three different parameter settings. STAT3P levels are known to increase in mock-transfected cells if they are grown in medium originating from US28 transfected cells due to the presence of IL-6 in the medium. Corresponding, the model gives increasing STAT3P levels in response to extracellular IL-6 in all three different parameter settings (Figures 7A-C).

When US28 is active, the model gives a constant production of IL-6 due to NF-kB activation (Figures 7D-F). The parameters of the positive feedback module determine the additional amount of IL-6 production via the positive feedback mechanism. Because US28 activity is constant, so is the US28 induced IL6 production rate. Figures 7G-M show the production rate of IL-6 as a function of the IL6 concentration. The influence of US28 activity is the same at any IL6 concentration. This shows that the parameters of the US28 induced IL6 production do not influence the qualitative behavior of the model. It does influence the US28critcal and the steady state IL6 production in US28 active cells.

In a multicellular context the behavior of the model differs as a function of different parameter settings for the STAT3 phosphorylation level as a function of IL6 (Figure 8). Figure 8 shows a lattice of cells subjected to a high initial IL6. All cells present on

the plate are uninfected meaning that there will be no US28 induced IL6 production. When followed in time, the only multicellular model that is able to maintain the high IL6 levels is the lattice with irreversible bistable cells.
Analyses of the single cell model show the underlying reason for the behavior observed in the multicellular context. When the STAT3P level increases in a hyperbole manner as a function of increasing IL6, there is activation of STAT3 and additional production of IL6 present in a virus infected cell (Figure 7F,I,L,O). When there is no US28 activity in such a cell, there is also no steady state IL-6 production and, accordingly, no STAT3P (Figure 7C). Only when constantly activated by external IL-6 (originating from neighboring cells) such a cell can produce IL6 at a constant rate, but even then the degradation dominates (Figure 7I). In other words, the STAT3-positive phenotype is only present when US28 is present.
The same conclusions can be drawn for sigmoidal dependence between STAT3P and IL-6 that gives reversible bistable IL-6 production for US28 activity (Figure 7N). By increasing US28 activity the system switches to a high steady state of IL-6 level when a level of activity is passed. A second threshold exists that is crossed when the amount of US28 activity diminishes. This results in a rapid decrease in steady state IL6 that eventually returns to zero when no activity is left. Figure 7H and Figure 7K also show the tendency of the model to return to zero (net) IL6 production in US28 negative cells.
Sigmoidal dependence between STAT3P and IL6E can also give rise to an irreversible bistable IL6 production (Figure 7M). This means that the positive feedback loop is self-sustaining after a transient stimulus. This is an interesting property for such a system. In this case the virus is able to spread its proliferative phenotype to surrounding cell without infecting them (Figure 7P). This can be achieved by the secreted IL6 of infected cells, which is sufficient to activate the positive feedback loop for IL6 production in uninfected cells. In contrast to previous cases, the US28 induced IL6 production via NF-kB is not necessary to maintain IL6 production in the single cells (Figure 7G-I).
In the multicellular context, the behavior of the model is strikingly different for the chosen parameter settings. The irreversible bistable single cell model shows an irreversible activation of the proliferating phenotype once initiated by US28 or IL-6. This model implies a spreading of virus-induced phenotype in tissues without infecting individual cells. The following experimental setup may be useful to determine whether the positive feedback mechanism is indeed irreversible.
A first attempt at experimentally validating the model was made. Although only a limit amount of experiment was performed, we can conclude that several characteristics of the model can at least be partially validated. For example, the increased IL-6 expression 24 hours after a pulse with IL-6 indicates that NIH-3T3 cells can be triggered to produce new IL-6 after being subjected to a pulse with IL-6. Normal NIH-3T3 cells temporally exposed to IL-6 show induced STAT3 phosphorylation (Figures 10A,B, and D). Subsequently, activated STAT3 induces IL-6 production. Based on this experiment we propose an experimental setup as follows: Mock transfected

NIH-3T3 cells are to be exposed to medium originating from US28-expressing cells. The cells are subsequently washed, put in fresh medium and induced STAT3P levels are assessed. Because induced STAT3P will lead to IL-6 production, the medium will contain IL-6. If this medium is able to again induce STAT3P in normal NIH-3T3 cells to the same extend as before, the feedback loop may be considered to be self-sustaining/irreversible bistable.

If the feedback mechanism is indeed irreversible bistable, our model indicates that a single infected cell can enhance IL6 production in uninfected cells. High IL-6 means high levels of STAT3P and VEGF, which is of advantage for a tumor and its progression. When the system is not self sustainable, infected cells can induce STAT3 activation and IL6 production in uninfected cells but only locally and only for as long as the infection is present. This actually seems to fit quite well with the observations thus far made of US28 localization in tumors. Only a small subpopulation of the tumor is actually US28 positive, but besides their small number they would be able to influence the entire tumor by secreting factors like IL-6. This behavior may not be unique to HCMV either. The Kaposi Sarcoma associated Herpes Virus (KSHV) encoded GPCR, ORF74, has been shown to induce tumorigenesis in mice (22). Moreover, ORF74, like US28, induces STAT3 activation (23). Interestingly, immuno staining for ORF74 in Kaposi Sarcoma lesions show that only a small subset of the tumor cell population is ORF74 positive (24), which implies that a similar mechanism may be at play.

In conclusion, we present here a mathematical model describing US28-induced STAT3 activation. This model shows that STAT3-signaling in general has the potential to grow out of control. Considering its important role in the immune system, it seems logical that IL-6 signaling through STAT3 is very potent. However, there must be negative regulation at the same time to prevent the formation of positive feedback loops. One of these mechanisms is negative regulation by the Suppresors of Cytokine Signaling (SOCS), these proteins silence STAT3 signaling after activation by ligands (such as IL-6) (25). There are two general scenarios that allow for a positive feedback loop to form. The first scenario entails inactivating mutations in the SOCS genes. Such mutations have been described, and are associated with cancer development and progression (26, 27). The second scenario would involve US28 itself, in this case US28-induced IL-6 production overcomes silencing of STAT3 signaling by SOCS. In this case US28 renders a cell more susceptible to engage into a IL-6 drive positive feedback loop.

The model presented here is a first step in further understanding US28-induced STAT3 activation, and perhaps STAT3 activation in general. With this understanding it may be possible to formulate strategies of interfering in this feedback loop which may result in new therapeutic strategies against STAT3 associated diseases.

4.5 Materials and methods

Materials and reagents
Antibodies directed against phospho-STAT3 (Tyr705) and STAT3 were purchased from Cell Signaling Technology (Boston, MA, USA). Neutralizing antibody against murine IL-6 was from BD Biosciences (Franklin Lakes, NJ, USA). Tris base and cycloheximide were obtained from Sigma-Aldrich (St. Louis, MO); other chemicals were obtained from Applichem (Darmstadt, Germany). Murine IL-6 was obtained from Peprotech (Rocky Hill, NJ, USA). Dulbecco's Modified Eagle Medium (DMEM) was purchased from PAA Laboratories (Pasching, Austria). Bovine serum was purchased from Invitrogen.

Cell culture
Murine NIH-3T3 cells were cultured in Dulbecco's Modified Eagle Medium (DMEM) supplemented with 50 IU/ml penicillin, 50 µg/ml streptomycin, and 10% bovine serum. Stable clones of NIH-3T3 expressing US28 or US28 R129A mutant (12) were kept under a selective pressure of 400 µg/ml neomycin in the culture medium to ensure homogenous receptor expression in the cells. Expression of US28 in the NIH-3T3 cells was confirmed using [^{125}I]-CCL5 binding (specific binding was determined using CX3CL1 10^{-7} M), as previously described (28).

Western-blot analysis
A Biorad (Hercules, CA) minigel system was used to perform SDS/PAGE, and a Biorad electroblot system was used to transfer protein samples to a 0.45 µm polyvinylidene fluoride membrane. Cells were lysed in RIPA-buffer supplemented with α-complete protease inhibitor cocktail from Hoffmann-La Roche (Basel, Switzerland), 1 mM PMSF, 1 mM $NaVO_4$, and 1 mM NaF added. Samples were normalized using the BCA total protein determination kit obtained from Thermo Fisher Scientific (Rockford, IL, USA). Blots were quantified using ImageJ (Rasband, W.S., U. S. National Institutes of Health, Bethesda, MD, USA).

Quantitative RT-PCR
For assessing the amount of IL-6 mRNA cells were first scraped in ice-cold phosphate buffered saline (PBS). The cells were subsequently pelleted by centrifugation and stored as a pellet at -80°C until analysis. The RNA was isolated from the samples using the RNeasy kit from Qiagen (Hilden, Germany). Following RNA isolation, the amount of RNA obtained was determined by use of a NanoDrop from Thermo Fisher Scientific. For cDNA synthesis 200 ng RNA was used as template, and for the synthesis itself iScript cDNA synthesis kit from Biorad was utilized. PCR reactions were performed using SYBR Green mix with MyiQ Real-Time PCR detection system (Bio-Rad). The validated primers targeting murine IL-6 mRNA were obtained from Origene (Rockville, MD, USA).

Development of the mathematical models
For development of the models Mathematica 7.0 from Wolfram Research was used (Champaign, IL, USA).

Statistical analysis

All experiments were performed at least two times in duplicate. When comparisons between treated and vehicle-treated cell were made a Student T-test was performed using the GraphPad Prism software (San Diego, CA, USA). Bars and error bars represent the mean and SEM, respectively.

References

1. H. J. Snippert et al., Prominin-1/CD133 marks stem cells and early progenitors in mouse small intestine. Gastroenterology 136, 2187 (Jun, 2009).
2. M. K. Gandhi, R. Khanna, Human cytomegalovirus: clinical aspects, immune regulation, and emerging treatments. Lancet Infect Dis 4, 725 (Dec, 2004).
3. D. A. Mitchell et al., Sensitive detection of human cytomegalovirus in tumors and peripheral blood of patients diagnosed with glioblastoma. Neuro Oncol 10, 10 (Feb, 2008).
4. L. Harkins et al., Specific localisation of human cytomegalovirus nucleic acids and proteins in human colorectal cancer. Lancet 360, 1557 (Nov 16, 2002).
5. M. S. Chee, S. C. Satchwell, E. Preddie, K. M. Weston, B. G. Barrell, Human cytomegalovirus encodes three G protein-coupled receptor homologues. Nature 344, 774 (Apr 19, 1990).
6. U. A. Gompels, H. A. Macaulay, Characterization of human telomeric repeat sequences from human herpesvirus 6 and relationship to replication. J Gen Virol 76 (Pt 2), 451 (Feb, 1995).
7. M. Thelen, J. V. Stein, How chemokines invite leukocytes to dance. Nat Immunol 9, 953 (Sep, 2008).
8. F. Balkwill, Cancer and the chemokine network. Nat Rev Cancer 4, 540 (Jul, 2004).
9. J. R. Randolph-Habecker et al., The expression of the cytomegalovirus chemokine receptor homolog US28 sequesters biologically active CC chemokines and alters IL-8 production. Cytokine 19, 37 (Jul 7, 2002).
10. D. Maussang et al., The human cytomegalovirus-encoded chemokine receptor US28 promotes angiogenesis and tumor formation via cyclooxygenase-2. Cancer Res 69, 2861 (Apr 1, 2009).
11. E. Slinger et al., HCMV-encoded chemokine receptor US28 mediates proliferative signaling through the IL-6-STAT3 axis. Sci Signal 3, ra58 (Aug 3, 2010).
12. D. Maussang et al., Human cytomegalovirus-encoded chemokine receptor US28 promotes tumorigenesis. Proc Natl Acad Sci U S A 103, 13068 (Aug 29, 2006).
13. H. Sumimoto, F. Imabayashi, T. Iwata, Y. Kawakami, The BRAF-MAPK signaling pathway is essential for cancer-immune evasion in human melanoma cells. J Exp Med 203, 1651 (Jul 10, 2006).
14. N. Barker et al., Identification of stem cells in small intestine and colon by marker gene Lgr5. Nature 449, 1003 (Oct 25, 2007).
15. N. Barker et al., Lgr5(+ve) stem cells drive self-renewal in the stomach and build long-lived gastric units in vitro. Cell Stem Cell 6, 25 (Jan 8, 2010).
16. U. Fischer et al., A different view on DNA amplifications indicates frequent, highly complex, and stable amplicons on 12q13-21 in glioma. Mol Cancer Res 6, 576 (Apr, 2008).
17. K. Kemper, C. Grandela, J. P. Medema, Molecular identification and targeting of colorectal cancer stem cells. Oncotarget 1, 387 (Oct, 2010).
18. X. Liu et al., beta-Catenin overexpression in malignant glioma and its role in proliferation and apoptosis in glioblastma cells. Med Oncol, (Mar 19, 2010).
19. G. Niu et al., Constitutive Stat3 activity up-regulates VEGF expression and tumor angiogenesis. Oncogene 21, 2000 (Mar 27, 2002).
20. H. Wang et al., Targeting interleukin 6 signaling suppresses glioma stem cell survival and tumor growth. Stem Cells 27, 2393 (Oct, 2009).
21. H. Yu, M. Kortylewski, D. Pardoll, Crosstalk between cancer and immune cells: role of STAT3 in the tumour microenvironment. Nat Rev Immunol 7, 41 (Jan, 2007).
22. C. Bais et al., G-protein-coupled receptor of Kaposi's sarcoma-associated herpesvirus is a viral oncogene and angiogenesis activator. Nature 391, 86 (Jan 1, 1998).
23. M. Burger, T. Hartmann, J. A. Burger, I. Schraufstatter, KSHV-GPCR and CXCR2 transforming capacity and angiogenic responses are mediated through a JAK2-STAT3-dependent pathway. Oncogene 24, 2067 (Mar 17, 2005).
24. C. J. Chiou et al., Patterns of gene expression and a transactivation function exhibited by the vGCR (ORF74) chemokine receptor protein of Kaposi's sarcoma-associated herpesvirus. J Virol 76, 3421 (Apr, 2002).
25. D. J. Hilton, Negative regulators of cytokine signal transduction. Cell Mol Life Sci 55, 1568 (Sep, 1999).
26. F. Pierconti et al., Epigenetic silencing of SOCS3 identifies a subset of prostate cancer with an aggressive behavior. The Prostate, n/a (2010).
27. Y. C. Lin et al., Adenovirus-mediated SOCS3 gene transfer inhibits the growth and enhances the radiosensitivity of human non-small cell lung cancer cells. Oncol Rep 24, 1605 (Dec, 2010).
28. P. Casarosa et al., Constitutive signaling of the human cytomegalovirus-encoded chemokine receptor US28. J Biol Chem 276, 1133 (Jan 12, 2001).

5

Constitutive β-catenin signaling by the viral chemokine receptor US28

Adapted from:
Ellen V. Langemeijer*, Erik Slinger*, Sabrina de Munnik, Andreas Schreiber, David Maussang, Henry Vischer, Folkert Verkaar, Rob Leurs, Marco Siderius and Martine J. Smit
PLoS One (In press)

* authors contributed equally to this manuscript

5.1 Abstract

Chronic activation of Wnt/β-catenin signaling is found in a variety of human malignancies including melanoma, colorectal and hepatocellular carcinomas. Interestingly, expression of the HCMV-encoded chemokine receptor US28 in intestinal epithelial cells promotes intestinal neoplasia in transgenic mice, which is associated with increased nuclear accumulation of β-catenin. In this study we show that this viral receptor constitutively activates β-catenin and enhances β-catenin-dependent transcription. Our data illustrate that this viral receptor does not activate β-catenin via the classical Wnt/Frizzled signaling pathway. Analysis of US28 mediated signaling indicates the involvement of the Rho-Rho kinase (ROCK) pathway in the activation of β-catenin. Moreover, cells infected with HCMV show significant increases in β-catenin stabilization and signaling, which is mediated to a large extent by expression of US28. The modulation of the β-catenin signal transduction pathway by a viral chemokine receptor provides alternative regulation of this pathway, with potential relevance for the development of colon cancer and virus-associated diseases.

5.2 Introduction

The Wnt/β-catenin signaling pathway plays critical roles in embryonic development, stem cell self-renewal and regeneration (*1, 2*). Perturbations in this signaling cascade have been implicated in the pathogenesis of cancer. Notably, chronic activation of Wnt/β-catenin signaling is found in a variety of human malignancies including melanoma, colorectal and hepatocellular carcinomas (*3, 4*). Accordingly, components of the Wnt/β-catenin pathway are important targets for cancer therapeutics (*3*). In the absence of an extracellular Wnt ligand, cytoplasmic β-catenin is phosphorylated through the action of the "destruction complex", a large protein assembly that contains the Ser/Thr kinases casein kinase 1α (CK1), glycogen synthase kinase 3 (GSK-3) and the tumor suppressors Axin and Adenomatous polyposis coli (APC) (*1*). Phosphorylation of β-catenin targets it for ubiquitin-mediated proteasomal degradation. However, upon stimulation of the seven-transmembrane receptor Frizzled and the single-pass low-density lipoprotein receptor-related protein LRP5/6 by a Wnt ligand, the destruction complex function is compromised through a not fully understood mechanism. As a result, β-catenin will not be phosphorylated and will no longer be subject to degradation, and will subsequently translocate to the nucleus (*5*). Nuclear β-catenin functions as a transcriptional co-activator of target genes such as c-*myc* and cyclin D1, which are involved in proliferation, survival and oncogenic transformation (*6-8*).

The importance of GPCR-mediated signaling in onset and development of various types cancer (*9*) is underscored by the observation that β-catenin activation is triggered by a 7TM spanning receptor, Frizzled which is activated by its cognate ligand Wnt (*1*). Besides Frizzled receptors, a few other G protein-coupled receptors (GPCRs) mediate β-catenin induced transcriptional activation (*10, 11*). The lysophosphatidic acid LPA2 receptor and LPA3 both trigger β-catenin stabilization and cell proliferation via protein kinase C activation (*12*). Additionally, the pro-inflammatory metabolite prostaglandin E2 activates β-catenin through activation of its cognate receptor (*13*). The human protease-activated receptor-1 (PAR-1) stabilizes β-catenin through phosphorylation of GSK-3b at Ser9 . Altogether, these pathways converge on the Wnt signaling route to induce cytoplasmic β-catenin accumulation, nuclear localization, and enhanced transcriptional activation (*14*).

In this study we show that the human cytomegalovirus (HCMV)-encoded GPCR US28 positively modulates β-catenin signaling, resulting in enhanced β-catenin-dependent transcription. US28 is one of four GPCRs encoded by the HCMV (*15*). Interestingly, this widely spread b-herpesvirus (*16*) has been associated with vascular diseases (*17*) and is suggested to act as an oncomodulator (*18*). All four HCMV-encoded GPCRs (vGPCRs) show high homology to human chemokine receptors, which play a fundamental role in the control and regulation of the immune system and in the progression of cancer and metastasis (*19, 20*). US28 is able to signal in a constitutive, ligand-independent, manner via $G\alpha_q$ and Gβγ but also in a ligand-dependent manner via $G\alpha_{12}$ to proliferative and pro-angiogenic signaling pathways (*15, 21, 22*).

US28 has oncogenic properties as US28-expressing NIH-3T3 cells promote tumorigenesis when injected into nude mice (*23*). Moreover, US28 expression was detected in human glioblastomas and medulloblastomas, which was associated with increased STAT3/IL-6 and COX-2 activity (*24-26*) Moreover, transgenic mice expressing US28 in intestinal epithelial cells, including LGR5-positive stem cells, develop adenomas and adenocarcinomas, associated with increases in β-catenin protein stabilization and nuclear localization (*27*). Additionally, transcriptional profiling of US28-expressing fibroblasts indicated also an overrepresentation of genes involved in the Wnt/β-catenin signaling pathway (*28*). These observations suggest that US28 may facilitate transformation and development of intestinal neoplasia via activation of β-catenin (*27*).
In this study we show that the viral chemokine receptor US28 positively modulates the β-catenin pathway via a non-conventional novel pathway, involving Rho kinase.

5.3 Results

5.3.1 Viral chemokine receptor US28 activates the β-catenin pathway.

Transgenic mice expressing US28 in intestinal epithelial cells develop adenomas and adenocarcinomas that express high levels of nuclear β-catenin protein (*27*). Additionally, US28-mediated up-regulation of genes associated with β-catenin signaling was described (*28*). These findings and the role of β-catenin in oncogenesis (*1, 2*), prompted us to investigate the mechanism by which this viral GPCR activates β-catenin signaling. Since this receptor displays constitutive active properties (*29*) we used the wild type (WT) as well as a G protein-uncoupled mutant receptor (US28-$R^{129}A$) in these studies. US28-WT expressing NIH-3T3 cells displayed [^{125}I]-CCL5 binding and increased inositol phosphate production compared to mock-transfected cells (Fig. 1A,B), indicative of proper plasma membrane targeting and functionality of the receptor. Cells expressing the G protein-uncoupled mutant US28 (US28-$R^{129}A$) receptor displayed [^{125}I]-CCL5 binding but no constitutive signaling (Figure 1A, B). Using Western blot analysis, non-phospho (active) β-catenin levels were shown to be elevated in US28-expressing NIH-3T3 cells compared to mock-transfected and US28-$R^{129}A$ expressing cells (Figure 1C). Further indication for US28-mediated activation of β-catenin signaling was generated using a β-catenin-specific reporter gene construct containing TCF/Lef binding sites (TOPflash) (*30*). Analysis of activation of TOPflash in the NIH-3T3 cells stably expressing US28 confirmed US28-mediated activation of β-catenin signaling (Figure 1D). As expected stable expression of the G protein-uncoupled mutant (US28-$R^{129}A$) did not display β-catenin activation. Also in HEK293T cells, increasing expression of US28 resulted in dose-dependent activation of the β-catenin signaling pathway as demonstrated using the TOPflash reporter gene (Figure 1E). A reporter gene containing mutant TCF/Lef-binding sites (FOPflash), used as a negative control, was not induced in US28 expressing cells (data not shown). In accordance with the Western blot data, cells expressing the G protein-uncoupled mutant US28-$R^{129}A$ did not display TOPflash reporter gene activity,

indicating the importance of G-protein signaling in US28-induced activation of the β-catenin signaling pathway (Figure 1E). Treatment of US28 transfected cells with the US28 small molecule inverse agonist VUF6064 (*31*) at a 10μM concentration, prevented activation of the Tcf-Lef reporter gene construct (Figure 1E).
To investigate whether US28-mediated β-catenin signaling can be modulated by chemokine ligands, we stimulated US28-expressing cells with CCL5, which enhances US28-dependent signaling through $G\alpha_q$ and Gα12 pathways (*32*). Stimulation of US28 with 100 nM CCL5 yielded a small but significant increase in TOPflash reporter gene activity (Figure 1F). Expression of CCR1, a human chemokine receptor displaying close homology to US28, did not induce activation of TOPflash, neither in a constitutive manner, nor upon stimulation with 100 nM of its endogenous ligand CCL5 (Figure 1F).

5.3.2 US28 activates β-catenin/TOPflash via a non-classical signal transduction pathway.

We next compared the mechanism by which the classical activator of the Wnt/Frizzled pathway Wnt3a and US28 activate β-catenin signaling. As depicted in Figure 2A, both Wnt3a [200 ng/ml] and US28 expression induced stabilization of β-catenin in NIH3T3 cells. Activation of β-catenin through the classical Wnt/Frizzled pathway involves the CK1g/GSK3b-mediated phosphorylation of LRP 5/6, which leads to recruitment of Axin and Dishevelled to the plasma membrane, culminating in the disruption of the destruction complex (*33, 34*). Analysis of LRP6 phosphorylation in US28-expressing cells indicated that in contrast to Wnt3a-stimulated β-catenin activation of either mock or US28 transfected cells, LRP6 phosphorylation was absent at serine residue 1490, suggesting an alternative mechanism of β-catenin activation for US28 (Figure 2B and Figure S1). In line with this notion, activation of TOPflash activity through Wnt3a and US28 were additive (Figure 2C), suggesting parallel modes of pathway activation. These data illustrate that US28 does not activate β-catenin via the classical Wnt/Frizzled signaling pathway. To investigate this alternative mechanism of US28-mediated β-catenin signaling, various inhibitors of potential effectors of the GSK-3b/APC destruction complex, such as PLC (U73122), PKC (203291), Akt (124005), PI3K (Wortmannin and LY294002), Src (PP-2) and STAT-3 (Stattic) were analysed as potential modulators of US28-mediated β-catenin activation. Neither of these showed any effect on US28-induced TOPflash reporter gene activation (data not shown).
Earlier studies attributed a role for COX-2 in US28-mediated cellular responses (*24, 28*). Since COX-2 activation has been linked to activation of the β-catenin pathway (*13*) we analysed the effect of celecoxib (COX-2 inhibitor) on US28-mediated β-catenin-dependent reporter gene activity. Celecoxib treatment inhibited the TOPflash reporter gene activity only partially at relatively high celecoxib concentrations, indicating only a minor contribution of COX-2 (Figure 2D).

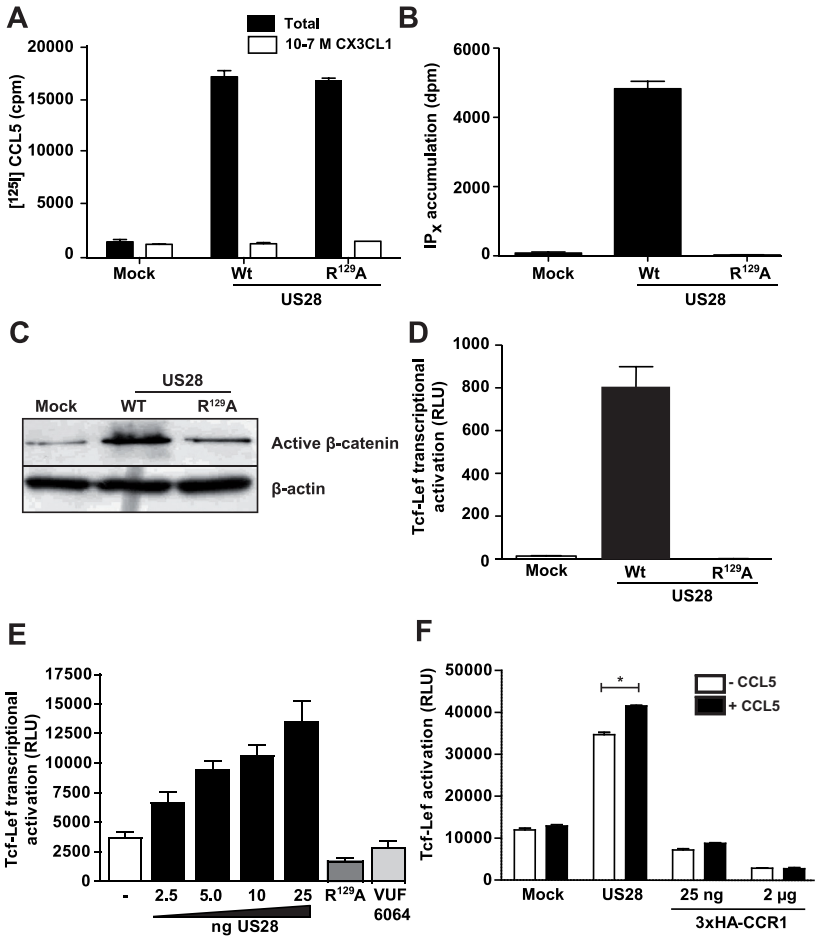

Figure 1. US28 induces constitutively activates β-catenin signaling. US28 is expressed and functional in NIH-3T3 cells. (**A**) Whole cell binding of ^{125}[I]-CCL5 on NIH-3T3 cells expressing wild-type (WT), mutant R^{129}A or HA-tagged US28 is displaced by fractalkine (CX3CL1). (**B**) US28-WT constitutively stimulates inositol phosphate (IPx) accumulation in NIH-3T3, while the non-G protein-coupling mutant US28-R^{129}A shows no activation. (**C**) Total cell extracts of NIH-3T3 cells stably expressing US28, the non G-protein-coupling mutant and empty plasmid control (mock) were analysed on Western blot with antibodies recognizing the non-phospho (active) β-catenin, total β-catenin and actin. (**D**) NIH-3T3 cells stably expressing US28 and the non G-protein coupling US28 mutant R^{129}A were transfected with the Tcf-Lef reportergene construct. Luciferase activity was measured 24hr after transfection. (**E**) US28 dose-dependently induces Tcf-Lef transcriptional activation in HEK293T cells. The non-G protein coupling mutant US28 R^{129}A does not display activation of the reportergene at 25ng DNA transfected (dark grey bar). Treatment of HEK293T cells transfected with 25ng US28 DNA with inverse agonist VUF 6064 (10 µM) prevents activation of Tcf-Lef reortergene (light grey bar). (**F**) HEK293T cells transfected with the human chemokine receptor CCR1 and the Tcf-Lef reportergene construct do not show Tcf-Lef activation nor after exposure to 100 nM CCL5 (RANTES). US28 expressing HEK293T cells display constitutive signaling to the Tcf-Lef reportergene, which is significantly enhanced by exposure to 100 nM CCL5 (RANTES).

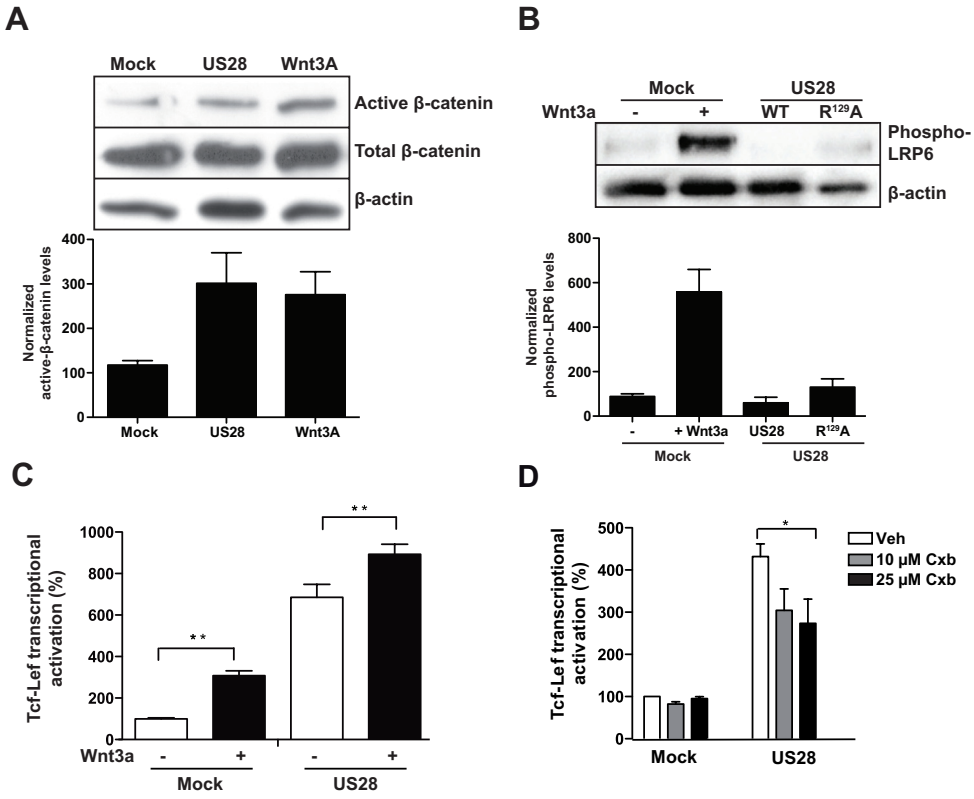

Figure 2. Classical Wnt/Frizzled/β-catenin signaling is not involved in US28-mediated Tcf-Lef activation. (**A**) Western blot analysis of total cell extracts of NIH-3T3 cells, stably expressing US28 or an empty plasmid (mock) which were treated with Wnt3a-(overnight, 200ng/ml) and vehicle treated mock cells. The blot was probed with antibodies recognizing the non-phosphorylated (active) β-catenin, total β-catenin and actin. A representative blot is shown and normalized quantifications of (active) β-catenin of independent experiments are shown below the blot. (**B**) Western blot analysis of total cell extracts of NIH-3T3 cells stably expressing US28, the non G-protein coupling US28 mutant $R^{129}A$ or an empty plasmid (mock) and Wnt3a-treated mock cells. The blot was probed with antibodies recognizing Lrp6-phospho-ser^{1490} and β-actin. A representative blot is shown and normalized quantifications of Lrp6-phospho-ser^{1490} of independent experiments are shown below the blot. (**C**) HEK293T cells co-transfected with the Tcf-Lef reporter gene construct and either US28-expressing or an empty control plasmid (mock) exposed to Wnt3a (overnight, 200 ng/ml). Luciferase activity was measured 24hr after transfection and is displayed here as the percentage of the non-treated mock control that is set at 100%. (**D**) HEK293T cells co- transfected with the Tcf-Lef reportergene and an US28-expressing construct or empty plasmid control (mock) were exposed to various concentrations (ON, 10-25 μM) of the COX2 inhibitor celecoxib (Cxb). Tcf-Lef reporter gene activation was measured 24hr after transfection and is displayed here as the percentage of the mock control that is set at 100%.

5.3.3 G protein involvement in US28 enhanced TOPflash reporter gene activation. The complete lack of activity of the G protein-uncoupled receptor US28-$R^{129}A$ mutant towards β-catenin signaling suggested that G protein coupling is essential for activation of β-catenin by US28. The involvement of G-proteins in US28-mediated TOPflash reporter gene activation was further examined by co-expressing different G protein subunits or by co-expressing constructs known to negatively regulate G protein function. Co-transfection of the Ga-proteins $G\alpha_s$, $G\alpha_{i2}$, $G\alpha_{i3}$, $G\alpha_{11}$, $G\alpha_{13}$ with US28 did not influence TOPflash reporter gene activation nor did overnight treatment with the $G\alpha_i$–specific inhibitor pertussis toxin (PTX) (data not shown). Co-expression of $G\alpha_q$ enhanced US28-mediated TOPflash reporter gene activation, while knocking down $G\alpha_q$ with $shG\alpha_q$ resulted in over 50% inhibition of US28-mediated TOPflash activation (Figure 3A). Downregulation of $G\alpha_q$ protein levels was confirmed by Western blot analysis (Figure 3B). Expression of the regulator of G protein signal-

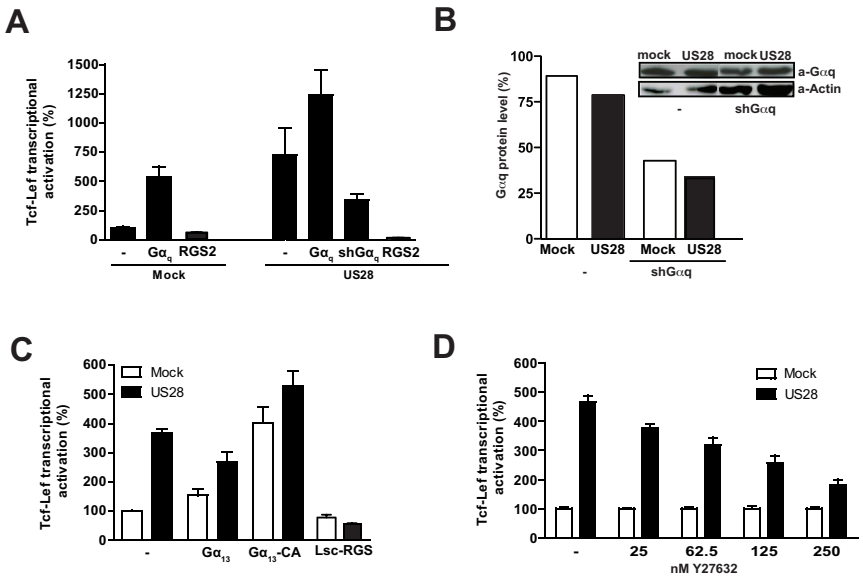

Figure 3. G protein involvement in US28-mediated Tcf-Lef activation. (**A**) HEK293T cells were co-transfected with the Tcf-Lef reporter gene construct, a US28-expressing construct or empty plasmid control (mock) and various constructs expressing Gα-proteins as indicated, $G\alpha_{q\text{-}11}$ shRNA construct or a construct expressing regulator of G protein signaling 2 (RGS2), known to specifically interfere with $G\alpha_q$ signaling. Tcf/Lef reporter gene activation was measured 24hr after transfection and is displayed here as the percentage of the mock control that is set at 100%. (**B**) HEK293T cells were co-transfected with the Tcf-Lef reporter gene construct, US28-expressing construct or empty plasmid control (mock) and an shRNA construct to decrease protein levels of Gαq. Total cell extracts were analysed on Western blot using antibodies recognizing $G\alpha_q$ or β-actin (insert). Bars represent level of $G\alpha_q$ protein level compared to the actin levels, with the ratio in non-treated mock cells set at 100%. (**C**) HEK293T cells were co-transfected with the Tcf/Lef reporter gene construct, a US28-expressing construct or empty plasmid control (mock) and various constructs expressing $G\alpha_{13}$, a constitutive active (CA) $G\alpha_{13}$ or Lsc-RGS, encoding the RGS domain of the Rho GTPase guanine nucleotide exchange factor (Rho-GEF) Lsc, known to specifically interfere with transmembrane signaling mediated by activated $G\alpha_{12/13}$. Tcf/Lef reporter gene activation was measured 24hr after transfection and is displayed here as the percentage of the mock control that is set at 100%. (**D**) HEK293T cells co-transfected with the Tcf/Lef reporter gene construct, a US28-expressing construct or empty plasmid control (mock) were treated (overnight) with various concentrations of the ROCK inhibitor Y27632 as indicated.

ing 2 (RGS2), which is known to specifically interfere with $G\alpha_q$-mediated signaling (*35*) strongly reduced US28-induced TOPflash activation (Figure 3A). Interestingly, co-transfection of a constitutively active mutant of $G\alpha_{13}$ ($G\alpha_{13}$-CA), but not wild type $G\alpha_{13,}$ resulted in enhanced TOPflash activation in mock cells (Figure 3C). This effect was enhanced when US28 was co-transfected. Finally, we co-transfected cells with US28 and the Lsc-RGS scavenger, encoding the RGS domain of the Rho GTPase guanine nucleotide exchange factor (Rho-GEF) Lsc. Lsc-RGS is known to specifically interfere with transmembrane signaling mediated by activated $G\alpha_{12/13}$ signaling (*35, 36*). Expression of Lsc-RGS in US28-expressing cells resulted in a strong inhibition of US28-mediated TOPflash reporter gene activation (Figure 3C), indicating an important role for $G\alpha_{12/13}$ proteins.

As $G\alpha_q$ and $G\alpha_{12/13}$ proteins mediate activation of Rho via the Rho-GEFs p63 and p115 (*36, 37*), respectively and Rho in turn is known to activate ROCK kinase (Rho ROCK REF), we investigated the role of the Rho-Rho kinase (ROCK) pathway in US28-mediated signaling to β-catenin. Exposure of US28-expressing cells to increasing concentrations of the ROCK inhibitor Y27632 resulted in a dose-dependent attenuation of the US28 mediated TOPflash activation (Figure 3D), indicating involvement of Rho-ROCK signaling in the US28-induced β-catenin activation pathway.

5.3.4 Role for US28 in HCMV induced activation of β-catenin signaling

The HCMV Titan 2B strain (referred to as WT) (*28*) and a strain deficient for the US28 gene (HCMV-DUS28) were used to examine the ability of HCMV, and the possible contribution of US28, in activating β-catenin signaling after infection. Infection of human foreskin fibroblasts (HFFs) with HCMV-WT resulted in increased presence of active β-catenin in cytoplasm and nuclei of infected cells, as evidenced by the expression of the immediate early antigen (IEA) (Figure 4A). Cells infected with the deletion mutant HCMV-DUS28 showed only marginal active β-catenin in these cells and no active β-catenin was apparent in non-infected cells (Figure 4A). Since HFFs

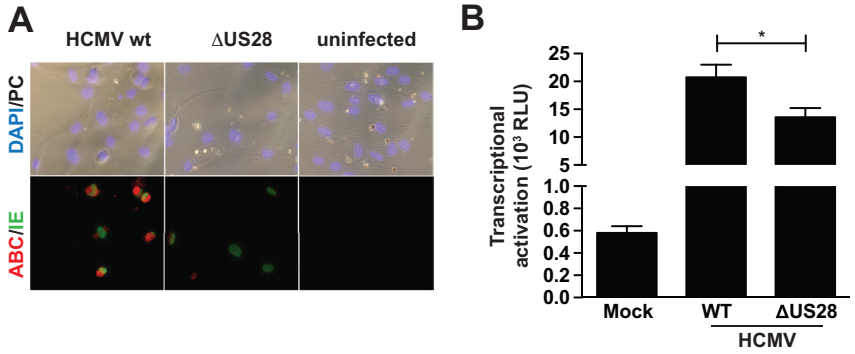

Figure 4. HCMV-infected cells stimulate activation of β-catenin in a US28 dependent manner. (**A**) HFF cells were infected with HCMV-WT or HCMV-ΔUS28 with a M.O.I of 1 on IBIDI slides. Cells were fixed 24 hours post-infection (hpi) and stained with antibodies recognizing the HCMV immediate early antigen (IEA) and activated β-catenin respectively. (**B**) U373-MG cells transfected with Tcf-Lef reporter gene were either infected with HCMV-WT or HCMV-ΔUS28 with a M.O.I. of 2, or left uninfected (mock). Luciferase activity was measured 48h post-infection.

show low transfection efficiencies we used U373-MG glioma cells to transfect the TOPflash reporter gene construct to monitor β-catenin-dependent transcriptional activation after HCMV infection. U373-MG glioma cells were transfected with the TOPflash reporter gene construct, followed by infection with either HCMV-WT or HCMV-DUS28. Cells infected with HCMV-WT showed strong β-catenin-dependent transcriptional activation (Figure 4B), while cells infected with the deletion mutant HCMV-DUS28 displayed a significantly lower level of TOPflash reporter gene activity (Figure 4B). The levels of infection between HCMV-WT and HCMV-DUS28 were similar, as determined by back titration (Figure S2). These data clearly indicate a role for US28 in regulation of β-catenin signaling during HMCV-infection.

5.5 Discussion

We have demonstrated that HCMV partly through expression of the constitutively active chemokine receptor US28 induces β-catenin signaling upon infection. Indeed, mounting evidence links viral infection to β-catenin hyperactivation. For instance, the Epstein-Barr virus (EBV) activates β-catenin in latently infected B lymphocytes (*38*). The human papillomavirus (HPV) E6 and E7 oncogenes appear to contribute to activation of β-catenin signaling in HPV16-positive oropharyngeal squamous carcinoma cells (*39*) and the hepatitis C virus (HCV) encoded core protein potentiates Wnt/β-catenin signaling in hepatocellular carcinoma cells (*40*). For the human immunodeficiency virus (HIV), however, active Wnt/β-catenin signaling plays a significant role in repression of HIV-1 replication in multiple cell targets (*41, 42*).
Interestingly, expression of the HCMV-encoded chemokine receptor US28 in intestinal epithelial cells promotes intestinal neoplasia in transgenic mice (*27*), which is associated with increased accumulation of β-catenin in the nucleus. In this study we show that this viral receptor leads to activation of β-catenin and enhanced β-catenin-dependent transcription in a manner distinct from conventional Wnt-mediated signaling when expressed in NIH3T3 cells or HEK293T cells. Classical Wnt-mediated β-catenin signaling entails the phosphorylation of LRP 5/6, ultimately leading to the nuclear accumulation of β-catenin (*1, 43*). The absence of LRP6 phosphorylation in US28-expressing cells supports the notion that US28 activates the β-catenin pathway through alternative routes. Unlike some of the lysophosphatidic acid, prostaglandin and protease activated receptors shown to stabilize β-catenin at the level of the destruction complex (*12*), US28-induced TOPflash activation is not PI3K- nor PKC-dependent. COX-2, via concomitant production of prostaglandins and activation of their cognate receptors in US28 expressing cells (Maussang, Langemeijer et al. 2009) is partially involved and does not account for the large increase in β-catenin activity observed in US28 expressing cells.
In this study it is shown for the fist time that a GPCR, the viral chemokine receptor US28, activates β-catenin signaling through the Rho-ROCK pathway. Our data show that coupling of US28 to both $G\alpha_q$ and $G\alpha_{12/13}$ proteins is essential for the observed activation of β-catenin signaling. Overexpression, scavenging and/or downmod-

ulation of either G protein greatly affect US28 mediated β-catenin signaling. The reported ligand-independent, constitutive, activity displayed by US28 is primarily exerted through activation of $G\alpha_q$ proteins (*29, 44*). Earlier, US28 was shown to also constitutively activate the serum response factor via $G\alpha_q$ proteins and RhoA, the small G protein that is activated by $G\alpha_q$ proteins through RhoGEF (*35, 37*). The ligand-dependent activity of US28 directs smooth muscle migration via $G\alpha_{12/13}$ and RhoA (*45*). Interestingly, several regulators of the Wnt/β-catenin signaling pathway were found to be associated with pro-migratory signaling of US28 via activation of the Pyk2 kinase (*46*). In view of the importance of $G\alpha_q$ and $G\alpha_{12/13}$ in US28 mediated β-catenin signaling and reported coupling of US28 to RhoA we postulated a role for its downstream target Rho kinase (ROCK) in US28 mediated activation of β-catenin. Inhibition of ROCK, with the specific inhibitor Y27632, substantiates a role for Rho-ROCK axis in the US28 induced activation of the β-catenin pathway. Exposure of US28 expressing cells to the chemokine CCL5 result in further increases in β-catenin signaling, infering involvement of $G\alpha_{12/13}$ proteins which is in line with previous studies indicating the involvement of these G proteins in US28-mediated responses (*47*). Altogether, our studies demonstrate that US28 activates β-catenin signaling in a ligand dependent and independent manner, involving $G\alpha_{12/13}$ and $G\alpha_q$ proteins converging at RhoA/ROCK (Figure 5). Additional experiments are currently ongoing to elucidate the molecular mechanism by which ROCK stabilizes β-catenin and induces TOPflash activation.

Of importance is that significant increases of β-catenin stabilization and signaling are observed in HCMV-infected HFFs and glioblastoma cells. This increase in β-cat-

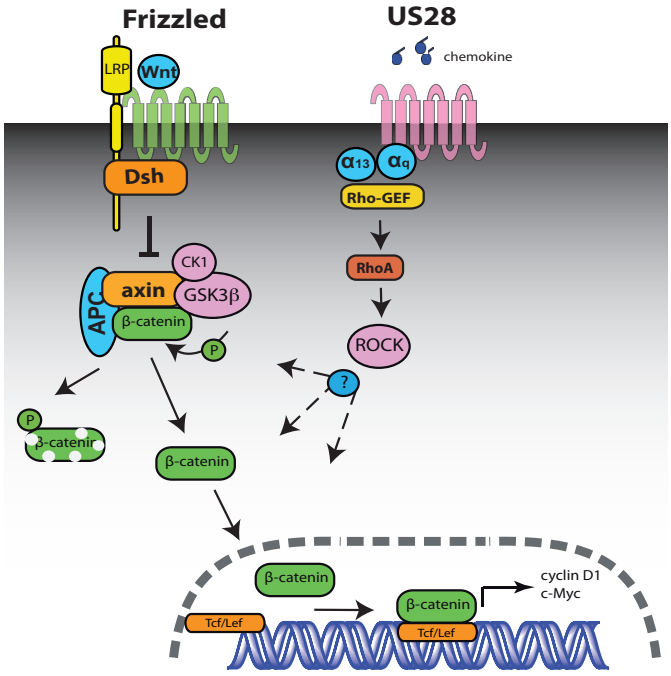

Figure 5. Schematic representation of the classic Wnt signaling pathway and model of US28-mediated activation of β-catenin signaling pathway.
The left side of the model indicates components of the classic Wnt/Frizzled mediated activation of β-catenin. In this pathway the disruption complex (Axin, APC) that enables GSK3β– and Caseine kinase 1 (CK1)-mediated phosphorylation of β-catenin leading to its degradation, is disrupted in a Dishevelled-mediated way upon Wnt binding to Frizzled/LRP. US28 activates β-catenin signaling in a ligand-dependent and independent manner, involving respectively $G\alpha_{12/13}$ and $G\alpha_q$ proteins and respective RhoGEFs, converging at RhoA/ROCK, resulting in increased Tcf/Lef transcriptional activation.

enin signaling upon HCMV infection is mediated to a large extent by expression of US28, as shown using the deletion mutant HCMV-DUS28. Besides US28, other CMV encoded proteins, including another viral GPCR UL33, also contribute to the observed increase in β-catenin signaling upon HCMV infection (Figure S3). Increases in β-catenin nuclear localization were also reported upon infection of murine CMV (*48*), reinforcing a role of HCMV-encoded proteins, like US28, in regulating β-catenin signaling. Sustained activation of the Wnt/β-catenin pathway induced by gain-of-function mutations of activators of the Wnt pathway, for e.g. mutations in the β-catenin gene that enhance its stability, or mutations in genes that control β-catenin stability like APC, the Axins, or E-cadherin, is found in various cancers (*3, 4*). Hence, the ability of US28 to constitutively activate β-catenin signaling, as well as other oncogenic signaling pathways (*22, 24, 25, 28, 49*) illustrates that this viral receptor may contribute to a malignant phenotype in HCMV positive cells. The fact that expression of US28 promotes development of intestinal dysplasia and cancer in transgenic mice (*27*) suggest that CMV infection may facilitate development of intestinal neoplasia in humans. Moreover, β-catenin and components of the Wnt canonical pathway are commonly overexpressed in glioblastoma multiforme (*50*). The high incidence of HCMV infection and detection of expression of US28 in human glioblastomas (*24, 25*) further underscores the relevance of this receptor in cancer development.

Taken together, in this study we have shown an alternative regulation of the β-catenin pathway. The viral chemokine receptor US28, induces activation of β-catenin, via the Rho-ROCK pathway. By expression of viral receptor proteins viruses might be able to rewire β-catenin signaling, contributing to malignant phenotypes.

5.5 Materials and methods

Cell culture and transfections

Human HEK293T, human glioblastoma U373-MG, human foreskin fibroblasts (HFF) and NIH-3T3 mouse fibroblast cells were all obtained from ATCC, and cultured in Dulbecco's Modified Eagle's Medium (DMEM) (PAA Laboratories), supplemented with penicillin (50 IU/ml), streptomycin (50 mg/ml) (PAA Laboratories) and 10% fetal bovine serum (FBS) (PAA Laboratories), heat-inactivated FBS and bovine serum (Gibco) respectively. NIH-3T3-stable cell lines (Mock, US28, HA-US28 and US28-R^{129}A mutant) were kept under the selective pressure of neomycin (400 mg/ml) (Sigma) to ensure homogenous receptor expression. Transient transfections of HEK293T cells were performed with the polyelthyleneimine (PEI) method (*51, 52*) followed by luciferase activity measurement the next day. Transient transfections of NIH-3T3 and U373-MG cells were performed with the Lipofectamine2000 method (Invitrogen).

Reporter gene analysis

10^6 HEK293T cells were transfected with plasmids encoding a TOP-flash reporter construct (TOPflash or the negative control Fopflash, kindly provided by Prof. H. Clevers and Dr. M. vd Wetering) and 25 ng of US28 receptor DNA (wild type or G-protein-uncoupled mutant R^{129}A) unless indicated differently and 25 ng of DNA encoding G-proteins (RGS2 and Lsc-RGS G protein scavengers were kindly provided by Dr. B. Moepps). Comparable TOPflash reportergene transfection protocols were used for U373-MG and NIH-3T3 cells, respectively. Total DNA amounts were kept constant by addition of empty vector. Inhibitors Y27632 (Rock, Sigma) were incubated overnight and added directly after transfection. 200ng/ml human recombinant Wnt3a (R&D systems, 5036-WN-010) was incubated overnight to activate the canonical Wnt signaling pathway. Luciferase activity was measured 24 h post transfection (RLU, relative light units) with a Victor^2 multilabel plate reader from (PerkinElmer Life Sciences). Statistical analyses, * or ** indicating $p<0.05$ or $p<0.001$, using Anova and Bonferroni post test 95% confidence interval.

Virus infection

Human Foreskin Fibroblasts (HFF) infected at a multiplicity of infection (MOI) of 1 on IBIDI slides with the TB40wt and TB40-DUS28 strains, respectively. Anti-IEA (Milipore) and anti-non-phospho-β-catenin antibodies (Cell Signaling Technology) were used to visualize IEA and activated β-catenin. After transfection of the TOPflash reporter gene in U373-MG cells (24 h), different HCMV Titan strains (WT or -DUS28) were used to infect U373-MG at an MOI of 2. Multiple viral stocks (3 for HCMV-WT, 4 for -DUS28) were assayed in triplicate. The rate of infectivity was controlled by back titration and IEA staining on parallel clear plates (data not shown). 48h post-infection luciferase activity was measured.

Chemokine binding and inositol phosphate accumulation experiments

Stably transfected NIH-3T3 cells (Mock, HA-US28 and US28) were analyzed for radiolabelled chemokine binding and inositol phosphate accumulation as previously described (*15*).

Western Blot Analysis

Biorad minigel and electroblot systems (Biorad) were used to perform SDS-PAGE and subsequent protein transfer onto 0.45 mm nitrocellulose or PVDF membranes. After an overnight serum starvation in medium containing 0.5% bovine serum, NIH-3T3 stable cell lines (Mock,

US28 and US28-$R^{129}A$) were lysed in radioimmunoprecipitation assay buffer supplemented with a-Complete Protease Inhibitor Cocktail (Hoffmann-la Roche), 1 mM PMSF, 1 mM $NaVO_4$ and 1 mM NaF. Samples were normalized using the BCA total protein determination kit (Thermo Fisher Scientific, Rockford lL, USA). Antibodies were used for detection of active β-catenin (Millipore and Cell Signaling Technology), total β-catenin (BD Transduction Laboratories), mouse monoclonal b-actin expression (Sigma), $G\alpha_q$ (Santa-Cruz) and P-LRP6 (Ser^{1490}) (Cell Signaling Technology).

Acknowledgements
We thank Rana Vatanparast for technical assistance. Alexandra Pelgrom is acknowledged for discussion and technical input. We thank Prof. H. Clevers and Dr. M. v.d. Wetering (Hubrecht Laboratory, Utrecht, The Netherlands) for providing the pTopFlash and pFopflash constructs for the TOPflash activation assay, Dr. B. Moepps (Inst. Pharmacol. Toxicol. Univ Ulm, Ulm, Germany) for the RGS2 and Lsc-RGS scavenger constructs. This work was supported by The Netherlands Organization for Scientific Research (to E. L., S.d.M, F.V. and M.J.S.), The Royal Netherlands Academy of Arts and Sciences (to M.J.S.) and Echo grant (to E.S.)

References

1. H. Clevers, Wnt/beta-catenin signaling in development and disease. *Cell* **127**, 469 (Nov 3, 2006).
2. B. T. MacDonald, K. Tamai, X. He, Wnt/beta-catenin signaling: components, mechanisms, and diseases. *Dev Cell* **17**, 9 (Jul, 2009).
3. N. Barker, H. Clevers, Mining the Wnt pathway for cancer therapeutics. *Nat.Rev.Drug Discov.* **5**, 997 (2006).
4. P. Polakis, Wnt signaling and cancer. *Genes Dev.* **14**, 1837 (2000).
5. H. Aberle, A. Bauer, J. Stappert, A. Kispert, R. Kemler, beta-catenin is a target for the ubiquitin-proteasome pathway. *EMBO J* **16**, 3797 (Jul 1, 1997).
6. T. C. He *et al.*, Identification of c-MYC as a target of the APC pathway. *Science* **281**, 1509 (Sep 4, 1998).
7. M. Shtutman *et al.*, The cyclin D1 gene is a target of the beta-catenin/LEF-1 pathway. *Proc Natl Acad Sci U S A* **96**, 5522 (May 11, 1999).
8. O. Tetsu, F. McCormick, Beta-catenin regulates expression of cyclin D1 in colon carcinoma cells. *Nature* **398**, 422 (Apr 1, 1999).
9. R. Lappano, M. Maggiolini, G protein-coupled receptors: novel targets for drug discovery in cancer. *Nat Rev Drug Discov* **10**, 47 (Jan, 2011).
10. S. Lin *et al.*, The absence of LPA2 attenuates tumor formation in an experimental model of colitis-associated cancer. *Gastroenterology* **136**, 1711 (May, 2009).
11. E. Lara *et al.*, Epigenetic repression of ROR2 has a Wnt-mediated, pro-tumourigenic role in colon cancer. *Mol Cancer* **9**, 170 (2010).
12. M. Yang *et al.*, G protein-coupled lysophosphatidic acid receptors stimulate proliferation of colon cancer cells through the {beta}-catenin pathway. *Proc Natl Acad Sci U S A* **102**, 6027 (Apr 26, 2005).
13. M. D. Castellone, H. Teramoto, B. O. Williams, K. M. Druey, J. S. Gutkind, Prostaglandin E2 promotes colon cancer cell growth through a Gs-axin-beta-catenin signaling axis. *Science* **310**, 1504 (Dec 2, 2005).
14. M. D. Castellone, H. Teramoto, J. S. Gutkind, Cyclooxygenase-2 and colorectal cancer chemoprevention: the beta-catenin connection. *Cancer Res* **66**, 11085 (Dec 1, 2006).
15. P. Casarosa *et al.*, Constitutive signaling of the human cytomegalovirus-encoded chemokine receptor US28. *J Biol Chem* **276**, 1133 (Jan 12, 2001).
16. M. K. Gandhi, R. Khanna, Human cytomegalovirus: clinical aspects, immune regulation, and emerging treatments. *Lancet Infect Dis* **4**, 725 (Dec, 2004).
17. F. R. Stassen, X. Vega-Cordova, I. Vliegen, C. A. Bruggeman, Immune activation following cytomegalovirus infection: more important than direct viral effects in cardiovascular disease? *J Clin Virol* **35**, 349 (Mar, 2006).
18. J. Cinatl, Jr., J. U. Vogel, R. Kotchetkov, H. Wilhelm Doerr, Oncomodulatory signals by regulatory proteins encoded by human cytomegalovirus: a novel role for viral infection in tumor progression. *FEMS Microbiol Rev* **28**, 59 (Feb, 2004).
19. J. A. Burger, T. J. Kipps, CXCR4: a key receptor in the crosstalk between tumor cells and their microenvironment. *Blood* **107**, 1761 (Mar 1, 2006).
20. A. M. Fulton, The chemokine receptors CXCR4 and CXCR3 in cancer. *Curr Oncol Rep* **11**, 125 (Mar, 2009).
21. D. N. Streblow *et al.*, Human cytomegalovirus chemokine receptor US28-induced smooth muscle cell migration is mediated by focal adhesion kinase and Src. *J Biol Chem* **278**, 50456 (Dec 12, 2003).
22. D. Maussang *et al.*, Human cytomegalovirus-encoded chemokine receptor US28 promotes tumorigenesis. *Proc Natl Acad Sci U S A* **103**, 13068 (Aug 29, 2006).
23. D. Maussang *et al.*, The human cytomegalovirus-encoded chemokine receptor US28 promotes angiogenesis and tumor formation via cyclooxygenase-2. *Cancer Res* **69**, 2861 (Apr 1, 2009).
24. E. Slinger *et al.*, HCMV-encoded chemokine receptor US28 mediates proliferative signaling through the IL-6-STAT3 axis. *Sci Signal* **3**, ra58 (Aug 3, 2010).
25. L. Soroceanu *et al.*, Human Cytomegalovirus US28 Found in Glioblastoma Promotes an Invasive and Angiogenic Phenotype. *Cancer Research* **71**, 6643 (Nov 1, 2011).
26. N. Baryawno *et al.*, Detection of human cytomegalovirus in medulloblastomas reveals a potential therapeutic target. *J Clin Invest* **121**, 4043 (Oct, 2011).
27. G. Bongers *et al.*, The cytomegalovirus-encoded chemokine receptor US28 promotes intestinal neoplasia in transgenic mice. *J Clin Invest* **120**, 3969 (Nov 1, 2010).
28. D. Maussang *et al.*, The human cytomegalovirus-encoded chemokine receptor US28 promotes angiogenesis and tumor formation via cyclooxygenase-2. *Cancer Res* **69**, 2861 (Apr 1, 2009).
29. P. Casarosa *et al.*, Constitutive signaling of the human cytomegalovirus-encoded chemokine receptor US28. *Journal of Biological Chemistry* **276**, 1133 (Jan 12, 2001).

30. V. Korinek *et al.*, Constitutive transcriptional activation by a beta-catenin-Tcf complex in APC-/- colon carcinoma. *Science* **275**, 1784 (Mar 21, 1997).
31. J. W. Hulshof *et al.*, Synthesis and pharmacological characterization of novel inverse agonists acting on the viral-encoded chemokine receptor US28. *Bioorganic & medicinal chemistry* **14**, 7213 (Nov 1, 2006).
32. J. Vomaske *et al.*, Differential ligand binding to a human cytomegalovirus chemokine receptor determines cell type-specific motility. *PLoS Pathog* **5**, e1000304 (Feb, 2009).
33. G. Davidson *et al.*, Casein kinase 1 gamma couples Wnt receptor activation to cytoplasmic signal transduction. *Nature* **438**, 867 (Dec 8, 2005).
34. X. Zeng *et al.*, A dual-kinase mechanism for Wnt co-receptor phosphorylation and activation. *Nature* **438**, 873 (Dec 8, 2005).
35. B. Moepps *et al.*, Constitutive serum response factor activation by the viral chemokine receptor homologue pUS28 is differentially regulated by Galpha(q/11) and Galpha(16). *Cell Signal* **20**, 1528 (Aug, 2008).
36. S. Siehler, Regulation of RhoGEF proteins by G12/13-coupled receptors. *Br J Pharmacol* **158**, 41 (Sep, 2009).
37. S. Lutz *et al.*, The guanine nucleotide exchange factor p63RhoGEF, a specific link between Gq/11-coupled receptor signaling and RhoA. *J Biol Chem* **280**, 11134 (Mar 25, 2005).
38. J. Shackelford, C. Maier, J. S. Pagano, Epstein-Barr virus activates beta-catenin in type III latently infected B lymphocyte lines: association with deubiquitinating enzymes. *Proc Natl Acad Sci U S A* **100**, 15572 (Dec 23, 2003).
39. T. Rampias *et al.*, Activation of Wnt signaling pathway by human papillomavirus E6 and E7 oncogenes in HPV16-positive oropharyngeal squamous carcinoma cells. *Mol Cancer Res* **8**, 433 (Mar, 2010).
40. J. Liu *et al.*, Enhancement of canonical Wnt/beta-catenin signaling activity by HCV core protein promotes cell growth of hepatocellular carcinoma cells. *PLoS One* **6**, e27496 (2011).
41. A. Kumar *et al.*, Active beta-catenin signaling is an inhibitory pathway for human immunodeficiency virus replication in peripheral blood mononuclear cells. *J Virol* **82**, 2813 (Mar, 2008).
42. S. D. Narasipura *et al.*, Role of beta-catenin and TCF/LEF family members in transcriptional activity of HIV in astrocytes. *J Virol* **86**, 1911 (Feb, 2012).
43. K. Willert, K. A. Jones, Wnt signaling: is the party in the nucleus? *Genes Dev* **20**, 1394 (Jun 1, 2006).
44. R. Minisini *et al.*, Constitutive inositol phosphate formation in cytomegalovirus-infected human fibroblasts is due to expression of the chemokine receptor homologue pUS28. *Journal of Virology* **77**, 4489 (Apr, 2003).
45. R. M. Melnychuk *et al.*, Human cytomegalovirus-encoded G protein-coupled receptor US28 mediates smooth muscle cell migration through G alpha 12. *Journal of Virology* **78**, 8382 (Aug, 2004).
46. J. Vomaske *et al.*, HCMV pUS28 initiates pro-migratory signaling via activation of Pyk2 kinase. *Herpesviridae* **1**, 2 (2010).
47. R. M. Melnychuk *et al.*, Human cytomegalovirus-encoded G protein-coupled receptor US28 mediates smooth muscle cell migration through Galpha12. *J Virol* **78**, 8382 (Aug, 2004).
48. M. Melnick, E. S. Mocarski, G. Abichaker, J. Huang, T. Jaskoll, Cytomegalovirus-induced embryopathology: mouse submandibular salivary gland epithelial-mesenchymal ontogeny as a model. *BMC Dev Biol* **6**, 42 (2006).
49. D. N. Streblow *et al.*, Human cytomegalovirus chemokine receptor US28-induced smooth muscle cell migration is mediated by focal adhesion kinase and Src. *J Biol Chem* **278**, 50456 (Dec 12, 2003).
50. M. Nager *et al.*, beta-Catenin Signalling in Glioblastoma Multiforme and Glioma-Initiating Cells. *Chemother Res Pract* **2012**, 192362 (2012).
51. E. J. Schlaeger, K. Christensen, Transient gene expression in mammalian cells grown in serum-free suspension culture. *Cytotechnology* **30**, 71 (Jul, 1999).
52. D. Maussang, H. F. Vischer, A. Schreiber, D. Michel, M. J. Smit, Pharmacological and biochemical characterization of human cytomegalovirus-encoded G protein-coupled receptors. *Methods Enzymol* **460**, 151 (2009).

Supplemental figures

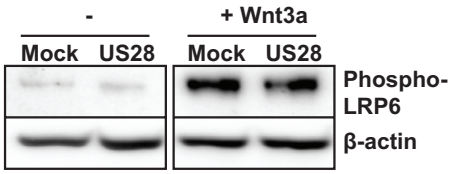

Figure S1. Wnt3a induces LRP6 phosphorylation at serine 1490 in US28-transfected NIH3T3 cells. Mock cells and US28 expressing cells were treated with 500 ng/ml recombinant Wnt3a. Subsequently, LRP6 Ser1490 phosphorylation was analysed by Western blot analysis.

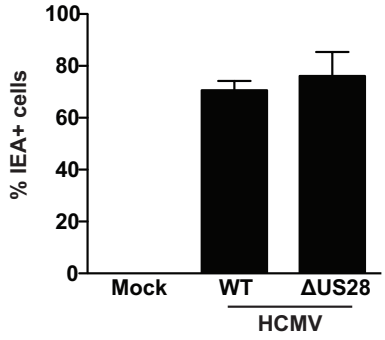

Figure S2. Back titration of wild-type HCMV and HCMV ΔUS28. The levels of infection were assessed by staining for Immediate Early (IEA). The amount of IEA+ cells is not significantly different between the different viral strains. This backtitration was performed on the samples that were used for the analysis shown in Figure 4B.

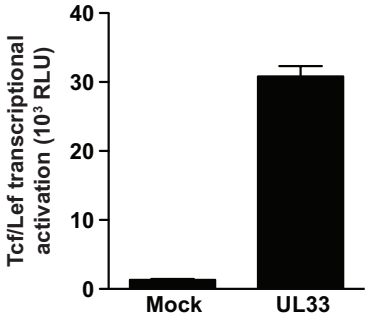

Figure S3. Activation of Tcf/Lef by UL33. UL33 and TOPflash were co-transfected, and luciferase activity was analysed 24 hours post-transfection. UL33 induces Tcf/Lef activation strongly.

6

Characterization of the US28 signalosome

6.1 Abstract

The human cytomegalovirus genome contains several genes encoding chemokine receptor homologs. One of these homologs is US28, a constitutive active receptor that activates several signaling pathways and which is capable of inducing proliferation. In order to understand how US28 can elicit such behavior, several signaling pathways have already been analyzed to date. However, there are still significant caveats in our understanding of US28 signaling. To address this, the US28 signalosome was characterized using a methodology designed for isolating receptor complexes. The obtained complexes were analyzed using liquid chromatography coupled online to a tandem mass-spectrometer. Analysis of the signalosome using Ingenuity Pathway Analysis software and STRING has revealed several pathways to be overrepresented. The data from these analyses was used to further investigate the nature of US28-induced Tcf/Lef signaling. These data represent a first view of a viral G-protein coupled receptor's signalosome.

6.2 Introduction

The virally encoded G-protein coupled receptor (GPCR) US28 has been shown to possess oncogenic properties in an earlier study (1). Since the first description of this receptor's oncogenic potential, the molecular mechanisms by which US28 induces a proliferative phenotype have been investigated. These investigations have shown that US28 activates multiple pathways that are required for the US28-induced proliferation. The first factor that was shown to be critical for proliferation instigated by US28 is cyclooxygenase-2 (COX2). Using the non-steroidal inflammatory inhibitor (NSAID) Celecoxib, COX2 activity was shown to be required for both the increased cellular growth rate and tumorigenic potential displayed by US28 expressing cells (2). Another cellular factor shown to be of import to US28-induced proliferation is STAT3 (see **Chapter 3** of this thesis). This transcription factor was shown, like COX2, to be a key factor for inducing the US28-related proliferative and oncogenic phenotype (3). Treating cells with the STAT3 inhibitor JSI-124 resulted in decreased proliferation as well as reduced focus formation. Finally, β-catenin signaling, a transcription factor that is associated with many cancers, in particular colon cancer, is also influenced by US28 (see **Chapter 5** of this thesis). A study using transgenic mice expressing US28 targeted to the intestine showed that these mice developed tumors in the small intestine and these tumors display constitutive β-catenin activation (4).

These examples clearly show that US28 activates multiple cellular pathways. An analysis of the US28 signalosome was performed to gain more understanding of US28 signaling. The signalosome can be defined as the proteins that form a complex with a receptor to facilitate (receptor-) signaling, in the case of GPCRs the signalosome contains, among others, proteins such as the G-proteins (5). In this study we have employed an immunoprecipitation technique using N-terminally HA-tagged US28 which, following immunoprecipitation and sample preparation was subjected to liquid chromatography tandem mass-spectrometry (LC-MS/MS). The resulting list of proteins was then analyzed for gene ontology and potential interactions, using Ingenuity Pathway Analysis software.

A STRING analysis was used on the same dataset in combination with other experimental data to build an interaction map. Based on the result of these analyses, and the data shown in **Chapter 5**, the link between US28 induced Rho/ROCK signaling and Tcf/Lef activation was further investigated.

In this study a general technique for performing immunoprecipitations on GPCRs leaving protein-protein interactions intact is described, as well as a workflow for preparing the eluates from the immunoprecipitations for LC-MS/MS analysis. The obtained knowledge about the signalosome will aid in identifying novel signaling pathways through which US28 signals.

6.3 Results

6.3.1 Characterization of N-terminally HA-tagged US28 expressing cells

Although it is possible to perform immunoprecipitation using antibodies raised against US28 in conjuction with protein-A conjugated agarose, such an approach is not as efficient as using a more direct approach using antibodies that are conjugated to agarose. Therefore, we chose to use anti-HA conjugated agarose. For our purposes we used a HA-tag fused N-terminally to US28. In Figure 1A shows US28 binding to [^{125}I]-CCL5 in transiently transfected HEK293T. With expression being confirmed by the aforementioned binding assay, functionality was confirmed using a reportergene assay measuring transcriptional activity of NFAT (Figure 1B). Furthermore, NIH-3T3 cells stably expressing HA-US28 display a similar proliferative phenotype as the wild-type US28 expressing NIH-3T3 (Figure 1C).

6.3.2 Immuno-precipitation of HA-US28

Following confirmation of expression and functionality, HA-US28 was immuno-precipitated from transiently transfected cells. For this purpose a lysis buffer preserving as many protein-protein interactions as possible, while still efficiently lysing the cells was required. Subsequently, the obtained eluates were first separated by SDS/PAGE. Presence of US28 was confirmed by Western-blot analysis, using anti-HA antibodies (Figure 2A). Coomassie brilliant blue (CBB) staining was used to assess the

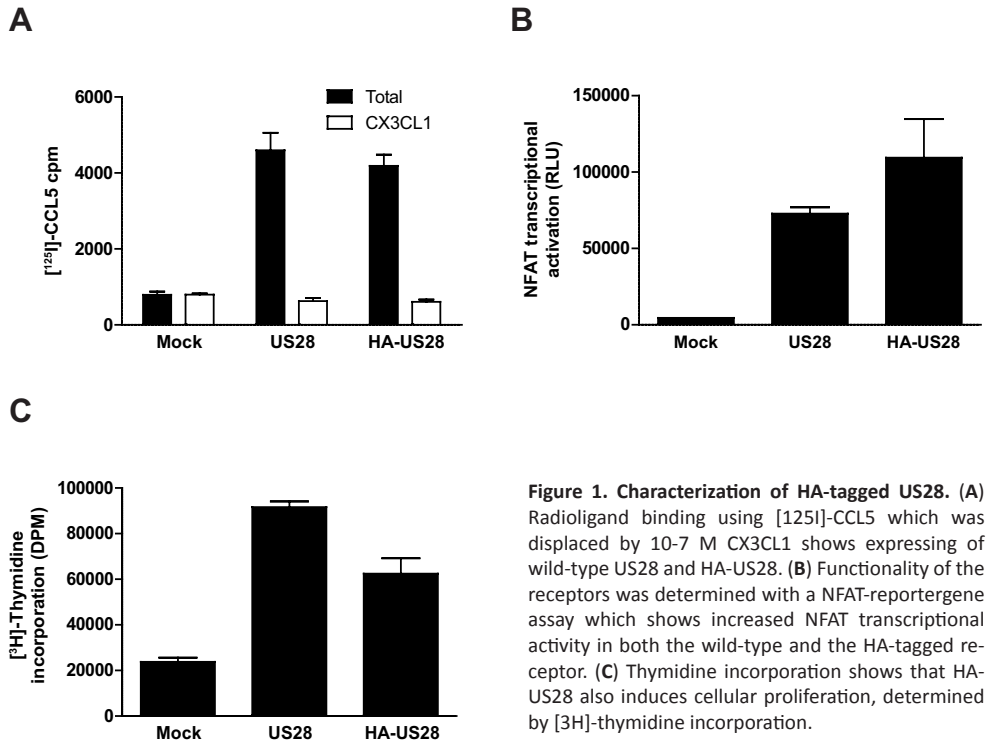

Figure 1. Characterization of HA-tagged US28. (**A**) Radioligand binding using [125I]-CCL5 which was displaced by 10-7 M CX3CL1 shows expressing of wild-type US28 and HA-US28. (**B**) Functionality of the receptors was determined with a NFAT-reportergene assay which shows increased NFAT transcriptional activity in both the wild-type and the HA-tagged receptor. (**C**) Thymidine incorporation shows that HA-US28 also induces cellular proliferation, determined by [3H]-thymidine incorporation.

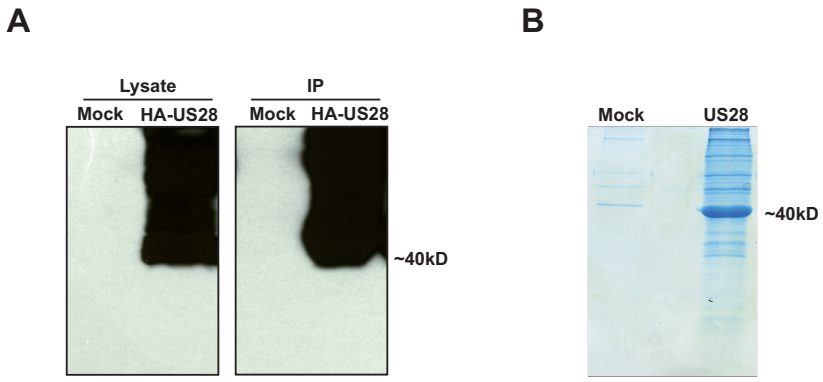

Figure 2. Immuno-precipitation of the US28 signalosome. (**A**) Western-blot using antibodies raised against the HA-tag. Both US28 wild-type and US28 R129A mutant are present in either the lysate and the immuno-precipitated proteins (IP). The predicted mass of US28 is marked at the side. (**B**) Coomassie Brilliant Blue staining of a SDS/PAGE on which IP proteins was loaded. Again the approximate size of US28 is marked at the side. The difference between the mock pull-down and the wild-type pulldown is visible as a lower amount of bands.

amount of proteins that were co-precipitated (Figure 2B). This gel was then further processed and the co-precipitating proteins were identified by LC-MS/MS. The LC-MS/MS analysis yielded 491 proteins that were specifically co-precipitating with US28, and these proteins are listed in Table S1 (Supplemental data). The spectral counts indicate the abundance of the proteins in the immuno-precipitation, with a higher number indicating a greater abundance of protein.

6.3.3 Further analysis of the US28 signalosome

In order to gain further insight in the roles of the proteins listed in Table 1, the dataset for US28 was analyzed using Ingenuity Pathway Analysis (IPA) software. Proteins that were more or less expected to be present in the dataset, such as Ga_i were found to be present in the dataset. The functional annotation is shown in Figure 3. This analysis shows that 28% of the identified proteins are enzymes and 13% of the proteins are transporters. IPA was also used to perform a core analysis on the different datasets. These datasets were subsequently cross-analyzed in order to

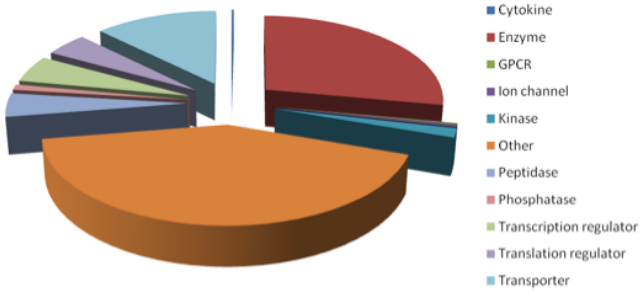

Figure 3. Distribution of cellular functions among proteins present in the US28 signalosome. The different protein functions are denoted in colors and the size of each portion of the pie-chart is representative of the percentage of proteins that were identified within the signalosome.

identify overrepresented pathways. As expected, several pathways associated with the regulation of cell survival and proliferation, were found to be overrepresented (threshold was set at p<0.05, using Fisher's Exact Test). Among the proteins present in the pathways associated with proliferation and survival were several mitochondrial proteins. This may reflect changes in cellular metabolism that are induced by US28. Another set of proteins that stands out are the 14-3-3 proteins, which are important mediators of cellular signaling (6). All the canonical pathways of which proteins were found to be significantly overrepresented are listed in Figure 4 in descending order of significance. In total 42 pathways were found to contain proteins that were found in the co-immunoprecipitation.

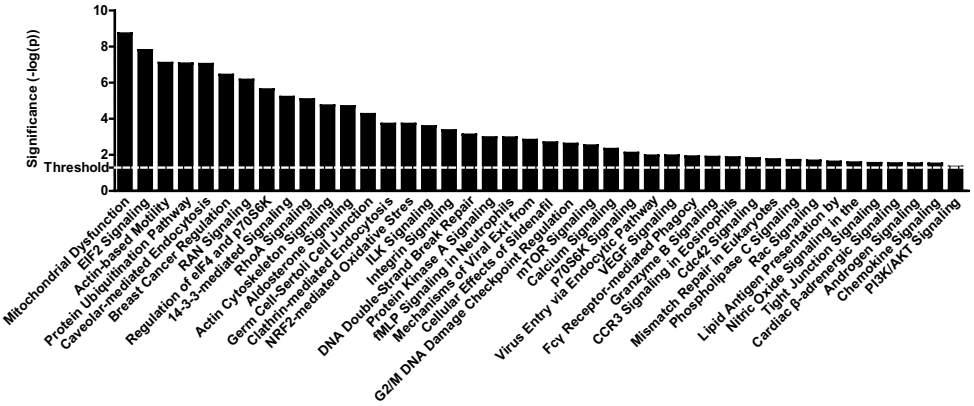

Figure 4. Canonical pathways that are overrepresented in the list of proteins of the US28 signalosome. On the X-axis significance is shown in –log(p) where p is the result of a Fisher's Exact Test. The threshold is indicated as the white dotted line and is set at p<0.05 (-log(p)=1.3).

6.3.4 14-3-3 proteins interact with Cby and potentially influence β-catenin signaling

As mentioned above, analysis of the signalosome revealed that several pathways were overrepresented. Among these pathways is RhoA signaling. In **Chapter 5**, experiments with the ROCK inhibitor Y-27632 show that US28-induced Tcf/Lef activation is dependent on ROCK. G-protein signaling can activate Rho (7, 8), which in turn can activate ROCK (9). We decided to further investigate the proteins that were found to play a role in these pathways. When we were first exploring US28-induced Tcf/Lef activation, one of the mechanisms that was considered was US28-induced activation of Akt, which then phosphorylates Gsk3b resulting in disruption of the destruction complex. However, further investigation showed that this was not the case, as US28 does not induce Akt phosphorylation. In fact, US28 appears to inhibit Akt phosphorylation (Figure 6A). Therefore, a protein-protein interaction analysis with the Search Tool for the Retrieval of Interacting Genes/Proteins (STRING) was

performed on proteins found in the signalosome as well as proteins that are known to associate with factors found in our dataset based on experimental data. Proteins that were included from the mass-spectrometry dataset and reported to play a role in Tcf/Lef activation are ROCK1, RHOA, ARHGEF11, the 14-3-3 proteins (YWHAx), PPP2R1A (PP2A subunit). CTNNB1 (β-catenin) was included because of the data shown in Chapter 5, and Akt was included based on the data described above. Since PTEN is regulated by ROCK and controls Akt activity and CBY1 is phosphorylated by Akt and reported to play a role in b-catenin signaling (10, 11) these proteins were also included in the STRING analysis. Immunoprecipitation experiments revealed that US28 is co-immunoprecipitating with PTEN and CBY1 (data not shown). Figure 5 shows that a protein-protein interaction map of these proteins can be built that links to b-catenin.

Cby is a protein that controls the intracellular distribution and function of β-catenin. Another protein that plays a pivotal role in this interaction map is Akt. As mentioned above, US28-expressing cells show lower phosphorylation of Akt S473 (Figure 6A), which is consistent with lower Akt activity (12). When Cby and β-catenin are both phosphorylated by Akt, they are recognized by 14-3-3 proteins (Note that the protein symbol for 14-3-3 proteins is YWHAx). Subsequently the complex is then exported out of the nucleus and b-catenin is degraded (10). Indeed, when Cby function is impaired in SW480 colon carcinoma cells, their growth is suppressed (13). In this light, the presence of known inhibitory factors (such as the PP2A subunit PPP2R1A) of Akt in the US28 signalosome is intriguing since this suggests a novel way for US28 to influence β-catenin signaling.

To test whether inhibitory factors like PTEN or PP2A are controlling US28-induced b-catenin signaling, we treated cells with inhibitors against PTEN (bpV) and PP2A (okadaic acid). Figure 6B shows that both bpV and okadaic acid can inhibit US28-induced activation of Tcf-Lef. To investigate the role of 14-3-3 in US28-induced Tcf-

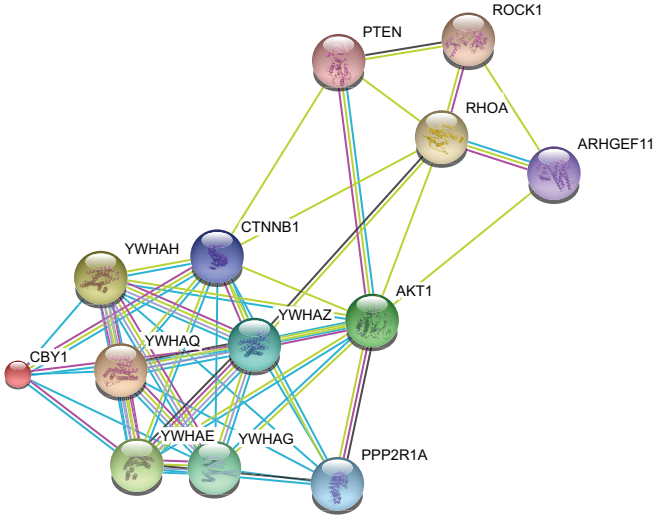

Figure 5. Protein-protein interaction map connecting the 14-3-3 pathway with the RhoA signaling pathway. The STRING program was used to build this interaction map. Proteins involved in either pathway, which were found in either the signalosome or that were known to be involved from earlier studies where used as input. The lines indicate different sources of evidence for the interactions. Neighborhood (green), gene fusion (red), co-occurrence (blue), co-expression (black), experiments (purple), databases (cyan), text mining (yellow).

Lef activation, we made use of the phytotoxin fusicoccin. Fusicoccin has been described as a stabilizer of 14-3-3 interactions in both plants as well as in human cells (14-16). Because of its ability to promote 14-3-3 interactions with client proteins, and the data we obtained with bpV and okadaic acid, we expected fusicoccin to inhibit US28-induced Tcf-Lef activation. Figure 6C shows that treatment with fusicoccin showed a dose-dependent reduction in Tcf-Lef activation, confirming our hypothesis. To investigate the interaction between Cby and b-catenin we used a bioluminescence resonance energy transfer (BRET) assay. Therefore 14-3-3e and Cby

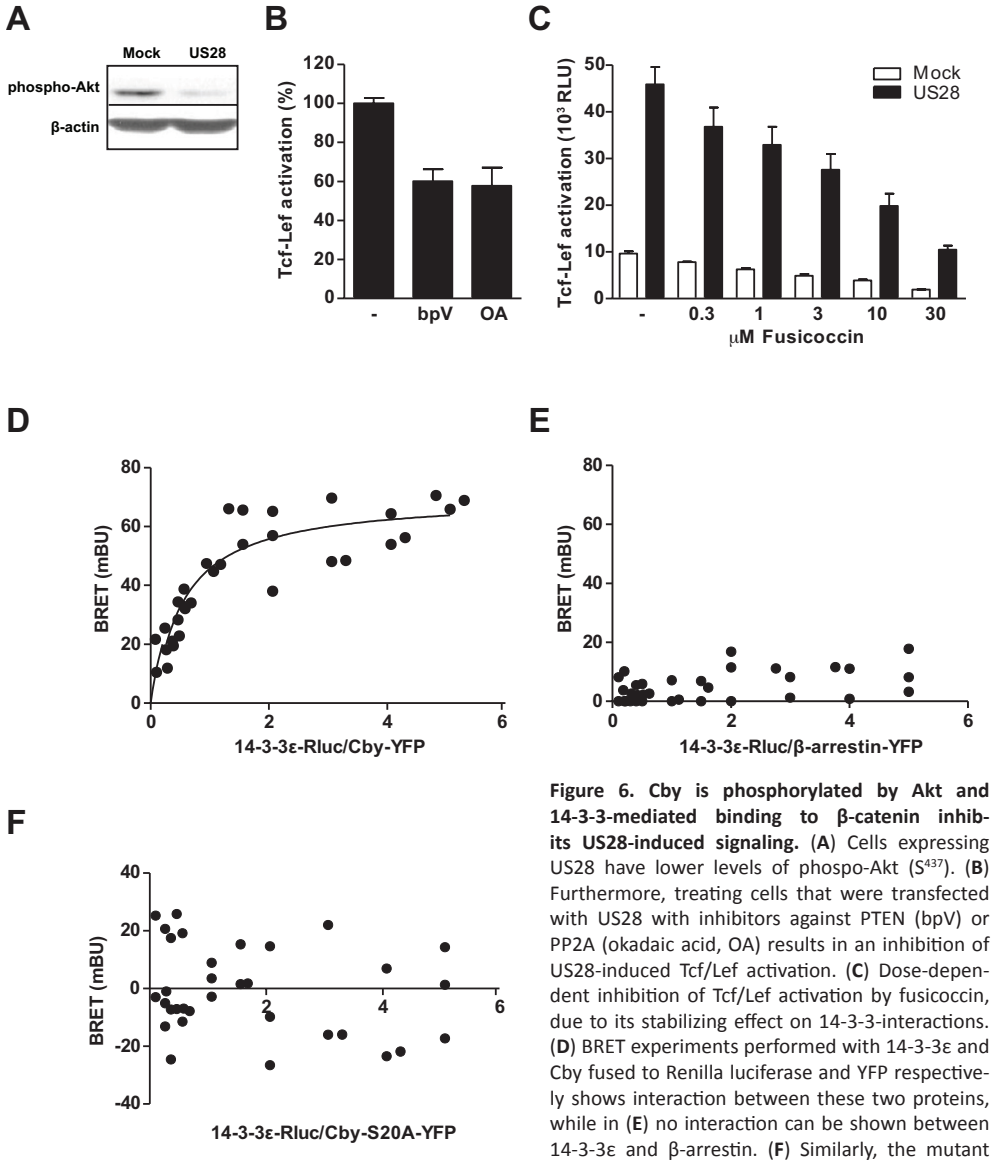

Figure 6. Cby is phosphorylated by Akt and 14-3-3-mediated binding to β-catenin inhibits US28-induced signaling. (**A**) Cells expressing US28 have lower levels of phospo-Akt (S^{437}). (**B**) Furthermore, treating cells that were transfected with US28 with inhibitors against PTEN (bpV) or PP2A (okadaic acid, OA) results in an inhibition of US28-induced Tcf/Lef activation. (**C**) Dose-dependent inhibition of Tcf/Lef activation by fusicoccin, due to its stabilizing effect on 14-3-3-interactions. (**D**) BRET experiments performed with 14-3-3ε and Cby fused to Renilla luciferase and YFP respectively shows interaction between these two proteins, while in (**E**) no interaction can be shown between 14-3-3ε and β-arrestin. (**F**) Similarly, the mutant S^{20}A form of Cby does not show any interaction with 14-3-3ε.

were tagged with Rluc and YFP, respectively. In this assay the light emitted by the donor 14-3-3e-Rluc is used to excite the Cby-YFP in case of close proximity of the proteins (energy transfer). In BRET analysis, the donor DNA concentration is kept constant, while the acceptor is varied in a wide range in transfection. Saturation of the energy transfer indicates close proximity of the two assessed proteins. BRET with 14-3-3e-Rluc and Cby-YFP shows a saturable BRET signal (Figure 6D), indicating an affinity of both proteins for each other. In contrast, the energy transfer from 14-3-3e-Rluc to b-Arrestin-YFP protein was found not to be saturable, which indicates that there is no or very low affinity between these two partners (Figure 6E). Studies with Cby-S20A-YFP, which lacks the phosphorylation site that is required for interacting with 14-3-3, and the 14-3-3e-Rluc also showed a complete loss of affinity (Figure 6F). These data show that phosphorylation of Cby is required to be able to interact with 14-3-3 proteins. Furthermore, the experiments performed with the different inhibitors suggest that Cby may be a factor in US28-induced b-catenin signaling.

6.4 Discussion

In recent years proteomic analysis has become an important tool to gain further understanding of the proteome. Powerful analysis techniques like LC-MS/MS have been instrumental in this effort. In this study the US28 signalosome was analyzed in an effort to further clarify the manner by which US28 signals. To this end we endeavored to isolate US28 and its associated proteins by way of immunoprecipitation. The results shown in this study show that we are able to efficiently isolate US28 and their associated proteins. Analysis of these pull-downs identified 491 proteins to specifically co-precipitate with either US28

The US28 signalosome was analyzed using the IPA software. This resulted in a number of pathways that were overrepresented in the signalosome. Some of these pathways were expected to be present, such as clathrin-mediated endocytosis (involved in GPCR internalization), calcium signaling, and phospholipase C (PLC) signaling (both are associated with $G\alpha_q$ signaling). The pathways related to internalization are expected to be there since US28 displays constitutive internalization, while calcium signaling and PLC signaling are both function of $G\alpha_q$ activation. Analysis of the US28 signalosome shows over-representation of proteins involved in proliferation and survival. Examples of affected pathways are: breast cancer regulation, RhoA signaling, mTOR signaling, Cdc42 signaling, and PI3K/Akt signaling. A set of proteins that was identified in the US28 signalosome were the 14-3-3 proteins. This protein family is composed of 7 members (14-3-3β, γ, ε, σ, ζ, τ, and η), which are important mediators of signaling, that act by facilitating protein-protein interactions (e.g. kinase-substrate) (6). These proteins are present in all eukaryotes and well conserved, indicating their vital role in cellular function. While, removal of one of the 14-3-3 members generally does not result in a phenotype in the presence of the other members, removal of all 14-3-3s results in (cell-) death. Several studies

have indicated that 14-3-3 proteins may have a role in mediating GPCR signaling. For example, 14-3-3ζ was shown to occupy a Raf-binding site on the α2-Adrenergic receptor (α2AR) and could be displaced with phosphorylated Raf-1 (24). In this case 14-3-3ζ is proposed to anchor receptors to the cell-surface, and when the receptors are activated the 14-3-3 anchors are released. Subsequently, α2AR will undergo the cycle of activation, inactivation, and internalization. Membrane expression of the HIV co-receptor GPR15 is stabilized in a similar manner by 14-3-3 proteins (25), which suggests the existence of a general mechanism where 14-3-3 proteins regulate the subcellular localization of GPCRs. The presence of 14-3-3 proteins in the vicinity of US28 could be evidence of such a role for 14-3-3 in US28 localization. Additionally, US28 may bind so much 14-3-3 that it impairs the functionality of the 14-3-3 proteins by sequestering a large fraction of the 14-3-3 proteins. Further analysis using STRING suggests that the presence of 14-3-3 proteins and proteins involved in RhoA signaling may be a consequence of US28 influencing b-catenin signaling by inhibiting a regulatory component, Cby. Experiments with inhibitors of PP2A and PTEN seem to confirm this. Furthermore, when US28-expressing cells are treated with fusicoccin, a compound that promotes 14-3-3 interactions, US28-induced Tcf-Lef signaling is inhibited. In Figure 7, this proposed model is shown, where signaling by US28 increases PP2A and PTEN activity. This results in dephosphorylation of Akt, which inactivates Akt. Subsequently, Cby phosphorylation is diminished. This process 'unlocks' b-catenin which is now far more likely to be retained in the nucleus, thus potentiating any signaling through b-catenin, as is shown in Figure 7.
Pathways like mitochondrial dysfunction may be a result of apoptotic factors that were found in the pull-downs (eg. annexins like ANXA6 and ANXA5). Alternatively, these proteins may reflect US28-induced changes in cell metabolism considering

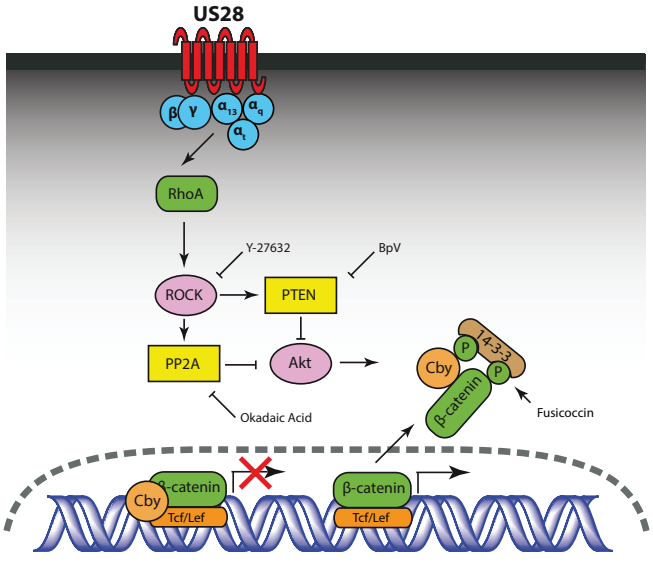

Figure 7. Model of US28-induced inhibition of Cby function. US28 induces signaling through RhoA. This results in activation of ROCK, which subsequently phosphorylates and activates PTEN and PP2A. Both phosphatases can inhibit Akt function, which results inhibition of Cby phosphorylation. Phosphorylation of Cby is required for its interaction with 14-3-3 proteins, which promotes the interaction of Cby with β-catenin.

that HCMV is known to change the cellular metabolism (26). Such virus-induced changes in metabolism are of interest, since transformed cells often display an altered metabolism. This is known as the Warburg effect and is characterized by the switch from pyruvate oxidation to lactic acid fermentation (27). The Warburg effect is a common effect in more than 90% of cancers (28). Indeed, KSHV has been shown to induce the Warburg effect in infected cells. Moreover, inhibiting glycolysis resulted in apoptosis of latently infected cells, which suggests that the metabolic changes effected by the Warburg effect circumvents apoptosis that would otherwise by induced by virally encoded factors (29). Whether the Warburg effect only facilitates proliferation or actively promotes transformation in the setting of US28-induced proliferation remains to be seen.

A list of proteins that were co-immunoprecipitated with US28 can be found in Table S1. An analysis of the function of the protein in Table 1 shows that most of them are enzymes, which fits with a role of these proteins in signaling. Interestingly, one cytokine, Macrophage migration Inhibitory Factor (MIF), was found to co-precipitate with US28. MIF is a pro-inflammatory cytokine, which also possesses characteristics reminiscent of chemokines. While CD74 is considered the cognate receptor for MIF (17), binding to the chemokine receptors CXCR4 and CXCR2 has also been described to bind to MIF (18). Furthermore, MIF has also been shown to be capable of promoting tumorigenesis and has been associated with several types of cancers (19, 20). The link of MIF with brain tumors, and glioblastomas in particular (21), is intriguing considering the data in Chapter 3, where US28 was shown to be present in glioblastoma tumors, mediating STAT3 responses (3). In glioblastomas MIF appears to be mainly involved in the neovascularization of the tumors (21). The presence of this cytokine in the pull-downs may be an indication of direct binding of MIF to US28, but could also be evidence of interaction of US28 with another receptor. In the latter case this could either be a chemokine receptor like CXCR2 or CXCR4, but it could also be CD74. Support for an interaction of CD74 with US28 exists, as CD74 has been shown to functionally interact with CXCR4 (22). However, arguing against such a dimerization model, the US28 pull-downs contain neither chemokine receptors nor CD74. Further experiments using labeled MIF should be able to address this question.

While US28 can be expected to be present on the plasma membrane and in particular in the cytoplasm based on current knowledge of US28 localization (23), the presence of nuclear proteins is somewhat puzzling. However, a similar analysis performed on the Histamine H1-receptor (H1R) has also yielded similar nuclear proteins (data not shown). A possible explanation could be that these proteins are involved in GPCR protein synthesis and maturation, although this does not explain the presence of DNA-repair enzymes.

The data presented in this study are an important first step in understanding the US28 signalosome. Furthermore, a methodology for isolating GPCRs and their associated proteins has been established. However, several challenges still remain to be met. First of all, more information about the US28 signalosome could be obtained if

the immunoprecipitation is performed on the different cellular compartments separately. This could be accomplished by sucrose-gradient separation, which allows for separation of all the different cellular compartments. However, alternative methods are available if one is mainly interested in the plasma membrane. First sulfo-NHS-SS-biotin can be used to biotinylate proteins that have extra-cellular domains and are thus considered to be present on the plasma membrane. Using streptavidin conjugated agarose these biotinylated proteins can be separated from the rest of the proteins (30). Another technique for isolating plasma membrane proteins entails the use of the lectin concanavalin A immobilized on magnetic beads (31).
Further development of the techniques discussed above will result in a better characterization of the US28 signalosome. Together with pathway analysis of the obtained data, this should lead to increased understanding of US28 mediated signaling.

6.5 Materials and methods

Materials and reagents

Anti-HA conjugated agarose was obtained from Sigma-Aldrich (St. Louis, MO, USA). The anti-HA monoclonal antibodies were purchased from Hoffman-La Roche (Basel, Switzerland). Rabbit anti-rat conjugated to horseradish peroxidase was purchased from Thermo Fisher Scientific (Rockford, IL, USA). All other chemicals were purchased from Applichem (Darmstadt, Germany).

Cell culture

Human HEK293T cells were cultured were cultured in Dulbecco's Modified Eagle Medium (DMEM) supplemented with 50 IU/ml penicillin, 50 µg/ml streptomycin, and 10% fetal bovine, heat inactivated fetal bovine serum. Transient transfections of HEK293T cells were performed using the polyethylenimine method (32). Expression of US28 in HEK293T cells was confirmed using [^{125}I]-CCL5 binding (specific binding was determined using CX3CL1 10^{-7} M), as previously described (33).

Western-blot analysis

A Biorad (Hercules, CA) minigel system was used to perform SDS/PAGE, and a Biorad electroblot system was used to transfer protein samples to a 0.45 µm polyvinylidene fluoride membrane from PerkinElmer (Waltham, MA, USA). Primary antibodies were incubated overnight in Tris-buffered saline with 0.1% Tween20 (TBST) added. Secondary antibodies were incubated for 90 minutes in TBST, and subsequently ECL from PerkinElmer was used to visualize the bound antibodies.

Co-immunoprecipitation and Mass-spectrometry

Analysis of the US28 signalosome was done by immuno-precipitating HA-tagged US28. To this end, the cells were lysed in 1% NP-40, 1 mM EDTA, 150 mM NaCl, 10% glycerol, and 1 mM $CaCl_2$. After 30 minutes incubation on ice, the lysates were clarified by centrifugation. Subsequently, anti-HA conjugated agarose (Sigma) was added to the lysate and left to incubate for 90 minutes at 4°C. The conjugated agarose was then washed 3 times with a wash buffer containing 0.1% Triton X-100, 50 mM Tris, 300 mM NaCl, and 5 mM EDTA, the pH was set at 7.5 with HCl. The proteins were eluted from the conjugated agarose with Laemmli buffer. The eluted proteins were separated on a 12% poly-acryl-amide gel, which was subsequently stained with Coomassie blue. Protein lanes from Coomassie stained SDS-PAGE gels were excised and prepared for LC-MS/MS analysis as previously described (34, 35). Peptides were separated by an Ultimate 3000 nanoLC-MS/MS system (Dionex LC-Packings, Amsterdam, The Netherlands) equipped with a 20 cm × 75 µm ID fused silica column custom packed with 3 µm 120 Å ReproSil Pur C18 aqua (Dr Maisch GMBH, Ammerbuch-Entringen, Germany). After injection, peptides were trapped at 30 µl/min on a 5 mm × 300 µm ID Pepmap C18 cartridge (Dionex LC-Packings, Amsterdam, The Netherlands) at 2% buffer B (buffer A: 0.05% formic acid in MQ; buffer B: 80% ACN + 0.05% formic acid in MQ) and separated at 300 nl/min in a 10–40% buffer B gradient in 60 min. Eluting peptides were ionized at 1.7 kV in a Nanomate Triversa Chip-based nanospray source using a Triversa LC coupler (Advion, Ithaca, NJ). Intact peptide mass spectra and fragmentation spectra were acquired on a LTQ-FT hybrid mass spectrometer (Thermo Fisher, Bremen, Germany). Intact masses were measured at resolution 50.000 in the ICR cell using a target value of 1 X 10^6 charges.

In parallel, following an FT pre-scan, the top 5 peptide signals (charge-states 2^+ and higher) were submitted to MS/MS in the linear ion trap (3 amu isolation width, 30 ms activation, 35% normalized activation energy, Q value of 0.25 and a threshold of 5000 counts). Dynamic exclusion was applied with a repeat count of 1 and an exclusion time of 30s.
The obtained MS/MS spectra were searched against the Human IPI database (v3.59; 80128 entries) using Sequest (version 27, rev 12), which is part of the BioWorks 3.3 data analysis package (Thermo Fisher, San Jose, CA). MS/MS spectra were searched with a maximum allowed deviation of 10 ppm for the precursor mass and 1 amu for fragment masses. Methionine oxidation and cysteine carboxamidomethylation were allowed as variable modifications, two missed cleavages were allowed. Scaffold (version Scaffold 2.01.02, Proteome Software Inc., Portland, OR) was used to validate MS/MS based peptide and protein identifications. Peptide identifications were accepted when established at greater than 95,0% probability as specified by the Peptide Prophet algorithm (36). Protein identifications were accepted when established at greater than 99,0% probability and contained at least 2 identified peptides. Protein probabilities were assigned by the Protein Prophet algorithm (37). Proteins that contained similar peptides and could not be differentiated based on MS/MS analysis alone were grouped to satisfy the principles of parsimony. Proteins were quantified by spectral counting (i.e. the sum of all MS/MS spectra per identified protein) (Liu H, Sadygov RG, Yates JR, III. A model for random sampling and estimation of relative protein abundance in shotgun proteomics. Anal.Chem. 76(14), 4193-4201 (15-7-2004). Old WM, Meyer-Arendt K, Aveline-Wolf L et al. Comparison of label-free methods for quantifying human proteins by shotgun proteomics. Mol.Cell Proteomics. 4(10), 1487-1502 (2005).)). The beta-binominal statistical test (Pham TV, Piersma SR, Warmoes M, Jimenez CR. On the beta-binomial model for analysis of spectral count data in label-free tandem mass spectrometry-based proteomics. Bioinformatics. 26(3), 363-369 (1-2-2010).) was used to calculate fold changes and p-values between U28HA and mock.

Bioluminescence Energy Transfer (BRET)
For BRET measurements, 14-3-3ε was C-terminally fused to Renilla reniformus luciferase to function as the donor. As acceptor, Cby C-terminally fused to enhanced yellow fluorescent protein (eYFP) was used. In BRET analysis, the donor DNA concentration is kept constant, while the acceptor is varied in a wide range in transfection. Both constructs were co-transfected into HEK293T and seeded into a 96-well white bottom plate. Measurements were taken 24 hours post-transfection, using a Victor^3 multi label plate reader (PerkinElmer Life Sciences). The donor signal was detected as luminescence at 460 nm, while acceptor fluorescence was measured at 535 nm, after 10 minute incubation with 5 µM coelenterazine-H (Promega). The BRET ratio was calculated by dividing the fluorescence by the luminescence which was then plotted against the different cDNA ratios. Saturation of the energy transfer indicates close proximity of the two assessed proteins.

Reporter Gene Analysis
10^6 HEK293T cells were transfected with plasmids encoding a Tcf-Lef reporter construct (TOP-flash or the negative control Fop-flash) and 25 ng of US28 receptor DNA (wild type or G-protein-uncoupled mutant $R^{129}A$) unless indicated differently and 25 ng of DNA encoding G-proteins in cotransfection. Total DNA amounts were kept constant by addition of empty vector. Inhibitors bpV (PTEN, Alexis Biochemicals) and Okadaic acid (PP2A, Calbiochem), Fucicoccin (FC, Calbiochem) were incubated overnight and added directly after transfection.

Luciferase activity was measured 24 h post transfection (RLU, relative light units) with a Victor^2 multilabel plate reader from (PerkinElmer Life Sciences). The TOP-flash and FOP-flash reporter gene plasmids to study Tcf-Lef activation were kindly provided by Prof. H. Clevers and Dr. M. vd Wetering.

References

1. D. Maussang et al., Human cytomegalovirus-encoded chemokine receptor US28 promotes tumorigenesisProc Natl Acad Sci U S A 103, 13068 (Aug 29, 2006).
2. D. Maussang et al., The human cytomegalovirus-encoded chemokine receptor US28 promotes angiogenesis and tumor formation via cyclooxygenase-2. Cancer Res 69, 2861 (Apr 1, 2009).
3. E. Slinger et al., HCMV-encoded chemokine receptor US28 mediates proliferative signaling through the IL-6-STAT3 axis. Sci Signal 3, ra58 (Aug 3, 2010).
4. G. Bongers et al., The cytomegalovirus-encoded chemokine receptor US28 promotes intestinal neoplasia in transgenic mice. The Journal of Clinical Investigation 0, 0 (2010).
5. M. L. Halls, D. M. F. Cooper, Sub-picomolar relaxin signalling by a pre-assembled RXFP1, AKAP79, AC2, [beta]-arrestin 2, PDE4D3 complex. EMBO J 29, 2772 (2010).
6. D. K. Morrison, The 14-3-3 proteins: integrators of diverse signaling cues that impact cell fate and cancer development. Trends Cell Biol 19, 16 (Jan, 2009).
7. S. Siehler, Regulation of RhoGEF proteins by G12/13-coupled receptors. Br J Pharmacol 158, 41 (Sep, 2009).
8. S. Lutz et al., The guanine nucleotide exchange factor p63RhoGEF, a specific link between Gq/11-coupled receptor signaling and RhoA. J Biol Chem 280, 11134 (Mar 25, 2005).
9. K. Fujisawa, A. Fujita, T. Ishizaki, Y. Saito, S. Narumiya, Identification of the Rho-binding domain of p160ROCK, a Rho-associated coiled-coil containing protein kinase. J Biol Chem 271, 23022 (Sep 20, 1996).
10. K. Takemaru, V. Fischer, F. Q. Li, Fine-tuning of nuclear-catenin by Chibby and 14-3-3. Cell Cycle 8, 210 (Jan 15, 2009).
11. F. Q. Li, A. Mofunanya, K. Harris, K. Takemaru, Chibby cooperates with 14-3-3 to regulate beta-catenin subcellular distribution and signaling activity. J Cell Biol 181, 1141 (Jun 30, 2008).
12. D. R. Alessi et al., Mechanism of activation of protein kinase B by insulin and IGF-1. EMBO J 15, 6541 (Dec 2, 1996).
13. V. Fischer, D. A. Brown-Grant, F. Q. Li, Chibby suppresses growth of human SW480 colon adenocarcinoma cells through inhibition of beta-catenin signaling. J Mol Signal 7, 6 (May 31, 2012).
14. L. Camoni, C. Di Lucente, S. Visconti, P. Aducci, The phytotoxin fusicoccin promotes platelet aggregation via 14-3-3-glycoprotein Ib-IX-V interaction. Biochem J 436, 429 (Jun 1, 2011).
15. A. H. de Boer, I. J. de Vries-van Leeuwen, Fusicoccanes: diterpenes with surprising biological functions. Trends Plant Sci 17, 360 (Jun, 2012).
16. A. Richter, R. Rose, C. Hedberg, H. Waldmann, C. Ottmann, An optimised small-molecule stabiliser of the 14-3-3-PMA2 protein-protein interaction. Chemistry 18, 6520 (May 21, 2012).
17. A. A. Sablina, M. Hector, N. Colpaert, W. C. Hahn, Identification of PP2A complexes and pathways involved in cell transformation. Cancer Res 70, 10474 (Dec 15, 2010).
18. M. Sunde et al., TC-1 is a novel tumorigenic and natively disordered protein associated with thyroid cancer. Cancer Res 64, 2766 (Apr 15, 2004).
19. T. Clahsen, F. Schaper, Interleukin-6 acts in the fashion of a classical chemokine on monocytic cells by inducing integrin activation, cell adhesion, actin polymerization, chemotaxis, and transmigration. J Leukoc Biol 84, 1521 (Dec, 2008).
20. S. Fiorentini et al., Human Cytomegalovirus productively infects lymphatic endothelial cells and induces a secretome that promotes angiogenesis and lymphangiogenesis through IL-6 and GM-CSF. J Gen Virol, (Dec 1, 2010).
21. S. Botto et al., IL-6 in human cytomegalovirus secretome promotes angiogenesis and survival of endothelial cells through the stimulation of survivin. Blood 117, 352 (Jan 6, 2011).
22. J. B. Friedman, E. B. Brunschwig, P. Platzer, K. Wilson, S. D. Markowitz, C8orf4 is a transforming growth factor B induced transcript downregulated in metastatic colon cancer. Int J Cancer 111, 72 (Aug 10, 2004).
23. A. Fraile-Ramos et al., The human cytomegalovirus US28 protein is located in endocytic vesicles and undergoes constitutive endocytosis and recycling. Mol Biol Cell 12, 1737 (Jun, 2001).
24. L. Prezeau, J. G. Richman, S. W. Edwards, L. E. Limbird, The zeta isoform of 14-3-3 proteins interacts with the third intracellular loop of different alpha2-adrenergic receptor subtypes. J Biol Chem 274, 13462 (May 7, 1999).
25. Y. Okamoto, S. Shikano, Phosphorylation-dependent C-terminal Binding of 14-3-3 Proteins Promotes Cell Surface Expression of HIV Co-receptor GPR15. J Biol Chem 286, 7171 (Mar 4, 2011).
26. J. Munger, S. U. Bajad, H. A. Coller, T. Shenk, J. D. Rabinowitz, Dynamics of the Cellular Metabolome

during Human Cytomegalovirus Infection. PLoS Pathog 2, e132 (2006).
27. O. Warburg, On the origin of cancer cells. Science 123, 309 (Feb 24, 1956).
28. I. F. Robey, A. D. Lien, S. J. Welsh, B. K. Baggett, R. J. Gillies, Hypoxia-inducible factor-1alpha and the glycolytic phenotype in tumors. Neoplasia 7, 324 (Apr, 2005).
29. T. Delgado et al., Induction of the Warburg effect by Kaposi's sarcoma herpesvirus is required for the maintenance of latently infected endothelial cells. Proc Natl Acad Sci U S A 107, 10696 (Jun 8, 2010).
30. T. Sato et al., Single Lgr5 stem cells build crypt-villus structures in vitro without a mesenchymal niche. Nature 459, 262 (May 14, 2009).
31. L. G. van der Flier et al., Transcription factor achaete scute-like 2 controls intestinal stem cell fate. Cell 136, 903 (Mar 6, 2009).
32. E. J. Schlaeger, K. Christensen, Transient gene expression in mammalian cells grown in serum-free suspension culture. Cytotechnology 30, 71 (Jul, 1999).
33. P. Casarosa et al., Constitutive signaling of the human cytomegalovirus-encoded chemokine receptor US28. J Biol Chem 276, 1133 (Jan 12, 2001).
34. A. Shevchenko, M. Wilm, O. Vorm, M. Mann, Mass spectrometric sequencing of proteins silver-stained polyacrylamide gels. Anal Chem 68, 850 (Mar 1, 1996).
35. S. R. Piersma et al., Proteomics of the TRAP-induced platelet releasate. J Proteomics 72, 91 (Feb 15, 2009).
36. A. Keller, A. I. Nesvizhskii, E. Kolker, R. Aebersold, Empirical statistical model to estimate the accuracy of peptide identifications made by MS/MS and database search. Anal Chem 74, 5383 (Oct 15, 2002).
37. A. I. Nesvizhskii, A. Keller, E. Kolker, R. Aebersold, A statistical model for identifying proteins by tandem mass spectrometry. Anal Chem 75, 4646 (Sep 1, 2003).

Supplemental table S1. Proteins identified by LC-MS/MS, sorted by subcellular location. Abundance is indicated as normalized spectral counts in the rightmost columns.

Function/Description	Symbol	Localization	Function	Spectral counts
macrophage migration inhibitory factor (glycosylation-inhibiting factor)	MIF	Extracellular Space	cytokine	5
acyl-CoA dehydrogenase family, member 9	ACAD9	Cytoplasm	enzyme	5
acetyl-CoA acetyltransferase 1	ACAT1	Cytoplasm	enzyme	10
ATP citrate lyase	ACLY	Cytoplasm	enzyme	8
adenosylhomocysteinase	AHCY	Cytoplasm	enzyme	10
aldo-keto reductase family 1, member B1 (aldose reductase)	AKR1B1	Cytoplasm	enzyme	2
aldehyde dehydrogenase 3 family, member A2	ALDH3A2	Cytoplasm	enzyme	2
adenine phosphoribosyltransferase	APRT	Cytoplasm	enzyme	0
ADP-ribosylation factor 1	ARF1	Cytoplasm	enzyme	7
ADP-ribosylation factor 4	ARF4	Cytoplasm	enzyme	8
asparagine synthetase (glutamine-hydrolyzing)	ASNS	unknown	enzyme	6
5-aminoimidazole-4-carboxamide ribonucleotide formyltransferase/IMP cyclohydrolase	ATIC	unknown	enzyme	9
HLA-B associated transcript 1	BAT1	Nucleus	enzyme	5
carbonic anhydrase II	CA2	Cytoplasm	enzyme	12
cell division cycle 42 (GTP binding protein, 25kDa)	CDC42	Cytoplasm	enzyme	2
CDP-diacylglycerol--inositol 3-phosphatidyltransferase	CDIPT	Cytoplasm	enzyme	0
CDP-diacylglycerol synthase (phosphatidate cytidylyltransferase) 2	CDS2	Cytoplasm	enzyme	5
cytochrome c oxidase subunit Va	COX5A	Cytoplasm	enzyme	5
citrate synthase	CS	Cytoplasm	enzyme	5
cytochrome b-245, alpha polypeptide	CYBA	Cytoplasm	enzyme	0
cytochrome c-1	CYC1	Cytoplasm	enzyme	1
aspartyl-tRNA synthetase	DARS	Cytoplasm	enzyme	9
DEAD (Asp-Glu-Ala-Asp) box polypeptide 1	DDX1	Nucleus	enzyme	4
DEAD (Asp-Glu-Ala-Asp) box polypeptide 3, X-linked	DDX3X	Nucleus	enzyme	3
DEAD (Asp-Glu-Ala-Asp) box polypeptide 5	DDX5	Nucleus	enzyme	9
DEAD (Asp-Glu-Ala-Asp) box polypeptide 6	DDX6	Nucleus	enzyme	4
7-dehydrocholesterol reductase	DHCR7	Cytoplasm	enzyme	3
DEAH (Asp-Glu-Ala-His) box polypeptide 15	DHX15	Nucleus	enzyme	2
DEAH (Asp-Glu-Ala-His) box polypeptide 30	DHX30	Nucleus	enzyme	2
DEAH (Asp-Glu-Ala-His) box polypeptide 9	DHX9	Nucleus	enzyme	11
dihydrolipoamide dehydrogenase	DLD	Cytoplasm	enzyme	4
DnaJ (Hsp40) homolog, subfamily A, member 2	DNAJA2	Nucleus	enzyme	11
deoxyuridine triphosphatase	DUT (includes EG:1854)	Nucleus	enzyme	1
eukaryotic translation initiation factor 4A3	EIF4A3 (includes EG:9775)	Nucleus	enzyme	3
fatty acyl CoA reductase 1	FAR1	Cytoplasm	enzyme	5

phenylalanyl-tRNA synthetase, alpha subunit	FARSA	Cytoplasm	enzyme	3
phenylalanyl-tRNA synthetase, beta subunit	FARSB	Cytoplasm	enzyme	3
fatty acid synthase	FASN	Cytoplasm	enzyme	25
flap structure-specific endonuclease 1	FEN1	Nucleus	enzyme	2
fumarate hydratase	FH	Cytoplasm	enzyme	2
FK506 binding protein 4, 59kDa	FKBP4	Nucleus	enzyme	10
GTPase activating protein (SH3 domain) binding protein 1	G3BP1	Nucleus	enzyme	7
glucosidase, alpha; neutral AB	GANAB	Cytoplasm	enzyme	5
galactosidase, alpha	GLA	Cytoplasm	enzyme	1
glutaredoxin 3	GLRX3	Cytoplasm	enzyme	3
glutamate dehydrogenase 1	GLUD1	Cytoplasm	enzyme	4
guanine nucleotide binding protein (G protein), alpha inhibiting activity polypeptide 3	GNAI3	Cytoplasm	enzyme	3
guanine nucleotide binding protein (G protein), beta polypeptide 2-like 1	GNB2L1	Cytoplasm	enzyme	9
glutamic-oxaloacetic transaminase 2, mitochondrial (aspartate aminotransferase 2)	GOT2	Cytoplasm	enzyme	5
glucose-6-phosphate isomerase	GPI	Extracellular Space	enzyme	16
glutathione reductase	GSR	Cytoplasm	enzyme	2
glutathione S-transferase omega 1	GSTO1	Cytoplasm	enzyme	4
glutathione S-transferase pi 1	GSTP1	Cytoplasm	enzyme	3
hydroxyacyl-CoA dehydrogenase/3-ketoacyl-CoA thiolase/enoyl-CoA hydratase (trifunctional protein), alpha subunit	HADHA	Cytoplasm	enzyme	5
hydroxyacyl-CoA dehydrogenase/3-ketoacyl-CoA thiolase/enoyl-CoA hydratase (trifunctional protein), beta subunit	HADHB	Cytoplasm	enzyme	3
heme oxygenase (decycling) 1	HMOX1	Cytoplasm	enzyme	0
hypoxanthine phosphoribosyltransferase 1	HPRT1	Cytoplasm	enzyme	4
hydroxysteroid (17-beta) dehydrogenase 10	HSD17B10	Cytoplasm	enzyme	1
hydroxysteroid (17-beta) dehydrogenase 12	HSD17B12	Cytoplasm	enzyme	1
isoleucyl-tRNA synthetase	IARS	Cytoplasm	enzyme	3
isocitrate dehydrogenase 2 (NADP+), mitochondrial	IDH2	Cytoplasm	enzyme	2
inositol-3-phosphate synthase 1	ISYNA1	unknown	enzyme	6
KH-type splicing regulatory protein	KHSRP	Nucleus	enzyme	2
leucyl-tRNA synthetase	LARS	Cytoplasm	enzyme	3
lysophosphatidylcholine acyltransferase 1	LPCAT1	Cytoplasm	enzyme	5
leukotriene A4 hydrolase	LTA4H	Cytoplasm	enzyme	5
magnesium transporter 1	MAGT1	Plasma Membrane	enzyme	1
malate dehydrogenase 2, NAD (mitochondrial)	MDH2	Cytoplasm	enzyme	36
NADH dehydrogenase, subunit 5 (complex I)	MT-ND5	Cytoplasm	enzyme	6
methylenetetrahydrofolate dehydrogenase (NADP+ dependent) 1, methenyltetrahydrofolate cyclohydrolase, formyltetrahydrofolate synthetase	MTHFD1	Cytoplasm	enzyme	2

NADH dehydrogenase (ubiquinone) 1 alpha subcomplex, 13	NDUFA13	Cytoplasm	enzyme	0
NADH dehydrogenase (ubiquinone) 1 beta subcomplex, 10, 22kDa	NDUFB10	Cytoplasm	enzyme	5
NADH dehydrogenase (ubiquinone) 1 beta subcomplex, 9, 22kDa	NDUFB9	Cytoplasm	enzyme	0
NADH dehydrogenase (ubiquinone) Fe-S protein 2, 49kDa (NADH-coenzyme Q reductase)	NDUFS2	Cytoplasm	enzyme	6
NADH dehydrogenase (ubiquinone) Fe-S protein 3, 30kDa (NADH-coenzyme Q reductase)	NDUFS3	Cytoplasm	enzyme	4
NADH dehydrogenase (ubiquinone) Fe-S protein 8, 23kDa (NADH-coenzyme Q reductase)	NDUFS8	Cytoplasm	enzyme	1
NADH dehydrogenase (ubiquinone) flavoprotein 1, 51kDa	NDUFV1	Cytoplasm	enzyme	4
NADH dehydrogenase (ubiquinone) flavoprotein 2, 24kDa	NDUFV2	Cytoplasm	enzyme	3
ornithine aminotransferase	OAT	Cytoplasm	enzyme	6
oxidase (cytochrome c) assembly 1-like	OXA1L	Cytoplasm	enzyme	3
prolyl 4-hydroxylase, beta polypeptide	P4HB	Cytoplasm	enzyme	9
phosphoribosylaminoimidazole carboxylase, phosphoribosylaminoimidazole succinocarboxamide synthetase	PAICS	unknown	enzyme	5
protein-L-isoaspartate (D-aspartate) O-methyltransferase	PCMT1	Cytoplasm	enzyme	0
pyruvate dehydrogenase (lipoamide) beta	PDHB	Cytoplasm	enzyme	5
protein disulfide isomerase family A, member 6	PDIA6	Cytoplasm	enzyme	12
phosphoribosylformylglycinamidine synthase	PFAS	Cytoplasm	enzyme	2
phosphogluconate dehydrogenase	PGD	Cytoplasm	enzyme	3
phosphatidylinositol glycan anchor biosynthesis, class S	PIGS	Cytoplasm	enzyme	4
purine nucleoside phosphorylase	PNP	Nucleus	enzyme	1
peptidylprolyl isomerase B (cyclophilin B)	PPIB	Cytoplasm	enzyme	2
peroxiredoxin 1	PRDX1	Cytoplasm	enzyme	14
peroxiredoxin 3	PRDX3	Cytoplasm	enzyme	8
peroxiredoxin 4	PRDX4	Cytoplasm	enzyme	2
peroxiredoxin 5	PRDX5	Cytoplasm	enzyme	1
peroxiredoxin 6	PRDX6	Cytoplasm	enzyme	10
protein kinase C substrate 80K-H	PRKCSH	Cytoplasm	enzyme	2
protein arginine methyltransferase 5	PRMT5	Cytoplasm	enzyme	3
phosphoserine aminotransferase 1	PSAT1	Cytoplasm	enzyme	4
proteasome (prosome, macropain) 26S subunit, non-ATPase, 6	PSMD6	Cytoplasm	enzyme	3
polypyrimidine tract binding protein 1	PTBP1	Nucleus	enzyme	5
prostaglandin E synthase 3 (cytosolic)	PTGES3 (includes EG:10728)	Cytoplasm	enzyme	2
glutaminyl-tRNA synthetase	QARS	Cytoplasm	enzyme	2
RAB11B, member RAS oncogene family	RAB11B	Cytoplasm	enzyme	2
RAB1A, member RAS oncogene family	RAB1A	Cytoplasm	enzyme	3

RAB2A, member RAS oncogene family	RAB2A	Cytoplasm	enzyme	0
RAB5B, member RAS oncogene family	RAB5B	Cytoplasm	enzyme	2
RAB5C, member RAS oncogene family	RAB5C	Cytoplasm	enzyme	4
RAB6A, member RAS oncogene family	RAB6A	Cytoplasm	enzyme	3
RAB7A, member RAS oncogene family	RAB7A	Cytoplasm	enzyme	3
RAP1B, member of RAS oncogene family	RAP1B	Cytoplasm	enzyme	0
arginyl-tRNA synthetase	RARS	Cytoplasm	enzyme	6
ras homolog gene family, member A	RHOA	Cytoplasm	enzyme	0
SAR1 homolog A (S. cerevisiae)	SAR1A	Cytoplasm	enzyme	0
succinate dehydrogenase complex, subunit A, flavoprotein (Fp)	SDHA	Cytoplasm	enzyme	2
septin 2	SEPT2	Cytoplasm	enzyme	4
serine hydroxymethyltransferase 2 (mitochondrial)	SHMT2	Cytoplasm	enzyme	4
superoxide dismutase 1, soluble	SOD1	Cytoplasm	enzyme	0
serine palmitoyltransferase, long chain base subunit 1	SPTLC1	Cytoplasm	enzyme	2
STT3, subunit of the oligosaccharyltransferase complex, homolog B (S. cerevisiae)	STT3B (includes EG:201595)	unknown	enzyme	3
transaldolase 1	TALDO1	Cytoplasm	enzyme	2
threonyl-tRNA synthetase	TARS	Nucleus	enzyme	2
thioredoxin-related transmembrane protein 1	TMX1	Cytoplasm	enzyme	0
TNF receptor-associated protein 1	TRAP1	Cytoplasm	enzyme	9
thioredoxin	TXN	Cytoplasm	enzyme	5
ubiquitin-like modifier activating enzyme 1	UBA1	Cytoplasm	enzyme	9
ubiquinol-cytochrome c reductase binding protein	UQCRB	Cytoplasm	enzyme	0
ubiquinol-cytochrome c reductase core protein II	UQCRC2	Cytoplasm	enzyme	8
vinculin	VCL	Plasma Membrane	enzyme	3
valosin-containing protein	VCP	Cytoplasm	enzyme	16
X-ray repair complementing defective repair in Chinese hamster cells 5 (double-strand-break rejoining)	XRCC5	Nucleus	enzyme	5
X-ray repair complementing defective repair in Chinese hamster cells 6	XRCC6	Nucleus	enzyme	17
tyrosyl-tRNA synthetase	YARS	Cytoplasm	enzyme	2
tyrosine 3-monooxygenase/tryptophan 5-monooxygenase activation protein, zeta polypeptide	YWHAZ	Cytoplasm	enzyme	13
sigma non-opioid intracellular receptor 1	SIGMAR1	Plasma Membrane	G-protein coupled receptor	3
chloride intracellular channel 1	CLIC1	Nucleus	ion channel	1
translocase of outer mitochondrial membrane 40 homolog (yeast)	TOMM40	Cytoplasm	ion channel	4
adenylate kinase 1	AK1	Cytoplasm	kinase	1
adenylate kinase 2	AK2	Cytoplasm	kinase	2
aldehyde dehydrogenase 18 family, member A1	ALDH18A1	Cytoplasm	kinase	5
hexokinase 1	HK1	Cytoplasm	kinase	3
non-metastatic cells 3, protein expressed in	NME3	Cytoplasm	kinase	0

phosphoglycerate kinase 1	PGK1	Cytoplasm	kinase	12
phosphatidylinositol 4-kinase, catalytic, alpha	PI4KA	Cytoplasm	kinase	3
protein kinase, cAMP-dependent, regulatory, type II, alpha	PRKAR2A	Cytoplasm	kinase	6
actin, beta-like 2	ACTBL2	unknown	other	3
actinin, alpha 1	ACTN1	Cytoplasm	other	25
ARP2 actin-related protein 2 homolog (yeast)	ACTR2	Plasma Membrane	other	4
ARP3 actin-related protein 3 homolog (yeast)	ACTR3	Plasma Membrane	other	4
AHA1, activator of heat shock 90kDa protein ATPase homolog 1 (yeast)	AHSA1	Cytoplasm	other	2
allograft inflammatory factor 1-like	AIF1L	unknown	other	15
acidic (leucine-rich) nuclear phosphoprotein 32 family, member B	ANP32B	Nucleus	other	1
annexin A5	ANXA5	Plasma Membrane	other	7
annexin A6	ANXA6	Plasma Membrane	other	17
archain 1	ARCN1	Cytoplasm	other	4
Rho guanine nucleotide exchange factor (GEF) 11	ARHGEF11	Cytoplasm	other	2
actin related protein 2/3 complex, subunit 3, 21kDa	ARPC3	Cytoplasm	other	2
actin related protein 2/3 complex, subunit 4, 20kDa	ARPC4	unknown	other	7
ATPase family, AAA domain containing 3A	ATAD3A	Nucleus	other	12
ataxin 10	ATXN10	Cytoplasm	other	5
ancient ubiquitous protein 1	AUP1	Cytoplasm	other	6
BRI3 binding protein	BRI3BP	unknown	other	8
basigin (Ok blood group)	BSG	Plasma Membrane	other	6
chromosome 14 open reading frame 166	C14ORF166	Nucleus	other	0
complement component 1, q subcomponent binding protein	C1QBP	Cytoplasm	other	5
chromosome 22 open reading frame 28	C22ORF28	unknown	other	4
chromosome 8 open reading frame 41	C8ORF41	unknown	other	3
chromosome 8 open reading frame 55	C8ORF55	unknown	other	2
caldesmon 1	CALD1	Cytoplasm	other	16
calnexin	CANX	Cytoplasm	other	13
CAP, adenylate cyclase-associated protein 1 (yeast)	CAP1	Plasma Membrane	other	8
coiled-coil domain containing 47	CCDC47	Extracellular Space	other	6
chaperonin containing TCP1, subunit 3 (gamma)	CCT3	Cytoplasm	other	15
chaperonin containing TCP1, subunit 4 (delta)	CCT4	Cytoplasm	other	20
cell division cycle 37 homolog (S. cerevisiae)	CDC37	Cytoplasm	other	3
centrosomal protein 55kDa	CEP55	unknown	other	2
cofilin 1 (non-muscle)	CFL1	Nucleus	other	18

cofilin 2 (muscle)	CFL2	Nucleus	other	1
chromatin modifying protein 4B	CHMP4B	Cytoplasm	other	3
cytoskeleton-associated protein 4	CKAP4	Cytoplasm	other	8
CLPTM1-like	CLPTM1L	unknown	other	3
coronin, actin binding protein, 1B	CORO1B	Cytoplasm	other	9
cysteine and glycine-rich protein 2	CSRP2	Nucleus	other	6
cortactin	CTTN	Plasma Membrane	other	3
cytospin A	CYTSA	unknown	other	2
drebrin-like	DBNL	Cytoplasm	other	2
dynactin 2 (p50)	DCTN2	Cytoplasm	other	2
density-regulated protein	DENR (includes EG:8562)	unknown	other	2
dehydrogenase/reductase (SDR family) member 7B	DHRS7B	unknown	other	1
diablo homolog (Drosophila)	DIABLO	Cytoplasm	other	0
dermokine	DMKN	unknown	other	1
DnaJ (Hsp40) homolog, subfamily A, member 1	DNAJA1	Nucleus	other	14
DnaJ (Hsp40) homolog, subfamily B, member 11	DNAJB11	Cytoplasm	other	2
DnaJ (Hsp40) homolog, subfamily B, member 12	DNAJB12	Cytoplasm	other	2
DnaJ (Hsp40) homolog, subfamily C, member 7	DNAJC7	Cytoplasm	other	4
dedicator of cytokinesis 7	DOCK7 (includes EG:85440)	unknown	other	5
dymeclin	DYM	unknown	other	2
EF-hand domain family, member D2	EFHD2	unknown	other	4
eukaryotic translation initiation factor 3, subunit L	EIF3L	Cytoplasm	other	2
eukaryotic translation initiation factor 3, subunit M	EIF3M	unknown	other	2
erythrocyte membrane protein band 4.1-like 2	EPB41L2	Plasma Membrane	other	4
Fas associated factor family member 2	FAF2	unknown	other	4
family with sequence similarity 101, member B	FAM101B	unknown	other	3
Fanconi anemia, complementation group D2	FANCD2	Nucleus	other	7
Fanconi anemia, complementation group I	FANCI	unknown	other	5
FK506 binding protein 8, 38kDa	FKBP8	Cytoplasm	other	2
filamin C, gamma	FLNC	Cytoplasm	other	3
GDP dissociation inhibitor 2	GDI2	Cytoplasm	other	8
gem (nuclear organelle) associated protein 4	GEMIN4	Nucleus	other	2
growth factor receptor-bound protein 2	GRB2	Cytoplasm	other	1
GrpE-like 1, mitochondrial (E. coli)	GRPEL1	Cytoplasm	other	1
gelsolin	GSN	Extracellular Space	other	3
HCLS1 associated protein X-1	HAX1	Nucleus	other	5
histone cluster 1, H2bl	HIST1H2BL	Nucleus	other	2
heterogeneous nuclear ribonucleoprotein A1	HNRNPA1	Nucleus	other	9
heterogeneous nuclear ribonucleoprotein A2/B1	HNRNPA2B1	Nucleus	other	5

heterogeneous nuclear ribonucleoprotein H1 (H)	HNRNPH1	Nucleus	other	4
heterogeneous nuclear ribonucleoprotein K	HNRNPK	Nucleus	other	12
heat shock protein 90kDa alpha (cytosolic), class B member 1	HSP90AB1	Cytoplasm	other	16
heat shock protein 90kDa beta (Grp94), member 1	HSP90B1	Cytoplasm	other	8
heat shock 70kDa protein 4	HSPA4	Cytoplasm	other	7
heat shock 70kDa protein 5 (glucose-regulated protein, 78kDa)	HSPA5	Cytoplasm	other	18
heat shock 70kDa protein 9 (mortalin)	HSPA9	Cytoplasm	other	34
heat shock 27kDa protein 1	HSPB1	Cytoplasm	other	0
KIAA0368	KIAA0368	Cytoplasm	other	5
KIAA1211	KIAA1211	unknown	other	5
KIAA1524	KIAA1524	Cytoplasm	other	4
high-mobility group box 1-like 10	LOC100130561	Nucleus	other	4
RAN binding protein 1 pseudogene	LOC389842	Cytoplasm	other	4
leucine-rich PPR-motif containing	LRPPRC	Cytoplasm	other	5
leucine rich repeat containing 59	LRRC59	Cytoplasm	other	2
leucine zipper protein 1	LUZP1	Nucleus	other	11
myristoylated alanine-rich protein kinase C substrate	MARCKS	Plasma Membrane	other	2
membrane bound O-acyltransferase domain containing 7	MBOAT7	Plasma Membrane	other	2
malectin	MLEC	Plasma Membrane	other	1
mitochondrial ribosomal protein L47	MRPL47	Cytoplasm	other	1
mitochondrial ribosomal protein S26	MRPS26	Cytoplasm	other	0
mitochondrial carrier homolog 2 (C. elegans)	MTCH2	Cytoplasm	other	2
myosin, light chain 6, alkali, smooth muscle and non-muscle	MYL6	Cytoplasm	other	0
myosin XVIIIA	MYO18A	Cytoplasm	other	4
myosin IB	MYO1B	Cytoplasm	other	4
myosin IC	MYO1C	Cytoplasm	other	17
myosin ID	MYO1D	Plasma Membrane	other	9
myosin VI	MYO6	Cytoplasm	other	15
nucleosome assembly protein 1-like 1	NAP1L1	Nucleus	other	9
nucleosome assembly protein 1-like 4	NAP1L4	Nucleus	other	2
nuclear autoantigenic sperm protein (histone-binding)	NASP	Nucleus	other	3
nebulette	NEBL	Cytoplasm	other	2
non-POU domain containing, octamer-binding	NONO	Nucleus	other	7
5'-nucleotidase domain containing 2	NT5DC2	unknown	other	1
nuclear distribution gene C homolog (A. nidulans)	NUDC	Cytoplasm	other	5
Obg-like ATPase 1	OLA1	Cytoplasm	other	2
Parkinson disease (autosomal recessive, early onset) 7	PARK7	Nucleus	other	0
poly(rC) binding protein 2	PCBP2	Nucleus	other	5

proliferating cell nuclear antigen	PCNA	Nucleus	other	3
phosphatidylethanolamine binding protein 1	PEBP1	Cytoplasm	other	3
profilin 1	PFN1	Cytoplasm	other	11
progesterone receptor membrane component 1	PGRMC1	Plasma Membrane	other	0
plakophilin 1 (ectodermal dysplasia/skin fragility syndrome)	PKP1	Plasma Membrane	other	0
plastin 3	PLS3	Cytoplasm	other	24
proteasome (prosome, macropain) 26S subunit, non-ATPase, 11	PSMD11	Cytoplasm	other	5
proteasome (prosome, macropain) 26S subunit, non-ATPase, 12	PSMD12	Cytoplasm	other	3
proteasome (prosome, macropain) 26S subunit, non-ATPase, 3	PSMD3	Cytoplasm	other	6
proteasome (prosome, macropain) 26S subunit, non-ATPase, 7	PSMD7	Cytoplasm	other	3
paraspeckle component 1	PSPC1	Nucleus	other	2
protein tyrosine phosphatase-like A domain containing 1	PTPLAD1	Cytoplasm	other	40
glutaminyl-peptide cyclotransferase-like	QPCTL	unknown	other	2
RAD23 homolog B (S. cerevisiae)	RAD23B	Nucleus	other	2
Ran GTPase activating protein 1	RANGAP1	Cytoplasm	other	5
RNA binding motif protein, X-linked	RBMX	Nucleus	other	2
regulator of chromosome condensation 2	RCC2	Nucleus	other	4
reticulocalbin 2, EF-hand calcium binding domain	RCN2	Cytoplasm	other	7
RFT1 homolog (S. cerevisiae)	RFT1	unknown	other	4
ribonuclease/angiogenin inhibitor 1	RNH1	Cytoplasm	other	2
replication protein A1, 70kDa	RPA1	Nucleus	other	3
ribosomal protein L10a	RPL10A (includes EG:4736)	Cytoplasm	other	4
ribosomal protein L11	RPL11	Cytoplasm	other	6
ribosomal protein L13a	RPL13A	Cytoplasm	other	3
ribosomal protein L14	RPL14	Cytoplasm	other	6
ribosomal protein L17	RPL17	Cytoplasm	other	0
ribosomal protein L18	RPL18	Cytoplasm	other	3
ribosomal protein L22	RPL22	Nucleus	other	2
ribosomal protein L23	RPL23	Cytoplasm	other	7
ribosomal protein L26	RPL26	Cytoplasm	other	7
ribosomal protein L35a	RPL35A	Cytoplasm	other	0
ribosomal protein L36	RPL36 (includes EG:25873)	Cytoplasm	other	1
ribosomal protein L7a	RPL7A (includes EG:6130)	Cytoplasm	other	5
ribosomal protein L9	RPL9 (includes EG:6133)	Cytoplasm	other	3
ribosomal protein S10	RPS10	Cytoplasm	other	3
ribosomal protein S13	RPS13	Cytoplasm	other	11

ribosomal protein S16	RPS16	Cytoplasm	other	2
ribosomal protein S2	RPS2 (includes EG:6187)	Cytoplasm	other	14
ribosomal protein S27	RPS27	Cytoplasm	other	2
ribosomal protein S3A	RPS3A	Cytoplasm	other	4
ribosomal protein S5	RPS5	Cytoplasm	other	3
ribosomal protein S7	RPS7	Cytoplasm	other	2
ribosomal protein S9	RPS9	Cytoplasm	other	9
serum amyloid A-like 1	SAAL1	unknown	other	6
sorting and assembly machinery component 50 homolog (S. cerevisiae)	SAMM50	Cytoplasm	other	8
suprabasin	SBSN	unknown	other	0
SCO cytochrome oxidase deficient homolog 2 (yeast)	SCO2 (includes EG:9997)	Cytoplasm	other	2
stromal cell derived factor 4	SDF4	Cytoplasm	other	2
SEC22 vesicle trafficking protein homolog B (S. cerevisiae) (gene/pseudogene)	SEC22B	Cytoplasm	other	5
septin 7	SEPT7	Cytoplasm	other	5
SERPINE1 mRNA binding protein 1	SERBP1	Nucleus	other	4
splicing factor 3b, subunit 3, 130kDa	SF3B3	Nucleus	other	2
splicing factor proline/glutamine-rich	SFPQ	Nucleus	other	6
solute carrier family 25 (mitochondrial oxodicarboxylate carrier), member 21	SLC25A21	Cytoplasm	other	0
small nuclear ribonucleoprotein polypeptide A	SNRPA	Nucleus	other	2
SLIT-ROBO Rho GTPase activating protein 2	SRGAP2	unknown	other	3
signal recognition particle 68kDa	SRP68	Nucleus	other	2
serine/arginine-rich splicing factor 3	SRSF3	Nucleus	other	2
signal sequence receptor, gamma (translocon-associated protein gamma)	SSR3	Cytoplasm	other	7
signal sequence receptor, delta (translocon-associated protein delta)	SSR4	Cytoplasm	other	2
suppression of tumorigenicity 13 (colon carcinoma) (Hsp70 interacting protein)	ST13	Cytoplasm	other	3
stress-induced-phosphoprotein 1	STIP1	Cytoplasm	other	10
stathmin 1	STMN1	Cytoplasm	other	3
stomatin	STOM	Plasma Membrane	other	2
synaptotagmin binding, cytoplasmic RNA interacting protein	SYNCRIP	Nucleus	other	3
transgelin 2	TAGLN2	Cytoplasm	other	13
tubulin folding cofactor A	TBCA	Cytoplasm	other	0
t-complex 1	TCP1	Cytoplasm	other	15
trans-2,3-enoyl-CoA reductase	TECR	Plasma Membrane	other	5
TEL2, telomere maintenance 2, homolog (S. cerevisiae)	TELO2	unknown	other	2
transmembrane protein 109	TMEM109	Cytoplasm	other	3

transmembrane protein 126B	TMEM126B	unknown	other	1
transmembrane protein 161A	TMEM161A	unknown	other	6
transmembrane protein 165	TMEM165	Plasma Membrane	other	2
transmembrane protein 41B	TMEM41B	unknown	other	2
thymopoietin	TMPO	Nucleus	other	8
tropomyosin 1 (alpha)	TPM1	Cytoplasm	other	31
tropomyosin 4	TPM4	Cytoplasm	other	41
translocation associated membrane protein 1	TRAM1	Cytoplasm	other	2
tubulin, beta 2A	TUBB2A	Cytoplasm	other	4
tubulin, beta 2C	TUBB2C	Cytoplasm	other	12
tubulin, beta 3	TUBB3	Cytoplasm	other	2
tubulin, beta 4	TUBB4	Cytoplasm	other	3
tubulin, gamma 1	TUBG1	Cytoplasm	other	2
U2 small nuclear RNA auxiliary factor 2	U2AF2 (includes EG:11338)	Nucleus	other	2
VAMP (vesicle-associated membrane protein)-associated protein A, 33kDa	VAPA	Plasma Membrane	other	1
WD repeat domain 6	WDR6 (includes EG:11180)	unknown	other	2
exportin, tRNA (nuclear export receptor for tRNAs)	XPOT	Nucleus	other	14
YTH domain family, member 2	YTHDF2	unknown	other	2
tyrosine 3-monooxygenase/tryptophan 5-monooxygenase activation protein, epsilon polypeptide	YWHAE	Cytoplasm	other	40
tyrosine 3-monooxygenase/tryptophan 5-monooxygenase activation protein, gamma polypeptide	YWHAG	Cytoplasm	other	5
tyrosine 3-monooxygenase/tryptophan 5-monooxygenase activation protein, theta polypeptide	YWHAQ (includes EG:10971)	Cytoplasm	other	2
AFG3 ATPase family gene 3-like 2 (S. cerevisiae)	AFG3L2	Cytoplasm	peptidase	4
dynein, cytoplasmic 1, heavy chain 1	DYNC1H1	Cytoplasm	peptidase	4
leucine aminopeptidase 3	LAP3	Cytoplasm	peptidase	3
nicalin	NCLN	Cytoplasm	peptidase	2
protein disulfide isomerase family A, member 3	PDIA3	Cytoplasm	peptidase	14
presenilin 1	PSEN1	Plasma Membrane	peptidase	2
proteasome (prosome, macropain) subunit, alpha type, 1	PSMA1	Cytoplasm	peptidase	2
proteasome (prosome, macropain) subunit, alpha type, 3	PSMA3	Cytoplasm	peptidase	1
proteasome (prosome, macropain) subunit, alpha type, 4	PSMA4	Cytoplasm	peptidase	6
proteasome (prosome, macropain) subunit, alpha type, 7	PSMA7	Cytoplasm	peptidase	0
proteasome (prosome, macropain) subunit, beta type, 1	PSMB1	Cytoplasm	peptidase	1
proteasome (prosome, macropain) subunit, beta type, 2	PSMB2	Cytoplasm	peptidase	2
proteasome (prosome, macropain) subunit, beta type, 5	PSMB5	Cytoplasm	peptidase	2

proteasome (prosome, macropain) subunit, beta type, 6	PSMB6	Cytoplasm	peptidase	2
proteasome (prosome, macropain) subunit, beta type, 7	PSMB7	Cytoplasm	peptidase	4
proteasome (prosome, macropain) 26S subunit, ATPase, 1	PSMC1	Nucleus	peptidase	4
proteasome (prosome, macropain) 26S subunit, ATPase, 2	PSMC2	Nucleus	peptidase	1
SEC11 homolog A (S. cerevisiae)	SEC11A	Cytoplasm	peptidase	2
tubulin, gamma complex associated protein 2	TUBGCP2	Cytoplasm	peptidase	2
ubiquitin carboxyl-terminal esterase L1 (ubiquitin thiolesterase)	UCHL1	Cytoplasm	peptidase	4
YME1-like 1 (S. cerevisiae)	YME1L1	Cytoplasm	peptidase	10
protein phosphatase 1, catalytic subunit, alpha isozyme	PPP1CA	Cytoplasm	phosphatase	3
protein phosphatase 2, regulatory subunit A, alpha	PPP2R1A	Cytoplasm	phosphatase	10
protein tyrosine phosphatase, mitochondrial 1	PTPMT1	Cytoplasm	phosphatase	2
SAC1 suppressor of actin mutations 1-like (yeast)	SACM1L	Cytoplasm	phosphatase	3
SET nuclear oncogene	SET	Nucleus	phosphatase	4
calreticulin	CALR	Cytoplasm	transcription regulator	7
cullin-associated and neddylation-dissociated 1	CAND1	Cytoplasm	transcription regulator	3
ClpB caseinolytic peptidase B homolog (E. coli)	CLPB	Nucleus	transcription regulator	5
far upstream element (FUSE) binding protein 1	FUBP1	Nucleus	transcription regulator	2
histone deacetylase 1	HDAC1	Nucleus	transcription regulator	2
heterogeneous nuclear ribonucleoprotein D (AU-rich element RNA binding protein 1, 37kDa)	HNRNPD	Nucleus	transcription regulator	3
huntingtin	HTT	Cytoplasm	transcription regulator	0
interleukin enhancer binding factor 2, 45kDa	ILF2 (includes EG:3608)	Nucleus	transcription regulator	8
LAG1 homolog, ceramide synthase 2	LASS2	Nucleus	transcription regulator	8
MYB binding protein (P160) 1a	MYBBP1A	Nucleus	transcription regulator	2
nascent polypeptide-associated complex alpha subunit	NACA	Nucleus	transcription regulator	5
proliferation-associated 2G4, 38kDa	PA2G4	Nucleus	transcription regulator	5
PDZ and LIM domain 1	PDLIM1	Cytoplasm	transcription regulator	2
prohibitin	PHB (includes EG:5245)	Nucleus	transcription regulator	11
prolactin regulatory element binding	PREB	Nucleus	transcription regulator	2
proteasome (prosome, macropain) 26S subunit, ATPase, 3	PSMC3	Nucleus	transcription regulator	7
proteasome (prosome, macropain) 26S subunit, ATPase, 5	PSMC5	Nucleus	transcription regulator	2

retinoblastoma binding protein 7	RBBP7	Nucleus	transcription regulator	5
RuvB-like 1 (E. coli)	RUVBL1	Nucleus	transcription regulator	11
RuvB-like 2 (E. coli)	RUVBL2	Nucleus	transcription regulator	9
tripartite motif-containing 28	TRIM28	Nucleus	transcription regulator	3
thyroid hormone receptor interactor 13	TRIP13	Cytoplasm	transcription regulator	2
Y box binding protein 1	YBX1	Nucleus	transcription regulator	10
tyrosine 3-monooxygenase/tryptophan 5-monooxygenase activation protein, eta polypeptide	YWHAH	Cytoplasm	transcription regulator	1
basic leucine zipper and W2 domains 1	BZW1	Cytoplasm	translation regulator	4
eukaryotic translation elongation factor 1 alpha 2	EEF1A2	Cytoplasm	translation regulator	2
eukaryotic translation elongation factor 1 delta (guanine nucleotide exchange protein)	EEF1D	Cytoplasm	translation regulator	5
eukaryotic translation elongation factor 2	EEF2	Cytoplasm	translation regulator	42
eukaryotic translation initiation factor 2B, subunit 4 delta, 67kDa	EIF2B4	Cytoplasm	translation regulator	2
eukaryotic translation initiation factor 2, subunit 1 alpha, 35kDa	EIF2S1	Cytoplasm	translation regulator	3
eukaryotic translation initiation factor 3, subunit A	EIF3A	Cytoplasm	translation regulator	4
eukaryotic translation initiation factor 3, subunit B	EIF3B	Cytoplasm	translation regulator	2
eukaryotic translation initiation factor 3, subunit D	EIF3D	Cytoplasm	translation regulator	2
eukaryotic translation initiation factor 3, subunit E	EIF3E	Cytoplasm	translation regulator	4
eukaryotic translation initiation factor 3, subunit F	EIF3F	Cytoplasm	translation regulator	4
eukaryotic translation initiation factor 3, subunit H	EIF3H	Cytoplasm	translation regulator	3
eukaryotic translation initiation factor 4A1	EIF4A1	Cytoplasm	translation regulator	19
eukaryotic translation initiation factor 4 gamma, 1	EIF4G1	Cytoplasm	translation regulator	3
eukaryotic translation initiation factor 5A	EIF5A	Cytoplasm	translation regulator	3
GCN1 general control of amino-acid synthesis 1-like 1 (yeast)	GCN1L1	Cytoplasm	translation regulator	30
insulin-like growth factor 2 mRNA binding protein 1	IGF2BP1	Cytoplasm	translation regulator	8
methylthioribose-1-phosphate isomerase homolog (S. cerevisiae)	MRI1	Cytoplasm	translation regulator	2
poly(rC) binding protein 1	PCBP1 (includes EG:5093)	Nucleus	translation regulator	9

ribosomal protein S23	RPS23	Cytoplasm	translation regulator	2
Tu translation elongation factor, mitochondrial	TUFM	Cytoplasm	translation regulator	14
ATP-binding cassette, sub-family D (ALD), member 3	ABCD3	Cytoplasm	transporter	5
ATP-binding cassette, sub-family E (OABP), member 1	ABCE1	Cytoplasm	transporter	4
apolipoprotein D	APOD	Extracellular Space	transporter	2
ATP synthase, H+ transporting, mitochondrial Fo complex, subunit B1	ATP5F1	Cytoplasm	transporter	5
ATP synthase, H+ transporting, mitochondrial Fo complex, subunit d	ATP5H (includes EG:10476)	Cytoplasm	transporter	0
ATP synthase, H+ transporting, mitochondrial F1 complex, O subunit	ATP5O	Cytoplasm	transporter	4
ATPase, H+ transporting, lysosomal V0 subunit a1	ATP6V0A1	Cytoplasm	transporter	1
ATPase, H+ transporting, lysosomal 70kDa, V1 subunit A	ATP6V1A	Cytoplasm	transporter	10
ATPase, H+ transporting, lysosomal 31kDa, V1 subunit E1	ATP6V1E1	Cytoplasm	transporter	2
ATPase, H+ transporting, lysosomal 50/57kDa, V1 subunit H	ATP6V1H	Cytoplasm	transporter	5
calcium binding protein P22	CHP	Cytoplasm	transporter	3
coatomer protein complex, subunit alpha	COPA	Cytoplasm	transporter	9
coatomer protein complex, subunit beta 1	COPB1	Cytoplasm	transporter	4
coatomer protein complex, subunit beta 2 (beta prime)	COPB2	Cytoplasm	transporter	4
coatomer protein complex, subunit gamma	COPG	Cytoplasm	transporter	3
CSE1 chromosome segregation 1-like (yeast)	CSE1L	Nucleus	transporter	15
endoplasmic reticulum protein 29	ERP29	Cytoplasm	transporter	4
electron-transfer-flavoprotein, alpha polypeptide	ETFA	Cytoplasm	transporter	3
electron-transfer-flavoprotein, beta polypeptide	ETFB	Cytoplasm	transporter	2
hemoglobin, beta	HBB (includes EG:3043)	Cytoplasm	transporter	8
heterogeneous nuclear ribonucleoprotein U (scaffold attachment factor A)	HNRNPU	Nucleus	transporter	6
importin 4	IPO4	Nucleus	transporter	6
importin 5	IPO5	Nucleus	transporter	2
importin 7	IPO7	Nucleus	transporter	6
importin 8	IPO8	Nucleus	transporter	2
importin 9	IPO9	Nucleus	transporter	6
karyopherin alpha 2 (RAG cohort 1, importin alpha 1)	KPNA2	Nucleus	transporter	5
karyopherin (importin) beta 1	KPNB1	Nucleus	transporter	23
protein kinase C and casein kinase substrate in neurons 2	PACSIN2	Cytoplasm	transporter	4
sec1 family domain containing 1	SCFD1	Cytoplasm	transporter	5
Sec61 alpha 1 subunit (S. cerevisiae)	SEC61A1	Cytoplasm	transporter	7
SEC62 homolog (S. cerevisiae)	SEC62	Cytoplasm	transporter	4
sideroflexin 1	SFXN1	Cytoplasm	transporter	3

sideroflexin 4	SFXN4	Cytoplasm	transporter	2
solute carrier family 16, member 1 (monocarboxylic acid transporter 1)	SLC16A1	Plasma Membrane	transporter	14
solute carrier family 16, member 1 (monocarboxylic acid transporter 1)	SLC16A1	Plasma Membrane	transporter	2
solute carrier family 1 (neutral amino acid transporter), member 5	SLC1A5	Plasma Membrane	transporter	10
solute carrier family 25 (mitochondrial carrier; citrate transporter), member 1	SLC25A1	Plasma Membrane	transporter	4
solute carrier family 25 (mitochondrial carrier; oxoglutarate carrier), member 11	SLC25A11	Cytoplasm	transporter	14
solute carrier family 25, member 13 (citrin)	SLC25A13	Cytoplasm	transporter	10
solute carrier family 25 (mitochondrial thiamine pyrophosphate carrier), member 19	SLC25A19	Cytoplasm	transporter	3
solute carrier family 25 (mitochondrial carrier: glutamate), member 22	SLC25A22	Cytoplasm	transporter	4
solute carrier family 25 (mitochondrial carrier; phosphate carrier), member 3	SLC25A3	Cytoplasm	transporter	42
solute carrier family 35, member B2	SLC35B2	Cytoplasm	transporter	2
solute carrier family 39 (zinc transporter), member 14	SLC39A14	Plasma Membrane	transporter	6
solute carrier family 6 (neutral amino acid transporter), member 15	SLC6A15	Plasma Membrane	transporter	1
solute carrier family 7 (cationic amino acid transporter, y+ system), member 1	SLC7A1	Plasma Membrane	transporter	4
solute carrier family 7 (cationic amino acid transporter, y+ system), member 5	SLC7A5	Plasma Membrane	transporter	2
structural maintenance of chromosomes 2	SMC2	Nucleus	transporter	5
spinster homolog 1 (Drosophila)	SPNS1	Cytoplasm	transporter	2
synaptogyrin 1	SYNGR1	Plasma Membrane	transporter	1
transferrin receptor (p90, CD71)	TFRC	Plasma Membrane	transporter	5
transmembrane 9 superfamily member 1	TM9SF1	Plasma Membrane	transporter	2
transmembrane 9 superfamily member 3	TM9SF3	Cytoplasm	transporter	4
transmembrane emp24-like trafficking protein 10 (yeast)	TMED10	Cytoplasm	transporter	3
transportin 1	TNPO1	Nucleus	transporter	3
translocase of outer mitochondrial membrane 22 homolog (yeast)	TOMM22	Cytoplasm	transporter	7
translocase of outer mitochondrial membrane 70 homolog A (S. cerevisiae)	TOMM70A	Cytoplasm	transporter	3
exportin 4	XPO4	Nucleus	transporter	4
exportin 5	XPO5	Nucleus	transporter	4

7

The constitutively active HCMV-encoded receptor UL33 displays oncogenic potential

Adapted from: Erik Slinger[1], Ellen V. Langemeijer[1], Andreas Schreiber[1], Afsar Rahbar[2], Marijke Stigter-van Walsum[3], David Maussang[1], Marco Siderius[1], Guus van Dongen[3], Rob Leurs[1], Cecilia Söderberg-Nauclér[2] and Martine J. Smit[1]
(*Manuscript in preparation*)

[1]Leiden/Amsterdam Center for Drug Research, Faculty of Sciences, Division of Medicinal Chemistry, VU University Amsterdam, de Boelelaan 1083, 1081 HV Amsterdam, The Netherlands; [2]Department of Medicine, Center for Molecular Medicine, Karolinska University Hospital Solna and Karolinska Institutet, Stockholm, Sweden. [3]Department of Otolaryngology/Head and Neck Surgery, VU University Medical Center, Amsterdam, the Netherlands.

7.1 Abstract

The human cytomegalovirus (HCMV), associated with the development of malignancies, encodes the constitutively active G protein coupled receptors (GPCRs) UL33 and US28. As US28 possesses oncogenic properties and is expressed in CMV positive human glioblastomas, we set out to investigate the signaling properties of UL33. US28 expression is detected early after infection, whereas UL33 is expressed at later stages. In transient, as well as stable transfection systems, UL33, like US28, constitutively activates various proliferative, pro-angiogenic signal transduction pathways. In xenograft models, UL33 was shown to induce tumor growth. As shown previously for US28, UL33 expression was also detected in human glioblastoma. Interestingly, the distribution of UL33 in the primary glioblastoma samples was more dispersed, while expression of US28 was confined to the vascular niche. Taken together, our data indicate that the viral GPCR UL33 has oncogenic potential and could play a role in HCMV-associated malignancies. The differential kinetics of UL33 and US28 expression and pronounced expression of UL33 in human glioblastoma, indicate that HCMV has devised distinct means to engage or prolong proliferative signaling pathways upon infection through expression of these viral receptors.

7.2 Introduction

The mammalian line of defence against invasion of pathogens or injury depends on timely activation and proper targeting of leukocytes (1, 2). Chemokine-chemokine receptor interactions are crucial to control both onset and localization of leukocyte-mediated responses. Several b-herpesviruses have corrupted this system by hijacking and subverting components, both ligands and receptors, of the chemokine system (3-5). Human cytomegalovirus (HCMV, HHV-5), a member of the b-herpesvirus subfamily has successfully utilized this strategy resulting in high prevalence with up to 90% of the population harbouring a latent infection (5). While HCMV infection is asymptomatic in immune-competent individuals, it can cause severe pathologies in immune-compromised patients (6, 7). Moreover, HCMV infection during pregnancy is the leading infectious agent causing mental retardation and deafness of the unborn child (8). Furthermore, HCMV infection is associated with several pathologies, such as atherosclerosis (9), autoimmune diseases and cancers (6, 7, 10, 11). HCMV infection has been proposed to aggravate the malignant phenotype of e.g. colon cancer (12) malignant glioma (6, 13) and medulloblastoma (14). The HCMV-encoded chemokine receptor US28 is one of the HCMV-encoded proteins believed to contribute to the malignant phenotype (14-16).

US28 has been shown to scavenge and internalize different members of the CC family chemokines including CCL5 and CCL2, and also CX3CL1 (17). Furthermore, US28 has been shown to constitutively stimulate proliferative signaling (16, 18-20). Moreover, this GPCR have been implicated in oncomulation in vivo, as heterologous expression of US28 in mice, stimulates intestinal neoplasia (21). Furthermore, expression of US28 was correlated to proliferative signaling and poor prognosis in human glioblastoma (16).

Besides US28, HCMV encodes three other viral G protein coupled receptors (vGPCRs) with homology to human chemokine receptors; US27, UL33, and UL78 (3). These receptors and two chemokine homologues (vCXCL1 and 2) (22) may be utilized by the virus to deceive the host's immune system and could be instrumental in viral pathology. Homologues of UL33 and UL78 are conserved throughout the β-herpesvirus family (23). In contrast, US28 and US27 have been identified only in CMVs, closely related to HCMV, targeting primate hosts (24).

Like US28, UL33 has been shown to signal in a constitutive manner via Gaq, Gai, and Gas (25). The constitutive activation of both receptors could be instrumental in HCMV-mediated pathology. Therefore, it is crucial to determine the kinetics and cellular consequences of signaling mediated by these vGPCRs. The UL33 homologue in the murine cytomegalovirus (M33) was shown to be functional in viral dissemination (26). Interestingly, loss of M33 can be partially complemented with functional UL33, suggesting conservation of functionality. Both UL33 and US28 were found to co-localize with the viral envelop glycoproteins gB and gH (Margulies, Browne et al. 1996, Fraile-Ramos, Pelchen-Matthews et al. 2002). Although UL33 (27) and US28 (28) are dispensable for viral replication in respectively MCR5 and human forskin

fibroblasts, functional consequence of expressing vGPCRs on the viral particle may enhance binding of the virus particles to target cells. Alternatively, these receptors could exert their effect by rewiring cellular signaling of the host cells.
In this study we describe the UL33-mediated constitutive activation of proliferative signal transduction pathways, and consequences for cellular transformation. Moreover, we detected the expression of this vGPCR in human glioblastoma. As UL33 and US28 expression patterns after HCMV infection revealed different kinetics, our data suggest HCMV may use both UL33 and US28 to successfully engage proliferative signaling pathways in the host cell.

7.3 Results

7.3.1 UL33 is expressed with different kinetics compared to US28 in HCMV infection cycle

As both US28 and UL33 were previously shown to constitutively signal via multiple Ga-dependent signaling pathways, we examined the possibility of these events to occur in concert by monitoring expression of both receptors during the HCMV infection cycle. We evaluated the kinetics of US28 and UL33 expression after infection of human foreskin fibroblasts (HFF) using the HCMV TB40-BAC4 strain. We analyzed the kinetics of UL33 expression taking advantage of the N-terminally Flag tagged UL33 (TB40-BAC4-UL33ex1-FLAG). US28 was visualized using the antibody described (16). Intracellular distribution of both US28 and UL33 was similar as described earlier (35, 36) with UL33 mostly present in intracellular vesicles and US28 concentrated in the perinuclear area (data not shown). The kinetics of expression of both UL33 and US28 were investigated in situ and by Western analysis (Figure 1A and B). As can be seen in Figure 1A, expression of UL33ex1-FLAG was observed at 96, 120 and 144 hours post infection (h.p.i.), whereas US28 is already detectable 24 h.p.i., at low levels as indicated by Western blotting (Figure 1B). This may indicate an exclusive role of US28 early after infection and collective effects of both receptors, later in the infection cycle. Confirmation of US28 expression early in the HCMV infection cycle was obtained by means of radioligand binding assays, using [^{125}I]-CCL5, a chemokine known to bind US28. In these analyses, increased binding of [^{125}I]-CCL5 was observed 48 hrs after infection with the wild type HCMV strain (Wt) but not with the DUS28 (US28 deletion strain) - or UV-inactivated virus (Figure 1C). As no ligands for UL33 have been identified to date, these assays could not be performed for this vGPCR. To examine the functional consequence of differential expression of both viral GPCRs, PLC activation was measured in HCMV infected cells. For this purpose, TB40 wild type and mutant viral strains, deleted for UL33, US28 or both were used (33). All HCMV mutants used in this study displayed similar infection properties as confirmed by back titration (data not shown). Activation of PLC in HFF was significantly reduced for DUS28 and the double deletion mutant DUS28-DUL33 viral strains 48 h.p.i. (Figure 1D). Deletion of UL33 alone did not result in a significant reduction of PLC activation 48 h.p.i.

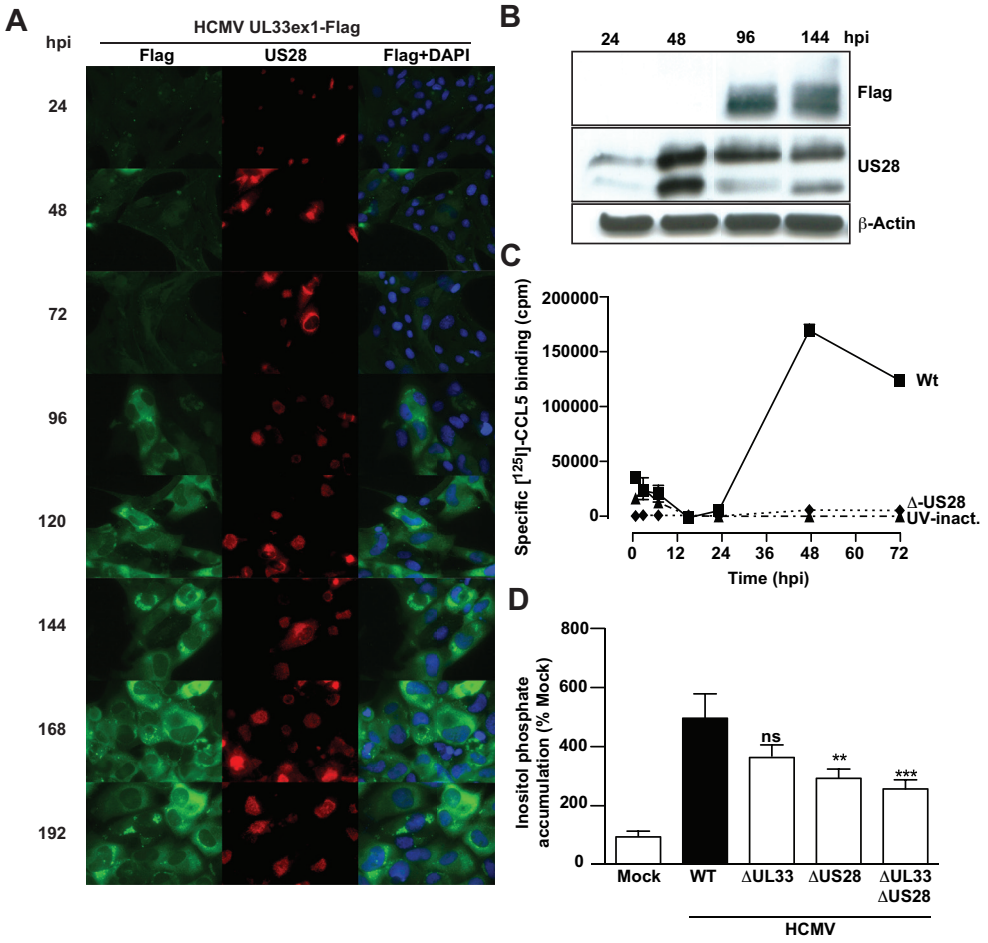

Figure 1. Kinetics of expression UL33 and US28 after HCMV infection. (**A**) UL33 receptor expression after infection with TB40 UL33ex1-FLAG (green) increases 96, 120, and 144 hours post infection in HFF cells. US28 (red) is expressed expression 24 hours post infection, with strongest expression from 48 hours post infection and onwards. All micrographs have been taken at 40x magnification. Nuclei of the cells were stained with DAPI (blue). (**B**) Western-blot analysis of both UL33ex1-FLAG and US28 expression in infected cells. The US28 typically antibody stains two bands of approximately 45 kD and 40 kD as shown in the panel. Expression of Flag-tagged UL33 (35 kDa) is observed at 96, 120 and 144 hours post infection (h.p.i.), whereas US28 is already detectable at low levels 24 h.p.i. Presence of US28 increases at later time-points. (**C**) [^{125}I]-CCL5 binding shows early kinetics of US28 protein expression in AD169-WT–infected cells with a peak at 48 h.p.i. No [^{125}I]-CCL5 binding is detected in cells infected with AD169-ΔUS28 mutant or in UV-inactivated WT virus infected cells. (**D**) PLC activation is significantly reduced in the absence of US28 in TB40-BAC4 deletion mutant virus infected cells 48 h.p.i. Inositol phosphate accumulation performed on HFF cells, infected with m.o.i. of 2 of different deletion HCMV TB40-BAC4 strains shows significant reduction in inositol phosphate accumulation by US28 and a double deletion mutant viral strain compared to wild-type infected cells (*$p < 0.05$, **$p < 0.01$, ***$p < 0.001$ respectively). Virus m.o.i. used in infections was confirmed to be comparable by back titration (data not shown).

7.3.2 HCMV-encoded UL33 constitutively activates multiple signaling pathways

As US28 was described to promiscuously trigger activation of various proliferative-, angiogenic- and inflammatory signaling pathways resulting in oncomodulatory effects (16, 32, 37), we evaluated UL33-mediated activation of these signaling pathways. As can be seen in Figure 2A, transfection of increasing amounts of pcDEF3-UL33 increased levels of UL33 protein as detected in an ELISA using anti-UL33 antibody (27). UL33 constitutively induced VEGF promotor activity in a dose-dependent manner, as was measured with a specific reportergene (Figure 2B). Likewise, UL33 expression induced activation of the NFAT pathway, COX2 promotor activity and STAT3 transcriptional activity as measured with specific reportergenes when expressed in HEK293T cells (Figure 2C-E).

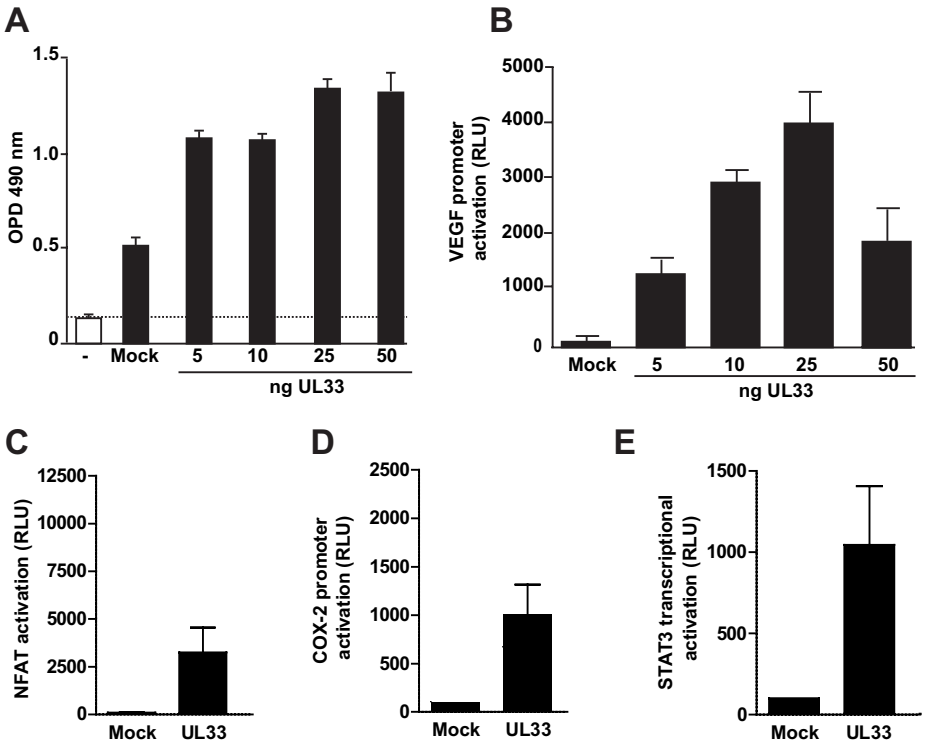

Figure 2. Viral chemokine receptor UL33 constitutively activates various signal transduction pathways. (**A**) ELISA of expression of UL33 after transfection with various amounts of the pcDEF3-UL33 to HEK293 cells. Bars represent the expression in permeabilized cells. Anti-UL33, kindly provided by Prof. W. Gibson, was used to detect UL33. (**B**) UL33 dose-dependently activates VEGF promotor activity. UL33 also induces NFAT transcriptional activation (**C**), COX-2 promoter activation (**D**), and STAT3 transcriptional activation (**E**). For all reporter gene assays HEK293T cells (1x106) are transiently transfected with 25 ng UL33 DNA in combination with the respective reporter constructs. Luciferase expression was determined 24 hrs post transfection. Results are presented in relative light units (RLU) and are all normalized (Mock is 100).

7.3.3 UL33 induces a transformed phenotype in NIH-3T3 cells

To investigate whether UL33 expression was associated with onset of transformation, as shown earlier for US28 (19), stable NIH-3T3 cell lines expressing UL33 were generated. To this end, wildtype UL33 and C-terminally eGFP-tagged UL33 constructs were used. Constitutive PLC activation indicated proper receptor functionality and expected signaling properties of both wt UL33 and eGFP-tagged UL33 receptors (Figure 3A). The observed increase in PLC activation in cell lines expressing UL33 was lower compared to those in US28-expressing NIH-3T3 cells

To examine the proliferative potential of UL33, a thymidine incorporation assay was done. Clearly, cell lines expressing UL33 displayed increased [^{3}H]-thymidine incorporation. DNA synthesis upon serum starvation was two-to four-fold higher in UL33-expressing cells compared to mock transfected cells. To confirm the oncogenic potential of UL33 a foci formation assay was performed. As depicted in Figure 3C UL33-eGFP expressing cells lost contact inhibition and formed foci as seen for US28-expressing cells, albeit with a lower efficiency compared to US28. In view of convergence of UL33 signaling into the STAT3 pathway, observed earlier for US28 (16), cells were treated with stattic, a small inhibitor molecule inhibitor targeting STAT3 (38). Stattic inhibited foci formation in UL33-expressing cells to a similar extent as seen in US28-expressing cells (Figure 3D).

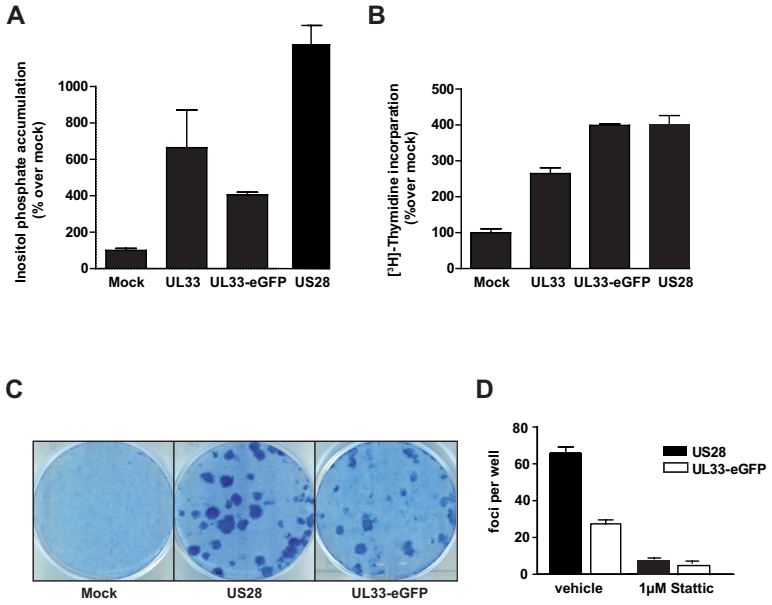

Figure 3. UL33 induces a proliferative phenotype in NIH-3T3. (**A**) UL33 shows constitutive inositol phosphate accumulation in NIH-3T3 cells stably expressing UL33 wt and UL33-eGFP. Constitutive accumulation of inositol phosphate in NIH-3T3 cells expressing US28 was used as positive control. (**B**) UL33 expressing NIH-3T3 cells display increased proliferation as measured by [^{3}H]-thymidine incorporation. Data are normalized over 3T3-Mock values. [^{3}H]-thymidine incorporation by NIH-3T3 cells stably expressing US28 was used as positive control. (**C**) NIH-3T3 cells expressing UL33-eGFP show loss of contact inhibition as evidenced by the appearance of foci, albeit to a lesser degree compared to NIH-3T3 cells expressing US28. (**D**) Inhibition of foci formation by NIH-3T3 cells stably expressing UL33-eGFP and US28, respectively, in the presence of 1 µM Stattic (specific inhibitor of STAT3 dimerization).

7.3.4 UL33 stimulates proliferative signaling

Since in vitro studies with UL33-expressing cells showed a transformed and proliferative phenotype, we determined whether UL33-eGFP expressing cells could also induce tumor formation in vivo. To this end, UL33-eGFP or US28 expressing NIH-3T3 cells were subcutaneously (s.c.) injected in the flanks of nude athymic mice (6 mice injected per cell line; 12 inoculations). First signs of tumor formation appeared as early as 1 week post injection for the mice injected with US28 expressing cells, and shortly after that for the mice injected with the UL33-eGFP cells, as shown in the Kaplan-Meier curve (Figure 4B). Tumours were clearly visible 2-3 weeks after inoculation (Figure 4A), after which animals were sacrificed. Some mice injected with UL33 expressing cells displayed smaller tumours at the exterior, however, large internal tumours were present in all cases. The mock group, as previously published (19), did not develop tumours up to 75 days after injection. Gene expression of US28 and UL33 was confirmed by RT-PCR in the tumours formed (Figure 4C). For US28 a much higher expression (>256x higher) was obtained than for UL33 mRNA.

7.3.5 UL33 expression in primary glioblastoma

Previous study from our laboratory has shown that US28 is expressed in primary glioblastoma tumors (16). To examine the potential presence of UL33 in primary glioblastoma, we examined tissue samples of 25 glioblastoma patients by immunohistochemistry using antibodies raised against UL33. UL33 was expressed at different levels in GBM tumors, mainly in the tumor cells that appear as patches in

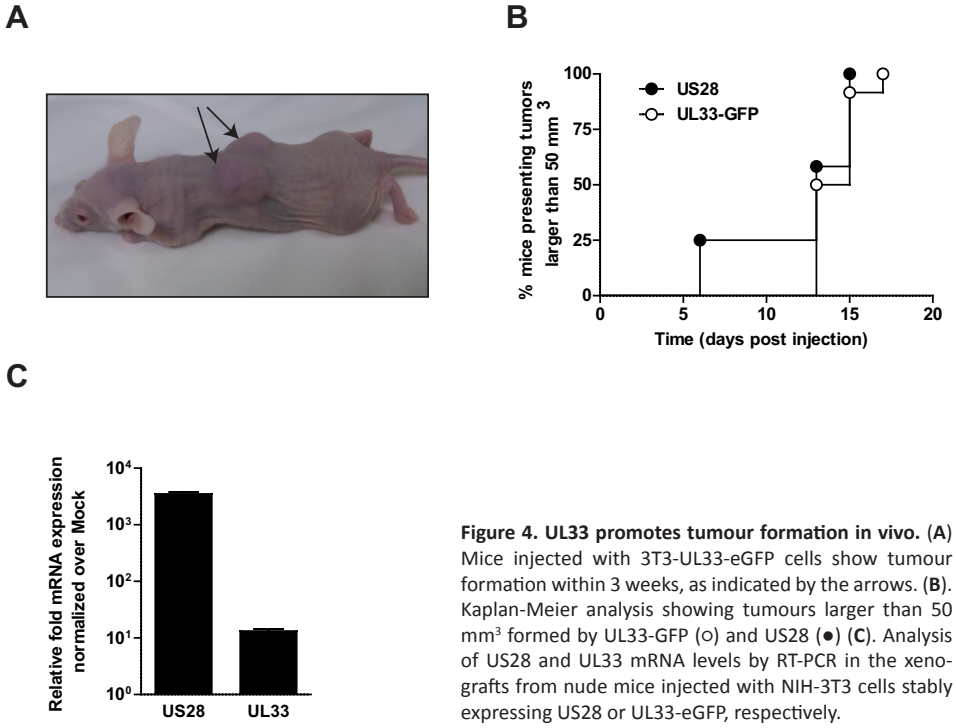

Figure 4. UL33 promotes tumour formation in vivo. (**A**) Mice injected with 3T3-UL33-eGFP cells show tumour formation within 3 weeks, as indicated by the arrows. (**B**). Kaplan-Meier analysis showing tumours larger than 50 mm^3 formed by UL33-GFP (○) and US28 (●) (**C**). Analysis of US28 and UL33 mRNA levels by RT-PCR in the xenografts from nude mice injected with NIH-3T3 cells stably expressing US28 or UL33-eGFP, respectively.

the tissue (Figure 5 B –D and F). UL33 staining is primarily cytoplasmic (Figure 5D). Patients were categorized in two groups (based on approximately percentage number of UL33 positive cells in their tumors (negative or grade1; <10% and grade 2; >10%-50%). UL33 was expressed in <10% of the tumor cells in 15/25 (60%), in >10-50% in 10/25 (40%). One of the samples tested in this study was negative for UL33. Median overall survival was 15.5 months in group 1 vs 13 months in group 2 of patients

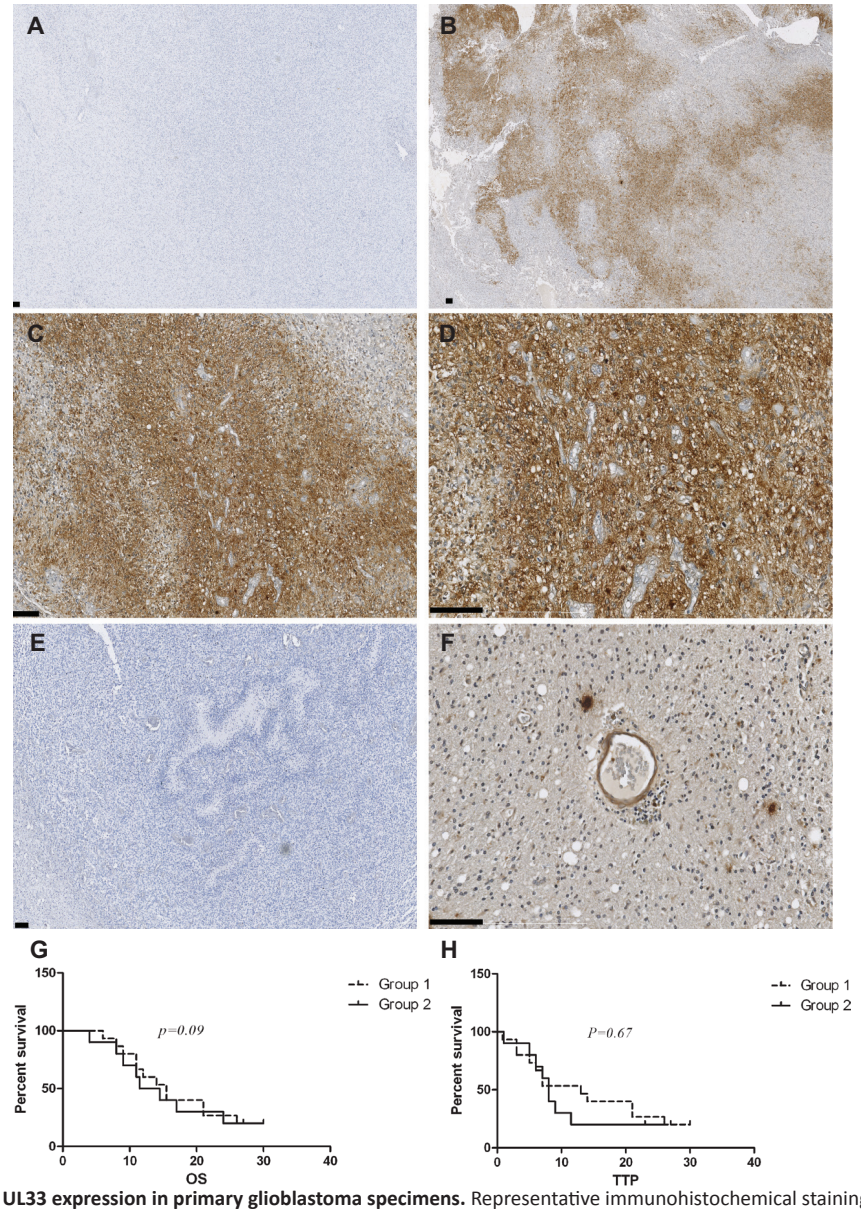

Figure 5 UL33 expression in primary glioblastoma specimens. Representative immunohistochemical stainings are shown. (**A** and **E**) Rabbit IgG isotype control staining (**B**, **C**, **D** and **F**) Samples stained with anti-UL33 antiserum (brown). Scale bars 100 µm. (**G**) Patient overall survival (OS), and (**G**) time to tumor progression (TTP) are not significantly affected by UL33 expression.

(p= 0.09, Figure 5G). Time to first tumor progression was 5 months longer in group 1 patients compared to group 2 patients (13 vs 8 months, p=0.67, Figure 5H). 5 patients were alive; 3 patients in group I and 2 patients in group 2.
Expression of UL33 around vessels, the main site for expression of US28 in primary glioblastoma, in these tissue samples (Figure 5F) was detected in 9 out of the 25 (36%) of tumor samples. In these cases mostly endothelial cells and smooth muscle cells (SMC) appeared to be positive for UL33 staining. Interestingly, infiltrating neutrophils and granulocytes appear to be strongly positive for UL33 in 8/25 (32%) of these patients (Figure 5F).

7.4 Discussion

Herpesviruses are known to alter cellular gene expression and cell function (39, 40). While the oncogenic potential of some viruses like Kaposi sarcoma associated herpes virus and human papilloma virus is well established (41, 42), HCMV is believed to possess oncomodulatory properties. In view of the oncomodulatory potential of the HCMV-encoded chemokine receptor US28 (4, 15, 19, 43, 44), we subjected UL33, another constitutively active viral encoded chemokine receptor homolog (25) to signaling and cell proliferation studies. In this study we clearly demonstrate that UL33, like US28, has oncogenic potential in vitro as well as in vivo. UL33 constitutively activates several signaling pathways (Figure 2), which play key roles in enhanced cellular proliferation and oncogenesis (45-47). UL33 stimulated transcriptional activation of NFAT and STAT3 (Figure 2C and 2E) and induced VEGF and COX-2 promoter activation (Figure 2B and 2D). NIH-3T3 cells stably expressing UL33 exhibit constitutive PLC activation, increases in DNA synthesis rate and loss of contact inhibition (Figure 3), properties indicative of transformation. UL33-eGFP expressing NIH-3T3 cells induce tumor growth within 3 weeks in a nude mice xenograft model (Figure 4). Tumor formation was apparent after 2 weeks, while did occur earlier for US28. The slower onset of tumor formation compared to mice injected with US28 expressing NIH-3T3 cells, can be explained by reduced increases in PLC activity and foci formation UL33 compared to US28 expressing NIH-3T3 cells. Moreover, the UL33 mRNA levels in the xenografts are significantly lower compared to US28 mRNA levels in US28-induced xenografts (Figure 5 C), suggesting that the oncomodulatory effects of both US28 and UL33 may differ, despite the overlap in receptor-induced signaling we have observed. Noteworthy, unlike for US28 (16), increased IL6 levels could not be detected in medium from NIH-3T3 cells stably expressing UL33 (data not shown) nor could we measure increased PGE2 levels. Although both vGPCRs can activate a comparable set of signaling pathways, a certain threshold of activation may be required to induce rapid onset of turmorigenesis.
To study the expression kinetics of UL33 and US28 in HCMV infected cells, human foreskin fibroblasts (HFF) were infected with a mutant HCMV virus (BAC40-UL33ex1-Flag). Intracellular localization of both US28 and UL33 was comparable as described earlier (Fraile-Ramos, Pelchen-Matthews et al. 2002). The kinetics of expression of

both vGPCRs differ, with US28 being detectable 24 h.p.i., whereas UL33 only appeared after 72 h.p.i. Early expression kinetics of US28 was confirmed in a CCL5 binding assay and by measuring PLC activation 48 h.p.i. using HCMV TB40 WT and mutant strains lacking either US28, UL33 or both vGPCRs (33). Our data show that UL33, unlike US28, is expressed at a late stage of the HCMV replication cycle. This confirmed earlier observations on US28 and UL33 expression profiles in HFF and U373-MG cells (28, 36, 48). In a viral setting, both receptors could have modulatory functionalities important in HCMV pathology. As the UL33 expression kinetics is slower compared to that of US28, this may result in further activation of signaling pathways initially triggered by US28. For instance, the enhanced COX-2 promoter activity as previously described for US28 (32), could be prolonged by UL33 late expression. A comparable synergism could be postulated for the activation of STAT3 signaling important in US28 mediated oncomodulation (16). Yet, co-expression of both receptors could also result in antagonizing effects. Recently, UL33 was reported to co-localize and form heterodimers with US28 (49). Interestingly, the constitutive activation of the US28-mediated Gαq/phospholipase C pathway was not affected by receptor heteromerization, while UL33 was able to silence US28-mediated activation of the transcription factor NF-κB. These data imply that co-expression may result in inhibitory effects on downstream signaling. Further experiments are required to substantiate whether co-expression of both receptors does result in altered proliferative signaling.

Besides temporal synergy or modulatory function between the vGPCRs also a spatial complementarity between UL33 and US28 could affect HCMV-induced pathology. In this study we have shown that UL33 is expressed at detectable levels in primary glioblastomas (Figure 5). Compared to our earlier observation regarding expression of US28 in glioblastoma the pattern of UL33 expressed in these tumors is more pronounced. Whereas US28 is primarily expressed around the blood vessels within the so-called vascular niche (Slinger, Maussang et al. 2010), UL33 expression is detected in the vessel area as well within the cells that make up the tumor tissue and in immune cells invading the tissue. However, UL33 expression levels do not significantly correlate with patient outcome and survival.

Taken together, our data indicate that the viral GPCR UL33 has oncogenic potential and could play a role in HCMV-associated malignancies. The differential kinetics of UL33 and US28 expression and pronounced expression of UL33 in human glioblastoma, indicate that HCMV has devised distinct means to engage or prolong proliferative signaling pathways upon infection through expression of these viral receptors.

7.5 Materials and methods

Cell culture
HEK293T cells, human glioblastoma U373 cells, and mouse fibroblast NIH-3T3 cells were cultured in DMEM supplemented with penicillin/streptomycin (50 IU/ml) and 10% of fetal bovine, heat inactivated fetal bovine or bovine serum, respectively. Transfections were performed in HEK293T with the polyethylenimine (PEI) method (29). Transfections in U373 and NIH-3T3 cells were performed with the calcium phosphate method. Stably transfected NIH-3T3 cells were selected and maintained in culture with neomycin (400 mg/ml) to ensure expression of UL33 and US28 receptors, respectively.

Receptor characterization by inositol phosphate formation and thymidine Incorporation
UL33 or US28 expression and constitutive signaling were analyzed for inositol phosphate formation as previously described. As for thymidine incorporation measurement, the experiment was carried out upon serum starvation by using medium containing 0.5% calf serum. [6-^{3}H]-Thymidine was obtained from GE Healthcare Life Sciences (Buckinghamshire, UK) and used to label at a concentration of 1 µCi/ml [6-^{3}H]-Thymidine.

Reporter gene analysis
For the promoter activation measurements, 106 HEK293T cells were transfected with 0.5-1.5 mg of reporter-Luciferase plasmid and the indicated amounts (25 ng or 1 mg) of pcDEF3-UL33. To measure VEGF promoter activation, (500ng/1*106 cells) the pGL2-VEGF-Luciferaselucuciferase construct, kindly provided by Dr. G. Pages (Institute of Signaling Development Biology and Cancer, Nice, France) was used. The Ly6E STAT3-–response element luciferase construct (500ng/1*106 cells) (30) was used for STAT3 activity measurements. The NFAT reporter gene (500ng/1*106 cells), pNFAT-luc was purchased from Stratagene. Total DNA amounts were kept constant using empty vector pcDEF3. In U373 infected cells, transfection of the VEGF-Luciferase plasmid (19) was performed 2 h post infection (multiplicity of infection 1). Luciferase activities were measured 24 h after transfection with a Victor2 multilabel plate reader from Perkin-Elmer.

Focus formation assay
The focus formation assay was performed as described by (31) 400 stably transfected NIH-3T3 cells were cultured with 2000 untransfected NIH-3T3 cells for 2 weeks in regular culture medium without G418 in 6 well plates. Treatment with Stattic was initiated 12 hours after seeding. Medium containing Stattic was replaced every 48 hours after seeding. After 2 weeks, the cells were washed three times with phosphate buffered saline (PBS) and subsequently fixed in cold methanol for 10 min. Subsequently, the cells were stained with 0.4% methylene blue in H2O and the foci were counted.

Tumor formation in vivo

All animal experiments were performed according to the National Institutes of Health principles of laboratory animal care and Dutch national law and approved by the Dierexperimentencommissie from the VU Medical Center and performed in compliance with the protocol FaCh 05-02. Stably transfected NIH-3T3 cells (2*106) containing pcDEF3-US28, or pcDEF3-UL33-eGFP plasmids were injected s.c. into the flank of 8- to 10-week-old female nude mice (Hsd, athymic nu_nu, 25–32 g, Harlan Laboratories Cambridge Research Biochemicals; Zeist, The Netherlands).

RT-PCR

In the UL33-eGFP- and US28-expressing NIH-3T3 cells as well as the tumours formed, UL33 and US28 gene expression was checked using standard reverse transcriptase PCR (RT-PCR) as previously described (32). For detection of US28 mRNA the primers used were US28 forward 5-AGCGTGCCGTGTACGTTAC-3 and US28 reverse 5-ATAAAGACAAGCACGACC-3. For detection of UL33 mRNA the primers used were UL33 forward 5-GGAAAGTGCTGCTGACGCTAG-3 and UL33 reverse 5-GCTGTACGGTTGAGTAGAAGAAGG-3.

HCMV infections and Western blot analysis

U373 MG cells were infected with TB40-BAC4-HCMV (33) strains containing the wild type genotype or a mutant version. Using a recombinant virus encoding a FLAG-tagged UL33 expression and sub cellular localization of UL33 was studied after HCMV-infection. 2*105 HFF cells were seeded in 6-well plates and infected the next day at m.o.i. of 2. After 2 hrs, virus was removed and cells were washed 3 times with PBS to enable a synchronized infection. After indicated time (1, 2, 3, 4, 5, 6, 7 or 8 dpi) cells were washed 3 times with cold PBS, scraped and stored as a dry cell pellet at -20. Cell lysates were prepared in Ripa buffer containing protein inhibitors, lysates were sonicated for 10 sec. 12 µg of total protein was loaded on SDS-PAGE and after electrophoresis proteins were transferred to PVDF membranes by tank blotting (Biorad). Membranes were stained with anti-FLAG (Sigma polyclonal rabbit) to detect UL33ex1-FLAG expression. Loading on the gel was controlled by actin staining. Western blots were detected using anti rabbit-HRP conjugated secondary antibodies (BioRad) and chemiluminescent ECL substrate.

Patient Samples and Immunohistochemistry

Paraffin-embedded primary brain tumor specimens were available from 25 GBM patients who were admitted to the Karolinska University Hospital Sweden during 2009-2010. Tissue sections (6 um thick) were stained for UL33 using sensitive immunohistochemistry staining protocols as previously been described (Bellon and Nicot 2008). Briefly, the sections were deparaffinized in xylene (Sigma Aldrich), rehydrate in alcohol series, postfixed with 4% neutral buffered formalin (Apoteketpharmaci, Stockholm, Sweden), treated with pepsin (Biogenex, San Ramon, CA), and then incubated in citrate buffer (Biogenex). The sections were treated with 3% H2O2 (Sigma-Aldrich) to inactivate endogenous peroxidase, avidin/biotin blocking kit (DakoCytomation, Glostrup, Denmark), was used in order to block endogenous biotin/avidin and FC receptor blocker (Innovex Biosciences) to block FC-R. Finally, the tissue sections were treated with background buster (Innovex Biosciences). Incubation with primary polyclonal rabbit antibodies against human CMV-UL33 (Margulies, Browne et al. 1996) was done overnight at 4°C. Polyclonal rabbit IgG antibodies (R&D Systems, Minneapolis, MN) was used as isotype control. After incubation with primary antibodies, the

sections were incubated with biotinylated anti-rabbit (DakoCytomation) antibodies. Finally, the antibodies were visualized using streptavidin-conjugated horseradish peroxidase and diaminobenzidine (Innovex Biosciences). This study was approved by the ethics committees at Karolinska Institutet, Stockholm, Sweden (Dnr (2008/628-31/2).

Acknowledgements
We thank Stefan Dekker for technical assistance. Professor Wade Gibson is acknowledged for sharing the anti-UL33 antibody. This work was supported by The Netherlands Organization for Scientific Research (NWO) to E. Langemeijer, E. Slinger, D. Maussang and M.J. Smit, VIDI grant to M.J. Smit 700.54.425

References

1. F. Sallusto, A. Lanzavecchia, C. R. Mackay, Chemokines and chemokine receptors in T-cell priming and Th1/Th2-mediated responses. Immunol Today 19, 568 (Dec, 1998).
2. I. F. Charo, R. M. Ransohoff, The many roles of chemokines and chemokine receptors in inflammation. N Engl J Med 354, 610 (Feb 9, 2006).
3. H. F. Vischer, R. Leurs, M. J. Smit, HCMV-encoded G-protein-coupled receptors as constitutively active modulators of cellular signaling networks. Trends Pharmacol Sci 27, 56 (Jan, 2006).
4. E. Slinger, E. Langemeijer, M. Siderius, H. F. Vischer, M. J. Smit, Herpesvirus-encoded GPCRs rewire cellular signaling. Mol Cell Endocrinol 331, 179 (Jan 15, 2011).
5. M. K. Gandhi, R. Khanna, Human cytomegalovirus: clinical aspects, immune regulation, and emerging treatments. Lancet Infect Dis 4, 725 (Dec, 2004).
6. C. Soderberg-Naucler, Does cytomegalovirus play a causative role in the development of various inflammatory diseases and cancer? J Intern Med 259, 219 (Mar, 2006).
7. L. Soroceanu, C. S. Cobbs, Is HCMV a tumor promoter? Virus Res 157, 193 (May, 2011).
8. W. Britt, Manifestations of human cytomegalovirus infection: proposed mechanisms of acute and chronic disease. Curr Top Microbiol Immunol 325, 417 (2008).
9. J. L. Melnick, C. Hu, J. Burek, E. Adam, M. E. DeBakey, Cytomegalovirus DNA in arterial walls of patients with atherosclerosis. J Med Virol 42, 170 (Feb, 1994).
10. L. E. Harkins et al., Detection of human cytomegalovirus in normal and neoplastic breast epithelium. Herpesviridae 1, 8 (2010).
11. M. Michaelis, H. W. Doerr, J. Cinatl, The story of human cytomegalovirus and cancer: increasing evidence and open questions. Neoplasia 11, 1 (Jan, 2009).
12. L. Soroceanu, C. S. Cobbs, Is HCMV a tumor promoter? Virus Res 157, 193 (May, 2011).
13. K. Dziurzynski et al., Consensus on the role of human cytomegalovirus in glioblastoma. Neuro Oncol 14, 246 (Mar, 2012).
14. N. Baryawno et al., Detection of human cytomegalovirus in medulloblastomas reveals a potential therapeutic target. J Clin Invest 121, 4043 (Oct, 2011).
15. L. Soroceanu et al., Human cytomegalovirus US28 found in glioblastoma promotes an invasive and angiogenic phenotype. Cancer Res 71, 6643 (Nov 1, 2011).
16. E. Slinger et al., HCMV-encoded chemokine receptor US28 mediates proliferative signaling through the IL-6-STAT3 axis. Sci Signal 3, ra58 (Aug 3, 2010).
17. J. R. Randolph-Habecker et al., The expression of the cytomegalovirus chemokine receptor homolog US28 sequesters biologically active CC chemokines and alters IL-8 production. Cytokine 19, 37 (Jul 7, 2002).
18. P. Casarosa et al., Constitutive signaling of the human cytomegalovirus-encoded chemokine receptor US28. J Biol Chem 276, 1133 (Jan 12, 2001).
19. D. Maussang et al., Human cytomegalovirus-encoded chemokine receptor US28 promotes tumorigenesis. Proc Natl Acad Sci U S A 103, 13068 (Aug 29, 2006).
20. D. Maussang et al., The human cytomegalovirus-encoded chemokine receptor US28 promotes angiogenesis and tumor formation via cyclooxygenase-2. Cancer Res 69, 2861 (Apr 1, 2009).
21. G. Bongers et al., The cytomegalovirus-encoded chemokine receptor US28 promotes intestinal neoplasia in transgenic mice. J Clin Invest 120, 3969 (Nov, 2010).
22. M. Penfold, Z. Miao, Y. Wang, S. Haggerty, M. R. Schleiss, A macrophage inflammatory protein homolog encoded by guinea pig cytomegalovirus signals via CC chemokine receptor 1. Virology 316, 202 (Nov 25, 2003).
23. C. Vink, M. J. Smit, R. Leurs, C. A. Bruggeman, The role of cytomegalovirus-encoded homologs of G protein-coupled receptors and chemokines in manipulation of and evasion from the immune system. J Clin Virol 23, 43 (Dec, 2001).
24. A. Sahagun-Ruiz, A. M. Sierra-Honigmann, P. Krause, P. M. Murphy, Simian cytomegalovirus encodes five rapidly evolving chemokine receptor homologues. Virus Genes 28, 71 (Jan, 2004).
25. P. Casarosa et al., Constitutive signaling of the human cytomegalovirus-encoded receptor UL33 differs from that of its rat cytomegalovirus homolog R33 by promiscuous activation of G proteins of the Gq, Gi, and Gs classes. J Biol Chem 278, 50010 (Dec 12, 2003).
26. R. Case et al., Functional analysis of the murine cytomegalovirus chemokine receptor homologue M33: ablation of constitutive signaling is associated with an attenuated phenotype in vivo. J Virol 82, 1884 (Feb, 2008).
27. B. J. Margulies, H. Browne, W. Gibson, Identification of the human cytomegalovirus G protein-coupled receptor homologue encoded by UL33 in infected cells and enveloped virus particles. Virology 225, 111

(Nov 1, 1996).
28. J. Vieira, T. J. Schall, L. Corey, A. P. Geballe, Functional analysis of the human cytomegalovirus US28 gene by insertion mutagenesis with the green fluorescent protein gene. J Virol 72, 8158 (Oct, 1998).
29. E. J. Schlaeger, K. Christensen, Transient gene expression in mammalian cells grown in serum-free suspension culture. Cytotechnology 30, 71 (Jul, 1999).
30. P. T. Ram, C. M. Horvath, R. Iyengar, Stat3-mediated transformation of NIH-3T3 cells by the constitutively active Q205L Galphao protein. Science 287, 142 (Jan 7, 2000).
31. M. Burger et al., Point mutation causing constitutive signaling of CXCR2 leads to transforming activity similar to Kaposi's sarcoma herpesvirus-G protein-coupled receptor. J Immunol 163, 2017 (Aug 15, 1999).
32. D. Maussang et al., The human cytomegalovirus-encoded chemokine receptor US28 promotes angiogenesis and tumor formation via cyclooxygenase-2. Cancer Res 69, 2861 (Apr 1, 2009).
33. C. Sinzger et al., Cloning and sequencing of a highly productive, endotheliotropic virus strain derived from human cytomegalovirus TB40/E. J Gen Virol 89, 359 (Feb, 2008).
34. M. Bellon, C. Nicot, Regulation of telomerase and telomeres: human tumor viruses take control. Journal of the National Cancer Institute 100, 98 (Jan 16, 2008).
35. M. Waldhoer, T. N. Kledal, H. Farrell, T. W. Schwartz, Murine cytomegalovirus (CMV) M33 and human CMV US28 receptors exhibit similar constitutive signaling activities. J Virol 76, 8161 (Aug, 2002).
36. A. Fraile-Ramos et al., Localization of HCMV UL33 and US27 in endocytic compartments and viral membranes. Traffic 3, 218 (Mar, 2002).
37. P. Casarosa et al., Constitutive signaling of the human cytomegalovirus-encoded chemokine receptor US28. Journal of Biological Chemistry 276, 1133 (Jan 12, 2001).
38. J. Schust, B. Sperl, A. Hollis, T. U. Mayer, T. Berg, Stattic: a small-molecule inhibitor of STAT3 activation and dimerization. Chem Biol 13, 1235 (Nov, 2006).
39. H. Zhu, J. P. Cong, G. Mamtora, T. Gingeras, T. Shenk, Cellular gene expression altered by human cytomegalovirus: global monitoring with oligonucleotide arrays. Proc Natl Acad Sci U S A 95, 14470 (Nov 24, 1998).
40. G. Frascaroli et al., Human cytomegalovirus paralyzes macrophage motility through down-regulation of chemokine receptors, reorganization of the cytoskeleton, and release of macrophage migration inhibitory factor. J Immunol 182, 477 (Jan 1, 2009).
41. D. Ganem, KSHV and Kaposi's sarcoma: the end of the beginning? Cell 91, 157 (Oct 17, 1997).
42. N. Munoz et al., Epidemiologic classification of human papillomavirus types associated with cervical cancer. N Engl J Med 348, 518 (Feb 6, 2003).
43. G. Bongers et al., The cytomegalovirus-encoded chemokine receptor US28 promotes intestinal neoplasia in transgenic mice. The Journal of Clinical Investigation 0, 0 (2010).
44. N. Baryawno et al., Detection of human cytomegalovirus in medulloblastomas reveals a potential therapeutic target. J Clin Invest 121, 4043 (Oct, 2011).
45. D. J. Dauer et al., Stat3 regulates genes common to both wound healing and cancer. Oncogene 24, 3397 (May 12, 2005).
46. R. T. Dorsam, J. S. Gutkind, G-protein-coupled receptors and cancer. Nat Rev Cancer 7, 79 (Feb, 2007).
47. R. J. Flockhart, J. L. Armstrong, N. J. Reynolds, P. E. Lovat, NFAT signalling is a novel target of oncogenic BRAF in metastatic melanoma. Br J Cancer 101, 1448 (Oct 20, 2009).
48. A. Fraile-Ramos et al., The human cytomegalovirus US28 protein is located in endocytic vesicles and undergoes constitutive endocytosis and recycling. Mol Biol Cell 12, 1737 (Jun, 2001).
49. P. Tschische, K. Tadagaki, M. Kamal, R. Jockers, M. Waldhoer, Heteromerization of human cytomegalovirus encoded chemokine receptors. Biochem Pharmacol 82, 610 (Sep 15, 2011).

8

Discussion and future perspectives

In the previous chapters, US28 has been shown to activate a plethora of cellular pathways. In contrast to most chemokine receptors, which tend to couple to $G\alpha_i$, US28 couples to multiple different Gα subunits. A second difference with the human chemokine receptors is the constitutive activation that is displayed by US28. Similar to the KSHV-encoded receptor ORF74, US28 constitutively signals through $G\alpha_q$ that, in turn, stimulates phospholipase C resulting in increased inositol-1,4,5-triphosphate levels which bind to intracellular inositol receptors triggering Ca^{2+} release into the cytosol. This ultimately results in the activation of target genes like the nuclear factor of activated T-cells (NFAT) (1). Another factor activated by US28 via $G\alpha_q$ is NF-κB (1). This transcription factor is an important mediator of many cellular responses, including stress- and immune responses (2). The NF-κB signaling pathway appears to play an important role in US28, and it is pivotal in the activation of the COX-2 and STAT3 pathways (3, 4).

Multiple signaling pathways are activated by US28, and at least some of these pathways converge to induce a proliferative phenotype. The COX-2 and STAT3 pathways are both required for US28-induced VEGF production, and inhibition of either pathway results in reduced proliferation. In order to gain more insight in the role of US28 in tumor biology, two signaling routes activated by US28 have been characterized in this thesis, the IL-6/STAT3-axis (**Chapter 3, 4**) and Wnt/b-catenin (**Chapter 5**) signaling. Furthermore, a first characterization of the US28 signalosome is shown **Chapter 6**, which may lead to a more in-depth understanding of US28-induced signaling. Finally, the oncogenic properties of another HCMV-encoded GPCR, UL33 were investigated (**Chapter 7**).

8.1 US28 and UL33 constitutively induce STAT3 activation

In **Chapter 3**, US28 is shown to constitutively induce STAT3 signaling. The first hints of the activation of this pathway were measurements of angiogenic factors in the medium of US28-expressing NIH-3T3 cells. These measurements showed that US28 induces NIH-3T3 cells to secrete IL-6 and VEGF. In addition, CCL2 concentration in the growth medium is diminished which fits the proposed role of US28 as a chemokine sink. Following IL-6 secretion, its cognate receptor is activated. Subsequently, STAT3 is phosphorylated by JAK1, resulting in dimerization and transcriptional activation (5). Additionally, UL33 is shown in **Chapter 7** to also induce STAT3 activity, although it is still unknown whether this is mediated via a mechanism similar to US28. **Chapter 3** represents the first observation of US28 protein expression in glioblastoma clinical samples. Moreover, we demonstrate that STAT3 is phosphorylated in the same niche of the tumor, which suggests that a similar mechanism that we observed in our in vitro models is taking place within these tumors. Finally, the extent of STAT3 phosphorylation in the tumor correlates with patient survival and tumor progression, meaning that a high extent of STAT3 phosphorylation results in a poor prognosis.

The activation of STAT3 by US28 can be interfered with on multiple levels, on the transcriptional level by either the NF-κB inhibitor BAY11-7082 (6) or a STAT3 inhibitor like JSI-124 (7) or Stattic (8). Inhibition at the level of IL-6 and the IL-6 receptor is accomplished via neutralizing antibodies against IL-6 or small molecules inhibiting IL-6 receptor function (9). The fact that conditioned medium derived from US28-expressing cells also results in STAT3 phosphorylation together with the knowledge that STAT3 can induce IL-6 production by itself (10) indicates the possibility of a positive feedback loop. In **Chapter 4** this positive feedback loop is further investigated, using a mathematical model described US28-induced STAT3 activation and IL-6 secretion. Using this model it is clear that IL-6/STAT3 signaling has the potential to generate a positive feedback loop that has the potential to run out of control. Moreover, once a certain critical amount of cells is producing IL-6, the positive feedback loop may force the production of the cytokine in the whole (cancerous) tissue creating an inflamed region. It should be noted that STAT3-signaling may be induced with multiple ligands. For example, IL-5 was found to be over-expressed in HCMV-infected cells to the same extent as IL-6 (11). Such other factors may be able to induce a positive feedback loop on their own, or facilitate one for another factor. Naturally, several mechanisms, which have been discussed in **Chapter 2**, are in play to prevent such a runaway feedback loop from happening. The Silencers Of Cytokine Signaling (SOCS), in particular, are important negative regulators of STAT-signaling (12). An exogenous factor such as US28 may disturb the balance between positive feedback and negative feedback for signaling networks like the STAT3 controlled pathway(s). An important question rises however, why does HCMV induce IL-6 production and what role does it play in the viral life cycle. At a first glance, it seems counter-intuitive for a virus to induce pro-inflammatory signaling in the

cells it infects. However, activation of STAT3 signaling by IL-6 also has anti-apoptotic effects (13) which may be beneficial to the virus. Additionally, since HCMV can infect macrophages (14) and monocytes (15), increased IL-6 secretion may act as a bait to attract new cells for HCMV to infect as IL-6 induces chemotaxis in both macrophages and monocytes (16). Under normal circumstances, increased IL-6 signaling would have no severe effects by virtue of the negative regulation of STAT3 activation. However, if a cell has impaired regulation of STAT3, US28-induced IL-6 signaling either in an autocrine or in a paracrine fashion may result in a proliferative phenotype like the one that is observed in the NIH-3T3 cells. HCMV-induced IL-6 production itself is correlated with aberrant angiogenesis (17, 18). Of course, dysregulation of angiogenesis in the right context is in itself a potent mediator of tumorigenesis (19).
In conclusion, US28-induced IL-6 production may create a favorable microenvironment for proliferation of HCMV. While US28 is solely responsible for HCMV-induced IL-6 production in the host cell at an early time-point of infection, at later stages during infection other viral factors may also induce IL-6 production. One such factor may be UL33, which was shown in **Chapter 7** to also constitutively activate STAT3. In **Chapter 7**, UL33 is further described to be expressed at later time points in infection. UL33 has earlier been described to be present on the virus particle (20). Yet, the amount of UL33 at early time points may be too little to result in appreciable signaling. In this light it would be interesting to investigate whether UL33 conditioned medium can induce STAT3 phosphorylation in other cells. Additionally, it would be interesting to analyze UL33-induced secretion of proteins. This can be done in two ways, one focusing on angiogenic factors with an approach using an antibody array. This approach is sensitive enough for detecting low levels of proteins in the medium, but is biased towards angiogenic factors. The second approach entails using mass-spectrometry to identify factors from the supernatant. While this approach is less sensitive it is unbiased and will allow for a full characterization of factors whose production is induced by UL33.

8.2 US28 induces β-catenin activation

In **Chapter 5**, constitutive activation of β-catenin signaling is described. The involvement of this pathway in US28 signaling was first based on the same micro-array study where US28-induced COX-2 expression was detected (3). The micro-array data also indicated up-regulation of factors involved in Wnt/β-catenin signaling. Further investigation, using the TOP-Flash reporter gene revealed that US28 constitutively induces β-catenin signaling to Tcf-Lef. This was further confirmed by means of Western-blot analysis, showing increased levels of non-phosphorylated β-catenin. Interestingly, US28 activates β-catenin signaling in a non-canonical manner in NIH-3T3. However, another model system, using transgenic mice expressing US28 in the intestine shows canonical β-catenin activation (21). This clearly indicates that the mechanism by which US28 induces β-catenin signaling is very much dependent

on the cellular context.
As mentioned above, US28 induces β-catenin signaling via a non-canonical pathway. In the canonical β-catenin signaling pathway Wnt/Frizzled is usually accompanied with LRP6 phosphorylation. However, the signaling through β-catenin that is induced by US28 in NIH-3T3 is of a different nature. US28-induces signaling via Ga_q and $Ga_{12/13}$, which subsequently results in activation of Rho/ROCK signaling. Further downstream this leads to Tcf/Lef activation.
Further investigation, detailed in **Chapter 6**, suggests that in the NIH-3T3 background US28 inhibits Akt phosphorylation by activating Rho-associated protein kinase (ROCK) via RhoA. Acting further downstream in this signaling route are two protein phosphatases, PP2A and PTEN. Both PP2A and PTEN have a key role in the regulation of different signaling routes, including oncogenic pathways. In the case of US28-induced signaling, where either or both PP2A and PTEN are activated by US28, which may result in decreased Akt activation.
Further downstream, the transcriptional regulator Chibby (Cby) has been identified as an important factor in regulating b-catenin signaling (22). Interestingly, Cby's antagonistic function is counteracted by TC1 (23). Moreover, TC1 is reported to be overexpressed in thyroid cancer (23) and metastatic colon cancer (24). In the case of colon cancer, increased TC1 expression is correlated with poor prognosis. This observation fits well with our current understanding of the molecular mechanisms by which Cby asserts its influence on β-catenin signaling. Indeed, US28 may have a similar effect as TC1 on Cby/β-catenin interaction albeit via another mechanism. Besides the difference in the mechanisms by which US28 and TC1 accomplish functional inhibition of Cby, in both cases it results in a removal of the 'brakes' on β-catenin signaling. It is unlikely that inhibiting Cby will directly result in transforma-

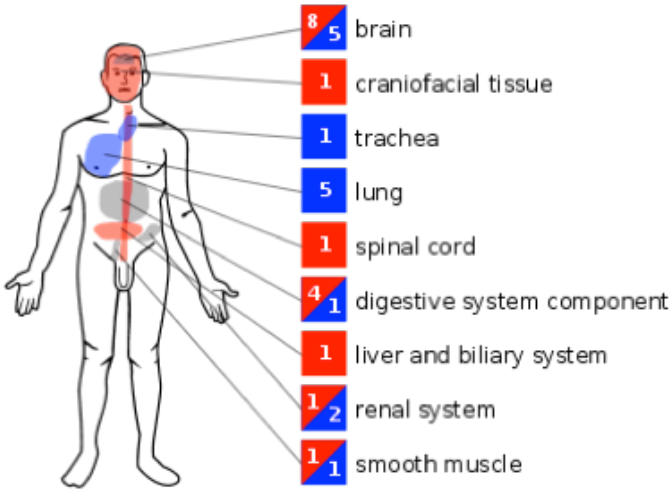

Figure 2. Schematic depiction of Lgr5 expression in humans. Data analyzed by the Atlas project from EMBL shows studies reporting over-expression in red and under-expression in blue. Most expression data is available about the brain and the digestive system.

tion of cells. But in a cell where β-catenin signaling is already hyperactivated, loss of Cby's antagonistic function will exacerbate the transformed phenotype. It will therefore be interesting to express US28 in a cellular background in which β-catenin signaling is already aberrant (eg. APC-mutants or knock-outs). One could imagine that US28-related interference with Cby functioning may add to canonical signaling and thus result in extra activation of B-catenin signaling.

The pathway identified in NIH-3T3 and the canonical Wnt/β-catenin pathway, thus seem to be mutually exclusive, due to the differences in regulation of GSK3b phosphorylation. However, 'unlocking' of b-catenin by US28 may render cells more responsive to b-catenin signaling, resulting in a hyper response to otherwise normal triggers. Treating those cells with an agonist, such as Wnt, should then result in higher activation as measured, for instance, with the Tcf-Lef reporter system that was utilized in **Chapter 5**. If US28 does impart increased sensitivity to Wnt-activation, it may be an explanation of the observed tumor formation in transgenic mice (21).

In the US28-expressing transgenic mice expression is driven by the murine villin promoter. This results in high expression levels throughout the intestinal epithelium. The intestinal epithelium is constantly replaced with new cells, which originate from the intestinal crypts. At the bottom of these crypts reside the intestinal stem cells that give rise to all the different epithelial cells, these cells express the GPCR Lgr5 and are defined as Lgr5+ cells (25). In the case of the transgenic mice mentioned above, US28 is also expressed by the Lgr5+ cells. Since deletion of APC in these cells results in rapid formation of adenomas (26), the presence US28 in Lgr5+ cells may be part of the mechanism that results in the formation of tumors in these mice. Interestingly, Lgr5+ cells can autonomously form intestinal crypt structures; these structures have been termed organoids. The presence of Paneth cells increases the efficiency of this process (27, 28). Lgr5+ cells are not only present in the intestine, Lgr5 is expressed in various tissues as shown in Figure 1. Organoids have been successfully cultured from Lgr5+ cells obtained from the stomach (29). Especially Lgr5 expression in the brain is interesting, considering the presence of US28 in glioblastoma that was described in **Chapter 3**. The LGR5 gene was found to be amplified in recurrent glioblastomas. (30). Moreover, knock-down of Lgr5 in brain cells

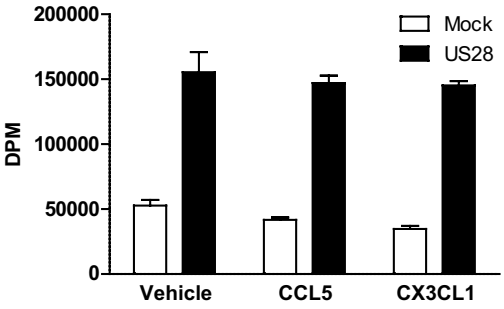

Figure 2. CCL5 and CX3CL1 have no effect on US28-induced proliferation. For this experiments NIH-3T3 cells were subjected to a similar proliferation experiment as detailed in **Chapter 2**. Briefly, the cells were incubated for 24 hours with either CCL5 or CX3CL1 in medium containing [^{3}H]-thymidine. The concentration used for either chemokines was 10-7 M.

with a cancer-stem cell profile induces apoptosis (31). Recently, cancer stem cells have been shown to play a pivotal role in tumor maintenance in murine models for intestinal tumors and glioblastoma (32, 33). This raises the question whether US28 is also expressed in cancer stem cells in patients suffering from HCMV-associated cancers.
Since Lgr5+ cells are dependent on a variety of factors among which Wnt3a, it will be interesting to see whether Lgr5+ cells that express US28 will exhibit a different phenotype compared to wild-type organoids. To further study the tentative link between US28 and Lgr5+ stem cells, and their role in HCMV-associated cancers, it will be necessary to show combined US28 and Lgr5 expression in these cancers. While US28 expression has been shown in glioblastomas, analyzing Lgr5 expression in these tumors will be difficult as there is no reliable antibody yet. An alternative method would be to perform in situ RNA hybridizations to detect other stem cell markers such as Olfm4 or Ascl2. Both these genes have been successfully used as markers in mice and appear to be very specific (28, 34). Whether this is also the case in humans remains to be seen, but the fact that both these genes are highly conserved suggests that this may be the case.
In conclusion, US28 induces β-catenin activation via two possible signaling routes. A canonical route that was described in the transgenic mouse model (21) and a non-canonical route, through Rho and ROCK, whose increased activity results in increased Tcf/Lef activity. Our data in **Chapter 6** suggests that US28-induced activation of Rho and ROCK results in dysregulation of Akt-regulated phosphorylation of Cby and b-catenin. To what extent induction of β-catenin by US28 is responsible for the induction of HCMV associated cancers remains to be clarified. It will be interesting to see whether β-catenin activation by US28, like STAT3, can be correlated in glioblastoma. Especially since β-catenin over-expression is associated with glioblastoma growth (35, 36). Even more interesting, targeting the β-catenin in these cancers results in the down-regulation of several other signaling factors among which STAT3 (2). This suggests that there may be interplay between these two pathways.

8.3 Role of ligand-induced US28 signaling

In general, constitutive signaling appears to be a hallmark for US28. However, CCL5 and CX3CL1 which both bind to US28 can influence signaling to a certain extent (1, 37). While CCL5 generally acts as an agonist, potentiating calcium release induced by US28 (38), it has no effect of inositol phosphate accumulation (1). Moreover, CCL5 and CCL2 are both capable of inducing chemotaxis in vascular smooth muscle cells (39), which is a clear indication of ligand-dependent pathways controlled by US28. CX3CL1, on the other hand, acts in some cases as an inverse agonist on US28, inhibiting inositol phosphate accumulation. In the context of calcium signaling, however, it acts as an agonist (1, 37). Furthermore, CCL5 can increase US28-induced Tcf/Lef activity. It is likely that the reponse of US28 to a ligand is dependent on the cellular context. The clinical data presented in **Chapter 3** indicates that US28-ex-

pression appears to be localized in a specific subset of cells. This possibly highlights the importance of cellular context, and the need for a relevant model system for in vitro studies. Despite these concerns, the data presented in this thesis, as well as data from earlier studies indicate that ligand-induced signaling is not critical for US28-induced proliferation. In Figure 2, this is further demonstrated in a thymidine incorporation experiment. However, the fact that ligands do not seem to play a direct role in US28-induced proliferative signaling does not exclude a role for them in tumorigenesis. Especially considering the recent data from Bongers et al., where CCL2 over-expressing mice were crossed with mice expressing US28 in the intestine. This crossing exacerbated tumor formation in these mice (21). The vascular smooth muscle cell migration mentioned earlier may be an indication for a role of US28 in tumor angiogenesis.

8.4 To what extent is UL33 mirroring US28 signaling?

In **Chapter 7** signaling by another HCMV encoded chemokine receptor homolog is explored in further detail. Earlier research had already shown that, like US28, UL33 signals in a constitutive manner through NF-κB (40). Besides this data, not much was known about UL33's signaling. The discovery of US28's propensity for inducing proliferation in NIH-3T3 cells together with the fact that both proteins display constitutive activity prompted us to investigate UL33's oncomodulatory properties. Moreover, immunohistochemistry staining of glioblastoma tumor samples shows presence of UL33 in these tumors. In contrast with the US28 stainings shown in **Chapter 3**, UL33 appears to be present in large portions of the tumor. Double staining for US28 and UL33 may give further insights in the role that either receptor plays in the tumor biology of glioblastoma.

Our data show that there is a large degree of overlap between signaling by US28 and UL33, which may indicate that both receptors can take over each other signaling. This could provide HCMV with a degree of redundancy. However, arguing against redundancy, US28 is present at early stages of infection, whereas UL33 is present only at 96 hours post infection. Alternatively, UL33 and US28 may potentiate each others signaling. Work by Tschische et al. has shown that UL33 and UL78 can form heterodimers with US28, and may influence the constitutive signaling displayed by US28 (41). Considering the differences in temporal expression of both US28 and UL33 this may represent a way for HCMV to regulate signaling of both molecules.

One of the attractive features of UL33 is that, unlike US28, there is a mouse cytomegalovirus (MCMV) homolog, M33. Moreover, deletion of M33 from the MCMV genome results in a virus that displays impaired dissemination as well as attenuated infection of the spleen and pancreas (42). Reactivation was also negatively affected in the M33 deletion strain (38). Recently, complementation experiments using a strain of MCMV in which the gene encoding M33 is deleted (MCMV ΔM33) have shown that both US28 and UL33 can both functionally replace M33 in MCMV ΔM33 (43). It will be interesting to see whether US28 and UL33 in this model can have on-

comodulatory effects. To answer this question, these recombinant viruses may be used in combination with existing mouse models for different cancers.

8.5 Mathematical modeling of US28's modulation of the STAT3 signaling pathway

Cellular responses are the result of the integration of multiple signaling events that are relayed through different signal transduction routes. To add to the complexity of signaling many pathways also engage in crosstalk with each other. The relatively new field of systems biology seeks to describe, model, and ultimately predict these signaling networks. In **Chapter 4** US28-induced signaling through the IL-6/STAT3 axis is described in great detail. Because of its paracrine nature, induction of the IL-6/STAT3 axis by an external factor was modeled. This model shows that STAT3 signaling has the potential to become engaged in a positive feedback loop. The model also reveals that STAT3 signaling needs to be tightly controlled, as it is prone to enter a positive feedback loop. One can imagine that it is reasonable for a rapid response system to exhibit such behavior. Experiments corroborated this model and showed that picomolar concentrations of IL-6 can already trigger a STAT3 response in cells. Moreover, the same experiments show that treatment with IL-6 induces the expression of IL-6 and prolonged STAT3 phosphorylation.
Considering that US28 induces IL-6 production via NF-kB, these data suggest that US28 may significantly influence the external milieu even when the amount of cells that actually express US28 is very small. It should be noted though, that STAT3 signaling is normally tightly controlled by several negative feedback mechanisms, amongst which are the SOCS proteins as discussed in **Chapter 2**. It is known that in many cancers the STAT3 pathway is affected, either by mutations in STAT3 itself or by mutations in the associated receptors and regulatory proteins. Mutations that render STAT3 constitutively active have been shown to be able to induce angiogenesis (44), although such mutations remain to be demonstrated in patient samples. Another level at which IL-6/STAT3 signaling can be altered is at the IL-6 receptor. Mutations in the transactivating gp130 subunit of the IL-6 receptor can result in constitutive activation of the IL-6/STAT3 pathway that, in turn, results in increased production of IL-6. Such mutations have been described in hepatocellular tumors, which interestingly are always accompanied by mutations in β-catenin signaling proteins (45). Regulation of IL-6 expression itself can also be affected as was shown by Iliopoulis et al. where they demonstrated that transient activation of NF-kB can result in permanent downregulation of Let7 miRNAs. Let7 is an inhibitory factor of IL-6 expression, which thus results in increased IL-6 levels (46). Finally, overexpression of SOCS3 has been reported to inihibit growth of human non-small cell lung cancer cells as well as rendering them more sensitive to radiation (47). Also, epigenetic silencing of SOCS3 has been reported in several cancers (48-50). These data all indicate the effect of changes in signaling through the IL-6/STAT3 axis are dependent on the cellular context.
While the model proposed in **Chapter 4** certainly has predictive value, its real use-

fulness will become apparent when it can be linked to the other pathways engaged by US28. Until now, we have mainly described how the different pathways are activated via the viral receptors. However, if the signaling through the different routes can be integrated into one model that would greatly increase our understanding of US28 signaling and perhaps even allow for predictions in what kind of cells or tissue US28 may exert its oncomodulatory effects.

8.6 What new insights does the US28 signalosome offer?

Although the efforts described in this thesis as well as those of others have shed light on several important facets of US28 signaling, there are still significant caveats in our understanding of US28-induced signaling. In order to gain more understanding of US28-induced signaling, we analyzed the US28 signalosome in **Chapter 6**. The proteins that interact with a receptor and mediate its signaling are referred to as the signalosome. To be able to isolate this subset of proteins a methodology for isolating US28 with its interacting partners had to be developed. As described in **Chapter 6**, a modified immuno-precipitation protocol was used to perform pull-downs of US28 and its interacting partners, using anti-HA conjugated agarose and N-terminally HA-tagged US28. The co-precipitating proteins were then identified by way of liquid chromatography tandem mass-spectrometry.
While such an approach is immensely powerful, one major drawback is that the shear amount of data obtained by these analyses can be daunting. For now, this limits the use of proteomics for understanding cellular signaling. Of course, this is partly due to the fact that most experimental setups for analyzing cellular signaling by mass-spectrometry have been in the development phase for the last few years. As the techniques mature and the data analysis is standardized, it will be possible to assign reliability scores to the different datasets instead of the current practice of collecting all proteomics results regardless of data quality.
The 14-3-3 proteins are overrepresentated in the US28 signalsome. Because of the important role these proteins have in cellular signaling, this may result in aberrant signaling across many signaling pathways. An example of this was discussed earlier in **Chapter 6** where the binding of 14-3-3s by US28 is proposed to interfere with β-catenin regulation by Cby. Several factors that are normally associated with mitochondrial function were also found to co-precipitate with US28. This was a surprising finding, which suggests an important role for intracellular US28 in the alteration of cellular signaling and may also be indicative for a role for US28 in the HCMV-induced shift from oxidative phosphorylation to glycolysis by cytosolic lactic acid fermentation (also known as the Warburg effect) (51).
The current technique for co-immunoprecipitation of the US28 signalosome has proven to be reliable and reproducible. However, this analysis cannot distinguish between the different cellular compartments. An analysis of the differences between intracellular versus the US28 that is present on the plasma membrane would shed light on which of the US28 populations is responsible for the different signal-

ing pathways. In order to address this issue a methodology for isolating the different US28 populations needs to be developed. We have explored two different approaches. First a classical biochemical approach using sucrose gradients to separate the different cellular compartments was employed. The main advantage of this approach is that it allows for analysis of the different compartments using the same preparation. However, while it was no problem to isolate US28 from the plasma membrane compartment as well as from other compartments, we found that it was difficult to obtain enough protein for mass-spectrometry analysis. Furthermore, reproducibility was also an issue using this approach. Therefore an alternative method, using selective biotinylation of plasma membrane proteins with NHS-SS-biotin was explored. This method takes advantage of the fact that NHS-SS-biotin cannot cross the plasma membrane leading to biotinylation of only extracellular lysines. Following biotinylation the cells expressing HA-tagged US28 can be subjected to the established co-immunoprecipitation method. Subsequently, the eluted US28 with their associated proteins are subjected to a biotin pull-down, using streptavidin. The resulting protein fraction will consist of biotinyated US28 and its associated proteins. Initial experiments have shown that it is possible using this method to not only purify biotinylated US28 (Figure 3A), but also associated proteins as shown by silverstaining of the resulting protein mixture (Figure 3B). Another promising technique involves the use of the lectin concanavalin A to isolate the plasma membrane compartment. Concanavalin A binds to the α-D-glucose and α-D-mannose of glycosylated membrane proteins (52). Lee and colleagues have developed a method using concanavalin A bound to magnetic beads that can be used to quickly and reliably purify the plasma membrane fraction. Hence, using the above mentioned techniques, the signalosomes of plasma membrane bound US28 and intracellular US28 can be analyzed which may result in an increased understanding how US28 redirects cellular signaling.

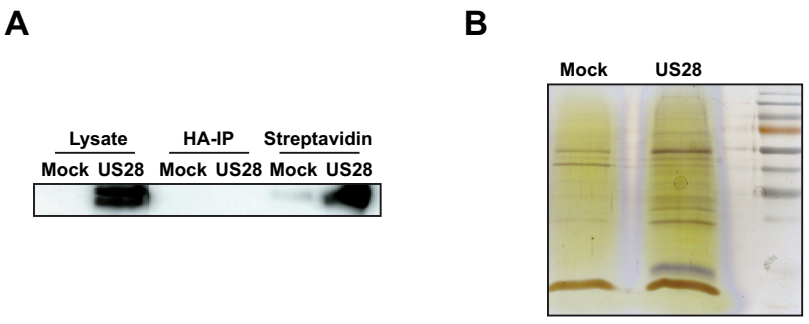

Figure 3. (**A**) Western-blot analysis showing successful isolation of HA-US28 from HEK293T cells transfected with DNA encoding HA-US28. (**B**) A silverstaining showing co-precipitating proteins that are co-isolated with US28, while some proteins are isolated in a non-specific manner as shown in the Mock sample, the majority of proteins are specifically co-precipitating with US28.

8.7 Pharmaceutical intervention strategies, target US28 and UL33 or its pathways?

Considering that a significant portion of the population is HCMV sero-positive, US28 may have an important impact on tumor biology in general. We have shown for the first time that in at least one type of cancer, glioblastoma, US28-associated signaling has a significant effect on tumor progression and patient survival. Efforts to target US28 signaling with inverse agonists have been made (53-55). While these compounds are useful research tools, their potential as drugs is limited due to poor water solubility and low potency.
Considering the knowledge we now have of US28-induced signaling, it may actually be more advantageous to target the pathways that are induced by US28 instead of the receptor itself. Especially considering the paracrine effects that US28 has on surrounding cells. For example, treatment with STAT3 inhibitors may be a viable way of interfering with US28-mediated STAT3 activation. One drawback of targeting the signal transduction pathway instead of the receptor is the potential loss of specificity since these pathways are present in many different cells.
Systems biology approaches will play an important role in addressing the first issue of specificity. By understanding how the different signal transduction routes interact which each other, the models can be predictive and provide insight how to target these pathways to get the desired cellular response (eg. death of a tumor cell).
Another HCMV-encoded GPCR, UL33, was found to have similar tumorigenic properties as US28. In **Chapter 7** the way UL33 induces a proliferative phenotype is similar to US28. Moreover, both US28 and UL33 can be found in glioblastoma tumor samples. The fact that these two proteins are expressed at similar times during infection (albeit that US28 is also expressed at early stages of infection) suggests that US28 and UL33 can act as back-up for each other. Therefore, a pharmacological intervention strategy aimed at inhibiting HCMV-induced proliferative signaling should take into account both US28 and UL33.

To this end, the work described in this thesis has contributed to understanding the way viral GPCRs like US28 and UL33 induce oncomodulatory behavior and which may result in new strategies for treating HCMV-related cancers like glioblastoma.

References

1. P. Casarosa et al., Constitutive signaling of the human cytomegalovirus-encoded chemokine receptor US28. J Biol Chem 276, 1133 (Jan 12, 2001).
2. X. Yue et al., Interruption of beta-catenin suppresses the EGFR pathway by blocking multiple oncogenic targets in human glioma cells. Brain Res 1366, 27 (Dec 17, 2010).
3. D. Maussang et al., The human cytomegalovirus-encoded chemokine receptor US28 promotes angiogenesis and tumor formation via cyclooxygenase-2. Cancer Res 69, 2861 (Apr 1, 2009).
4. E. Slinger et al., HCMV-encoded chemokine receptor US28 mediates proliferative signaling through the IL-6-STAT3 axis. Sci Signal 3, ra58 (Aug 3, 2010).
5. P. C. Heinrich, I. Behrmann, G. Muller-Newen, F. Schaper, L. Graeve, Interleukin-6-type cytokine signalling through the gp130/Jak/STAT pathway. Biochem J 334 (Pt 2), 297 (Sep 1, 1998).
6. M. Lappas, K. Yee, M. Permezel, G. E. Rice, Sulfasalazine and BAY 11-7082 interfere with the nuclear factor-kappa B and I kappa B kinase pathway to regulate the release of proinflammatory cytokines from human adipose tissue and skeletal muscle in vitro. Endocrinology 146, 1491 (Mar, 2005).
7. M. A. Blaskovich et al., Discovery of JSI-124 (cucurbitacin I), a selective Janus kinase/signal transducer and activator of transcription 3 signaling pathway inhibitor with potent antitumor activity against human and murine cancer cells in mice. Cancer Res 63, 1270 (Mar 15, 2003).
8. J. Schust, B. Sperl, A. Hollis, T. U. Mayer, T. Berg, Stattic: a small-molecule inhibitor of STAT3 activation and dimerization. Chem Biol 13, 1235 (Nov, 2006).
9. M. Hayashi et al., Suppression of bone resorption by madindoline A, a novel nonpeptide antagonist to gp130. Proc Natl Acad Sci U S A 99, 14728 (Nov 12, 2002).
10. H. Sumimoto, F. Imabayashi, T. Iwata, Y. Kawakami, The BRAF-MAPK signaling pathway is essential for cancer-immune evasion in human melanoma cells. J Exp Med 203, 1651 (Jul 10, 2006).
11. J. Dumortier et al., Human cytomegalovirus secretome contains factors that induce angiogenesis and wound healing. J Virol 82, 6524 (Jul, 2008).
12. I. D. Dimitriou et al., Putting out the fire: coordinated suppression of the innate and adaptive immune systems by SOCS1 and SOCS3 proteins. Immunol Rev 224, 265 (2008).
13. Y. Liu, P.-K. Li, C. Li, J. Lin, Inhibition of STAT3 Signaling Blocks the Anti-apoptotic Activity of IL-6 in Human Liver Cancer Cells. J Biol Chem 285, 27429 (August 27, 2010, 2010).
14. Q. Wang, L. E. Limbird, Regulation of alpha2AR trafficking and signaling by interacting proteins. Biochem Pharmacol 73, 1135 (Apr 15, 2007).
15. J. V. Olsen, M. Mann, Effective representation and storage of mass spectrometry-based proteomic data sets for the scientific community. Sci Signal 4, pe7 (2011).
16. T. Clahsen, F. Schaper, Interleukin-6 acts in the fashion of a classical chemokine on monocytic cells by inducing integrin activation, cell adhesion, actin polymerization, chemotaxis, and transmigration. J Leukoc Biol 84, 1521 (Dec, 2008).
17. S. Botto et al., IL-6 in human cytomegalovirus secretome promotes angiogenesis and survival of endothelial cells through the stimulation of survivin. Blood 117, 352 (Jan 6, 2011).
18. S. Fiorentini et al., Human Cytomegalovirus productively infects lymphatic endothelial cells and induces a secretome that promotes angiogenesis and lymphangiogenesis through IL-6 and GM-CSF. J Gen Virol, (Dec 1, 2010).
19. D. Hanahan, R. A. Weinberg, The hallmarks of cancer. Cell 100, 57 (Jan 7, 2000).
20. A. Fraile-Ramos et al., Localization of HCMV UL33 and US27 in endocytic compartments and viral membranes. Traffic 3, 218 (Mar, 2002).
21. G. Bongers et al., The cytomegalovirus-encoded chemokine receptor US28 promotes intestinal neoplasia in transgenic mice. The Journal of Clinical Investigation 0, 0 (2010).
22. K. Takemaru, V. Fischer, F. Q. Li, Fine-tuning of nuclear-catenin by Chibby and 14-3-3. Cell Cycle 8, 210 (Jan 15, 2009).
23. M. Sunde et al., TC-1 is a novel tumorigenic and natively disordered protein associated with thyroid cancer. Cancer Res 64, 2766 (Apr 15, 2004).
24. J. B. Friedman, E. B. Brunschwig, P. Platzer, K. Wilson, S. D. Markowitz, C8orf4 is a transforming growth factor B induced transcript downregulated in metastatic colon cancer. Int J Cancer 111, 72 (Aug 10, 2004).
25. N. Barker et al., Identification of stem cells in small intestine and colon by marker gene Lgr5. Nature 449, 1003 (Oct 25, 2007).
26. N. Barker et al., Crypt stem cells as the cells-of-origin of intestinal cancer. Nature 457, 608 (Jan 29, 2009).

27. T. Sato et al., Single Lgr5 stem cells build crypt-villus structures in vitro without a mesenchymal niche. Nature 459, 262 (May 14, 2009).
28. T. Sato et al., Paneth cells constitute the niche for Lgr5 stem cells in intestinal crypts. Nature, (Nov 28).
29. N. Barker et al., Lgr5(+ve) stem cells drive self-renewal in the stomach and build long-lived gastric units in vitro. Cell Stem Cell 6, 25 (Jan 8, 2010).
30. U. Fischer et al., A different view on DNA amplifications indicates frequent, highly complex, and stable amplicons on 12q13-21 in glioma. Mol Cancer Res 6, 576 (Apr, 2008).
31. S. Nakata et al., LGR5 is a marker of poor prognosis in glioblastoma and is required for survival of brain cancer stem-like cells. Brain Pathol, (Jul 16, 2012).
32. A. G. Schepers et al., Lineage tracing reveals Lgr5+ stem cell activity in mouse intestinal adenomas. Science 337, 730 (Aug 10, 2012).
33. J. Chen et al., A restricted cell population propagates glioblastoma growth after chemotherapy. Nature, (Aug 1, 2012).
34. L. G. van der Flier et al., Transcription factor achaete scute-like 2 controls intestinal stem cell fate. Cell 136, 903 (Mar 6, 2009).
35. X. Liu et al., beta-Catenin overexpression in malignant glioma and its role in proliferation and apoptosis in glioblastma cells. Med Oncol, (Mar 19, 2010).
36. P. Pu et al., Downregulation of Wnt2 and beta-catenin by siRNA suppresses malignant glioma cell growth. Cancer Gene Ther 16, 351 (Apr, 2009).
37. M. Waldhoer, T. N. Kledal, H. Farrell, T. W. Schwartz, Murine cytomegalovirus (CMV) M33 and human CMV US28 receptors exhibit similar constitutive signaling activities. J Virol 76, 8161 (Aug, 2002).
38. R. D. Cardin, G. C. Schaefer, J. R. Allen, N. J. Davis-Poynter, H. E. Farrell, The M33 chemokine receptor homolog of murine cytomegalovirus exhibits a differential tissue-specific role during in vivo replication and latency. J Virol 83, 7590 (Aug, 2009).
39. R. M. Melnychuk et al., Mouse cytomegalovirus M33 is necessary and sufficient in virus-induced vascular smooth muscle cell migration. J Virol 79, 10788 (Aug, 2005).
40. P. Casarosa et al., Constitutive signaling of the human cytomegalovirus-encoded receptor UL33 differs from that of its rat cytomegalovirus homolog R33 by promiscuous activation of G proteins of the Gq, Gi, and Gs classes. J Biol Chem 278, 50010 (Dec 12, 2003).
41. P. Tschische, K. Tadagaki, M. Kamal, R. Jockers, M. Waldhoer, Heteromerization of human cytomegalovirus encoded chemokine receptors. Biochem Pharmacol 82, 610 (Sep 15, 2011).
42. R. Case et al., Functional analysis of the murine cytomegalovirus chemokine receptor homologue M33: ablation of constitutive signaling is associated with an attenuated phenotype in vivo. J Virol 82, 1884 (Feb, 2008).
43. H. E. Farrell et al., Partial Functional Complementation Between Human and Mouse Cytomegalovirus Chemokine Receptor Homologues. J Virol, (Apr 13, 2011).
44. G. Niu et al., Constitutive Stat3 activity up-regulates VEGF expression and tumor angiogenesis. Oncogene 21, 2000 (Mar 27, 2002).
45. S. Rebouissou et al., Frequent in-frame somatic deletions activate gp130 in inflammatory hepatocellular tumours. Nature 457, 200 (Jan 8, 2009).
46. D. Iliopoulos, H. A. Hirsch, K. Struhl, An epigenetic switch involving NF-kappaB, Lin28, Let-7 MicroRNA, and IL6 links inflammation to cell transformation. Cell 139, 693 (Nov 13, 2009).
47. Y. C. Lin et al., Adenovirus-mediated SOCS3 gene transfer inhibits the growth and enhances the radiosensitivity of human non-small cell lung cancer cells. Oncol Rep 24, 1605 (Dec, 2010).
48. F. Pierconti et al., Epigenetic silencing of SOCS3 identifies a subset of prostate cancer with an aggressive behavior. The Prostate, n/a (2010).
49. K. D. Sutherland et al., Differential hypermethylation of SOCS genes in ovarian and breast carcinomas. Oncogene 23, 7726 (Oct 7, 2004).
50. H. Isomoto, Epigenetic alterations in cholangiocarcinoma-sustained IL-6/STAT3 signaling in cholangiocarcinoma due to SOCS3 epigenetic silencing. Digestion 79 Suppl 1, 2 (2009).
51. J. Munger, S. U. Bajad, H. A. Coller, T. Shenk, J. D. Rabinowitz, Dynamics of the Cellular Metabolome during Human Cytomegalovirus Infection. PLoS Pathog 2, e132 (2006).
52. L. Bhattacharyya, M. Haraldsson, C. F. Brewer, Concanavalin A interactions with asparagine-linked glycopeptides. Bivalency of bisected complex type oligosaccharides. J Biol Chem 262, 1294 (Jan 25, 1987).
53. J. W. Hulshof et al., Synthesis and structure-activity relationship of the first nonpeptidergic inverse agonists for the human cytomegalovirus encoded chemokine receptor US28. J Med Chem 48, 6461 (Oct 6, 2005).

54. J. W. Hulshof et al., Synthesis and pharmacological characterization of novel inverse agonists acting on the viral-encoded chemokine receptor US28. Bioorg Med Chem 14, 7213 (Nov 1, 2006).
55. H. F. Vischer et al., Identification of novel allosteric nonpeptidergic inhibitors of the human cytomegalovirus-encoded chemokine receptor US28. Bioorg Med Chem 18, 675 (Jan 15, 2010).

NL

Nederlandse samenvatting

Het omleiden van signaaltransductie routes door HCMV-gecodeerde GPCRs

G-eiwit gekoppelde receptoren (GPCRs) vormen een grote groep membraan receptoren die gekarakteriseerd worden door de aanwezigheid van 7 transmembraan domeinen. GPCRs kunnen door een grote verscheidenheid aan liganden kunnen worden geactiveerd, variërend van licht tot aan eiwitten. Analoog aan de grote verscheidenheid aan liganden, leidt de activatie van GPCRs tot uiteenlopende responsen in de cel. De activatie van rhodopsine-receptoren op het netvlies door licht leidt bijvoorbeeld tot een elektrisch signaal dat naar de hersenen wordt gestuurd, terwijl activatie van chemokine-receptoren chemotaxis (migratie van cellen) tot gevolg heeft.

Een groot deel van de bevolking is besmet met het Humaan cytomegalovirus (HCMV). Een HCMV besmetting heeft normaal gesproken geen ernstige gevolgen, en zal in de meeste mensen een latent bestaan leiden. In mensen met een niet goed werkend immuun systeem (bijvoorbeeld kankerpatienten) kan een HCMV besmetting echter tot complicaties leiden, zoals pneumonitis (ontsteking van de longblaasjes) en retinitis (ontsteking van het netvlies). Ook wordt HCMV in verband gebracht met verschillende kankers, zoals glioblastoma en colon kanker. Dit verband is niet noodzakelijk rechtstreeks en men spreekt dan ook van een oncomodulair in plaats van een oncogeen effect. Het feit dat zo'n groot deel van de bevolking HCMV-positief is duidt erop dat HCMV zeer goed aangepast is om het immuunsysteem van zijn gastheer te omzeilen. Daartoe zijn er een aantal GPCRs 'gekaapt' uit het menselijk genoom, waaronder US28 en UL33, die afstammen van humane chemokine receptoren. Deze virale GPCRs (vGPCRs) verschillen op een aantal punten van de humane chemokine receptoren. Een belangrijk verschil is dat US28 en UL33, in tegenstelling tot chemokine receptoren, constitutieve activiteit vertonen. Verder bindt US28 een aantal verschillende chemokines, waaronder CCL2, CCL5 en CX3CL1. Doordat US28 deze chemokines bindt en internaleert, worden de de lokale concentratie van deze chemokines verlaagt. Dit effect wordt ook wel een 'chemokine-sink' genoem, hetgeen mogelijk bijdraagt aan de ontwijking van een immuun respons. Eerder onderzoek heeft uitgewezen dat constitutief actieve vGPCRs oncogene eigenschappen kunnen hebben. Eén van de eerste voorbeelden hiervan is de oncogene activiteit van ORF74, een vGPCR die door het Kaposi sarcoma herpes virus (KSHV) tot expressie wordt gebracht. Verscheidene onderzoeken hebben laten zien dat expressie van ORF74 leidt tot veranderingen in signaal transductie die tot oncogene transformatie kunnen leiden. Expressie van ORF74 in transgene muizen leidt tot laesies die erg lijken op laesies die worden gezien in Kaposi sarcoma. Er is ook gekeken of de vGPCRs gecodeerd door het HCMV dit soort effecten kunnen induceren. *In vitro* studies hebben laten zien dat expressie van US28 in NIH-3T3 cellen versnelde celdeling en een verlies van contact inhibitie veroorzaakt. Net zoals in het geval van ORF74 zijn er ook *in vivo* experimenten met US28 uitgevoerd. Een eerste *in vivo* experiment behelsde xenograft experimenten waarbij er NIH-3T3 cellen die

US28 tot expressie brengen in de flank van muizen waren geïnjecteerd. Deze injecties leidde tot de vorming van tumoren op de plek van injectie. Een later onderzoek liet zien dat expressie van US28 in de het darmepitheel van transgene muizen tot de vorming van adenomas leidt.
Het doel van dit proefschrift is om de moleculaire mechanismen die achter dit oncomodulaire gedrag van US28 zitten te ontrafelen. Tevens is er gekeken naar het oncogene/oncomodulaire potentieel van een andere vGPCR, namelijk UL33. In hoofdstuk 1 en 2 wordt de huidige kennis betreffende vGPCRs en een aantal oncogene signaaltransductie routes beschreven. **Hoofdstuk 1** is een introductie rond (virale) GPCRs, waarbij eerst de eigenschappen van GPCRs en chemokine receptoren in het bijzonder worden behandeld. Daarna worden de kenmerken van verschillende vGPCRs van verschillende herpesvirussen besproken. Daarbij wordt de nadruk gelegd op de signaaltransductie routes die door de verschillende vGPCRs worden geactiveerd en de gevolgen van activatie van deze routes door vGCPRs. In **hoofdstuk 2** worden er een aantal oncogene signalering routes beschreven, waaronder activatie en regulatie van STAT-, Wnt/β-catenin- en VEGF-signalering die in latere hoofdstukken terug komen.

Hoofdstuk 3 beschrijft hoe US28 de IL-6/STAT3-as activeert in NIH-3T3 en HEK293T cellen. Door middel van experimenten met verschillende specifieke inhibitors ontrafelen we hoe US28 deze signaal transductie route activeert. Daarbij zien we dat US28 in NIH-3T3 cellen IL-6 productie induceert. Dezelfde experimenten laten ook zien dat US28-afhankelijke STAT3 activatie via JAKs verloopt. De betrokkenheid van JAK duidt op een rol van de IL-6 receptor. Experimenten met geconditioneerd medium van cellen die US28 tot expressie brengen laten vervolgens zien dat deze cellen IL-6 aanmaken, wat vervolgens leidt tot STAT3 activatie. Dit kan worden onderbroken door middel van IL-6 neutraliserende antilichamen en met een inhibitor die op de IL-6-receptor werkt. Verder zien we dat inhibitie van STAT3 US28-afhankelijke VEGF activatie remt. Experimenten met recombinante virussen laten zien dat we deze observaties in een virale context kunnen dupliceren. Ook waren we in staat om voor het eerst de aanwezigheid van US28 aan te tonen in tumor monsters van glioblastoma patiënten. Belangrijker nog, we konden STAT3 activatie in dezelfde regio's van deze tumoren laten zien en de mate van STAT3 activatie correleren aan de hevigheid van dit type kanker.

In **hoofdstuk 4** wordt verder ingegaan op de eigenschappen van de US28-gerelateerde activatie van de IL-6/STAT3-as. Hierbij wordt er een eerste poging gedaan om US28-geinduceerde IL-6 productie en de daar bijhorende activatie van STAT3 te vatten in een wiskundig model. Hierbij zien we dat US28-geinduceerde activatie van STAT3 via IL-6 een bistabiel systeem lijkt te zijn waarbij er 2 steady-state toestanden zijn. Hierbij kan er een positieve terugkoppeling ontstaan wanneer er een minimum concentratie van IL-6 wordt overschreden. Dit resulteert erin dat het systeem de hoge steady-state waarde aanneemt. Als deze minimum concentratie niet

wordt bereikt zal het systeem de lage steady-state waarde aannemen en zal er geen positief terugkoppelings effect worden bereikt. In dit hoofdstuk worden ook een aantal eerste experimenten beschreven waarbij er is geprobeerd om dit model te verifiëren. Hoewel de eerste experimenten redelijk overeen lijken te komen met het model moet er nog meer werk worden verricht. Vooral het feit dat er voorbij wordt gegaan aan de negatieve regulatie van STAT3 is belangrijk en dit zal zeker worden meegenomen in toekomstige modellen van STAT3 signalering.

In de **hoofdstukken 5 en 6** wordt activatie van Tcf-Lef signalering via de Wnt/β-catenin route behandeld. In **hoofdstuk 5** zien we dat US28 Tcf-Lef signalering activeert en dat dit gepaard gaat met β-catenin activatie. Verdere experimenten laten echter zien dat er geen sprake is van LRP6 fosforylatie, hetgeen wel het geval zou zijn indien er sprake is van de standaard activatie van Tcf-Lef door Wnt/β-catenin. Verdere experimenten laten zien dat G-eiwit signalering via Rho-ROCK tot Tcf-Lef activatie leidt. Hoe activatie van Rho-ROCK Tcf-Lef activiteit kan op reguleren is nog niet duidelijk, en een reden dat in **hoofdstuk 6** het US28 signalosoom wordt geanalyseerd. Hierbij is het US28 signalosoom opgezuiverd door middel van co-immuno-precipitatie en massaspectrometrie. Vervolgens is er gekeken welke groepen van eiwitten op basis van ontologie over-gerepresenteerd zijn in de dataset. Daarbij viel de aanwezigheid van de 14-3-3 eiwitten op. Deze eiwitten spelen een belangrijke rol in het faciliteren van veel processen in de cel. Eén van deze processen is het binden van Cby aan β-catenin. Cby heeft normaal gesproken een remmende werking op β-catenin, maar om deze functie te kunnen uitvoeren is het belangrijk dat Cby wordt gefosforyleerd door Akt zodat 14-3-3 eiwitten kunnen binden aan Cby en β-catenin. Aangezien ROCK de activiteit van Akt indirect kan beïnvloeden door negatieve regulators van Akt te activeren, kan de controlerende functie van Cby op die manier worden opgeheven. Om te zien of Cby ook echt bindt aan 14-3-3 zijn er Bioluminiscence Resonance Energy Transfer (BRET) experimenten uitgevoerd waarbij deze interactie kon worden aangetoond. Als de interactie van 14-3-3 met client-eiwitten wordt gestabiliseerd met fusicoccin wordt Tcf-Lef signalering geremd. Hierbij moet wel worden opgemerkt dat dit niet noodzakelijk het gevolg hoeft te zijn van een stabilisatie van de interactie tussen 14-3-3 en Cby.

Hoofdstuk 7 beschrijft een eerste karakterisatie van de oncogene eigenschappen van UL33, een ander vGPCR die door HCMV tot expressie wordt gebracht. UL33 lijkt erg op US28 omdat het ook een constitutief actieve vGPCR is. In tegenstelling tot US28, bindt UL33 geen chemokines. Desondanks activeert UL33 vergelijkbare signaleringsroutes als US28 en induceert het een verhoogde celgroei *in vitro* en tumor vorming *in vivo*. Verder wordt de aanwezigheid van UL33 in glioblastoma tumoren aangetoond. In de virale levens cyclus komt UL33 later dan US28 tot expressie maar is er wel sprake van grote overlap en zijn beide receptoren voor een groot deel van de tijd beiden aanwezig op de celmembraan. Hierbij is het mogelijk dat beide receptoren met elkaar dimeriseren en elkaars activiteit beïnvloeden. Ook is het mogelijk

dat US28 en UL33 in bepaalde gevallen elkaars functie kunnen overnemen.

Zowel US28 als UL33 leiden signaaltransductie routes om zodat het virus beter kan overleven. Deze activiteit is echter ook verantwoordelijk voor het oncomodulaire gedrag van HCMV. In dit proefschrift worden de moleculaire mechanismen die US28 aanwendt om 2 belangrijke oncogene signaaltransductie routes te activeren beschreven. In het geval van IL-6/STAT3 activatie door US28 is er een begin gemaakt met een systeem biologische benadering door het opzetten van een eerste model dat probeert te beschrijven hoe US28 de IL-6/STAT3-as activeert. Activatie van Tcf-Lef door US28 lijkt op een niet-standaard manier te gebeuren en de analyse van het US28 signalosoom heeft belangrijke informatie opgeleverd over het mechanisme wat daar mogelijk achter zit. Ook is er een begin gemaakt met het beschrijven van de oncomodulaire eigenschappen van UL33.

LP

List of publications

Maussang D, Langemeijer E, Fitzsimons CP, Stigter-van Walsum M, Dijkman R, Borg MK, **Slinger E**, Schreiber A, Michel D, Tensen CP, van Dongen GA, Leurs R, Smit MJ. (2009) *The human cytomegalovirus-encoded chemokine receptor US28 promotes angiogenesis and tumor formation via cyclooxygenase-2.* Cancer Res 69(7):2861-9

Slinger E, Maussang D, Schreiber A, Siderius M, Rahbar A, Fraile-Ramos A, Lira SA, Söderberg-Nauclér C, Smit MJ. (2010) *HCMV-encoded chemokine receptor US28 mediates proliferative signaling through the IL-6-STAT3 axis.* Sci Signal 3(133):ra58

Slinger E, Langemeijer E, Siderius M, Vischer HF, Smit MJ. (2011) *Herpesvirus-encoded GPCRs rewire cellular signaling.* Mol Cell Endocrinol 331(2):179-84

Bongers G, Muniz LR, Pacer ME, Iuga AC, Thirunarayanan N, **Slinger E**, Smit MJ, Reddy EP, Mayer L, Furtado GC, Harpaz N, Lira SA. (2012) *A role for the epidermal growth factor receptor signaling in development of intestinal serrated polyps in mice and humans.* Gastroenterology 143(3):730-40

Langemeijer E, **Slinger E**, de Munnik S, Schreiber A, Maussang D, Vischer H, Verkaar F, Leurs R, Siderius M, Smit MJ. *Constitutive β-catenin signaling by the viral chemokine receptor US28.* PLoS ONE In press

Langemeijer E, **Slinger E**, Schreiber A, Rahbar A, Stigter-van Walsum M, Maussang D, Siderius M, van Dongen G, Söderberg-Nauclér C, Smit MJ. (In preparation) *The constitutively active HCMV-encoded receptor UL33 displays oncogenic potential*

Slinger E, Bruggeman F, Siderius M, Smit MJ. (In preparation) *A model describing STAT3 activation through US28-induced IL-6 production*

FW

Final words

Final words/Dankwoord

Hier is het dan, het proefschrift na 4 jaar bloed, zweet en tranen als AIO op de VU en 1,5 jaar op afstand als post-doc-achtige in New York. Het dankwoord is natuurlijk een van de belangrijkste (en ieder geval meest gelezen) delen van een proefschrift. Zes jaar geleden begon ik als promovendus aan dit project. Ik had destijds vooral ervaring met microbiologisch onderzoek, en vrijwel geen ervaring met het kweken van zoogdiercellen. Die microbiologische ervaring kwam later goed van pas met het spotten van besmetting (gelukkig niet te vaak).

Allereerst wil ik graag mijn promoter Martine en co-promoter Marco bedanken. Martine, bedankt voor alle hulp en ondersteuning en ook met het helpen realiseren van mijn avontuur in New York. Ik kon altijd bij je terecht met vragen, en ook manuscripten kwamen altijd snel terug met goede suggesties. Marco, jij was een belangrijke bron van inspiratie en altijd bereid om naar mijn soms 'crazy plans' te luisteren. Onze brainstorm sessies, soms na een paar biertjes op een borrel, hebben soms tot mooie ideeën geleid. De signaaltransductie trip naar Aken was ook een mooie ervaring compleet met een record brekende rit naar Amsterdam. En natuurlijk was de metro rit naar huis op het einde van de dag een mooi moment om de dag even door te spreken. Wat meer op afstand, maar zeker niet minder belangrijk, was de grote baas Rob. Jij hield ons altijd scherp met goed commentaar op presentaties en manuscripten en zonder jouw input had dit boekje er nooit gekomen.

Science doe je nooit alleen en ik ben geen uitzondering daarop. De praktische en morele ondersteuning van mijn collega's op de VU was altijd erg belangrijk. Ik heb een aantal lab- en kantoorgenoten gehad op mijn tocht door verschillende werkkamers en labs.

David, you were a great help with getting me started in the lab and my first kantoor-mate. You taught me the basics of cell culture and we were co-authors on several good papers. Andreas, thank you for all your help with the virus experiments. I still remember the time that we were walking with our recombinant, radioactive viruses in the RNC. You also taught me how to work with viruses, and told me about the existence of Ibidi slides, which saved me a lot of frustration with trying to get my cells to move onto a glass slide. Also thanks for the company during my drive to Italy (and the free breakfast near Ulm), and of course for inviting me for your marriage and later the skiing trip in Oberstdorf. Both were great experiences! I hope that the tulips are still doing well. Ellen, samen met Andreas, David en mij vormden we het vGPCR team, en ik ben blij dat we een mooi verhaal in PLoS ONE hebben kunnen publiceren. Hopelijk volgt het UL33 verhaal snel!

Jib, Anne en Herman thank you for being such good labmates and I hope that I

wasn't too much of annoyance with my sometimes somewhat dirty bench. Jib and Herman, we shared our office space for a while until one (Jib) left the lab and the other (Herman) moved to another room. Thank you for the fun moments even if it was for only a short time. Kim, jij was mijn wat langere termijn kantoorgenoot en we hebben altijd veel lol gehad in ons kantoortje. Hoewel we allebei een andere tak van wetenschapssport beoefenen konden we het altijd goed met elkaar vinden en heb ik veel aan jouw tips en trucs gehad. Ken, you were the last addition to our office. Thank you for the fun and for bringing sometimes strange candy, also thanks for teaching me how to swear in Cantonese.

Verder wil ik Jan-Paul, Saskia, Obbe en Leontien bedanken voor hun geweldige ondersteuning van het lab zowel op technisch gebied als op sociaal gebied. Zonder goede analisten kan geen enkel lab draaien en jullie waren/zijn geweldig.

Mijn AIO generatiegenoten: Anne, Danny en Petra moet ik natuurlijk ook opnoemen. Danny, de metro rit met jou en Marco was zoals eerder gezegd een mooi einde van de dag. Petra, onze jaarlijkse carpool naar de FIGON dagen was op het einde bijna een traditie aan het worden. Ook de warme chocolade melk voor Sinterklaas was een leuk initiatief. Anne, wij hebben lange tijd N249 (ik hoop dat ik het kamer nummer goed heb) gedeeld en konden altijd prima met elkaar opschieten, hoewel ik soms wel jaloers was op jouw keurig nette bench.

De next gen AIOs Azra, Sabrina en Saskia. Het was leuk om jullie te zien doorstromen van de laatste fases van jullie studie naar een AIO plek. De lunches en koffiepauzes waren altijd gezellig, helemaal met de baklava van Azra. Veel geluk met het afronden van jullie promoties!

De rest van de collega's: Dennis, Henry, Sven, Marola, Anitha, Iwan, Maikel, Chris, Luc, Rogier, Mark, Oscar, Ewald, Andrea, Laura, Cindy en wie ik verder nog mogelijk ben vergeten, bedankt voor gezelligheid tijdens de koffie, lunch en borrels.

Cecilia and Maral, thank you for the hospitality in Stockholm. Although I was there for only one week, we made sure it counted and the data we obtained was instrumental for the STAT3 paper.

Ik heb behoorlijk wat studenten in de loop der tijd begeleid en die wil ik graag allemaal bedanken. Ik hoop dat ik niemand vergeet, maar mocht dat zo zijn dan alvast mijn excuses. Dewy, Loes, Laura, Robert-Jan, Francisca, Mark, Martin, Hanneke, Claire, Selina, Maaike, Mirjam, en Ilse. Bedankt voor jullie inzet en bijdrages, waarvan er een aantal uiteindelijk in papers of dit proefschrift terecht zijn gekomen. Ik heb op mijn beurt veel van jullie geleerd over leiding en lesgeven.

FW

Although it was not a part of my Phd, I would like to thank the people that I worked with during my time at Mount Sinai in New York. Sergio, thank you for giving me the opportunity to work in your lab and for encouraging me to be more organized, which truth be told I could definitely use sometimes. I learned a lot of techniques which will really help me a lot in the rest of my scientific career. I had a great time living and working in New York, which was a great professional and personal experience. Glaucia, Michelle, Luciana, Monique, Lily, Alice, and Alan thank you for all the help and fun in and outside of the lab. I will most definitely come visit New York again as a tourist. Gerold, ook jij heel erg bedankt voor de hulp toen ik net was gearriveerd. Ik hoop dat je het nog lang naar je zin hebt in New York en ik zie je vast nog wel eens in Nederland of in New York.

Zonder ondersteuning van het thuisfront had ik het natuurlijk nooit gered en daarom wil graag Daniel, Bas, Jeroen en Jelger bedanken. Jullie zijn al sinds lange tijd goede vrienden en de avonden uit, korte vakanties en vis avonturen zijn altijd fantastisch geweest om even te ontspannen. Dat heb ik zeker gemist tijdens mijn tijd in Amerika en moeten we zeker inhalen de komende tijd.

Als laatste bedank ik mijn ouders en mijn broertje natuurlijk. Pap, Mam en Bart, bedankt voor jullie ondersteuning ook al was het soms lastig uit te leggen wat ik nou precies deed. Zonder jullie steun had ik dit nooit kunnen doen, heel erg bedankt daarvoor!